

APPENDIX L

GROUNDWATER FLOW FIELD DEVELOPMENT

This appendix describes the development of the regional-scale groundwater flow field used for the groundwater modeling that supports assessment of the groundwater quality impacts discussed in the *Draft and Final Tank Closure and Waste Management Environmental Impact Statement for the Hanford Site, Richland, Washington (TC & WM EIS)*, Chapters 5 and 6 and Appendices O and V. Included are an overview of groundwater flow at the site; the purpose and scope of the groundwater flow field development in the context of the overall groundwater modeling effort; changes in the groundwater flow field between the *Draft* and *Final TC & WM EIS*; model design variants to address uncertainty and sensitivity of the groundwater flow field; specifications of the model framework and inputs; the strategy and process of groundwater flow model calibration to head data; and sensitivity of the model to changes in input parameters. A thorough summary of the groundwater flow field results is also provided.

L.1 INTRODUCTION

This *Tank Closure and Waste Management Environmental Impact Statement for the Hanford Site, Richland, Washington (TC & WM EIS)* is being prepared in accordance with the National Environmental Policy Act (NEPA) of 1969, as amended (42 U.S.C. 4321 et seq.); U.S. Department of Energy (DOE) implementing procedures for NEPA (10 CFR 1021); and Council on Environmental Quality (CEQ) regulations for implementing the procedural provisions of NEPA (40 CFR 1500–1508). These regulations require that an environmental impact statement evaluate short- and long-term environmental impacts of the alternatives and the cumulative environmental impacts. This *TC & WM EIS* evaluates the impacts of Tank Closure, FFTF Decommissioning, and Waste Management alternatives on land resources, infrastructure, noise, air quality, geology and soils, water resources, ecological resources, cultural resources, socioeconomics (e.g., employment, regional demographics, housing and community services), public and occupational health and safety, environmental justice, and waste management activities. Contaminants in groundwater at the Hanford Site (Hanford) could potentially impact water resources, ecological resources, cultural resources, public health and safety, and environmental justice over the long term. In particular, the Columbia River and its associated ecological resources are highly valued resources that could be impacted by contaminants transported from Hanford through groundwater.

This *TC & WM EIS* quantifies impacts on the human and natural environment to the extent practicable, consistent with DOE's sliding-scale approach, taking into account available project information and design data. This approach to NEPA analysis implements CEQ's instruction to "focus on significant environmental issues and alternatives" (40 CFR 1502.1) and discuss impacts "in proportion to their significance" (40 CFR 1502.2(b)). This *TC & WM EIS* acknowledges uncertainty and incompleteness in the data and, where the uncertainty is significant or a major factor in understanding the impacts, explains how the uncertainty affects the analysis. Thus, this *TC & WM EIS* balances the dual goals of accuracy and comparability against the available information and the need for timely decisions.

Figure L-1 shows the components of the *TC & WM EIS* groundwater modeling system that was used to predict the long-term impacts on groundwater quality, human health, and ecological resources. This appendix specifically discusses the representation of the flow field used to support the long-term impact analyses. Topics discussed include the development of the flow field conceptualization, the groundwater flow observed at Hanford and predicted by the model, the model calibration process, and model sensitivities and uncertainties.

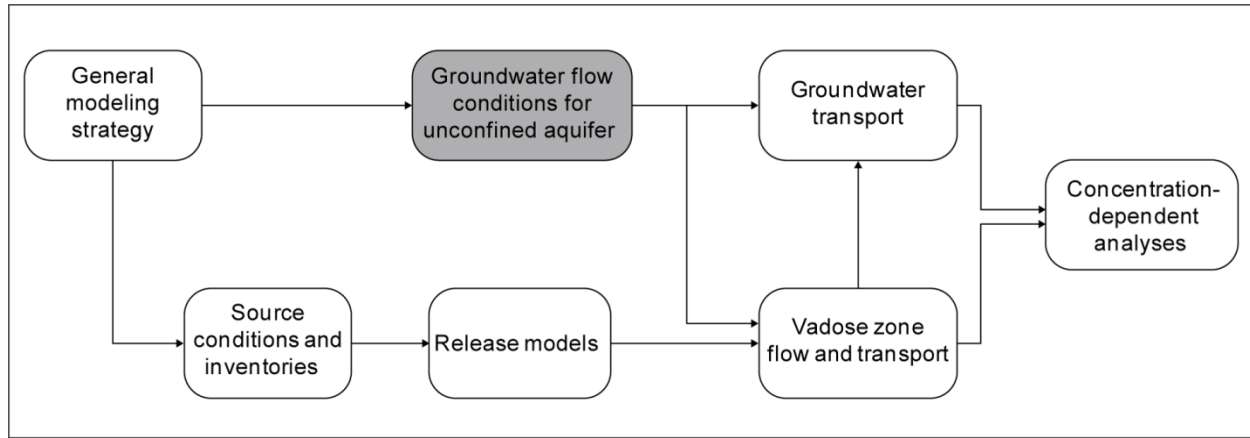


Figure L-1. Groundwater Modeling System Flowchart

L.1.1 Purpose

This appendix describes the development of a regional-scale groundwater flow field for Hanford. A groundwater flow field is a time-dependent, spatially varying representation of the direction and magnitude of groundwater flow. The Hanford groundwater flow field was critical to the evaluation and comparison of the potential long-term impacts of the *TC & WM EIS* alternatives, and evaluation of the long-term cumulative impacts on resources related to groundwater.

The groundwater flow field was calculated prior to simulation of contaminant transport in the vadose zone (the area of unsaturated soil and rock between the ground surface and the water table) and unconfined aquifer. The groundwater flow field provided the numerical representation of water table elevations and velocities that were necessary inputs to the vadose zone transport model, STOMP [Subsurface Transport Over Multiple Phases] (see Appendix N of this *TC & WM EIS*), and the saturated zone transport model (see Appendix O). A well-calibrated groundwater flow field provided connection and consistency between the vadose zone and saturated zone transport models that were used to evaluate alternative and cumulative impacts.

Three key criteria were considered in the development of the *TC & WM EIS* groundwater flow field based on NEPA requirements, as follows:

- The flow field must provide a basis for an unbiased evaluation of the impacts of the *TC & WM EIS* alternatives for the 10,000-year period of analysis (calendar years [CY] 1940–11,940).
- The flow field must provide a basis for understanding the *TC & WM EIS* alternatives in the context of cumulative impacts.
- The effects of uncertainties and gaps in input data (e.g., spatial distribution of well borings across the study area), modeling assumptions (e.g., conceptualization of the top of basalt [TOB] as a no-flow boundary), and numerical error (e.g., head and water balance residuals) must be evaluated and discussed.

This appendix describes how the *TC & WM EIS* groundwater flow field was developed to meet these requirements.

L.1.2 Scope

In describing the development of the *TC & WM EIS* groundwater flow field for Hanford, this appendix presents the following information:

- The fundamental features of the regional-scale flow field model specific to Hanford
- The data sources, data, and representation (encoding) of the data in the flow field model
- Model parameters and settings
- Algorithms selected for the model
- Calibration to existing water-level data and the results of calibration runs to check model sensitivity to varying boundary conditions

The model simulating the flow field for this *Final TC & WM EIS* was built by modifying the model used for the *Draft TC & WM EIS* groundwater analysis. Changes were made to the material types assigned in selected areas, and updates were made to the head observation data set.

L.1.3 Technical Guidance

The *Technical Guidance Document for Tank Closure Environmental Impact Statement Vadose Zone and Groundwater Revised Analyses (Technical Guidance Document)* (DOE 2005) specifies technical assumptions, model input parameters, and methods for proceeding with *TC & WM EIS* vadose zone and groundwater analyses. The technical bases supporting many of the assumptions result from various multiyear field- and science-based activities consistent with the Hanford Federal Facility Agreement and Consent Order, also known as the Tri-Party Agreement (Ecology, EPA, and DOE 1989); the Record of Decision for the *Tank Waste Remediation System, Hanford Site, Richland, Washington, Final Environmental Impact Statement (TWRs EIS)* (62 FR 8693); and the National Research Council's review of the *Draft TWRs EIS* (National Research Council 1996). This appendix indicates where design features or input data used in the development of the flow field are specified by the *Technical Guidance Document*.

The *Technical Guidance Document* specifies five key requirements for development of the *TC & WM EIS* groundwater flow field, as follows:

1. The flow field should be transient (i.e., change with time).
2. The factor driving the transient behavior should be operational recharge to the aquifer rather than time-changing boundary conditions.
3. The sitewide natural recharge rate should be 3.5 millimeters per year.
4. Both a Base Case and a Sensitivity (Alternate) Case should be investigated, and the difference between the two cases should take into account the uncertainty in the TOB elevation in the Gable Mountain–Gable Butte Gap (Gable Gap). The Sensitivity Case was presented in the *Draft TC & WM EIS* and is not presented again. Only the Base Case modifications and results are presented in this *Final TC & WM EIS*.
5. Flow field development should be consistent with the frameworks for vadose zone and contaminant transport modeling.

The TC & WM EIS groundwater flow model and simulated flow field meet these specifications.

L.1.4 Groundwater at the Hanford Site

Groundwater at Hanford is modeled on a regional scale. This regional-scaled approach results in, for analysis purposes, a single representation of the saturated zone beneath the site. This single representation requires some simplifying assumptions and does not allow for inclusion of all detailed site characterization data that may be available at particular areas of interest across the site. One example of a simplifying assumption used is that the Columbia and Yakima River stages are modeled as unchanging with time, although field observations show frequent river stage fluctuations for both. This and other simplifying assumptions incorporated into the regional-scaled groundwater model reflect a balance between representing the interaction of complex natural systems on a regional scale and the bounds of computational limitations in a production environment.

The conceptualization of groundwater flow at Hanford is that of an unconfined, heterogeneous aquifer bounded at the bottom by an impermeable basalt surface. Water enters the aquifer from the highlands on the southern and western sides of the region, from the Yakima River, and via natural and anthropogenic areal recharge (water applied at or near the ground surface). Water enters the groundwater and moves across Hanford to the east and north, discharging into the Columbia River. As groundwater flows across the site from the south and west, it encounters a groundwater divide in the 200 Areas. The location of this divide is uncertain as it is not well defined by field data; however, it dictates flow direction either to the north or to the east from the 200 Areas. Groundwater north and west of this divide moves to the north through Gable Gap (or Umtanum Gap) and then to the Columbia River north of Gable Mountain and Gable Butte. Groundwater south and east of this divide stays south of Gable Mountain and Gable Butte and continues generally eastward to the Columbia River. Refer to Figure L-2 for an overview of groundwater flow at Hanford.

Groundwater hydraulic head observation wells are dispersed across Hanford. Hydraulic head data have been collected over time starting in the 1940s. This database includes over 136,000 head observations from approximately 1,900 discrete locations. The field data indicate that the groundwater potentiometric surface changes over time, that it has continued to change up to the present day, and that it is higher and steeper in the western regions of the site and relatively flat in the eastern regions (CHPRC 2009a). The transient nature of the water table is due primarily to planned and unplanned discharges to the ground surface and directly to the water table during the Hanford operational period. The variable steepness in the potentiometric surface is due to the occurrence of materials with lower hydraulic conductivity in the west, causing a steeper water table; and materials of higher hydraulic conductivity in the east, resulting in a flatter surface.

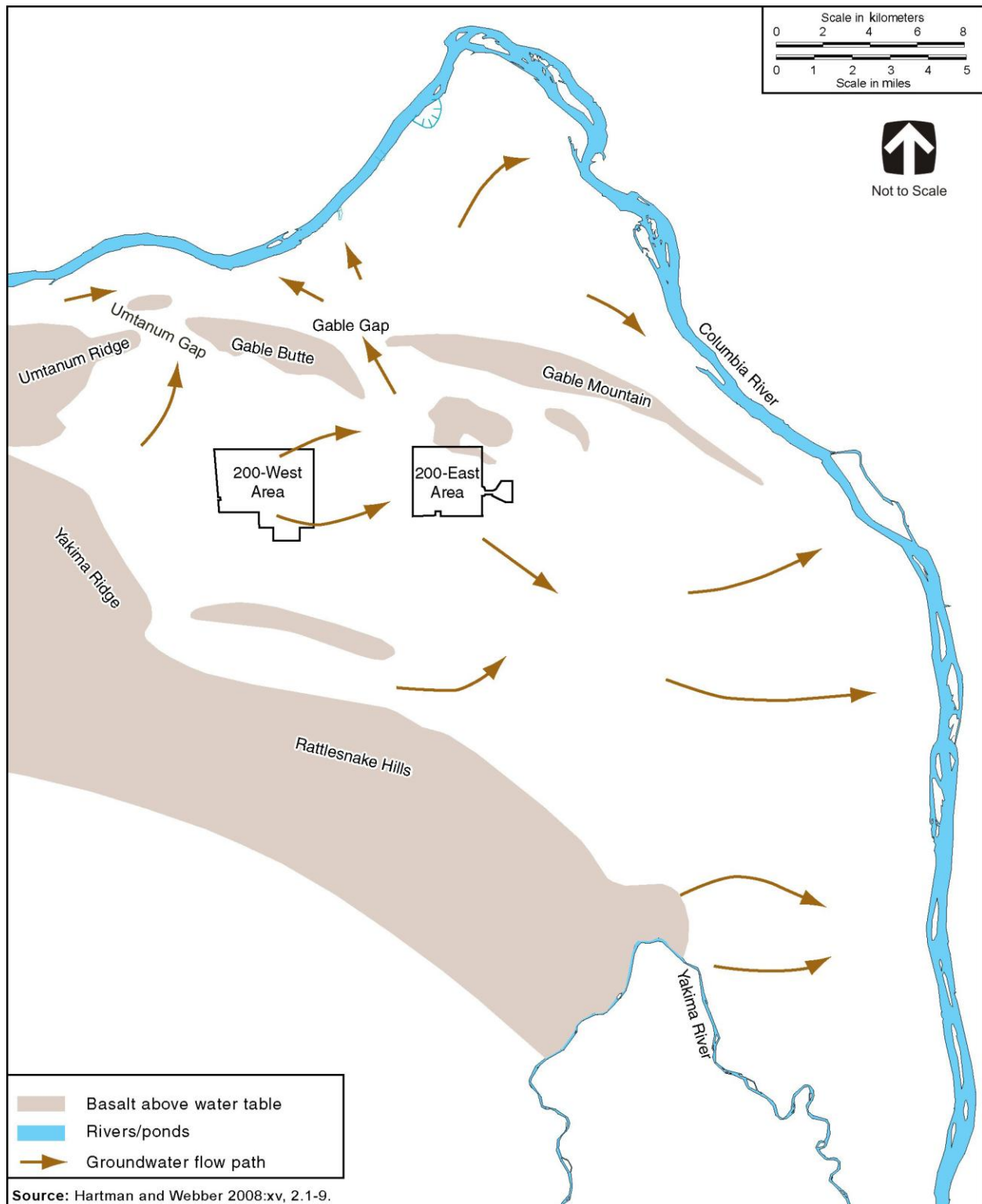


Figure L-2. Groundwater Flow at the Hanford Site

L.1.5 Summary of the *Draft TC & WM EIS* Groundwater Flow Model Results

The primary metric used to judge the acceptability of the groundwater flow model is the hydraulic head root mean square (RMS) error. RMS error is the result of a comparison of simulated hydraulic heads across the site and over time with the field-observed hydraulic heads at those same locations and times. The differences, or residuals, for all times and all locations are aggregated into a single RMS error for the groundwater flow model. For the *Draft TC & WM EIS* groundwater flow model, this error is between 2 and 3 meters (6.6 and 9.8 feet). The model residuals are reasonably well distributed with no obvious temporal or spatial biases (see the *Draft TC & WM EIS*, Appendix L, Section L.10.1).

As discussed in Section L.1.4 and shown in Figure L-2, groundwater flow across Hanford is generally from west to east, with some flow to the north through Gable Gap and Umtanum Gap. Additionally, it was hypothesized that adjusting the TOB surface cutoff elevation in Gable Gap within the uncertainty of the TOB well-boring log data may influence whether or not groundwater flows through Gable Gap. To test this hypothesis, the *Draft TC & WM EIS* included analysis of a flow model design variant (Alternate Case flow model). This model adjusted the TOB cutoff elevation in Gable Gap downward by 3 meters (9.8 feet) relative to the Base Case model. This lower cutoff elevation is the lowest reasonable elevation at which the cutoff can be expected based on the uncertainty in the available data. The results of the Alternate Case flow model evaluation in the *Draft TC & WM EIS* showed that although flow through Gable Gap can be affected by changes to the TOB cutoff elevation in this region, this cutoff elevation does not exclusively control flow direction. The analysis also showed that variations within the uncertainty of hydraulic conductivity values of the suprabasalt sediments have an influence on flow direction. Further, models with different cutoff elevations in Gable Gap could behave similarly during the historical timeframe with respect to their easterly versus northerly flow behavior yet diverge in the long-term future. This conclusion is supported by concentration-versus-time curves and concentration maps for a variety of contaminants as presented in Appendix O of the *Draft TC & WM EIS*. In summary, the *Draft TC & WM EIS* analysis of the uncertainty in the TOB cutoff elevation in the Gable Gap region found that this uncertainty does not affect the important features of the predicted flow field.

All contaminants of potential concern that were released to groundwater, as determined by the STOMP (vadose zone) analysis were analyzed for groundwater transport. Representative results of this groundwater transport analysis are published in the *Draft TC & WM EIS*. As with all modeling efforts, the modeled results vary from observations in the field. Figures L-3, L-4, and L-5 compare the *Draft TC & WM EIS* modeled contaminant plumes (2005) with the subsequent (2007) field-observed contaminant plumes for hydrogen-3 (tritium), technetium-99, and iodine-129, respectively. These figures are modified from isopleths produced in the *Draft TC & WM EIS*. The dark-green shading in the figures represents areas with higher modeled contaminant concentrations; the light-green shading, lower modeled contaminant concentrations. The beige lines representing the field-observed contaminant plumes from the 2007 Groundwater Monitoring Report (Hartman and Webber 2008) are included for comparison specifically with the areas of higher contaminant concentration (the dark-green areas). The comparisons show that, in terms of their modeled angles and extents, the modeled plumes vary from the field-observed plumes. Analysis of these variances shows that the modeled plumes could be made to more closely match field observations by making an eastward adjustment to the line where lower-conductivity sediments in the west transition to higher-conductivity sediments in the east. The red and blue lines running from the northwest to the southeast in each figure are schematic representations of changes made to the hydraulic conductivity zones in the *Final TC & WM EIS* groundwater flow model.

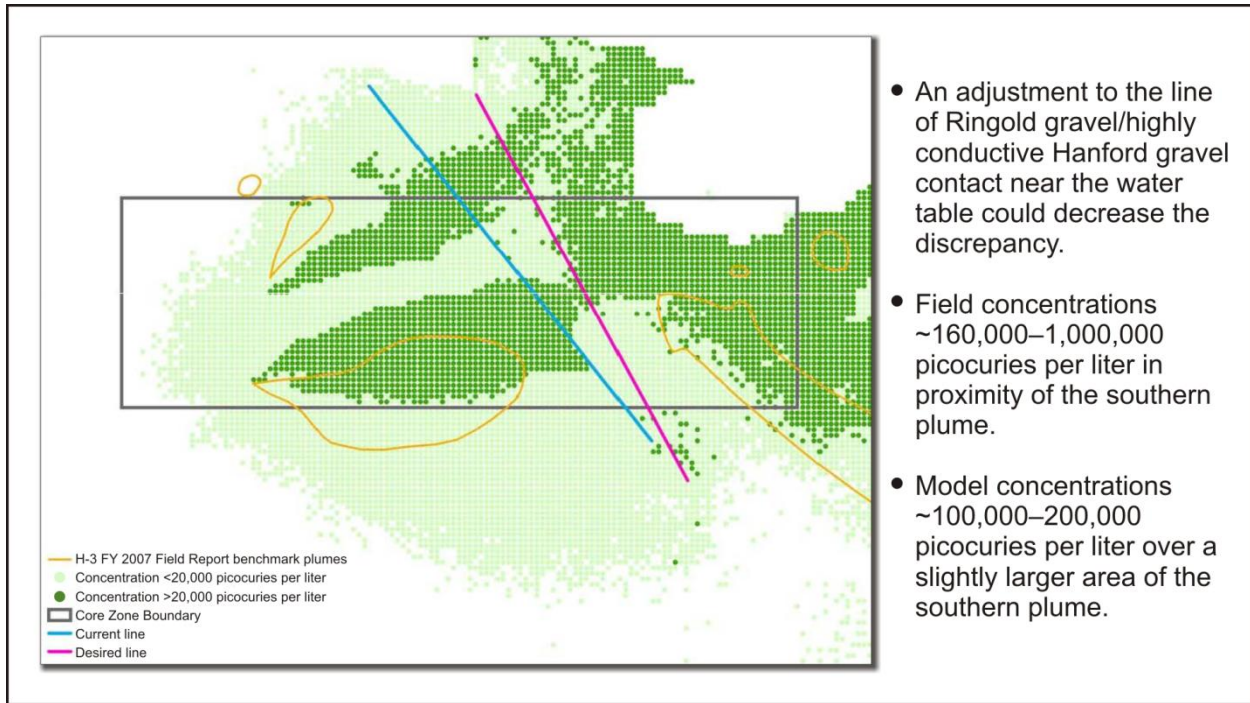


Figure L-3. Comparison of Draft TC & WM EIS Modeled Tritium Plumes to Field Observations in the 200-West Area

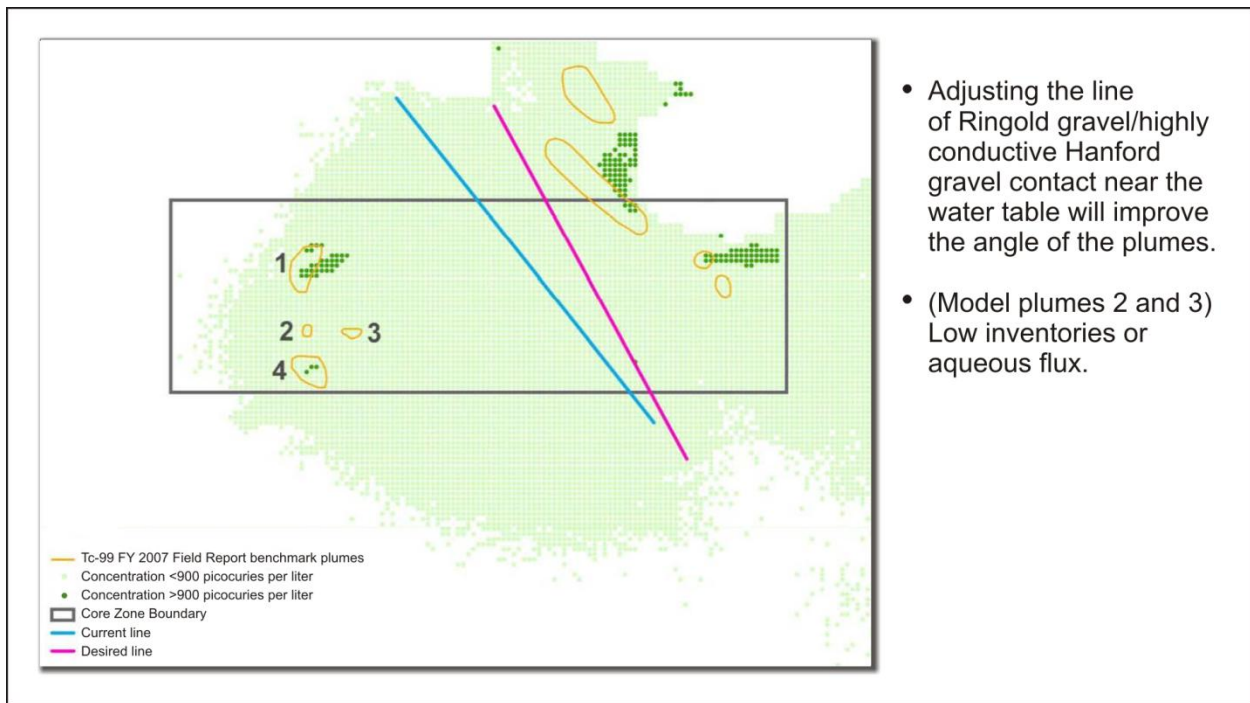


Figure L-4. Comparison of Draft TC & WM EIS Modeled Technetium-99 Plumes to Field Observations in the Core Zone

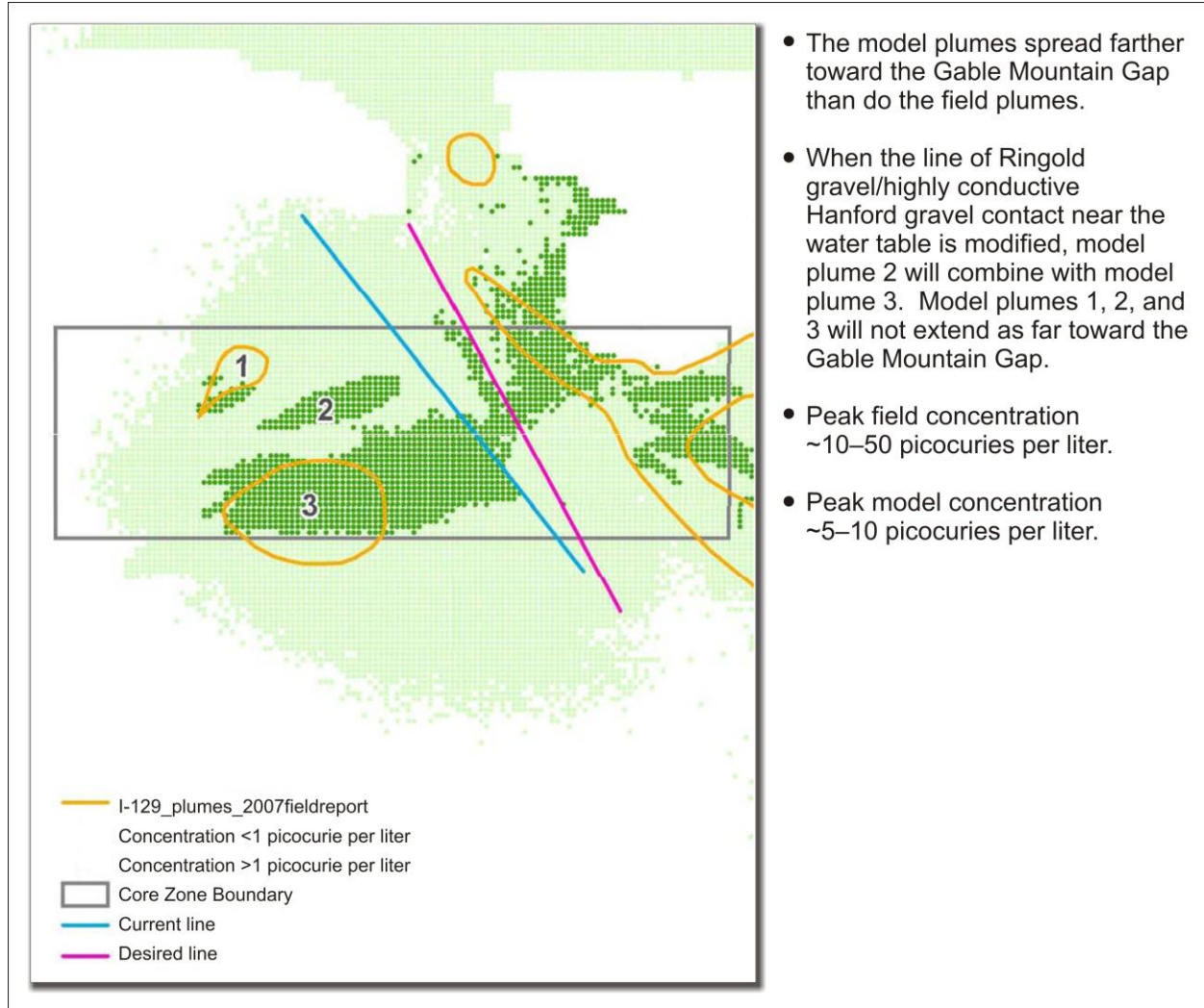


Figure L-5. Comparison of Draft TC & WM EIS Modeled Iodine-129 Plumes to Field Observations in the Core Zone

L.1.6 Significant Changes from the Draft TC & WM EIS to This Final TC & WM EIS

The groundwater flow model used to complete the analysis met the calibration acceptance criteria as described in the *Draft TC & WM EIS*, Appendix L, Table L-19. However, as described in the preceding section, the simulation of contaminant plumes could be improved by moving eastward the line that separates the lower-conductivity sediments in the west from the higher-conductivity sediments in the east. Figure L-6 shows the *Draft TC & WM EIS* model's hydraulic conductivity zones at model layer 11 (120 to 121 meters [394 to 397 feet] above mean sea level [MSL]); Figure L-7 shows the *Final TC & WM EIS* model's hydraulic conductivity zones at this same layer. A black line has been added to each figure to highlight the separation of the zones of lower hydraulic conductivity in the west from the zones of higher hydraulic conductivity in the east. Note that this black line is moved eastward in the *Final TC & WM EIS* model. This change in the hydraulic conductivity zones between the draft and this final environmental impact statements (EISs) is within the uncertainty of the interpretations made using the available borehole log data (CHPRC 2009b, 2010; Ecology 2003).

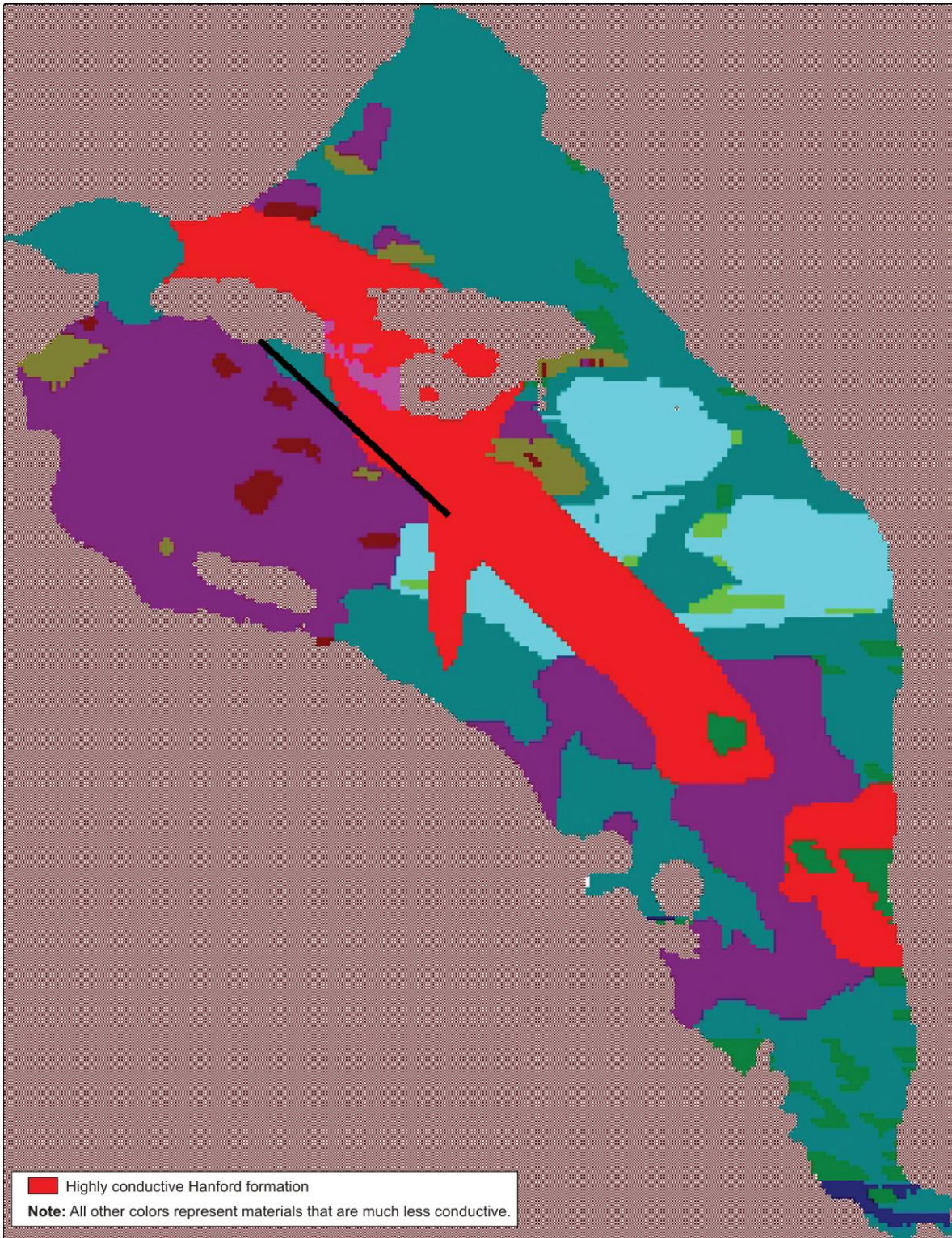


Figure L-6. Draft TC & WM EIS Flow Model Conductivity Zones – Layer 11 (120–121 meters above mean sea level)

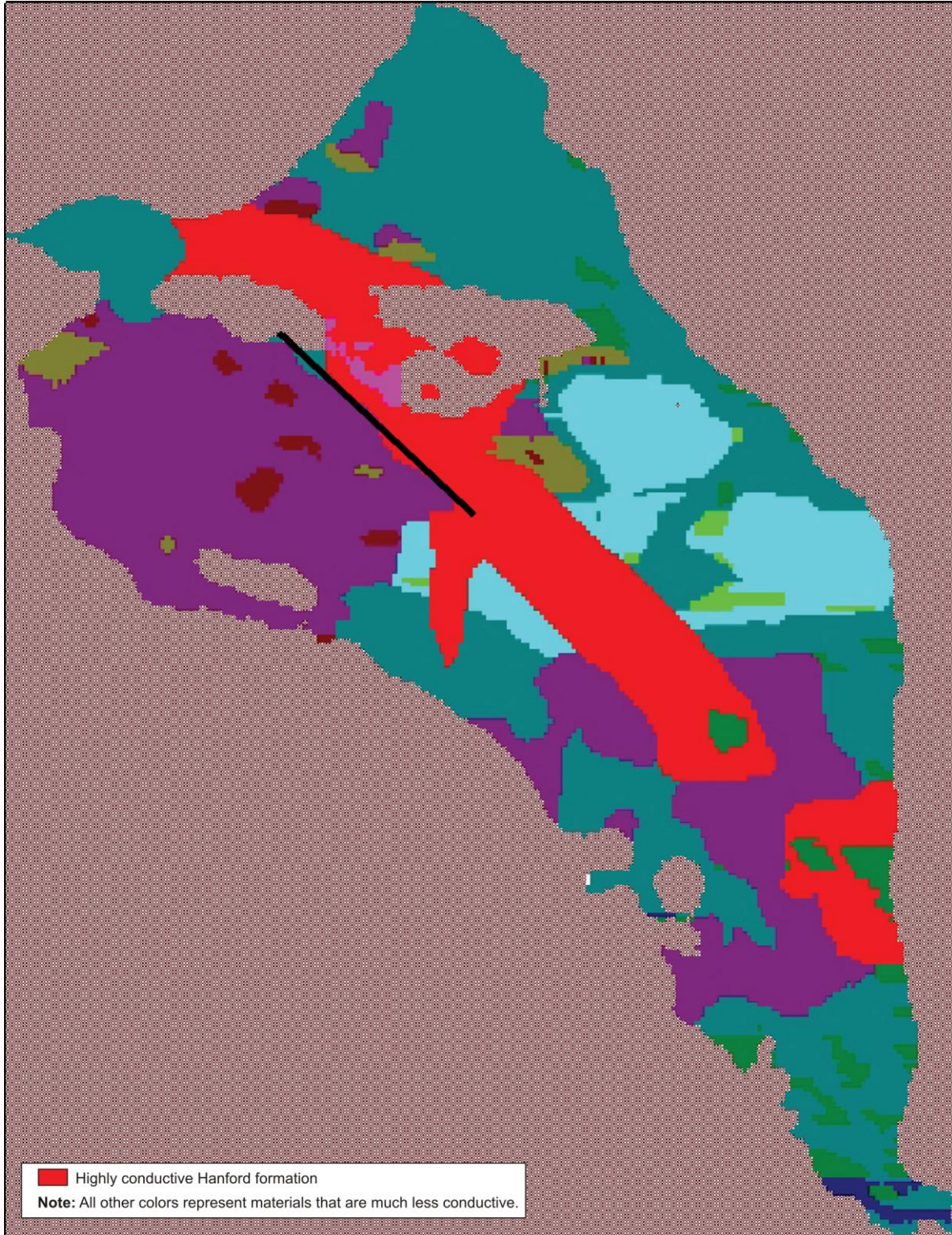


Figure L-7. Final TC & WM EIS Flow Model Conductivity Zones – Layer 11 (120–121 meters above mean sea level)

The other changes made to the *Draft TC & WM EIS* groundwater flow model include an update to the head observation data set and a change to the methodology used to process this updated data set for use in the *Final TC & WM EIS* groundwater flow model. The update to the data set included all quality-assurance-complete head observation records available as of December 2008. The head observation data set used in the *Draft TC & WM EIS* included head data available as of August 2006. In addition to updating the head data set, this *Final TC & WM EIS* used a different methodology for processing the data. In the *Draft TC & WM EIS*, the available data were partitioned into three calibration data sets and one validation data set. This methodology is described in the *Draft TC & WM EIS*, Appendix L, Section L.6.1. For this *Final TC & WM EIS*, a single data set was used for calibration. Since the data were not divided as they were for the *Draft TC & WM EIS*, more data points are present in this *Final TC & WM EIS* than were included in the *Draft TC & WM EIS*. This change in methodology tests the robustness of the data set by grouping it differently and checking to see if it produces a significantly different calibration error. The RMS error for the *Final TC & WM EIS* groundwater model, using this larger calibration data set, is between 2 and 3 meters (6.6 and 9.8 feet)—about the same as the RMS error for the *Draft TC & WM EIS* groundwater model.

Although not a significant change, Visual MODFLOW [modular three-dimensional finite-difference groundwater flow model], the graphic interface used to run MODFLOW 2000, was updated from Version 4.2 to Version 2009.1 (SWS 2009). Also not significant, the number of time steps used to solve the first stress period in the flow model was changed from 5 to 100. This time-stepping change was required because the model's conductivity zones were changed slightly from those used in the *Draft TC & WM EIS* groundwater model, as described above; however, no change was made to the initial head distribution. Therefore, additional time steps were needed to solve the first stress period in the simulation.

The following parameters/settings are unchanged in the *Final TC & WM EIS* groundwater flow model:

- Columbia River and Yakima River boundaries
- Background (natural) and anthropogenic recharge boundaries
- Generalized head boundaries (GHBs)
- Basalt surface boundary
- Horizontal and vertical model extents, including gridding
- Material properties
- Initial head distribution
- Rewetting methods
- Numerical engine and parameterization

Appendix O, Section O.2, contains a discussion of the changes in the groundwater transport model between the *Draft TC & WM EIS* and this *Final TC & WM EIS*. The most significant changes were adjustments to the dispersivity parameters to better match plume shapes. Appendix U contains a discussion of the correspondence between the model results and field data at the regional and subregional scales in light of changes to the groundwater flow field and transport parameters. Overall, shapes and extents of plumes originating in the eastern part of the Core Zone are in good agreement with field data. Groundwater velocities may be slightly too high for plumes originating in the northeastern part of the 200-West Area. These results are qualitatively similar to those of the *Draft TC & WM EIS*. Section L.8 contains a discussion of the uncertainty in the calibration, particularly with respect to the amount of flow north through Gable Gap and the effect on predicted technetium-99 concentrations versus time for Tank Closure Alternative 2B and Waste Management Alternative 2, Disposal Group 1, Subgroup 1-A. These results demonstrate that the differences in long-term groundwater impacts among the alternatives are discernible in light of the uncertainties in the calibration.

L.2 GROUNDWATER FLOW CONCEPTUAL MODEL

Figure L-8 provides a representation of the Hanford conceptual groundwater flow model. Water enters the region from the highlands in the west and the Yakima River in the south, and discharges into the Columbia River to the north and east. As modeled, aqueous recharge from anthropogenic and natural sources enters from the surface, and the basement is bounded by impermeable basalt. The geologic materials within the vertical and horizontal extents of the model consist of cataclysmic and quiescent deposits of well to poorly sorted sediments, resulting in highly variable hydraulic conductivity zones across the region.

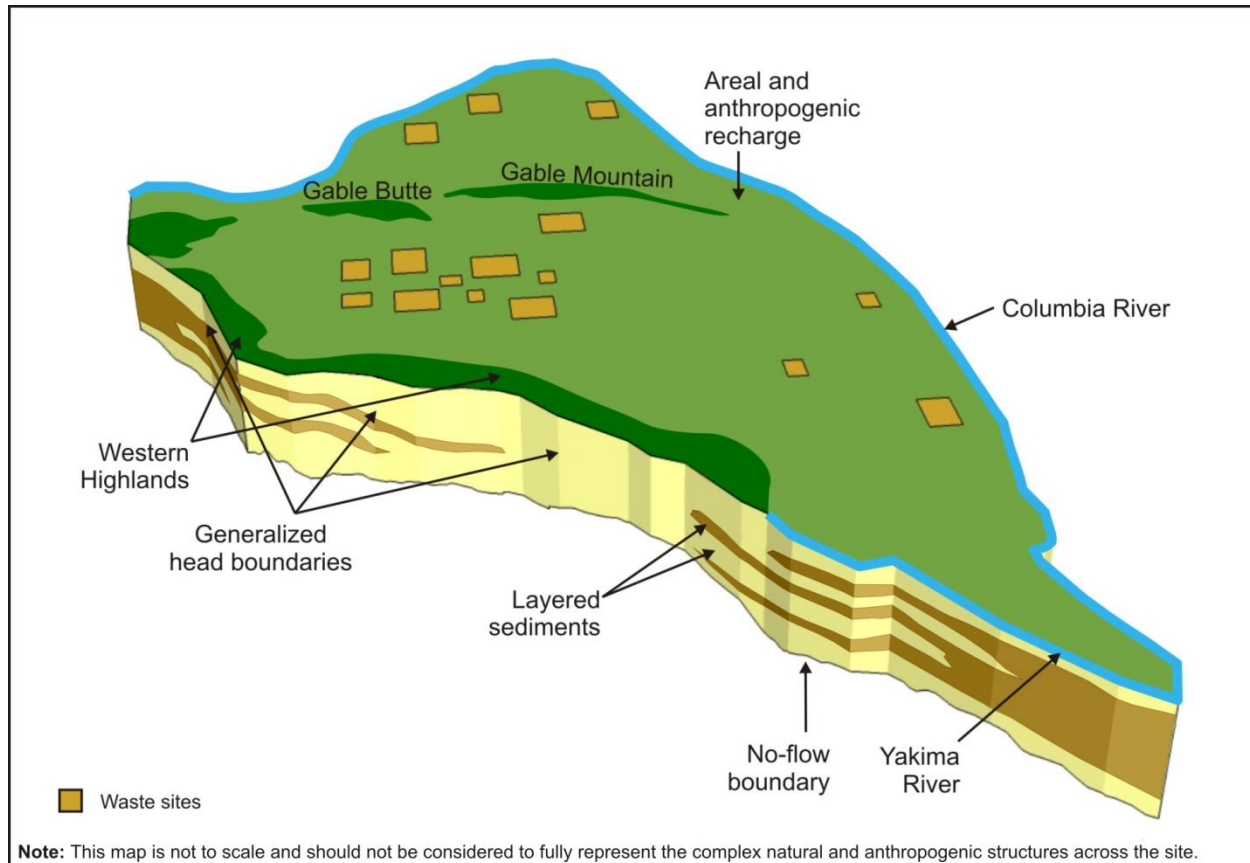


Figure L-8. Hanford Site Conceptual Groundwater Flow Model

L.2.1 Site Geometry

The Hanford groundwater flow model covers an area of approximately 152,000 hectares (375,000 acres). The Columbia River bounds the region to the north and east, stretching approximately 80 kilometers (50 miles) along the Hanford border. The Yakima River and western highlands border the region to the south and west.

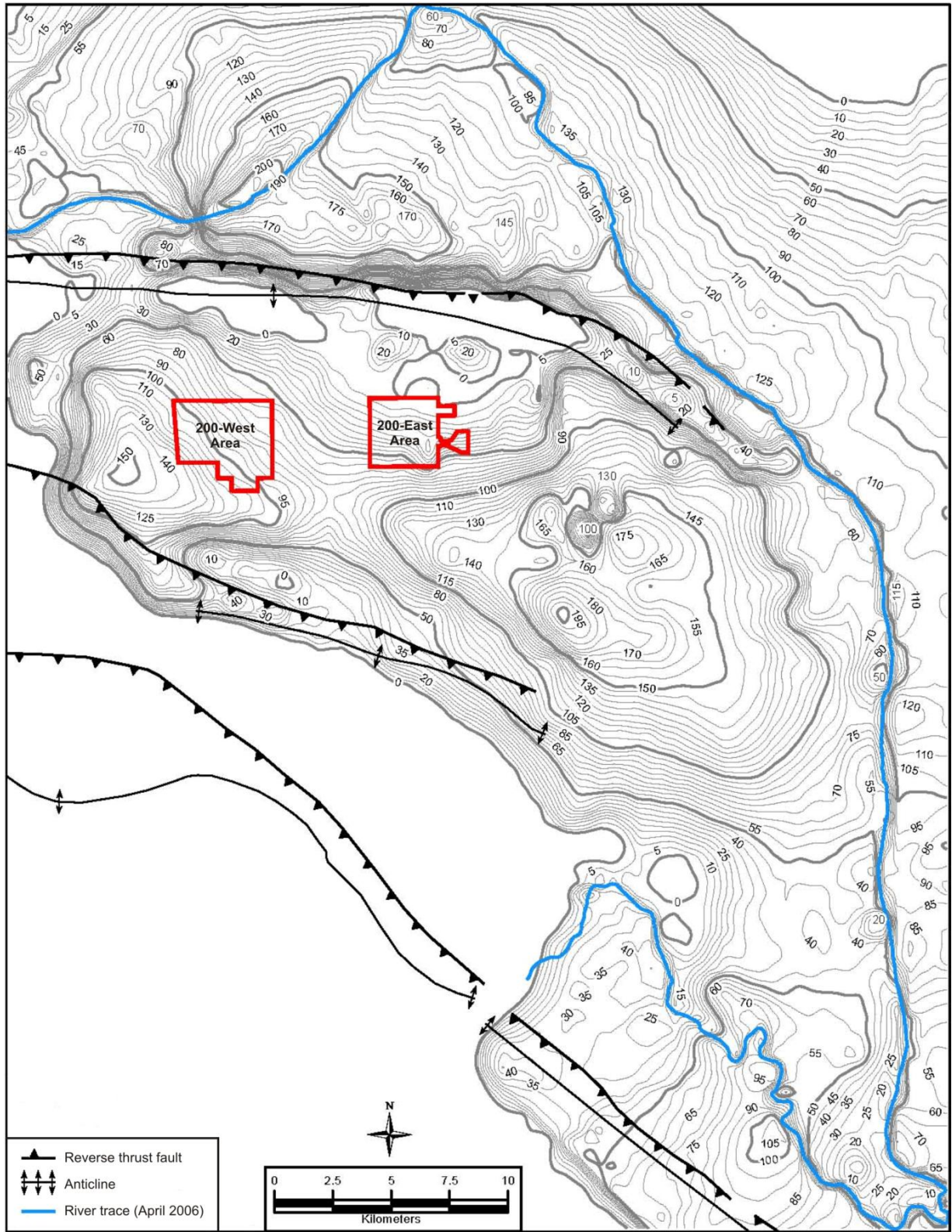
The hydrogeologic boundaries of the site include the Columbia River to the north and east, the Yakima River to the south, and western highlands of outcropping basalt above the water table along the Rattlesnake, Yakima, and Umtanum ridgelines. The highlands along the western boundary of the model domain are basalt outcrops above the water table and provide sources of groundwater flux into the model domain from ephemeral surface-water runoff, underground streams, and agricultural activities in these areas. The Columbia River is a groundwater sink, providing the location of eventual discharge for all

water entering the model domain. The Yakima River, due to its higher elevation and proximity to the Columbia River, is a source of water influx to the model.

The top of the aquifer is a phreatic surface bounded by highlands to the south and west and the Columbia River to the north and east. The site's water table is higher and steeper in the west, with hydraulic heads ranging between 125 and 160 meters (410 and 525 feet) above MSL. The water table gradient in this part of the site is the result of materials with low hydraulic conductivity. Horizontal hydraulic conductivities in the west range from less than 1 to around 20 meters (66 feet) per day. Highly conductive material zones in the central region of the site from Gable Gap through the eastern part of the 200-East Area, then south and east for several kilometers, result in an essentially flat water table in this area. Hydraulic heads here range between 120 and 122 meters (394 and 400 feet) above MSL. Horizontal hydraulic conductivity values in this region are around 4,000 meters (13,124 feet) per day. Moderately conductive material zones are typical of the northern, eastern, and southern portions of the site, resulting in a more gently sloping water table as groundwater moves to the Columbia River. Hydraulic heads in these regions range from 104 and 122 meters (341 and 400 feet) above MSL. Horizontal hydraulic conductivity values in these areas are less than 200 meters (656 feet) per day. Hydraulic heads in areas near the Columbia River are heavily influenced by its river stage, which is conceptualized as a constant head that ranges from 122 meters (400 feet) above MSL in the northwest to 104 meters (341 feet) above MSL in the southeast.

The aquifer thickness across the region ranges from 0 meters in areas where basalt is above the water table to as much as 180 meters (591 feet) due to the highly irregular topology of the TOB across the region. The areas where basalt is above the water table include the highlands along the western boundary and areas on and around Gable Mountain and Gable Butte. Gable Gap, the area between Gable Mountain and Gable Butte, has an uncertain TOB elevation, but data suggest that its elevation is near the water table and, therefore, the aquifer thickness here is estimated to be about 1 meter (3.3 feet) at its shallowest. North of Gable Mountain and Gable Butte the aquifer thicknesses reach up to 180 meters (591 feet). In the western region between Gable Gap and the western highlands the aquifer thicknesses approach 160 meters (525 feet), in part due to the higher water table in the west. The region southeast of Gable Gap, between the 200 Areas and the Columbia River, has aquifer thickness up to 200 meters (656 feet). Figure L-9 provides a graphic representation of the aquifer thickness across the region. This highly variable aquifer thickness is primarily due to the highly variable basalt surface in the region.

The basalt bounding the bottom of the aquifer is conceptualized as an impermeable layer. This basalt surface is highest along the western highlands, reaching elevations up to 1,000 meters (3,281 feet) above MSL. North and east of these highlands, the TOB dips to elevations as low as 80 meters (262 feet) below MSL, then rises again at Gable Mountain and Gable Butte to elevations up to around 200 meters (656 feet) above MSL. North of Gable Mountain and Gable Butte the basalt surface drops off abruptly, again reaching elevations as low as 60 meters (197 feet) below MSL. Figure L-10 provides a graphic representation of the basalt surface across the region.



Note: Contour units are in meters.

Figure L-9. Representation of Aquifer Thickness (meters) Across the Hanford Site

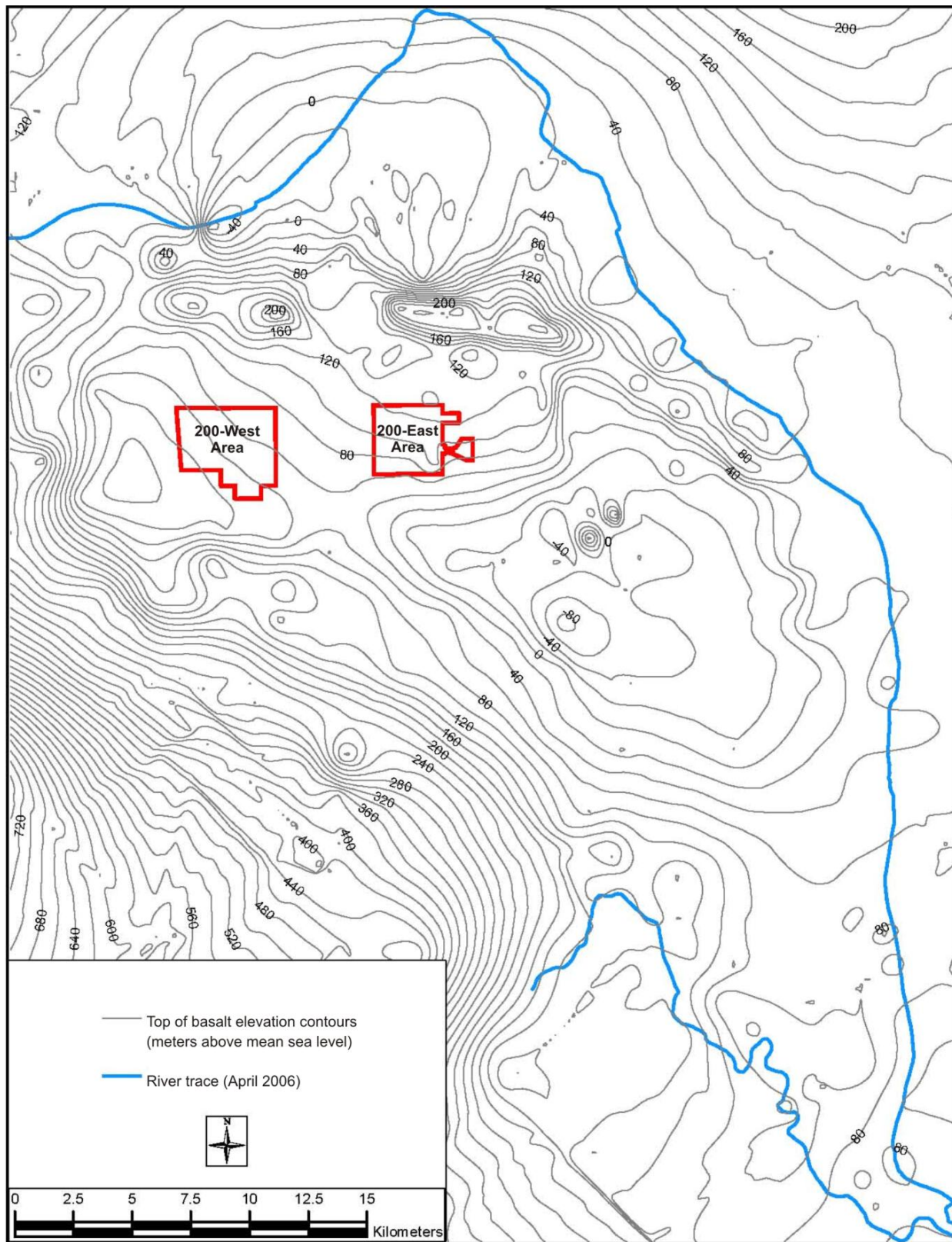


Figure L-10. Representation of the Basalt Surface Across the Hanford Site

L.2.2 Boundary Conditions

Water moves into the groundwater from the western and southern portions of the region, including Cold Creek Valley, Dry Creek Valley, Rattlesnake Mountain (runoff), and the Yakima River. Water also enters the model through natural and anthropogenic recharge to the ground surface. Water exits the model at the Columbia River, which bounds the model on its northern and eastern sides. Evapotranspiration is not explicitly modeled, but is taken into account as part of the natural areal recharge boundary condition.

Cold Creek Valley, Dry Creek Valley, and Rattlesnake Mountain runoff are modeled as GHB inputs to the model. Conceptually, a GHB represents a reservoir of water at a constant hydraulic head at some distance outside the model domain with a hydraulic conduction to the regional aquifer being modeled. GHBs allow water to move into and out of the modeled domain depending upon the difference between the time-varying hydraulic heads simulated inside the model and the constant heads at these simulated reservoirs outside the model.

The Yakima River and Columbia River are both modeled as constant hydraulic heads that vary with the elevation of the rivers. The Columbia River is a gaining stream, and it acts in the model as a groundwater sink, drawing water out of the model and forcing hydraulic heads in nearby modeled areas to be near its constant head value. Due to the Yakima River's elevation relative to the Columbia River, the Yakima River is a losing stream that acts in the model as a groundwater source.

Basalt, conceptualized and modeled as impermeable, bounds the bottom of the model. The TOB is a complex surface of variable depth that outcrops above the water table at the western and southern boundaries of the model and again rises above the water table in the Gable Mountain and Gable Butte area. Otherwise, basalt is generally below the water table and provides an impermeable surface through which water is not allowed to enter or exit the model.

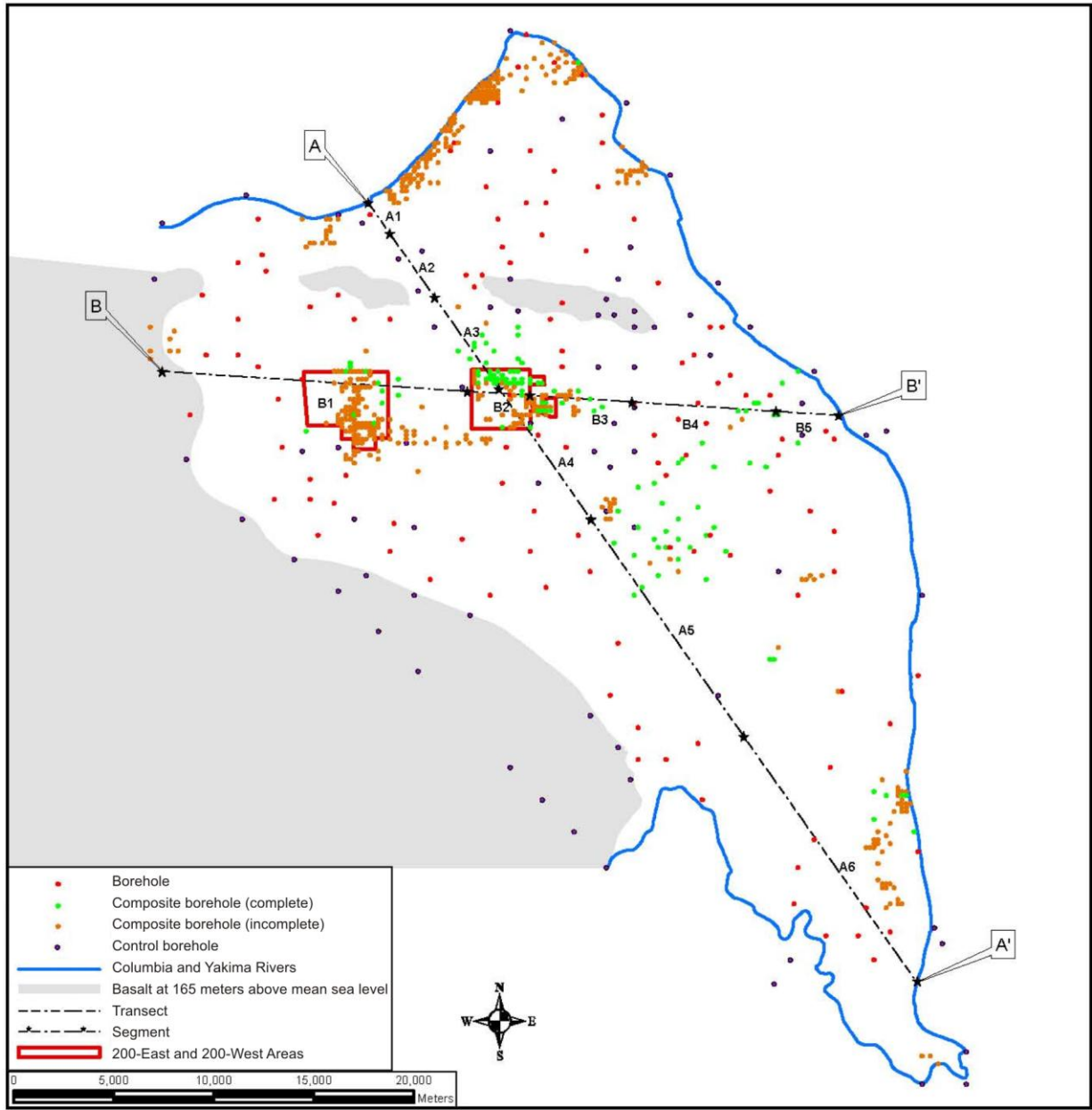
The top of the model is open to the atmosphere and subject to natural recharge (precipitation) and anthropogenic recharge. Anthropogenic recharge has been applied both at the ground surface and directly to the aquifer as a result of planned and unplanned releases at Hanford during the operational period. Significant anthropogenic water extractions from the aquifer are also modeled. In the model, all recharge is applied directly to the top of the aquifer. No vadose zone attenuation is considered.

Groundwater pump-and-treat activities are not considered in the *TC & WM EIS* groundwater model. The planned duration of these activities is short (DOE 2010) compared with the *TC & WM EIS* 10,000-year period of analysis. In addition, the final configuration of the groundwater pump-and-treat system was not established prior to the *Final TC & WM EIS* data cutoff date. Appendix U does contain a mass-removal sensitivity analysis illustrating the changes in concentration of carbon tetrachloride resulting from various degrees of removal from the aquifer system.

L.2.3 Geologic Materials

Hanford is located in south-central Washington in the Pasco Basin, which is part of the Columbia Plateau. The site is located in the Yakima Fold Belt and is characterized by a series of east–west-oriented anticlinal ridges and synclinal valleys (Lindsey 1995; Reidel and Chamness 2007). The general structure of the Pasco Basin includes bedrock composed of Miocene-aged tholeiitic flood basalts that are part of the Columbia River Basalt Group overlain by sedimentary materials of the Miocene-Pliocene Ringold Formation, Cold Creek Unit (Plio-Pleistocene Unit), and the Pleistocene Hanford formation. The basalt anticlinal structures have steeply dipping north flanks and gently dipping south flanks. In the 200 Areas located within the Hanford Central Plateau, basalt bedrock dips approximately 5 degrees to the south (Reidel and Chamness 2007).

The sedimentary materials overlying basalt bedrock form the suprabasalt aquifer system that contains the Hanford unconfined aquifer. Figure L–11 shows the locations of the geologic data points and two transects that illustrate the distribution of materials in the unconfined aquifer. The transects themselves (A-A' and B-B') are shown in Figures L–12 and L–13 at a vertical exaggeration of 5:1. The Ringold Formation, the oldest of the suprabasalt sediments deposited on top of the Columbia River Basalt Group, represents fluvial and lacustrine materials of the migrating, ancestral Columbia River and its tributaries (Reidel et al. 2006). Ringold material types range from coarser gravel and sand deposited in former river channels to finer overbank deposits of silt and mud that formed during periods of quiescence. Felsic minerals such as quartz and feldspar typically dominate Ringold sediments, and the sediment texture varies from moderately well- to well-sorted. The Hanford unconfined aquifer is found in Ringold sediments predominantly in the western and southern portions of Hanford west of the 200-East Area, and also to the north along the Columbia River near the 100-K, 100-N, and 100-D Areas.



Note: To convert meters to feet, multiply by 3.281.

Figure L-11. Geologic Materials – Borehole and Transect Locations

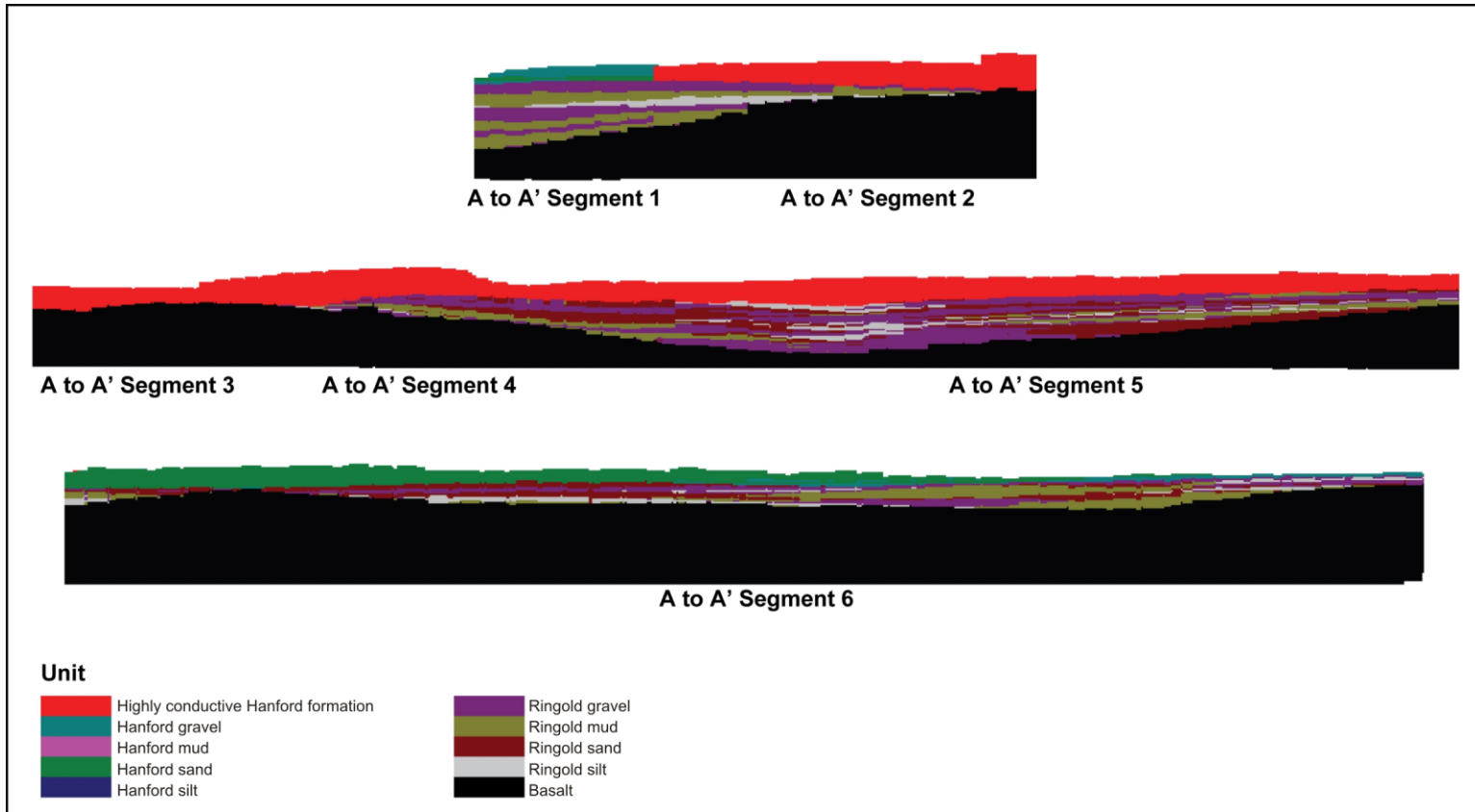


Figure L-12. Geologic Materials – Transect A-A'

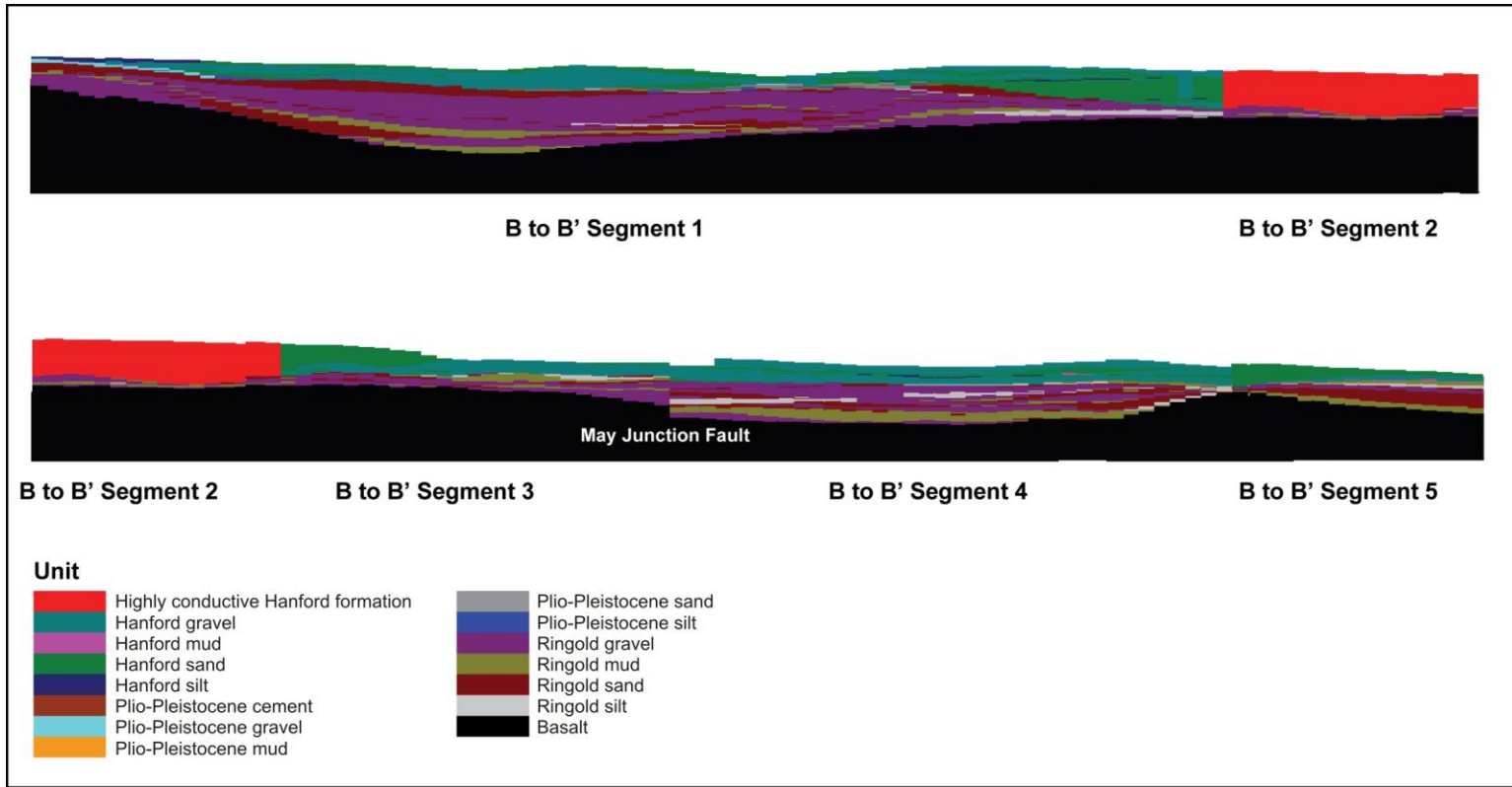
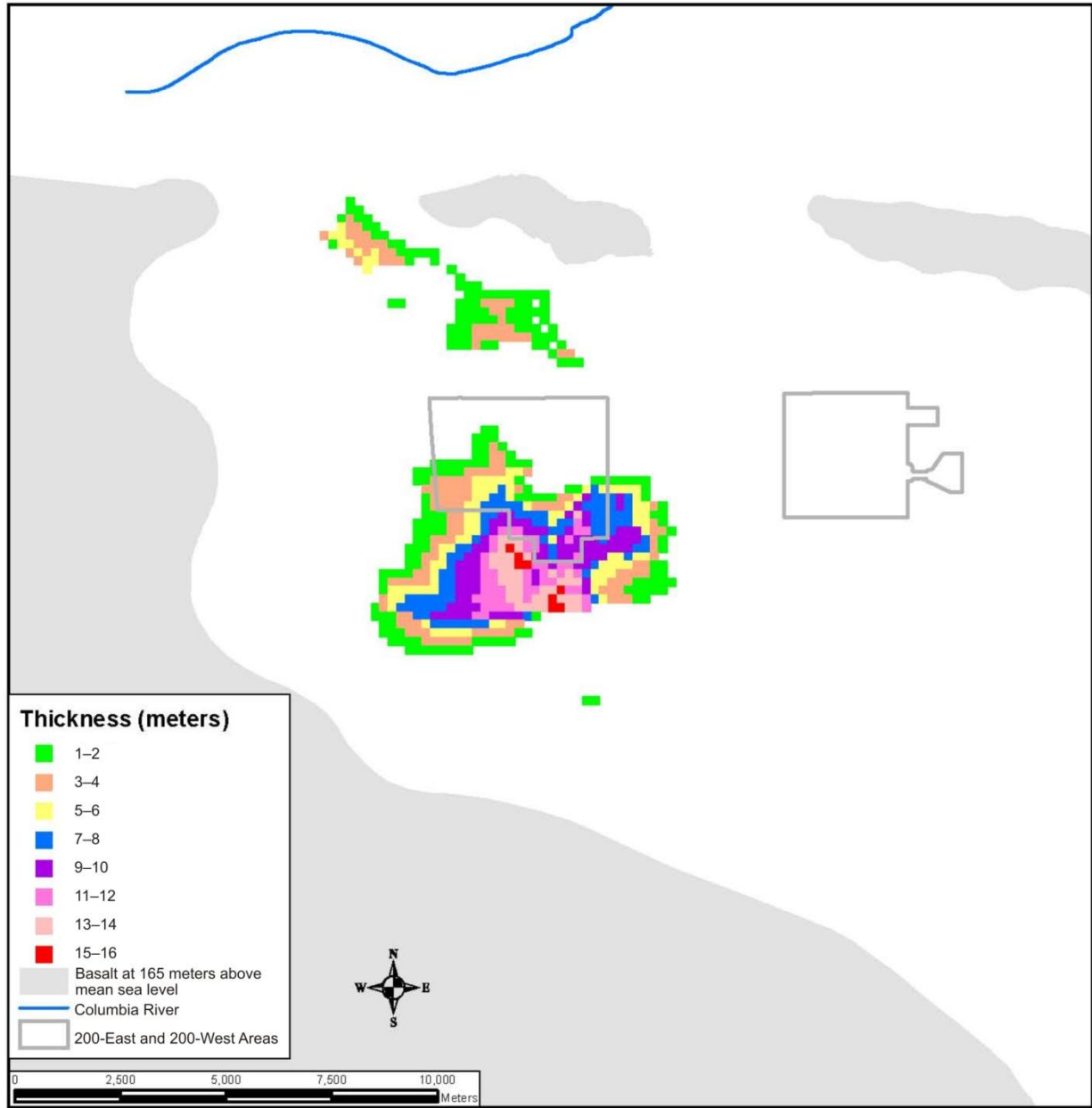


Figure L-13. Geologic Materials – Transect B–B'

The Hanford formation consists of glaciofluvial sediments resulting from high-energy cataclysmic flood events during the Pleistocene period from glacial Lake Missoula (Bjornstad and Lanigan 2007; Lindsey 1995; Serne et al. 2010). Hanford sediments tend to be dominated by mafic basaltic minerals rather than the felsic counterparts characterizing Ringold sediments and generally are poorly sorted to moderately well sorted. Hanford formation sediments are typically sand- or gravel-dominated and constitute most of the vadose zone on Hanford (Bjornstad and Lanigan 2007). Hanford formation sediments also constitute much of the saturated zone in the northern and eastern portions of Hanford.

The Cold Creek Unit represents fluvial and eolian sediments deposited during the late Pliocene to early Pleistocene period (Bjornstad and Lanigan 2007) between the Hanford formation and Ringold Formation. The Cold Creek Unit was deposited after the period of Columbia River incision that resulted in the deposition of the Ringold Formation and before the Pleistocene Missoula floods that deposited the Hanford formation (Reidel and Chamness 2007). The Cold Creek Unit in the 200-West Area is dominated by carbonate-rich paleosols and fine-grained sediments that represent eolian and flood materials found in the vadose zone. These sediments are also referred to as the “Plio-Pleistocene Unit” (e.g., Lindsey 1995). The spatial distribution of these fine-grained sediments in the 200-West Area below elevation 165 meters (541 feet) above MSL is shown in Figure L–14. Coarser Cold Creek gravels and sand, also referred to as “pre-Missoula gravels,” are the dominant material type at the water table across much of the east-central part of Hanford.

The contrast in the paleoenvironments responsible for the sedimentary deposition of materials ranging from boulders to mud results in a wide range of hydraulic properties across Hanford that span many orders of magnitude and are variable locally and regionally. The distribution of sediments at the water table interface is shown in Figure L–15. Higher hydraulic conductivities have been measured for the coarser gravel and sand materials relative to the lower-conductivity silt and mud lithologies. Typically, Hanford formation materials have much higher conductivities than either the Ringold Formation or Cold Creek Unit materials (Bjornstad et al. 2010; Thorne et al. 2006). The hydraulic conductivity of the three-dimensional mosaic of Hanford sediments and their spatial distribution is a major factor controlling the vertical moisture movement and contaminant transport in the vadose zone and the horizontal groundwater flow and contaminant transport in the saturated zone.



Note: To convert meters to feet, multiply by 3.281.

Figure L-14. Geologic Materials – Plio-Pleistocene Isopach Map

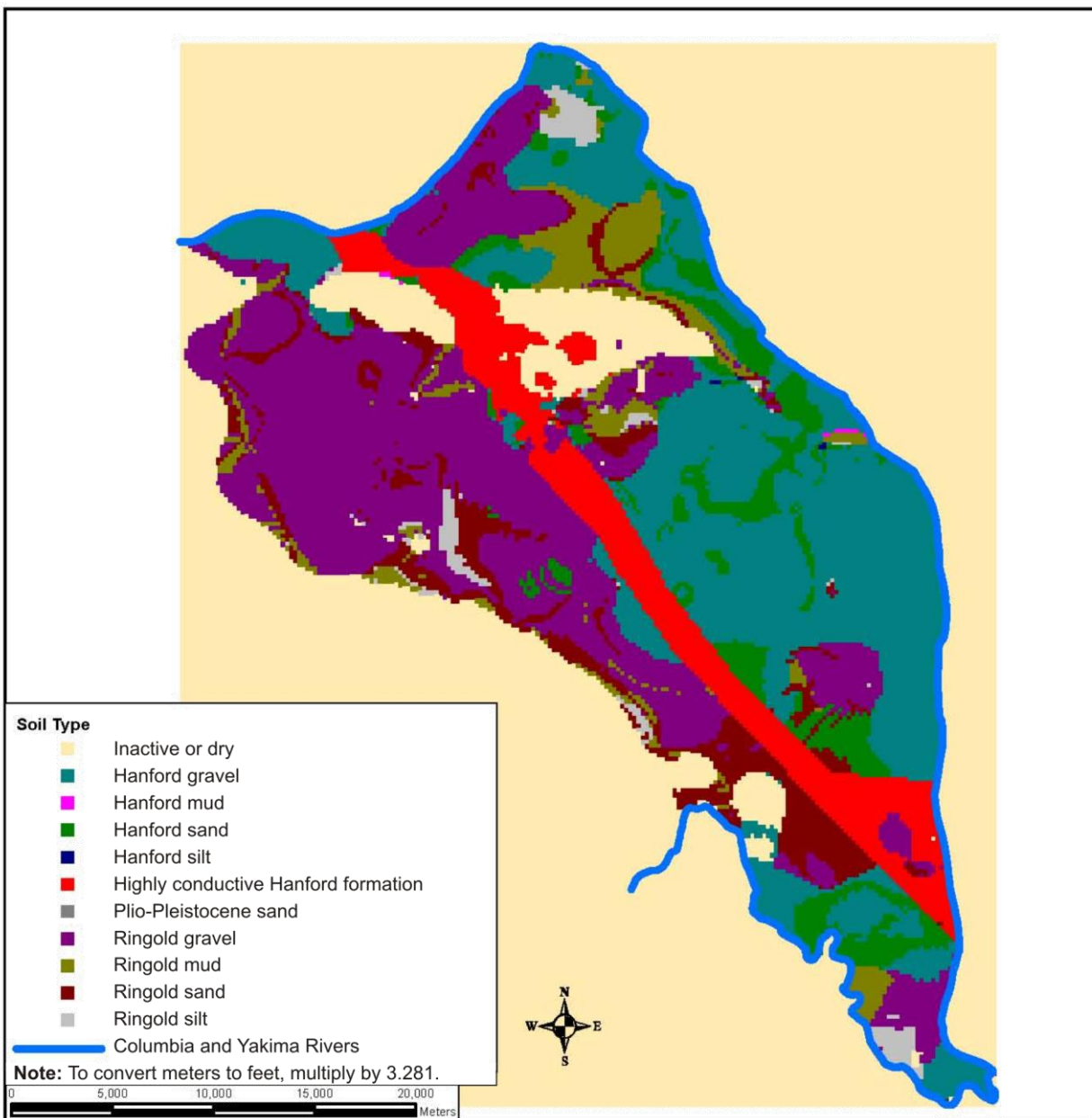


Figure L-15. Geologic Materials – Distribution of Sediments at the Water Table

L.2.4 Conclusion

The conceptual groundwater flow model was developed to solve the multidimensional problem of simulating groundwater elevations and movement over time across Hanford. Determining groundwater elevations and movement includes calculating the head, direction, and magnitude of groundwater at every location within the modeled domain consistent with the model’s gridding structure. Calculations for these heads, directions, and magnitudes were based on the site geometry, the site boundary conditions, and the site geology as described in the preceding paragraphs. The following section describes the implementation of these concepts into the Hanford groundwater flow model.

L.3 MODEL DEVELOPMENT FRAMEWORK

The *TC & WM EIS* groundwater flow model simulates the time-varying spatial distribution of the rate and direction of water movement in the unconfined aquifer. Groundwater flow through the unconfined aquifer is simulated using the U.S. Geological Survey (USGS) MODFLOW 2000 Engine, Version 1.15.00 (USGS 2004). The commercial version used in this *TC & WM EIS* is Visual MODFLOW, Version 2009.1 (SWS 2009). The resulting time-varying groundwater flow field is then used to simulate the transport of contaminants from their points of contact with the groundwater at various times in the history of the site to various receptor locations, including the Columbia River (see Appendix O).

The *TC & WM EIS* groundwater flow model was built using the best-available information for Hanford. The development of the groundwater flow model was based, in part, on the Site-Wide Groundwater Model (e.g., Thorne et al. 2006), when features of the work were adequately documented, traceable, and independently verifiable. Previously compiled site data were used when they could be traced to a source and were judged to be adequate. When compiled site data were unavailable or inadequate for the development methodology used, historical primary data were obtained and processed for use or additional data were collected. Published conceptualizations informed some modeling decisions when neither compiled site data nor historical primary data were available for direct use or as input to associated models. When the above sources did not provide the necessary information, the required inputs were derived through engineering judgment or became model calibration parameters. MODFLOW groundwater flow model inputs derived both directly and indirectly from site data and knowledge are described in Section L.4. Model calibration and uncertainty data are described in Section L.7.

The *Draft TC & WM EIS* MODFLOW groundwater flow model was developed in an incremental fashion, proceeding through a preliminary two-layer, steady-state realization to the final transient, multilayered, calibrated, and parameterized model. This appendix presents the *Final TC & WM EIS* flow model, updated as described in Section L.1.6, describing the technical bases for model modifications as well as the calibration and uncertainty analysis (see Section L.7).

L.3.1 MODFLOW 2000

Per direction from the DOE Office of River Protection, the numeric engine selected for simulating groundwater flow was MODFLOW 2000, Version 1.15.00 (USGS 2004). A numeric engine performs the calculations to solve the equations describing water flow through the unconfined aquifer. MODFLOW 2000, a modular three-dimensional finite-difference groundwater flow model, describes the flow of groundwater into and out of every active finite model cell for each discrete time step and along all three dimensions: two horizontal and the vertical.

L.3.2 Visual MODFLOW

Per direction from the DOE Office of River Protection, the MODFLOW interface software selected for this *TC & WM EIS* was Visual MODFLOW, Version 2009.1 (SWS 2009), a product that supports MODFLOW 2000 by providing tools for data input, model control, and presentation of model output. The MODFLOW 2000 numerical engine and its parameter settings in Visual MODFLOW, Version 2009.1, are discussed further in Section L.5.

L.4 MODEL INPUTS – CONCEPTUALIZATION, CHARACTERIZATION, AND ENCODING

This section describes the model inputs for defining the model grid design, cell properties, and flow boundary conditions. The encoding of these features of the *TC & WM EIS* groundwater flow model captures a conceptualization of the unconfined aquifer, its geomorphology, the hydrogeostratigraphic structure of the unconsolidated sediments, and its gross water budget based on underlying principles, data, and interpretation.

L.4.1 Discretization

“Discretization” of the groundwater flow model refers to the specification of the model domain (extent) and the compartmentalization (gridding) of the model domain in three dimensions: two horizontal and the vertical. Defining the model extent and the model grid is a matter of convenience informed by model purpose and computational considerations.

L.4.1.1 Extents

The *TC & WM EIS* groundwater flow model extents are determined by the Columbia and Yakima Rivers and by the top of the uppermost layer of basalt beneath the unconfined aquifer at Hanford.

The horizontal extents of the MODFLOW groundwater flow model are defined on the north, east, and south by the Columbia and Yakima Rivers. Review of hydrographs from wells along the river and comparison with river stage showed that the Columbia River is a reasonable hydrologic boundary. Coordinates for the Columbia and Yakima Rivers within the model domain were collected offshore within 25 meters (82 feet) of the nearshore bank using a global positioning system device in April 2006. The resulting river trace is shown in Figure L–16. The model extent on the west side is arbitrarily set at easting 557000, which is west of the Hanford boundary and the basalt ridge, Rattlesnake Mountain.

The minimum vertical extent is set at 90 meters (295 feet) below MSL, based on the lowest observed TOB elevation from boring logs for Hanford boreholes (CHPRC 2009b, 2010; Ecology 2003). The deepest estimated TOB elevation is 91 meters (299 feet) below MSL, which is rounded to –90 meters (–295 feet) in the model, given the uncertainties in elevation estimates. The maximum extent in the vertical direction is set at 165 meters (541 feet) above MSL, which is arbitrarily set above the maximum water table elevation (150 meters [492 feet] above MSL) for Hanford (Thorne et al. 2006:Figure 7.23).

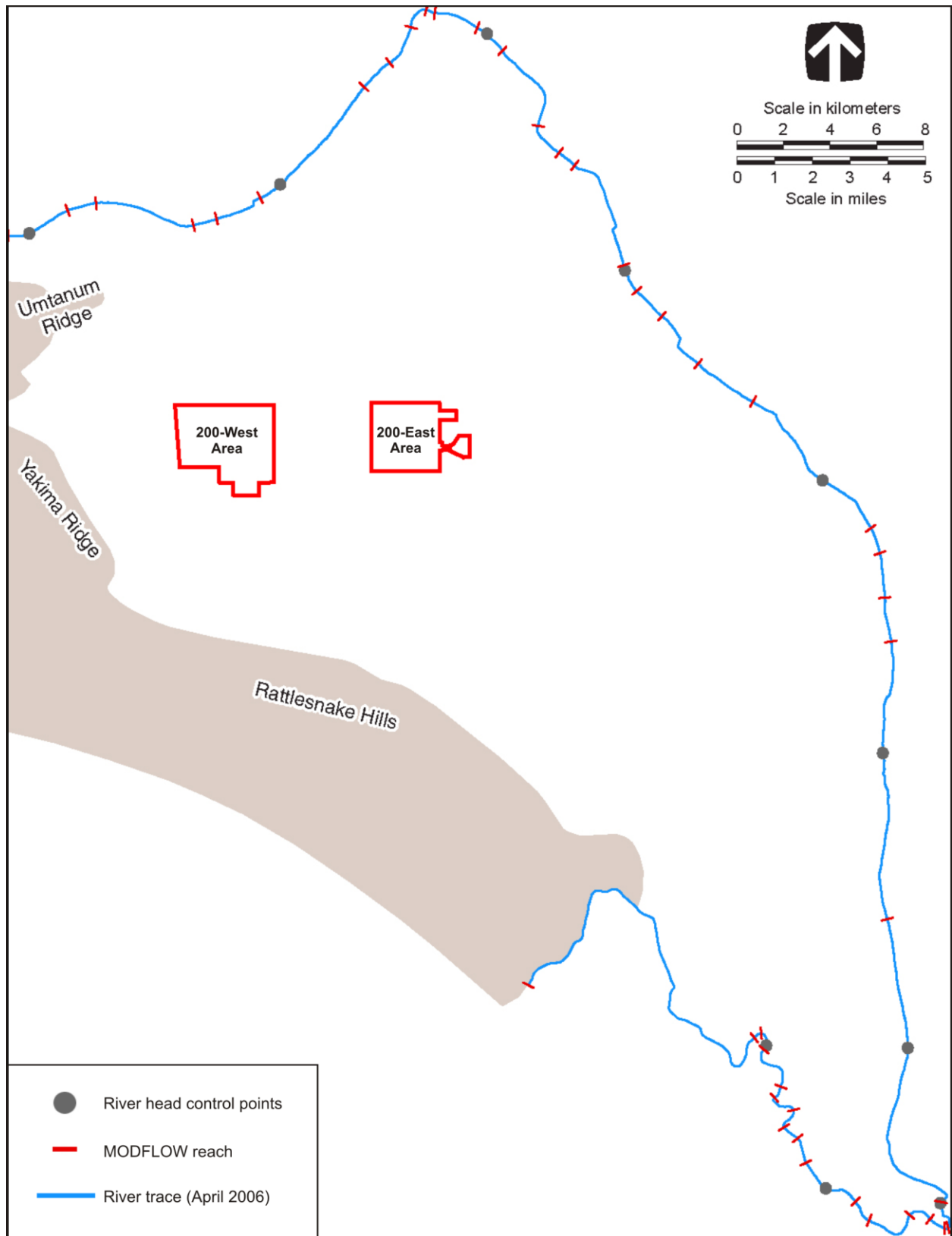


Figure L-16. MODFLOW Groundwater Flow Model Domain, Columbia and Yakima River Reaches, and River Head Control Points

L.4.1.2 Gridding

The *TC & WM EIS* MODFLOW groundwater flow model divides Hanford within the model domain into three-dimensional blocks or cells. The model domain is divided into a 200- by 200-meter (656- by 656-foot) horizontal grid, with a “fringe” of partial cells on the northern, eastern, and southern sides. The sizes of the partial cells are defined by the distance between the last full-size row and column and the model extent. The horizontal grid and the fringe on the eastern and southern edges of the *TC & WM EIS* MODFLOW groundwater flow model are depicted in Figure L–17.

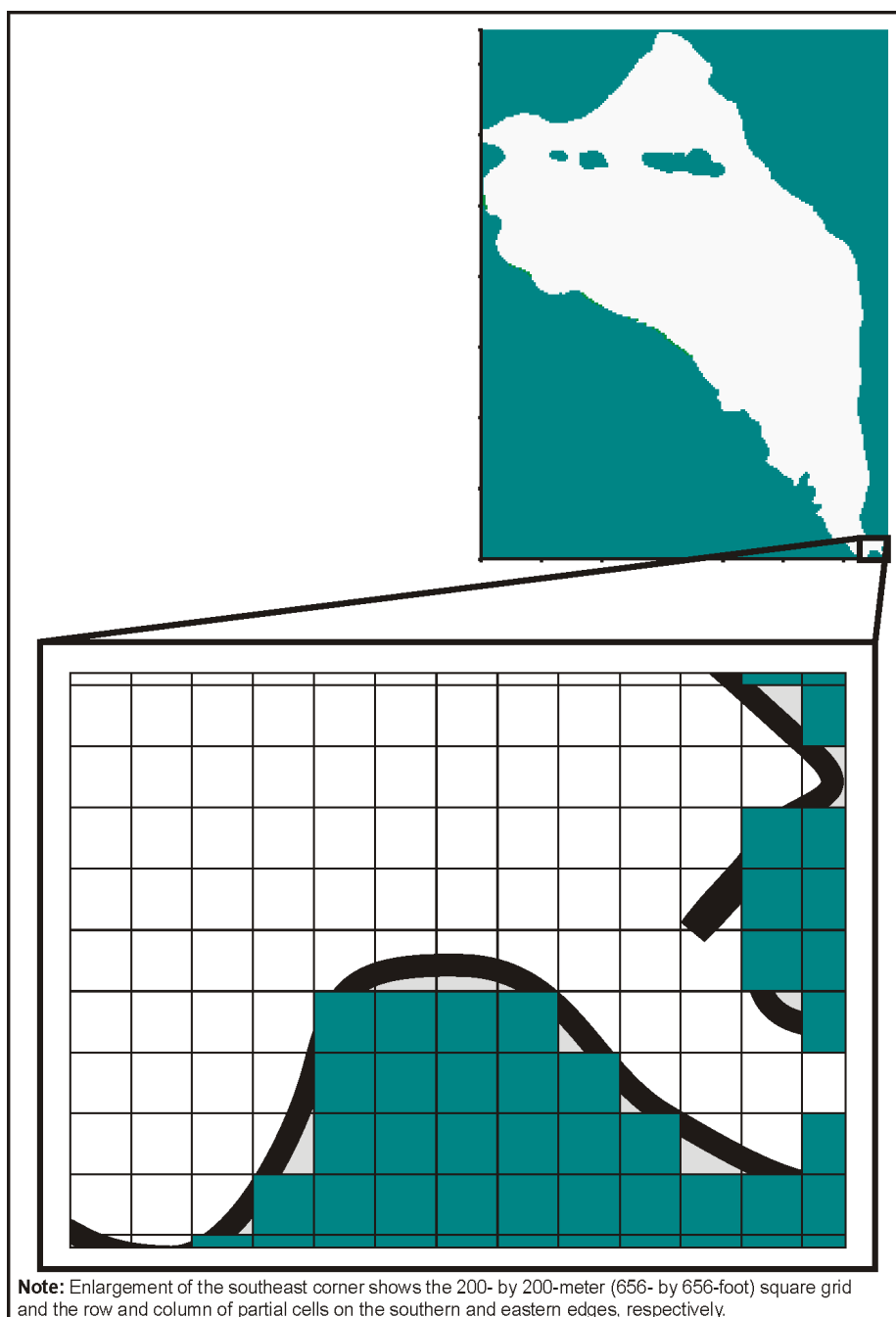


Figure L–17. Plan View of MODFLOW Horizontal Gridding

The horizontal grid size of 200 by 200 meters (656 by 656 feet) was selected based on two primary criteria: (1) a grid of such size that the heterogeneity of the hydrogeologic material types can be encoded to reasonably represent the suprabasalt sediments on a regional scale; and (2) a grid of such size that a reasonable flow mass balance (in the range of plus or minus 2 percent discrepancy) can be achieved. The horizontal grid size of 200 by 200 meters (656 by 656 feet) was initially selected to meet Criteria 1 because two grid cells cover approximately 0.5 kilometers, which can reasonably represent the minimum area of a particular material type to be encoded for a regional-scaled model. This grid size also achieved an acceptable flow mass balance discrepancy as discussed in Section L.8. No consideration was given to groundwater transport when selecting the grid size for the flow model because the groundwater transport model is not constrained by the flow model grid. See Appendix O for additional information on the groundwater transport model.

The interpolated elevation of the TOB surface in Gable Gap is not sensitive to the cell size of the horizontal grid. The lowest TOB elevation in Gable Gap (i.e., the “cutoff” elevation) determines the water level at which flow through the gap is possible. A comparison of 31 variants of the interpolated TOB surface for both a 200- by 200-meter (656- by 656-foot) grid and a 100- by 100-meter (328- by 328-foot) grid found that the elevation of the TOB surface in Gable Gap was not sensitive to grid size (see Table L-1).

**Table L-1. Top-of-Basalt “Cutoff”^a Elevation in Gable Mountain–Gable Butte Gap
by Grid Size and Aggregation Mean**

Run	Description	Elevation (meters)	
		100- by 100-meter grid ^b	200- by 200-meter grid ^c
Default	Geostatistical Analyst (Johnston et al. 2001) default settings.	121	121
Variant 1	Reduce major range from default (22,580 m) to 22,354 m.	121	121
Variant 1a	Reduce major range from default (22,580 m) to 21,451 m.	121	121
Variant 2	Reduce minor range to 22,354 m; model direction = 0 degrees.	121	121
Variant 2a	Reduce minor range to 21,451 m. Major range = 22,580 m and model direction = 0 degrees.	120	120
Variant 3	Minor range = 22,354 m; model direction = 356 degrees.	121	121
Variant 3a	Reduce minor range to 21,451 m and change model direction to 352 degrees (or 172 degrees).	121	121
Variant 4	Reduce partial sill from default (12,519 m) to 12,394 m.	121	121
Variant 4a	Reduce partial sill from default (12,519 m) to 11,893 m.	121	121
Variant 5	Increase nugget from default (0 m) to 15 m.	121	121
Variant 5a	Increase nugget from default (0 m) to 150 m.	121	120
Variant 6	Partial sill = 12,394 m; increase nugget to 125 m; constant sill.	121	120
Variant 6a	Reduce partial sill from default (12,519 m) to 11,893 m and increase nugget to 626 m.	120	120

Table L–1. Top-of-Basalt “Cutoff”^a Elevation in Gable Mountain–Gable Butte Gap by Grid Size and Aggregation Mean (continued)

Run	Description	Elevation (meters)	
		100- by 100-meter grid ^b	200- by 200-meter grid ^c
Variant 7	Increase number of neighbors to include per sector from default (5) to 6, “Include at Least” 2.	120	120
Variant 7a	Increase number of neighbors to include per sector from default (5) to 7, “Include at Least” 2.	120	120
Variant 8	Reduce lag size from default (4,859.2 m) to 4,810.7 m.	121	121
Variant 8a	Reduce lag size from default (4,859.2 m) to 4,616 m.	121	121
Variant 9	Increase number of lags to 13.	121	121
Variant 9a	Increase number of lags to 14.	121	121
Variant 10	Lag size 4,810.7 m; number of lags 13.	121	121
Variant 10a	Reduce lag size from default (4,859.2 m) to 4,616 m and increase number of lags to 14.	121	121
Random 1	Random Realization No. 1.	121	120
Random 2	Random Realization No. 2.	121	121
Random 3	Random Realization No. 3.	120	120
Random 4	Random Realization No. 4.	121	121
Random 5	Random Realization No. 5.	121	121
Random 6	Random Realization No. 6.	120	120
Random 7	Random Realization No. 7.	120	120
Random 8	Random Realization No. 8.	122	122
Random 9	Random Realization No. 9.	118	118
Random 10	Random Realization No. 10.	121	120

^a Lowest maximum elevation along MODFLOW flow path through Gable Mountain–Gable Butte Gap.

^b Environmental Systems Research Institute default mean.

^c Harmonic mean.

Note: To convert meters to feet, multiply by 3.281.

Key: m=meters; MODFLOW=modular three-dimensional finite-difference groundwater flow model.

The *TC & WM EIS* MODFLOW groundwater flow model is divided into 31 layers in the vertical direction. Each layer is a uniform (constant) thickness across the entire model domain in the horizontal directions. The layers range in thickness from 1 meter (3.281 feet) to 40 meters (131 feet). The layering of the *TC & WM EIS* MODFLOW groundwater flow model is depicted in Figure L–18. The model has 1-meter-thick (3.281-feet-thick) layers at depths between 115 and 125 meters (377 and 410 feet) above MSL, where the TOB surface is near the water table. These high-resolution layers span the TOB elevations simulated to occur in Gable Gap. Water levels fluctuate between these depths during the model simulation period. The thickest layers, which are greater than 15 meters (49 feet) thick, occur deep in the aquifer, where less resolution is required.

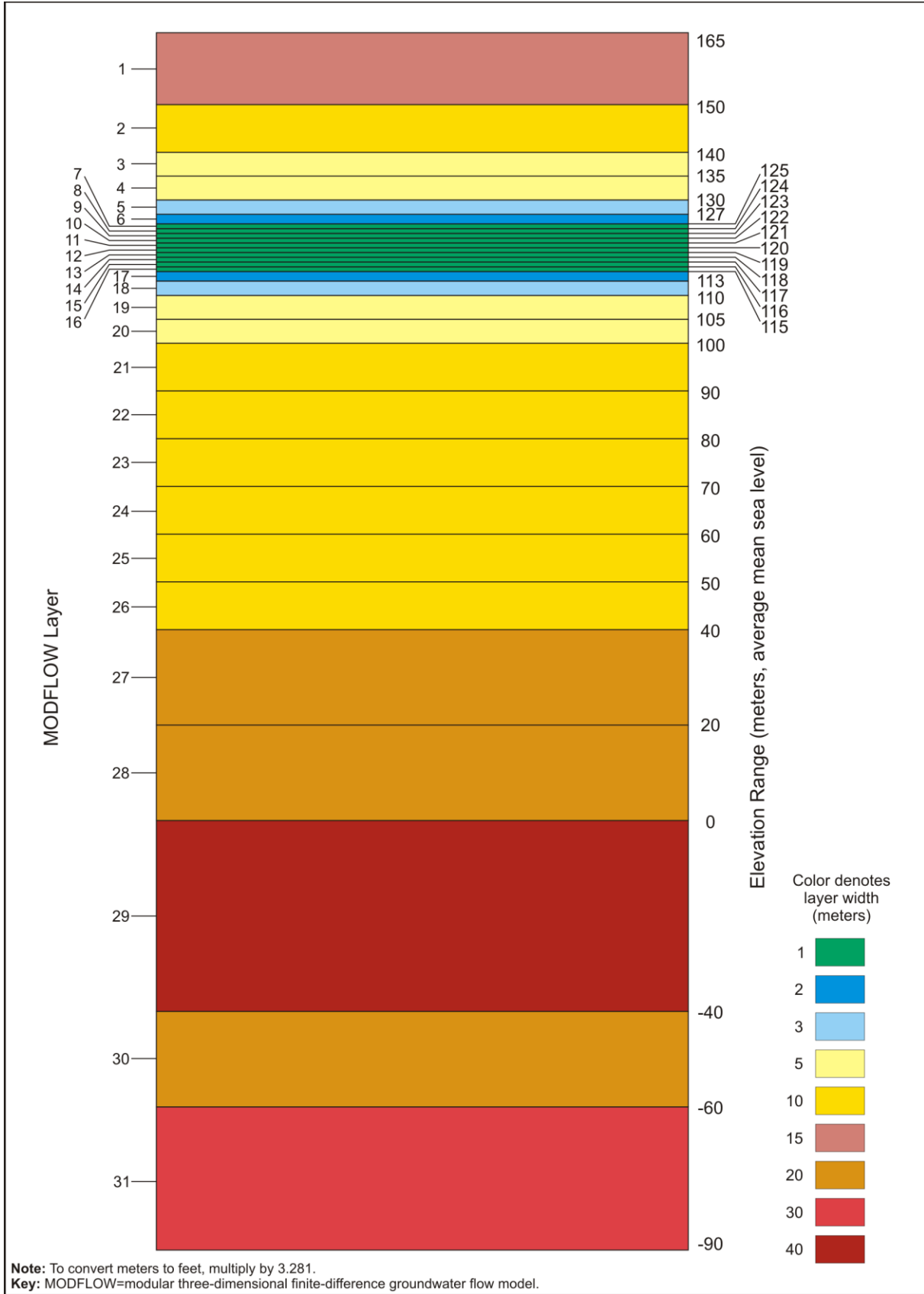


Figure L-18. Cross-Sectional View of MODFLOW Vertical Grid

L.4.2 Boundary Conditions

The boundary conditions for the *TC & WM EIS* groundwater flow model are defined by the Yakima and Columbia Rivers, the subsurface influx of water into the unconfined aquifer along Rattlesnake Mountain, the basalt layer beneath the unconfined aquifer, and recharge (anthropogenic and natural) at the ground surface. The Columbia and Yakima Rivers and naturally occurring subsurface influxes of groundwater to the unconfined aquifer at three discrete locations along the western boundary are modeled as GHBs. Except for the discrete GHB-encoded areas along the western boundary where mountain-front recharge is thought to occur (see Section L.4.2.3), the basalt layer beneath the unconfined aquifer is assumed to be a no-flow boundary, that is, no water enters the unconfined aquifer from the underlying basalt. For the *TC & WM EIS* groundwater flow model, the rivers, subsurface influx, basalt “basement,” and natural recharges are taken as constant. The only time-varying fluxes of water across the model boundary are anthropogenic areal recharges. These boundary conditions are discussed below.

L.4.2.1 Basalt Surface (No-Flow Boundary)

Massive basalts beneath the unconfined aquifer at Hanford define a no-flow boundary (aquiclude) in the *TC & WM EIS* groundwater flow model. A no-flow boundary represents a limit to flow within the unconfined aquifer. In this MODFLOW groundwater flow model, no water enters the unconfined aquifer from the underlying basalt. Except for a ridge of basalt in Gable Gap, the model cell in which the TOB surface is assigned and all lower cells are encoded in the model as “inactive.” Inactive cells do not allow water to flow to neighboring cells and do not accept flow coming from neighboring cells. For the ridge of basalt in Gable Gap, only cells at 115 meters (377 feet) above MSL and below are encoded as inactive; these elevations correspond to MODFLOW Layers 16 through 31. Cells above 115 meters (377 feet) above MSL that are encoded as basalt are made active, with a hydraulic conductivity 500 times lower than that of Hanford and Ringold muds (0.001 meters [0.00328 feet] per day). Active status prevents the MODFLOW cells from drying out during fluctuations of the water table; cells going dry cause model instabilities (see Section L.5.1.1).

L.4.2.2 Columbia and Yakima Rivers (River Package)

The *TC & WM EIS* groundwater flow model uses the Visual MODFLOW river package to encode the Columbia and Yakima Rivers. This package encodes surface-water/groundwater interaction via a seepage layer (riverbed) separating the surface-water body from the groundwater aquifer. The portions of the Columbia and Yakima Rivers in the *TC & WM EIS* MODFLOW groundwater flow model domain (see Figure L-16) are encoded in the model as an unbroken sequence of cells sharing a face or vertex. Each 200- by 200-meter (656- by 656-foot) cell encoded as river is assigned to a reach, and each reach is assigned a conductance, which is an inverse measure of the resistance to flow between the streambed and the underlying aquifer. For the *TC & WM EIS* groundwater flow model, conductance is a calibration parameter.

In the MODFLOW river package, conductance is a function of the length and width of a reach and the thickness and conductivity of the streambed. The *TC & WM EIS* MODFLOW groundwater flow model sets streambed thickness at 2 meters (6.6 feet) and conductivity at 0.0004 meters (0.0013 feet) per second. Reach width is a uniform 200 meters (656 feet). Reaches of different lengths are defined on the basis of slope. The river conductance parameter values in the *TC & WM EIS* MODFLOW groundwater flow model were varied to determine the model’s sensitivity to changes in these parameter values (see Section L.7). Because the length and width of each reach are fixed, adjusting conductance during calibration implies an adjustment of the ratio of streambed conductivity to streambed thickness.

In the *TC & WM EIS* MODFLOW groundwater flow model domain, 27 reaches, each with a relatively constant slope, are defined on the Columbia River, and 14 reaches are defined on the Yakima River

(see Figure L-16). Elevations were assigned to coordinates along the trace by interpolating from existing river elevation data developed by Pacific Northwest National Laboratory (PNNL) (Thorne et al. 2006). Elevations were assigned assuming constant slope between PNNL data points. The PNNL data set contains 700 data points for the Columbia River and 44 points for the Yakima River within the model extent. The entire Yakima River within the model domain is not modeled because the river upstream of Horn Rapids is assumed to be separate and distinct from (not connected to) the unconfined aquifer at Hanford.

The specified river stages, river bed thicknesses, and river bed conductances govern the interactions of the Columbia and Yakima Rivers with the unconfined aquifer. When the river stage is greater than the head in the aquifer immediately below, water flows from the river into the aquifer. The flow is reversed when the river stage is lower than the head in the aquifer immediately below. The former condition is described as a losing reach of the river, and the latter as a gaining reach. In general, the Columbia River gains throughout the modeled domain, and the Yakima River loses.

L.4.2.3 Mountain-Front Recharge (Generalized Head Boundary)

Groundwater is thought to enter the unconfined aquifer at Hanford from the underlying basalt layer in defined areas along the western boundary—Cold Creek Valley, Dry Creek Valley, and Rattlesnake Mountain (Thorne et al. 2006). Well-documented springs occur in Cold Creek Valley and Dry Creek Valley. Runoff from the eastern face of Rattlesnake Mountain is the third source of subsurface influx of groundwater along Hanford’s “upstream” boundary.

These three examples of mountain-front recharge are encoded in the *Final TC & WM EIS* groundwater flow model using the Visual MODFLOW GHB package (see Figure L-19). Figure L-19 provides the locations of the model-encoded GHB cells overlain onto a pictorial view of Hanford to show these encoded locations relative to the land features that they represent. With the GHB package, one defines groups of cells (zones) with specific values for head and parameters affecting conductance, the resistance to water flow into the cells of the zone. The head and conductance parameter values for each of the three GHB zones in the *TC & WM EIS* MODFLOW groundwater flow model were varied to determine the model’s sensitivity to changes in these parameter values (see Section L.7).

The Base Case groundwater flow model includes a simplifying assumption that mountain-front recharge does not vary with time. Field observations indicate that recharge, possibly from agricultural activities to the west of Hanford, is increasing with time. See Appendix V for an analysis of the model’s sensitivity to this and other features related to increased water fluxes into the model.

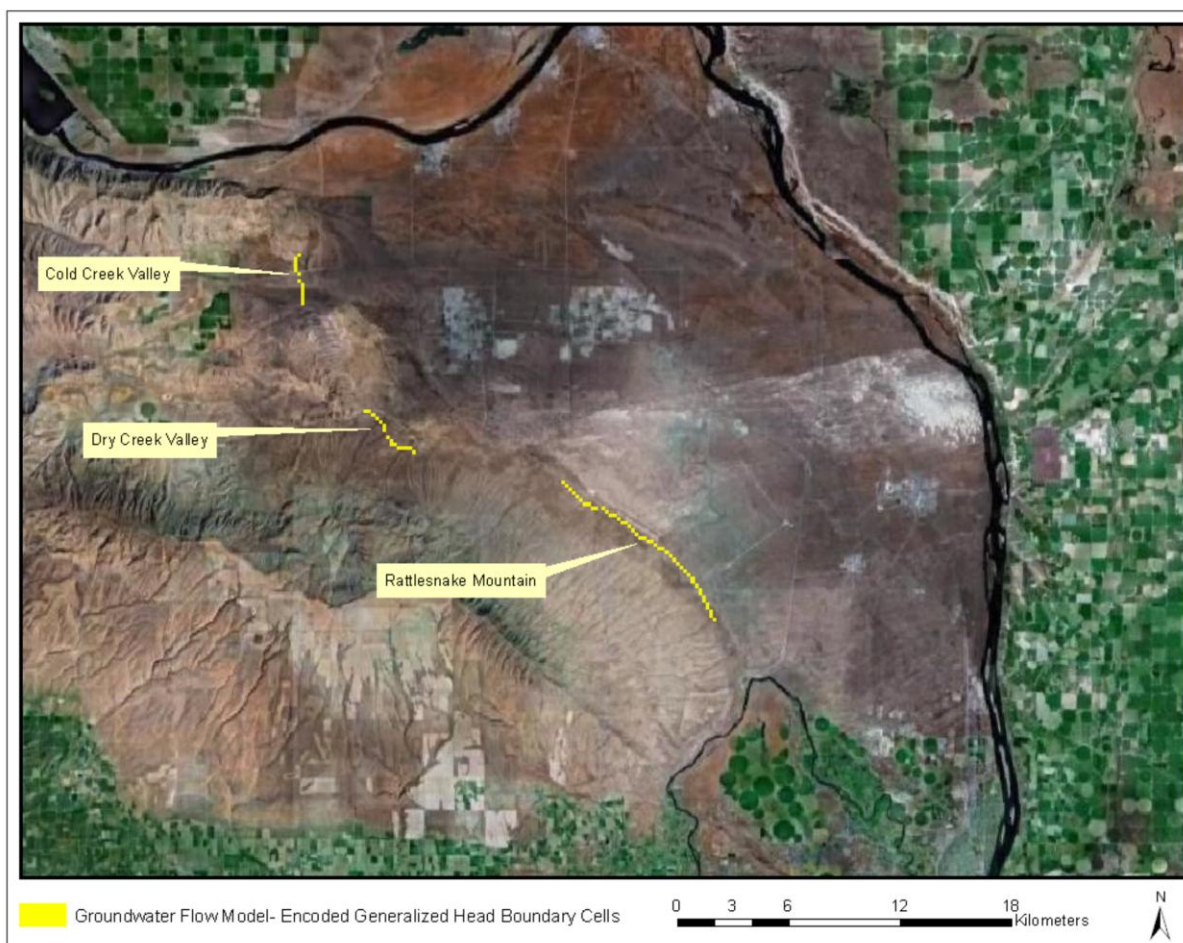


Figure L-19. Mountain-Front Recharge Zones

L.4.2.4 Natural Areal Recharge (Recharge Boundary)

The *TC & WM EIS* groundwater flow model incorporates natural recharge at the rates specified in the *Technical Guidance Document* (DOE 2005). Cribs and trenches (ditches) receive 50 millimeters (2 inches) of natural recharge per year, and tank farms receive 100 millimeters (4 inches) of natural recharge per year. Fifty millimeters per year is equivalent to 50 liters (13.2 gallons) per square meter per year. For situations where a particular facility does not completely cover a 200- by 200-meter (656- by 656-foot) MODFLOW grid cell, the full recharge value (e.g., 100 millimeters per year for tank farms) is applied across the entire MODFLOW cell that contains all or part of the facility. A fixed infiltration rate, 3.5 millimeters (0.14 inches) per year, representing precipitation on natural surfaces, is applied to the remaining areas not otherwise specified. These natural infiltration rates are also used in the STOMP vadose zone models (see Appendix N). The City of Richland and the sitewide recharge parameter values in the *TC & WM EIS* MODFLOW groundwater flow model were varied to determine the model's sensitivity to changes in these parameter values (see Section L.7).

L.4.2.5 Artificial Recharge (Recharge Boundary)

Anthropogenic recharge associated with Hanford operations and, to a lesser extent, extraction (water withdrawal) and irrigation beyond the Hanford boundary represents the important time-varying fluxes of water into and out of the aquifer during the model period of analysis (CYs 1940–11,940). Water originally taken from the Columbia River was discharged onto the ground surface during operations.

These anthropogenic recharge sources are the time-varying inputs that drive the transient behavior of the TC & WM EIS groundwater flow model.

Values for over 200 sources (or sinks) of water were taken from the Cumulative Impacts Inventory Database (SAIC 2006) and encoded into the model. These fluxes were encoded as constant flux boundary conditions in the MODFLOW cells that contain the sources and release sites. These recharge fluxes were also modeled using STOMP to simulate transport of contaminants through the vadose zone to the groundwater.

Of all the anthropogenic liquid sources identified in the Hanford inventory database, eight sites account for 88 percent of the total site recharge (see Table L-2). The volumes released at these sites range from 41 billion liters (10.8 billion gallons) at the 216-S-16P Pond to 300 billion liters (79.3 billion gallons) at the 116-K-2 Trench. All eight sites combined released roughly 1.43 trillion liters (0.38 trillion gallons). Five of these sites are located in the 200 Areas, and they were major contributors to the mounds of water that built up beneath the 200-East and 200-West Areas during operations from 1945 through the mid-1990s (SAIC 2006).

Table L-2. Major Total Recharge Sources on the Hanford Site (1940–Present)

WIDS ID	Site Type	Source Type	Centroid Easting	Centroid Northing	Volume (liters)	Cumulative Fraction
116-K-2	Trench	Liquid	569801	147701	300,000,000,000	0.21
216-A-25	Pond	Liquid	574970	139650	293,899,037,982	0.42
216-B-3	Pond	Liquid	576898	136687	282,689,367,700	0.61
216-U-10	Pond	Liquid	566318	134602	159,859,250,966	0.73
116-N-1	Crib	Liquid	571534	149782	83,700,000,000	0.78
316-1	Pond	Liquid	594283	116106	51,116,602,319	0.82
216-T-4A	Pond	Liquid	566475	137133	42,826,720,640	0.85
216-S-16P	Pond	Liquid	565412	133192	40,723,265,275	0.88

Note: To convert liters to gallons, multiply by 0.26417.

Key: WIDS ID=Waste Information Data System identification.

Anthropogenic areal recharge is encoded in the model in 1-year stress periods beginning in 1944. The model applies the estimated annual flux to the water table from each site in the appropriate 1-year stress periods, beginning in the first year of operations at the site and ending in the final year of operations. The total recharge applied to the water table in a given stress period fluctuates from year to year as the number of contributing sites and their fluxes vary. For example, Figures L-20 and L-21 show the timing and magnitude of flux from the dominant anthropogenic recharge sources in the 200-East and 200-West Areas, respectively.

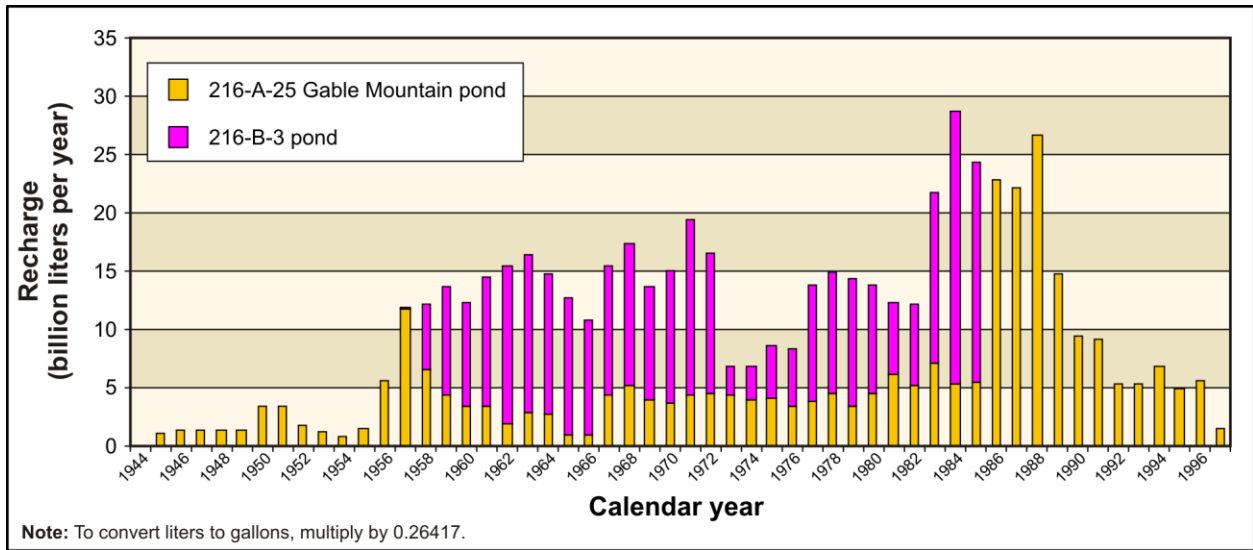


Figure L-20. Major Anthropogenic Recharge Sources in the 200-East Area

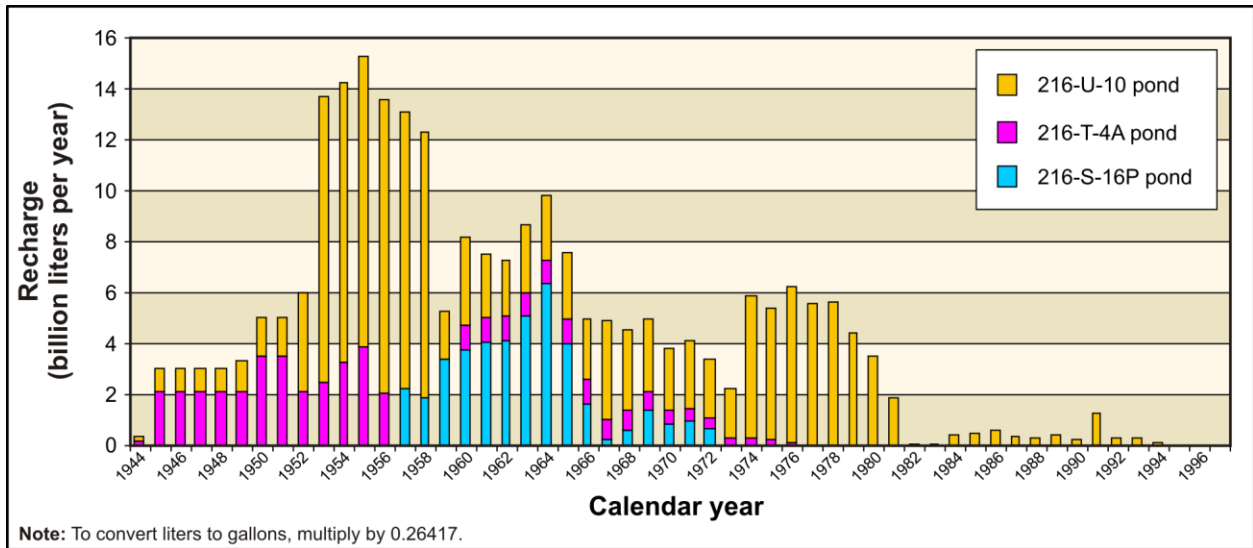


Figure L-21. Major Anthropogenic Recharge Sources in the 200-West Area

In addition to the liquid inventory sources, the model boundaries encompass three City of Richland water system well fields: North Richland, 1100B, and Wellsian Way. The pump houses at the North Richland and 1100B fields were constructed in 1978. Retention basins at these sites received Columbia River water, which was allowed to infiltrate to groundwater. Reference data for recharge from the retention basins and production wells were obtained from City of Richland water system reports dating from 1981 to 2006 (see Table L-3). Based on information provided in the water system reports, a 95th percentile upper confidence limit on mean net recharge was calculated and used for the time period from 1978 to 1981. For analysis purposes, future anthropogenic recharges were estimated based on past usage. The 95th percentile upper confidence limit on the mean was used for the CYs 2006 through 11,940 for all three City of Richland well field locations. The anthropogenic recharge parameter values in the *TC & WM EIS* MODFLOW groundwater flow model were varied to determine the model's sensitivity to changes in these parameter values (see Section L.7).

*Tank Closure and Waste Management Environmental Impact Statement for the
Hanford Site, Richland, Washington*

Table L-3. City of Richland Water Supply Data – Annual Summary Report

Year	Extraction North Richland (Mgal)	Extraction 1100B (Mgal)	Positive Recharge (Mgal) ^a	Positive Recharge/Extraction	Net Recharge (Mgal)	Net Recharge (gal)
1978	9.13×10 ²	6.86×10 ¹	3.70×10 ^{3b}	3.77	2.72×10 ³	2.72×10 ⁹
1979	9.13×10 ²	6.86×10 ¹	3.70×10 ^{3b}	3.77	2.72×10 ³	2.72×10 ⁹
1980	9.13×10 ²	6.86×10 ¹	3.70×10 ^{3b}	3.77	2.72×10 ³	2.72×10 ⁹
1981	9.13×10 ²	6.86×10 ¹	3.66×10 ³	3.73	2.68×10 ³	2.68×10 ⁹
1982	9.13×10 ²	6.86×10 ¹	2.36×10 ³	2.40	1.38×10 ³	1.38×10 ⁹
1983	9.13×10 ²	6.86×10 ¹	2.76×10 ³	2.82	1.78×10 ³	1.78×10 ⁹
1984	5.31×10 ²	0.00×10	3.61×10 ³	6.79	3.07×10 ³	3.07×10 ⁹
1985	5.42×10 ²	0.00×10	2.72×10 ³	5.01	2.17×10 ³	2.17×10 ⁹
1986	3.99×10 ²	1.08×10 ²	2.35×10 ³	4.63	1.84×10 ³	1.84×10 ⁹
1987	5.11×10 ²	1.02×10 ²	2.33×10 ³	3.80	1.72×10 ³	1.72×10 ⁹
1988	5.39×10 ²	1.08×10 ¹	1.94×10 ³	3.53	1.39×10 ³	1.39×10 ⁹
1989	1.08×10 ³	7.19×10	2.92×10 ³	2.69	1.83×10 ³	1.83×10 ⁹
1990	1.45×10 ³	4.07×10	2.70×10 ³	1.86	1.25×10 ³	1.25×10 ⁹
1991	1.13×10 ³	1.02×10 ¹	2.77×10 ³	2.44	1.64×10 ³	1.64×10 ⁹
1992	8.39×10 ²	4.35×10 ¹	1.71×10 ³	1.93	8.23×10 ²	8.23×10 ⁸
1993	6.01×10 ²	1.57×10 ¹	3.30×10 ³	5.35	2.68×10 ³	2.68×10 ⁹
1994	1.34×10 ³	6.17×10 ¹	2.64×10 ³	1.89	1.24×10 ³	1.24×10 ⁹
1995	5.72×10 ²	6.00×10 ¹	1.86×10 ³	2.94	1.23×10 ³	1.23×10 ⁹
1996	5.03×10 ²	5.84×10 ¹	2.34×10 ³	4.16	1.77×10 ³	1.77×10 ⁹
1997	6.23×10 ²	6.84×10 ¹	1.90×10 ³	2.75	1.21×10 ³	1.21×10 ⁹
1998	1.33×10 ³	1.47×10 ²	1.86×10 ³	1.26	3.85×10 ²	3.85×10 ⁸
1999	7.46×10 ²	1.11×10 ²	1.61×10 ³	1.88	7.54×10 ²	7.54×10 ⁸
2000	7.65×10 ²	3.64×10 ¹	1.83×10 ³	2.29	1.03×10 ³	1.03×10 ⁹
2001	5.34×10 ²	7.47×10 ¹	1.48×10 ³	2.44	8.76×10 ²	8.76×10 ⁸
2002	1.19×10 ³	6.85×10 ¹	3.05×10 ³	2.43	1.80×10 ³	1.80×10 ⁹
2003	5.35×10 ²	1.76×10 ¹	2.67×10 ³	4.83	2.12×10 ³	2.12×10 ⁹
2004	4.10×10 ²	5.79×10 ¹	1.69×10 ³	3.61	1.22×10 ³	1.22×10 ⁹
2005	5.39×10	1.33×10 ²	2.61×10 ³	18.86	2.47×10 ³	2.47×10 ⁹
2006–11,940	9.13×10 ²	6.86×10 ¹	3.70×10 ^{3b}	3.77	2.72×10 ³	2.72×10 ⁹
			Count	24.00		
			SD	1.35		
			Average	3.23		
			95% UCL	3.77		

^a Positive recharge taken from City of Richland water system reports for years 1981–2005 (Richland 1981–2005).

^b Used the 95th percentile UCL ratio.

Note: To convert gallons to liters, multiply by 3.7854.

Key: %=percent; gal=gallon; Mgal=million gallons; SD=standard deviation; UCL=upper confidence limit.

L.4.3 Lithology

Three major lithologic units that occur beneath Hanford are encoded in the *TC & WM EIS* groundwater flow model: Elephant Mountain basalt, Ringold Formation, and Hanford formation. The Elephant Mountain basalt represents the bottom of the unconfined aquifer (see Section L.4.3.2.1). The unconsolidated sediments of the Hanford and Ringold Formations constitute the unconfined aquifer. The sediments of these two formations represent the saturated zones through which groundwater flow is modeled.

L.4.3.1 Hydrogeologic Unit Definition

The *TC & WM EIS* groundwater flow model recognizes two major lithologic formations in the unconfined aquifer above the basalt, Hanford and Ringold, and two minor geologic units, the Cold Creek and Plio-Pleistocene Units. The Ringold Formation is the lower geologic unit of the unconfined aquifer, and, where it occurs, it directly overlies basalt. The Hanford formation overlies the Ringold Formation where the latter occurs and directly above the basalt where the Ringold is missing. Between the Hanford and Ringold Formations, the Cold Creek and Plio-Pleistocene Units locally occur at Hanford. Although the Cold Creek Unit is Plio-Pleistocene in age, for the purposes of the *TC & WM EIS* groundwater flow model, the Cold Creek Unit and the Plio-Pleistocene Unit have been identified as separate encoded material types. In the groundwater flow model, the Plio-Pleistocene Unit defines the fine-grained silts and caliche sediments prevalent in the 200-West Area, and the Cold Creek Unit refers to the coarse-grained, pre-Missoula gravels found farther to the east. Both the Hanford and the Ringold Formations consist of fluvial and lacustrine sequences of mud, silt, sand, and gravel. The coarse-grained multilithic facies of the Cold Creek Unit are thought to be more like Hanford formation gravel and sand than the harder, more cemented Ringold Formation gravel and sand (Thorne et al. 2006).

L.4.3.2 Hydrogeologic Unit Encoding

The *TC & WM EIS* groundwater flow model has been encoded with hydrogeologic data for the entire model domain developed from Hanford well borings completed as of September 2009 (CHPRC 2009b, 2010; Ecology 2003). Approximately 5,000 boring logs from Hanford and its surroundings were reviewed to determine whether the geologic units and discrete hydrostratigraphic layers could be recognized from the geologic descriptions. When multiple logs existed for a borehole, higher credibility was given to those descriptions recorded by a professional geologist. Logs were reviewed for specific identification of the Elephant Mountain basalt, Hanford and Ringold Formations, and Cold Creek and Plio-Pleistocene Units. The logs were further examined to discern textural types among the sedimentary units: mud, silt, sand, and gravel. Each of the resulting hydrogeologic units is encoded with unique properties (see Section L.4.4). The development of the hydrogeologic data for use in the *TC & WM EIS* groundwater flow model is described in the following sections.

L.4.3.2.1 Basalt Surface

The TOB surface encoded in the *TC & WM EIS* groundwater flow model was derived from boring logs, surface measurements, and geostatistical interpolation. The 5,000 boring logs used for hydrogeologic unit encoding were reviewed to determine whether the geologic descriptions accompanying the boring logs indicated the depth of the uppermost basalt layer underlying the unconfined aquifer. Only boreholes whose locations (coordinates) were known with some confidence were used. The TOB surface elevations at basalt outcroppings on or near Hanford were measured using a global positioning system device. Some TOB surface elevation values were taken from USGS topographic maps of Gable Mountain, Gable Butte, and Rattlesnake Mountain, which are massive outcroppings of the Elephant Mountain basalt, the formation underlying the unconfined aquifer at Hanford. Uncertainty estimates were assigned to each TOB elevation value.

The TOB surface encoded in the *TC & WM EIS* MODFLOW groundwater flow model is a geostatistical interpolation of the basalt-elevation data points from approximately 850 Hanford boring logs and 18 control points (see Figure L-22). Of the 18 control points, 12 are “structural,” representing site knowledge about TOB surface elevation where there were limited or no data available, and 6 are “visual,” added to improve the depiction of the TOB surface. Nine of the 12 structural control points were added along the Columbia River where it enters Hanford to position the TOB surface beneath the river. The other three structural control points were added at borehole (well) locations where the boring did not extend completely to the basalt, but only to the Ringold Formation Lower Mud Unit, which lies atop the basalt where it occurs. At these three locations, the TOB surface was estimated from other nearby borings that went deep enough to encounter the Ringold Formation Lower Mud Unit and the underlying basalt. Four of the six visual control points were added north of Gable Butte and Gable Mountain along the known position of the Gable Mountain Fault (see Figure L-22). The visual control points along the Gable Mountain Fault do not affect the simulated elevation of the TOB surface in Gable Gap (see Table L-4). The other two visual control points were added at Yakima Ridge. These two visual control points are not expected to affect the flow field in the operational areas of the site because of their distance from the operational areas (several kilometers to the south) and the predominant direction of groundwater flow (easterly).

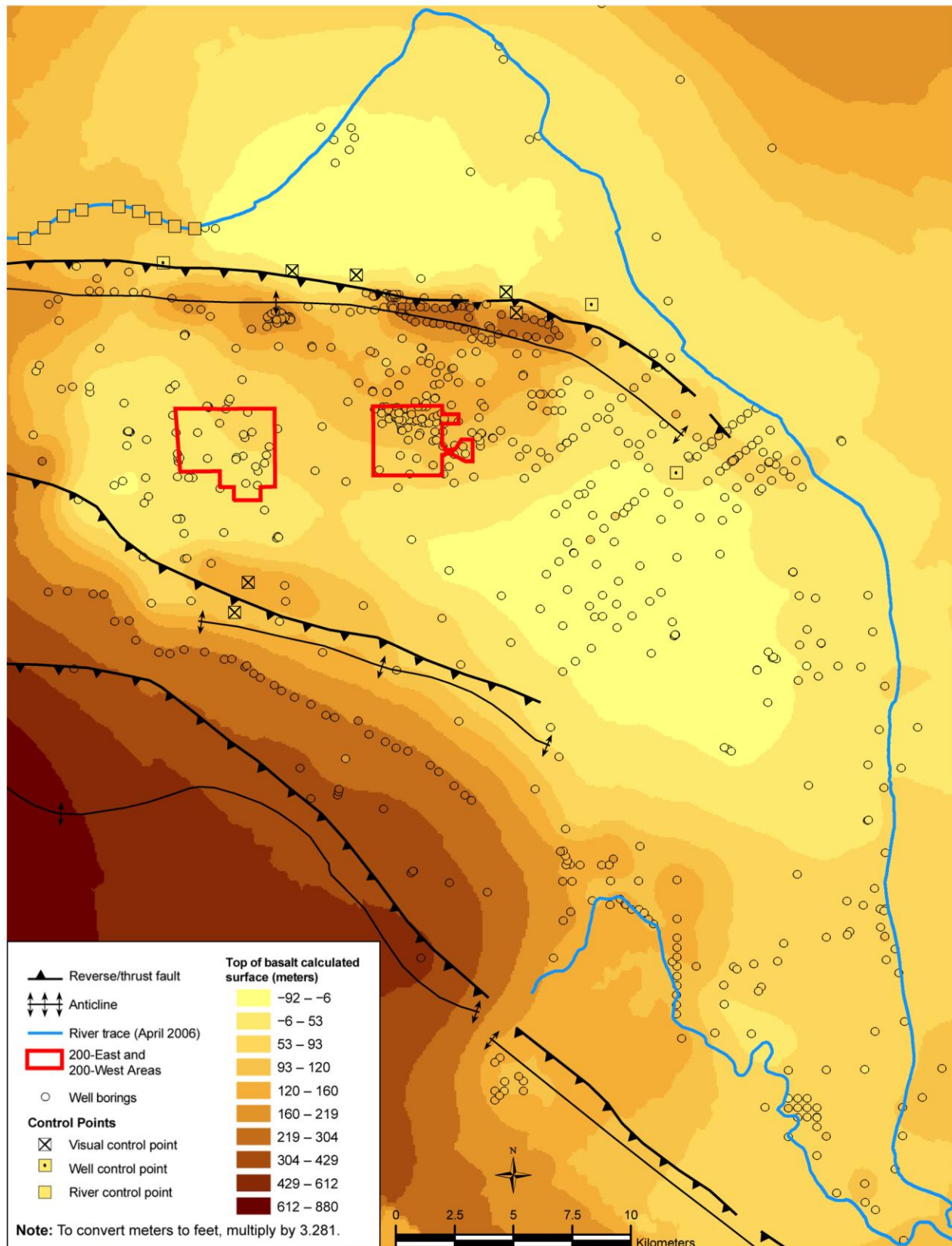


Figure L-22. Interpolated Top-of-Basalt Surface at the Hanford Site Showing Faults and Anticlines

Table L-4. Effect of Visual Control Points on Top-of-Basalt “Cutoff”^a Elevation in Gable Gap

Visual Control Points	Gable Gap Cutoff Elevation ^a (meters)	MODFLOW Layer (elevation in meters)	Notes
None	120.8407	11 (120–121)	–
5	120.8409	11 (120–121)	Includes new visual control points YRCP-1, YRCP-2, GMFCP-1, GMFCP-2, and GMFCP-3
6	120.8412	11 (120–121)	Includes five visual control points listed above and GMFCP-4 (closest to Gable Gap)

^a Lowest maximum elevation along MODFLOW flow path through Gable Gap.

Note: To convert meters to feet, multiply by 3.281.

Key: Gable Gap=Gable Mountain–Gable Butte Gap; MODFLOW=modular three-dimensional finite-difference groundwater flow model.

The TOB surface encoded into the *TC & WM EIS* groundwater flow model was interpolated from the data and control points using ArcGIS Version 9.1, ArcInfo Level with Geostatistical Analyst Extension (Johnston et al. 2001). The interpolated TOB surface is not sensitive to the parameter settings assigned in ArcGIS. To make this determination, the TOB surface for the MODFLOW flow field model domain was interpolated by ordinary kriging using ArcGIS for the cases listed in Table L-5. The resulting TOB Gable Gap cutoff elevations, also shown in Table L-5, indicate that the interpolated TOB surface is insensitive to the parameter settings assigned in ArcGIS.

Table L-5. Top-of-Basalt “Cutoff”^a Elevation in Gable Mountain–Gable Butte Gap Based on ArcGIS Parameter Settings

Run	Description	Top-of-Basalt Elevation (meters) ^b
Default	Geostatistical Analyst (Johnston et al. 2001) default settings.	121
Variant 1	Reduce major range from default (22,580 m) to 22,354 m.	121
Variant 1a	Reduce major range from default (22,580 m) to 21,451 m.	121
Variant 2	Reduce minor range to 22,354 m; model direction = 0 degrees.	121
Variant 2a	Reduce minor range to 21,451 m. Major range = 22,580 and model direction = 0.	121
Variant 3	Minor range 22,354 m; model direction = 356 degrees.	121
Variant 3a	Reduce minor range to 21,451 m and change model direction to 352 degrees (or 172 degrees).	121
Variant 4	Reduce partial sill from default (12,519 m) to 12,394 m.	121
Variant 4a	Reduce partial sill from default (12,519 m) to 11,893 m.	121
Variant 5	Increase nugget from default (0 m) to 15 m.	121
Variant 5a	Increase nugget from default (0 m) to 150 m.	121
Variant 6	Partial sill 12,394; increase nugget to 125 m; constant sill.	121
Variant 6a	Reduce partial sill from default (12,519 m) to 11,893 m and increase nugget to 626 m.	120
Variant 7	Increase number of neighbors to include per sector from default (5) to 6, “Include at Least” 2.	120
Variant 7a	Increase number of neighbors to include per sector from default (5) to 7, “Include at Least” 2.	120
Variant 8	Reduce lag size from default (4,859.2 m) to 4,810.7 m.	121
Variant 8a	Reduce lag size from default (4,859.2) to 4,616 m.	121

Table L-5. Top-of-Basalt “Cutoff”^a Elevation in Gable Mountain–Gable Butte Gap Based on ArcGIS Parameter Settings (*continued*)

Run	Description	Top-of-Basalt Elevation (meters) ^b
Variant 9	Increase number of lags to 13.	121
Variant 9a	Increase number of lags to 14.	121
Variant 10	Lag size 4,810.7 m; number of lags 13.	121
Variant 10a	Reduce lag size from default (4,859.2 m) to 4,616 m and increase number of lags to 14.	121

^a Lowest maximum elevation along MODFLOW flow path through Gable Mountain–Gable Butte Gap.

^b Grid is 200 by 200 m (harmonic mean).

Note: To convert meters to feet, multiply by 3.281.

Key: m=meter; MODFLOW=modular three-dimensional finite-difference groundwater flow model.

The final TOB surface was interpolated using ordinary kriging with the default settings (see Figure L-23). The resulting TOB surface was output to a raster file containing the elevation of the center point of each cell of the 200- by 200-meter (656- by 656-foot) grid of the *TC & WM EIS* groundwater flow model. These values were used to encode the TOB surface at the proper vertical layer in the MODFLOW groundwater flow model. For each MODFLOW cell, the TOB surface was assigned to the layer containing the TOB elevation if the TOB elevation was greater than the midpoint of the layer; otherwise, the TOB surface was assigned to the next-lower layer. The cell to which the TOB surface was assigned and all lower cells were made inactive, i.e., assigned the “no-flow” condition.

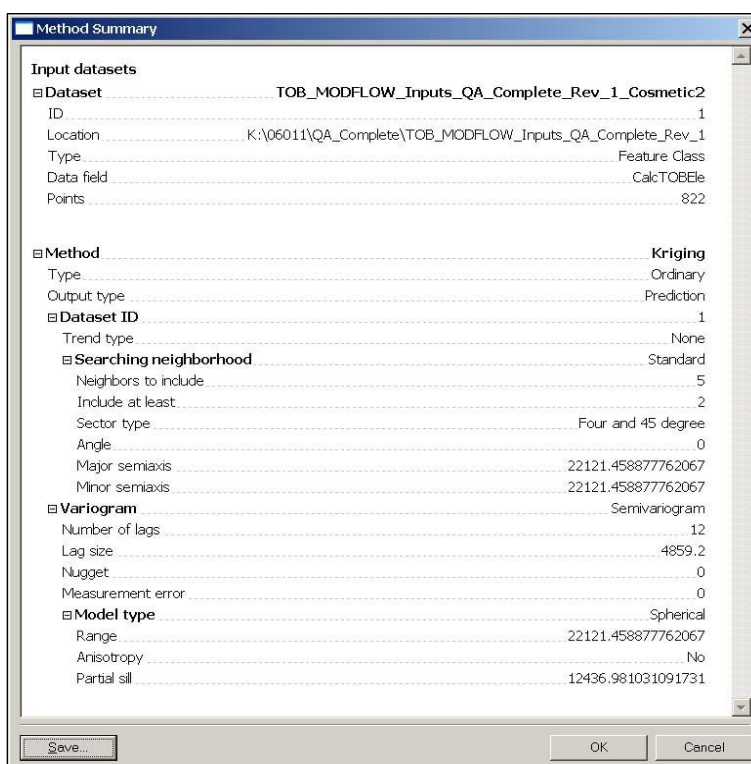


Figure L-23. Screen Print of Default Settings from Top-of-Basalt Surface Interpolation Using ArcGIS Geostatistical Analyst

The impact on the flow field of lower TOB elevations in Gable Gap is evaluated in the *Draft TC & WM EIS* (Appendix L, Sections L.2.2 and L.10.2). The lowest TOB elevation in Gable Gap, i.e., the “cutoff” elevation, determines the water level at which flow to the north through the gap is possible. One hundred TOB surfaces were created by randomly selecting the TOB elevation for each of the 849 borings and 12 structural control points from a normal distribution, with the mean equal to the reported TOB elevation and the interval size equal to twice the elevation uncertainty estimate. The results indicated that there are multiple possible locations for the gap to occur, with different elevation values. The mean elevations of the three most frequent locations correspond to cutoffs encoded in the groundwater flow model at approximately 118 meters (387 feet), 121 meters (397 feet), and 122 meters (400 feet) above MSL. Less than 5 percent of the realizations have a cutoff elevation lower than 118.5 meters (389 feet) above MSL. The TOB surface encoded in Gable Gap for the *Draft TC & WM EIS* groundwater flow model Alternate Case (Appendix L, Section L.2.2) was interpolated from a random TOB elevation data set with a cutoff value of 117.8 meters (387 feet) above MSL.

L.4.3.2.2 Suprabasalt Sedimentary Layers

Hanford boring logs were examined to discern textural layers of mud, silt, sand, and gravel within the Hanford and Ringold Formations and Cold Creek and Plio-Pleistocene Units. Individual layers were assigned to 1 of 13 material types (see Table L–6). The resulting lithological profiles—well name, well location, ground surface elevation, starting and ending depths of each layer, and each layer’s assignment to the textural types—were imported into a database program that generates geologic cross sections.

**Table L–6. Abundance of Textural Types in the
MODFLOW Final TC & WM EIS Groundwater Flow Model: Base Case**

Textural Type (Model Material Type Zone)	Unweighted (Cells)	Unweighted Percent	Weighted (km ³)	Weighted Percent
Hanford mud (1)	245	0.05	0.05	0.04
Hanford silt (2)	2,238	0.43	0.30	0.28
Hanford sand (3)	33,066	6.35	8.63	7.98
Hanford gravel (4)	131,826	25.30	17.69	16.37
Ringold sand (5)	27,333	5.25	10.27	9.51
Ringold gravel (6)	171,245	32.87	37.78	34.96
Ringold mud (7)	52,637	10.10	20.98	19.41
Ringold silt (8)	1,757	0.34	0.47	0.43
Plio-Pleistocene sand (9)	115	0.02	0.06	0.05
Plio-Pleistocene silt (10)	186	0.04	0.09	0.09
Cold Creek sand (11)	3,444	0.66	0.40	0.37
Cold Creek gravel (12)	31,724	6.09	2.35	2.18
Highly conductive Hanford formation (13)	64,223	12.33	8.97	8.30
Activated basalt (14) ^a	967	0.19	0.04	0.04

^a Zone 14 (Activated basalt) was assigned to mitigate rewetting problems (see Section L.5.1.1) and was encoded over nine model layers.

Note: To convert cubic kilometers to cubic miles, multiply by 0.2399.

Key: km³=cubic kilometers; MODFLOW=modular three-dimensional finite-difference groundwater flow model.

Hydrostratigraphic cross sections were constructed using HydroGeo Analyst, Version 3.0 (WHI 2005). Transects for these cross sections are located in the exact middle of a MODFLOW grid row (or column), and have a 100-meter (328-foot) buffer on either side. Thus, each cross section represents one row (or column) of the *TC & WM EIS* groundwater flow model. Transect length varies, but generally cross sections do not span the entire model domain. Lithological profiles for boreholes located within the

buffer area are projected onto the cross section for stratigraphic interpretation and interpolation. Elevations of contacts between the discrete geologic layers are determined by the resulting cross sections. Geologic layers within the cross section are encoded into the groundwater flow model based on elevation, from 165 meters (541 feet) above MSL down to the TOB surface. If more than one geologic layer is contained within one MODFLOW cell, the cell was assigned the properties of the hydrostratigraphic type with the largest total thickness over the range of elevations represented by the MODFLOW layer. At elevations near the water table (115 to 125 meters [377 to 410 feet]), this approach allows encoding of features on the order of several meters in thickness. At elevations deeper in the aquifer, the vertical grid spacing increases, and the minimum thickness of features that can be represented in the model ranges from several to tens of meters (see Figure L-18). The overall thickness of the model domain is approximately 250 meters (820 feet). At a minimum, features with thicknesses of about 10 percent of the overall model domain (25 meters [82 feet]) are represented in the model, which is appropriate for a regional-scale representation.

The hydrostratigraphy encoded into the *TC & WM EIS* groundwater flow model on the basis of HydroGeo Analyst cross sections was fine-tuned to remove artifacts associated with the encoding of adjacent transects, thus to ensure consistency with the final TOB surface, to eliminate rewetting problems (see Section L.5.1.1), and to add zonation within textural types. Fine-tuning involved re-encoding the MODFLOW stratigraphy to achieve the following:

- Remove incongruities due to extrapolation from the borehole out to the edge of the transect (seam).
- Remove incongruities due to truncation of the lithology that should extend out to the seam.
- Remove incongruities due to extrapolation of the lowest layer of the borehole down to the TOB surface.
- Remove incongruities due to the incorrect assignment to textural types.
- Remove inconsistent assignment to mud or silt from the same formation.
- Eliminate disconnects due to the lack of a shared face at the seam (edge contact only).
- Extend the lithology laterally or vertically to the TOB surface.
- Activate the basalt in the Gable Gap area at elevations where the water table fluctuates to mitigate rewetting problems. See Section L.5.1.1 for more-detailed information.
- Add a zone of high hydraulic conductivity extending from north of Gable Gap and through the Gable Gap, as well as south and southeast through the central area of the model domain. This change was a result of Local Users' Group input, Technical Review Group input, and testing that improved the match between model-simulated hydraulic heads and field-observed hydraulic heads across the model domain. See Section L.4.3.2.3 for additional details regarding this highly conductive material type.

In this *Final TC & WM EIS*, changes were made to the hydrostratigraphy to extend eastward the line where the hydrostratigraphy transitions from lower-conductivity materials in the 200-West Area to the higher-conductivity materials in the 200-East Area. A more detailed discussion of this change is included in Section L.1.6.

L.4.3.2.3 Identification of the Highly Conductive Hanford Formation

The *TC & WM EIS* groundwater flow model requires information about the spatial distribution of the hydraulic conductivity of sedimentary materials across the 1,518-square-kilometer (586-square-mile) Hanford Site. The sedimentary materials identified at Hanford include fluvial and lacustrine materials of the Miocene-Pliocene Ringold Formation, fluvial and eolian sediments of the Plio-Pleistocene and Cold Creek Units, and the Pleistocene glaciofluvial sediments resulting from cataclysmic flood events that are characteristic of the Hanford formation (Bjornstad and Lanigan 2007; Lindsey 1995; Reidel and Chamness 2007; Reidel et al. 2006; Serne et al. 2010). Sediments that make up the Hanford unconfined water table include members of all three units and vary spatially across the site.

Measured hydraulic conductivities of the Hanford sediments range from 0.0001 meters (0.00033 feet) per day for the finer Ringold mud sediments up to about 1 million meters (3,281,000 feet) per day for the Hanford coarser flood deposits (Cole et al. 2001; DOE 1988). The conductivity of the coarser sand- and gravel-dominated Hanford sediments is generally orders of magnitude greater than either the Cold Creek or Ringold sediments (Bjornstad et al. 2010). Estimates of the hydraulic conductivity for coarse Hanford materials range from about 10 to 6,000 meters (33 to 19,686 feet) per day, with an estimated maximum of 10,000 meters (32,810 feet) per day, in contrast to Ringold Formation sediments that have hydraulic conductivities ranging from 0.1 to approximately 200 meters (0.33 to approximately 656 feet) per day (Cole et al. 2001; DOE 1988). Cold Creek sediments have conductivities intermediate between Hanford and Ringold sediments (Bjornstad et al. 2010).

Several lines of evidence suggest that the spatial distribution and range of hydraulic conductivities of aquifer materials at Hanford have an important influence on the non-uniform, potentiometric surface that defines the water potential for the Hanford unconfined aquifer. The first is the field observation that the potentiometric surface is very steep across the western part of the Central Plateau near the 200-West Area and flattens considerably through Gable Gap and across the eastern parts of the Central Plateau near the 200-East Area (see Figures L-48, L-49, and L-50). The differences in the steepness of the groundwater potential gradient has been ascribed to contrasts in the lower hydraulic conductivities of Ringold sediments dominant in the 200-West Area relative to the higher hydraulic conductivities of Hanford and Cold Creek sediments that dominate aquifer materials near Gable Gap, the 200-East Area, and areas farther east (Bjornstad et al. 2010).

The second line of evidence is field measurements of hydraulic conductivity (see Figure L-42) that indicate the range in hydraulic conductivity among the geologic materials present at the Hanford water table. As Figure L-42 shows, the conductivity of Hanford (and Cold Creek) sediments implies a much higher and broader range of saturated hydraulic conductivities relative to the Ringold sediments. The highest hydraulic conductivities measured at Hanford occur in the Hanford and Cold Creek sediments that stretch in a southeast direction from the 100 B/C Area, through Gable Gap, across the Central Plateau through the 200-East Area, and into the 300 Area. Some of this area, particularly near Gable Gap and the 200-East Area, has been mapped as buried paleochannels, where the Pleistocene flooding has deposited Hanford formation materials directly on the TOB (Bjornstad et al. 2010).

The third line of evidence is available field data showing that the calibration of all groundwater flow models developed for the Hanford unconfined aquifer has required a zone of high-conductivity material at the water table to appropriately reproduce the contrast in the groundwater potential gradient from the western to eastern portion of Hanford (Cole et al. 2001; Thorne et al. 2006; Wurster et al. 1995). The location of those high-conductivity materials that ensure the best calibration of the models is based on the field data for hydraulic conductivity measured in aquifer pump tests (see Figure L-42).

L.4.4 Material Properties

The different textural types in the Hanford, Ringold, and other sedimentary hydrostratigraphic units are characterized by different material properties. Material properties required for the groundwater flow model include hydraulic conductivity, specific storage, and specific yield. Hydraulic conductivity is a measure of how easily water moves through pore spaces. Specific storage of a saturated aquifer is the amount of water that a given volume of aquifer material will release under a unit change in hydraulic head. Specific yield is the volumetric fraction of the bulk aquifer volume that an aquifer will yield when all the water is allowed to drain out of it under the forces of gravity.

Material properties for unconsolidated sediments below the water table are required for MODFLOW calculations. In MODFLOW, material of a given type can have only one value for a property, e.g., hydraulic conductivity. Each of the 14 material types encoded in the *TC & WM EIS* groundwater flow model (see Table L-6) has a unique combination of values for the several material properties. Material properties in the *Final TC & WM EIS* Base Case model are the same as the material properties used in the *Draft TC & WM EIS* Base Case model. The sensitivity of the *Final TC & WM EIS* Base Case model to changes in material properties, as well as to changes in other parameters, is evaluated and discussed further in Section L.7.

L.5 MODEL INPUTS – ALGORITHM SELECTION, PARAMETERS, AND SETTINGS

Some model inputs are independent of site data. These inputs include initial conditions and settings specifying how to make the calculations and how to modify the model to eliminate numerical instabilities that may arise. Some of the inputs are required by the MODFLOW software (e.g., rewetting rules), while others are common to all groundwater simulation models (e.g., time-stepping settings and initial conditions). These data-independent model inputs are discussed in the following sections.

L.5.1 Rewetting Methods

MODFLOW allows for cells to become dry (inactive) if the simulated head falls below the elevation of the cell bottom. Conversely, if the simulated head rises above the cell bottom or the laterally adjacent cells are wet, a currently dry cell can become wet. This process is called rewetting. The rewetting rules and parameters used to develop the *TC & WM EIS* groundwater flow model were generally the default parameters of MODFLOW 2000 (USGS 2004). The settings selected in Visual MODFLOW for the *TC & WM EIS* groundwater flow model are given in Table L-7.

Table L-7. Visual MODFLOW Rewetting Settings

Option	Setting
Activate cell wetting	On
Wetting threshold	0.1
Wetting interval	1 (iteration)
Wetting method	From below
Wetting head	Calculated from neighboring cells
Head value in dry cells	-1×10^{30} (meters)
Minimum saturated thickness for bottom layer	0.01 (meters)

Note: To convert meters to feet, multiply by 3.281.

Key: MODFLOW=modular three-dimensional finite-difference groundwater flow model.

L.5.1.1 Mitigation of Rewetting Problems

Rewetting problems emerged during model development that required mitigating actions. The rewetting problems were encountered in areas within the model where the water table and the TOB (inactive model cells) were at or near the same elevation and resulted in dry model cells in areas that should have been wet, based on the elevation of the water table in surrounding active model cells. Based on the model's rewetting settings, once an active model cell becomes dry, it can only be rewet from an active wet model cell below the active dry model cell. In the problem cases, the cell below the active dry model cell was an inactive cell that represented the TOB in that area within the model. This configuration would not allow the active dry model cell to rewet even though water table elevations in surrounding active wet model cells would normally result in rewetting of the problem dry model cell. This problem was significant enough that mitigation was required in the area of the model that represents Gable Gap.

To mitigate the rewetting problem in the Gable Gap area within the model, inactive cells that represented the TOB were made active and assigned hydraulic conductivity values that are more than 500 times lower than that of Hanford and Ringold muds (0.001 meters [0.00328 feet] per day). Making the inactive cell active and using a low hydraulic conductivity value allowed the active water table cells above the TOB to rewet from below, but maintained the TOB in this region as a low-permeability boundary. The TOB was activated in the Gable Gap area within the model between 124 meters (407 feet) above MSL and 115 meters (377 feet) above MSL.

L.5.2 Time-Stepping Settings

The *TC & WM EIS* groundwater flow model period of analysis is 10,000 years, from 1940—prior to the start of operations—to 11,940. In addition to the model preconditioning described in Section L.5.4, Initial Head Distribution, the model is further preconditioned by simulating CYs 1940 through 1943 (pre-Hanford) in transient mode prior to the occurrence of any anthropogenic recharge influxes (see Section L.4.2.5). The model then continues running in transient mode to capture the time-varying anthropogenic recharge influxes and the resulting water table fluctuations. Anthropogenic inputs are applied in 1-year stress periods beginning in 1944. The final stress period begins in 2022 and ends in 11,940. A stress period is defined as a period of time during the model simulation when all of the model's boundary conditions are static (i.e., unchanging).

L.5.3 Numerical Engine Selection and Parameterization

The numeric engine selected for simulating groundwater flow was MODFLOW 2000, Version 1.15.00 (USGS 2004), which is public domain software supported by Visual MODFLOW, Version 2009.1. The settings selected in Visual MODFLOW for the *TC & WM EIS* groundwater flow model are given in Table L-8.

Table L–8. Visual MODFLOW Numerical Solution Settings

Option	Setting
Simultaneous equation solver	Preconditioned conjugate-gradient (PCG2)
Preconditioning method	Modified incomplete Cholesky
Cholesky relaxation parameter	0.98
Maximum outer iterations	500
Maximum inner iterations	200
Head change criterion	0.01 (meter)
Residual criterion	5,000
Damping factor	1
Printout interval	10 (time steps)

Note: To convert meters to feet, multiply by 3.281.

Key: MODFLOW=modular three-dimensional finite-difference groundwater flow model.

The preconditioned conjugate-gradient package for solving simultaneous equations is described in USGS Water-Resources Investigations Report 90-4048 (Hill 1990). Modified incomplete Cholesky preconditioning of the hydrogeologic parameter matrix is efficient on scalar (nonvector) computers (SWS 2009). Outer iterations vary the preconditioned matrix of hydrogeologic parameters of the flow system (e.g., transmissivity, saturated thickness) in an approach toward the solution. Inner iterations continue until the user-defined maximum number of inner iterations has been executed or the final convergence criteria are met. Outer iterations continue until the final convergence criteria are met on the first inner iteration after an update. Both the head change and residual criteria determine convergence of the solver. The head change criterion is used to judge the overall solver convergence; the residual criterion is used to judge the convergence of the inner iterations of the solver. The damping factor allows the user to reduce the head change calculated during each successive outer iteration.

L.5.4 Initial Head Distribution

Pre-Hanford head observation data are not available. The *TC & WM EIS* groundwater flow model was assigned an initial arbitrarily high water table and run in transient mode for 500 years to simulate pre-Hanford (1940–1943) conditions with only natural recharges applied per the *Technical Guidance Document* (DOE 2005). This initial 500-year model run approached long-term, steady state conditions, which were assumed to represent pre-Hanford conditions.

L.5.5 Layer Properties

The layer property package used in the *TC & WM EIS* groundwater flow model is the Block-Centered Flow (BCF) package, which simulates flow in an unconfined aquifer. See Table L–9 for the BCF package run settings.

Table L–9. Visual MODFLOW BCF Package Settings

Settings	Values
CUNIT	1
Extension	.BCF
HDRY	-1×10^{30}
LUNIT	11

Key: BCF=Block-Centered Flow; MODFLOW=modular three-dimensional finite-difference flow model.

L.6 CALIBRATION STRATEGY

The *TC & WM EIS* groundwater flow model was calibrated to heads observed beginning in 1948. Artificial recharges during Hanford operations, especially those from 1944 to the mid-1990s, produced mounding of groundwater underneath the 200-East and 200-West Areas on the Central Plateau of Hanford (see Section L.4.2.5). Groundwater mounding influenced the local direction of flow and transport and consequently needed to be accurately represented in the long-term groundwater flow model.

Model calibration to head was conducted in the following three process steps:

1. Prepare a calibration data set consisting of observed groundwater (head) levels across Hanford during the calibration period of 1948–2008 and the preconditioning period of 1940–1943. This data set was updated between the *Draft* and *Final TC & WM EIS*.
2. Specify the model calibration criteria, that is, how similar model results need to be compared with the observations in the calibration data sets. The model calibration criteria are unchanged between the *Draft* and *Final TC & WM EIS*.
3. Conduct the final model calibration using structured and Monte Carlo optimization methods. This method was used when calibrating the *Draft TC & WM EIS* groundwater flow model, and the details of that calibration process are presented in the *Draft TC & WM EIS*, Appendix L, Section L.9.

For the *Final TC & WM EIS* groundwater flow model, a calibration and uncertainty analysis was conducted to determine the model's sensitivity to changes in a variety of parameter values. This sensitivity analysis was used as part of the final calibration.

The technical approach to these steps and the results are discussed in Sections L.6, L.7, and L.8.

L.6.1 Calibration Data Set

The *TC & WM EIS* groundwater flow model was calibrated to head data collected between 1948 and 2008 for a large number of selected wells scattered across the site. The data came from the HydroDat database of measured water table elevations provided by CH2M HILL and accepted by the *TC & WM EIS* team as quality assurance complete (CHPRC 2009a). This database includes approximately 136,000 observations at approximately 1,900 discrete locations. Wells were excluded from use in the head observation data set under the following conditions:

- They were closer than 600 meters (1,969 feet) to the Columbia River to remove the periodic fluctuations in the river stage from the head observation data.
- They were outside the active model domain because the model is not being calibrated in these areas.
- They were screened in basalt because these observations measure head values within confined aquifers that are not part of this flow model calibration.
- There were obvious data recording or entry errors, wells and/or observations with outlier data based on review of data in adjacent wells, or wells that were located in dry or inactive model cells.

Table L–10 details the number of well locations and observations that were removed from the original head observation data set.

Table L–10. Number of Well Locations and Head Observations Removed from Original Head Observation Data Set

Change	Number of Observations Remaining	Number of Wells Remaining
Original head observation data set	136,282	1,923
Removal of wells with data qualifiers	133,308	1,901
Removal of wells outside of the horizontal model domain	132,591	1,804
Removal of wells located within 600 meters (1,968 feet) of the Columbia River	99,224	1,430
Removal of wells screened in basalt	90,174	1,266
Removal of wells with duplicate locations	87,543	1,160
Averaging of observations for each well, screen, and year such that each well and/or screen has a single observation for each year	20,408	1,160
Edit and deletion of well locations and observations per detailed hydrograph and model review	15,996	713

The data from the remaining 713 wells were encoded into the flow model for use in the head calibration.

L.6.2 Calibration Criteria

The calibration data set was used to assess the ability of the model to accurately simulate water levels and flow direction in the past, which is an indication of its ability to accurately simulate water levels and flow direction in the future. The calibration criteria define acceptable model performance in terms of measures of similarity (difference) between observed and simulated values. The model calibration criteria are as follows:

- Residuals (differences between observed and modeled heads) should be reasonably distributed.
 - Residual distribution should be reasonably normal.
 - The mean residual should be approximately 0.
 - The number of positive residuals should approximate the number of negative residuals.
 - The correlation coefficient (calculated versus observed) should be greater than 0.9.
 - The RMS error (calculated versus observed) should be less than 5 meters (16.4 feet), approximately 10 percent of the gradient in the water table elevation.
- The residual distribution should meet the needs of this *TC & WM EIS*.
 - Residuals in the 200-East Area should be distributed similarly to those in the 200-West Area.
 - The residuals should be evenly distributed through the calibration period (1948–2008).
 - The residuals should be evenly distributed across the site.

- The calibrated parameters should compare reasonably well with field-measured values.
- Parameters should be reasonably uncorrelated. Correlation among the parameters is a symptom of a poorly posed problem with many nonunique solutions.

These criteria were used to assess the final head calibrations and are unchanged between the *Draft* and *Final TC & WM EIS*.

L.6.3 Development of Objective Function

The groundwater flow model was calibrated to observed hydraulic heads across Hanford during the calibration period (1948–2008). The objective of the head calibration was to minimize the difference between the model-simulated head values and the field-observed head values during the calibration period. All head observation data used in the head calibration were weighted equally. No concentration calibration was performed as part of the flow model development. Concentration calibration of the groundwater transport model is discussed in Appendix O.

L.7 CALIBRATION AND UNCERTAINTY ANALYSIS

The *Draft TC & WM EIS* analysis and results, along with public comments, led to a more detailed exploration of the model sensitivity to changes in the following model parameters:

- Hydraulic conductivity values
- Storage properties (specific yield [Sy])
- GHB head and conductance
- Background and anthropogenic recharge
- River conductance

RMS error was the measure of model sensitivity to each parameter.

L.7.1 Hydraulic Conductivity

No changes to hydraulic conductivity values were made in the *Final TC & WM EIS* flow model. To determine the sensitivity of the flow model to varying the hydraulic conductivity values across a reasonable range for the 13 material types used, a Monte Carlo analysis with 5,000 model realizations was developed. Table L-11 provides the range of hydraulic conductivity values applied in the analysis.

Table L–11. Range of Hydraulic Conductivity Values Used in Monte Carlo Analysis

Material Type (Model Zone)	Range of Horizontal Hydraulic Conductivity (Kh) Values (meters per day)
Hanford mud (1)	0.01 – 1.0
Hanford silt (2)	0.8 – 10.0
Hanford sand (3)	40.0 – 200.0
Hanford gravel (4)	75.0 – 300.0
Ringold sand (5)	0.5 – 5.0
Ringold gravel (6)	8.0 – 25.0
Ringold mud (7)	0.2 – 2.0
Ringold silt (8)	0.5 – 5.0
Plio-Pleistocene sand (9)	10.0 – 100.0
Plio-Pleistocene silt (10)	3.0 – 30.0
Cold Creek sand (11)	30.0 – 110.0
Cold Creek gravel (12)	0.1 – 120.0
Highly conductive Hanford formation (13)	1,500.0 – 5,000.0

Note: Vertical hydraulic conductivity = $K_h \times 0.1$. To convert meters to feet, multiply by 3.281

In each of the 5,000 realizations, all 13 material types were varied randomly across the ranges listed in Table L–11. The results of this analysis show that the model is sensitive (in terms of the RMS error metric) to changes in hydraulic conductivity values across the ranges listed. Figure L–24 shows the range of RMS error values resulting from the approximately 4,000 converged model runs.

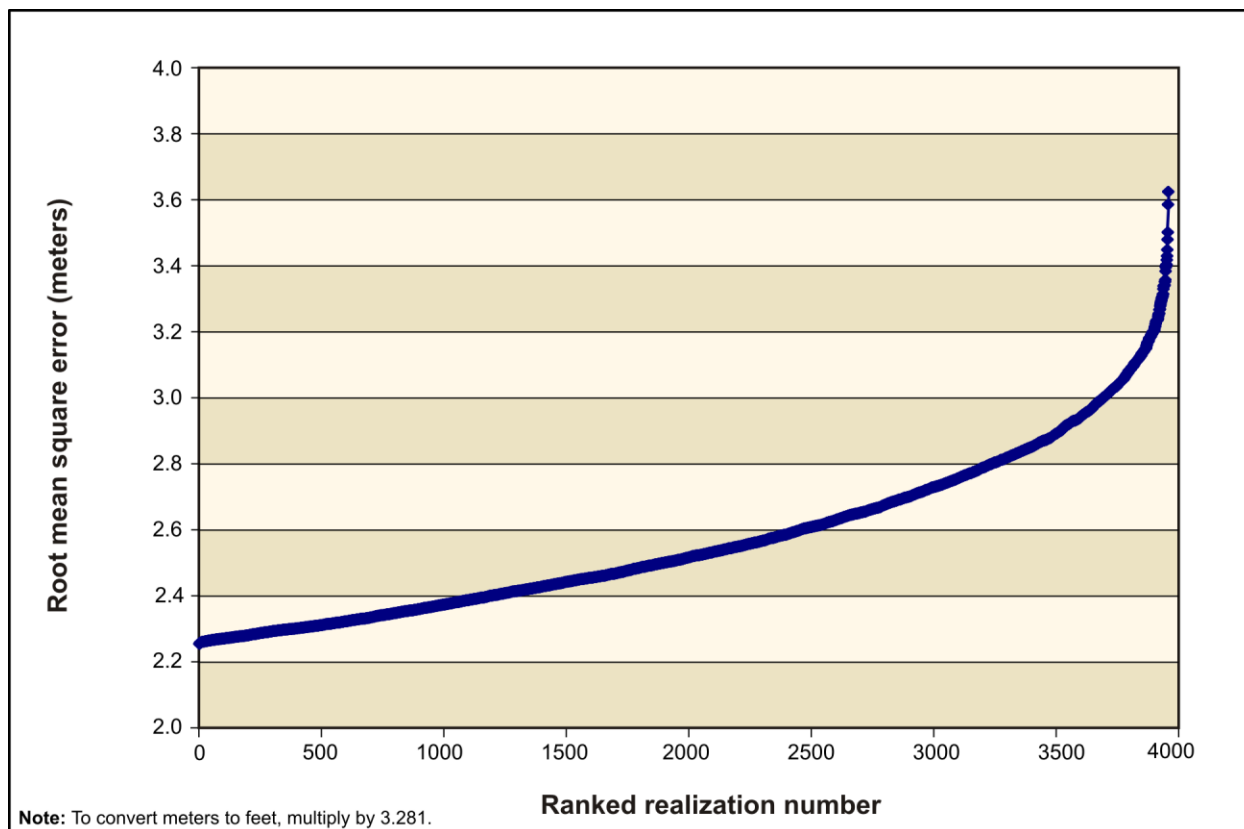


Figure L–24. Range of Root Mean Square Error for Varying Hydraulic Conductivity Values

L.7.2 Storage Properties (Specific Yield) Analysis

No changes to storage property values (expressed as Sy values) were made in the *Final TC & WM EIS* flow model. To determine the sensitivity of the model to varying the storage property values across a reasonable range for the 13 material types, a Monte Carlo analysis with 5,000 model realizations was developed. Approximately 4,700 were run to completion through the calibration period (1948 through 2008). Approximately 300 of the 5,000 runs did not converge. Table L-12 provides the range of Sy values applied in the analysis.

Table L-12. Range of Storage Property (Sy) Values Used in Monte Carlo Analysis

Material Type (Model Zone)	Range of Storage Property (Sy) Values
Hanford mud (1)	0.15 – 3.0
Hanford silt (2)	0.15 – 3.0
Hanford sand (3)	0.15 – 3.0
Hanford gravel (4)	0.15 – 3.0
Ringold sand (5)	0.15 – 3.0
Ringold gravel (6)	0.15 – 3.0
Ringold mud (7)	0.15 – 3.0
Ringold silt (8)	0.15 – 3.0
Plio-Pleistocene sand (9)	0.15 – 3.0
Plio-Pleistocene silt (10)	0.15 – 3.0
Cold Creek sand (11)	0.15 – 3.0
Cold Creek gravel (12)	0.15 – 3.0
Highly conductive Hanford formation (13)	0.15 – 3.0

Key: Sy=specific yield.

In each of the 5,000 realizations, all 13 material types were varied randomly across the ranges listed in Table L-12. The results of this analysis show that the model is not sensitive (in terms of RMS error) to changes in Sy values across the ranges listed. Figure L-25 shows the range of RMS error values resulting from the approximately 4,700 converged model runs.

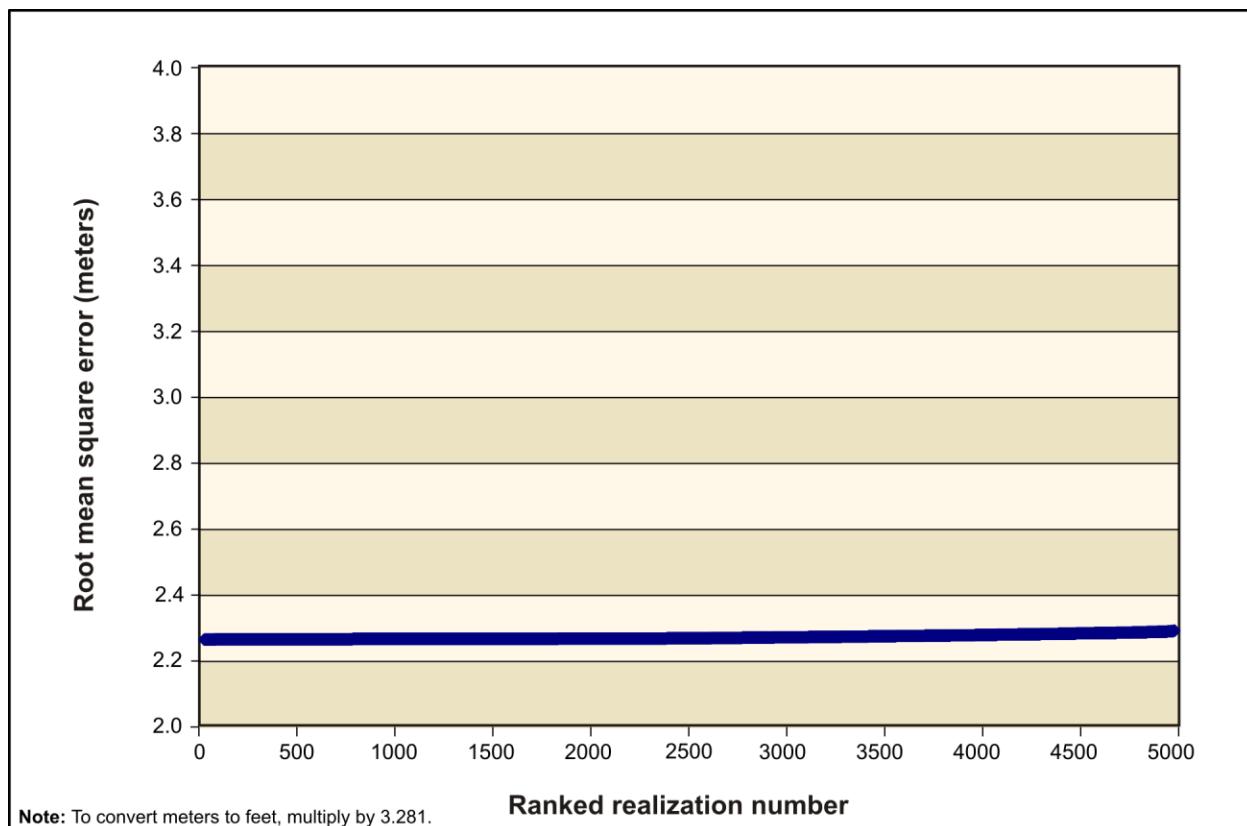


Figure L–25. Range of Root Mean Square Error for Varying Storage Property (Specific Yield) Values

L.7.3 GHB Head and Conductance

L.7.3.1 GHB Head

No changes to GHB head values were made in the *Final TC & WM EIS* flow model. To determine the sensitivity of the model to varying the GHB head values across a reasonable range, head values at each of the GHB areas in the model (Cold Creek, Dry Creek, and Rattlesnake Mountain) were varied by adjusting the base values by +4, +2, 0, -2, and -4 meters. This structured approach to varying the GHB head values resulted in 125 model realizations, all of which converged. The results of this analysis show that the model was not highly sensitive (in terms of RMS error) to changes in GHB head values across the ranges listed. Figure L–26 shows the range of RMS error values resulting from the 125 converged model runs.

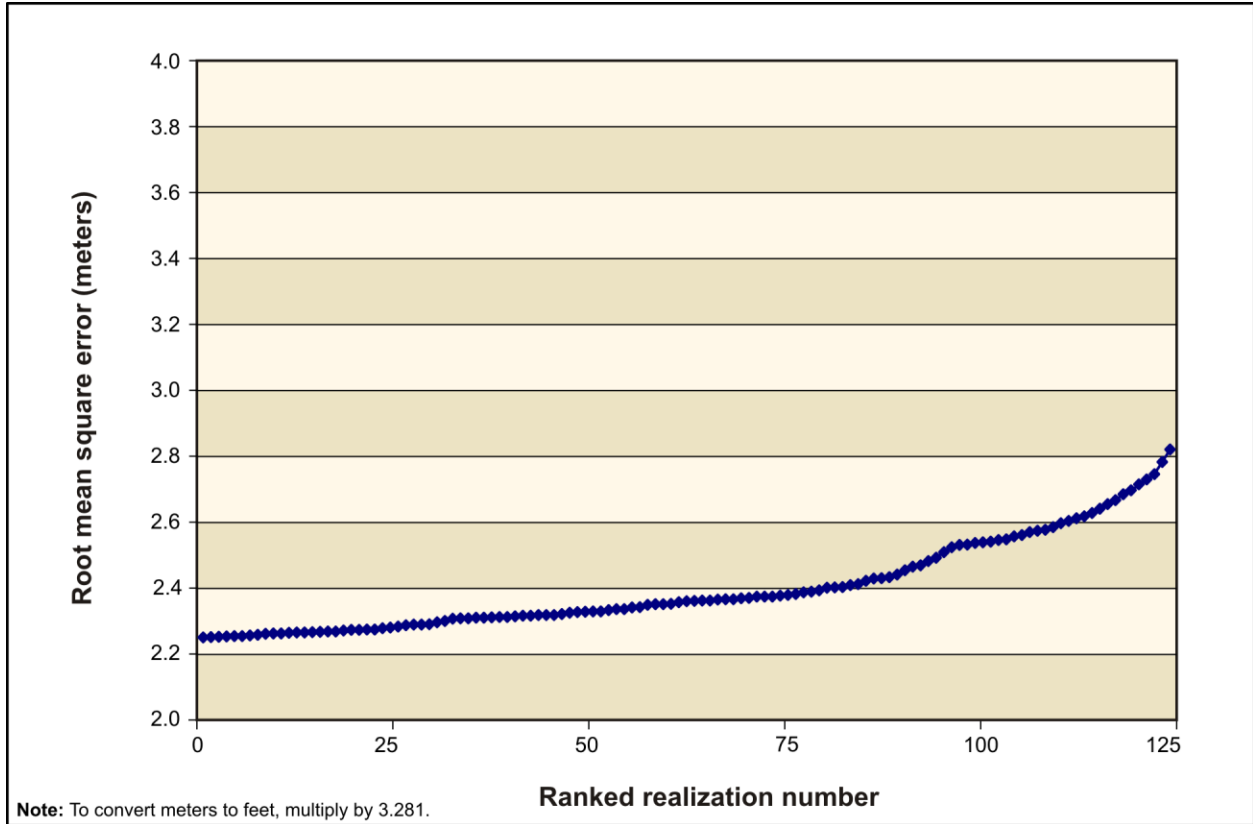


Figure L-26. Range of Root Mean Square Error for Varying Generalized Head Boundary Head Values

L.7.3.2 GHB Conductance

No changes to GHB conductance values were made in the *Final TC & WM EIS* flow model. To determine the sensitivity of the model to varying the GHB conductance values across a reasonable range, conductance values at each of the GHB areas in the model (Cold Creek, Dry Creek, and Rattlesnake Mountain) were varied by multiplying the base values by 0.1, 0.5, 1.0, 5.0, and 10.0. This structured approach to varying the GHB conductance values resulted in 125 model realizations, most of which converged. The results of this analysis show that the model was not highly sensitive (in terms of RMS error) to changes in GHB head values across the ranges listed. Figure L-27 shows the range of RMS error values resulting from the 122 converged model runs.

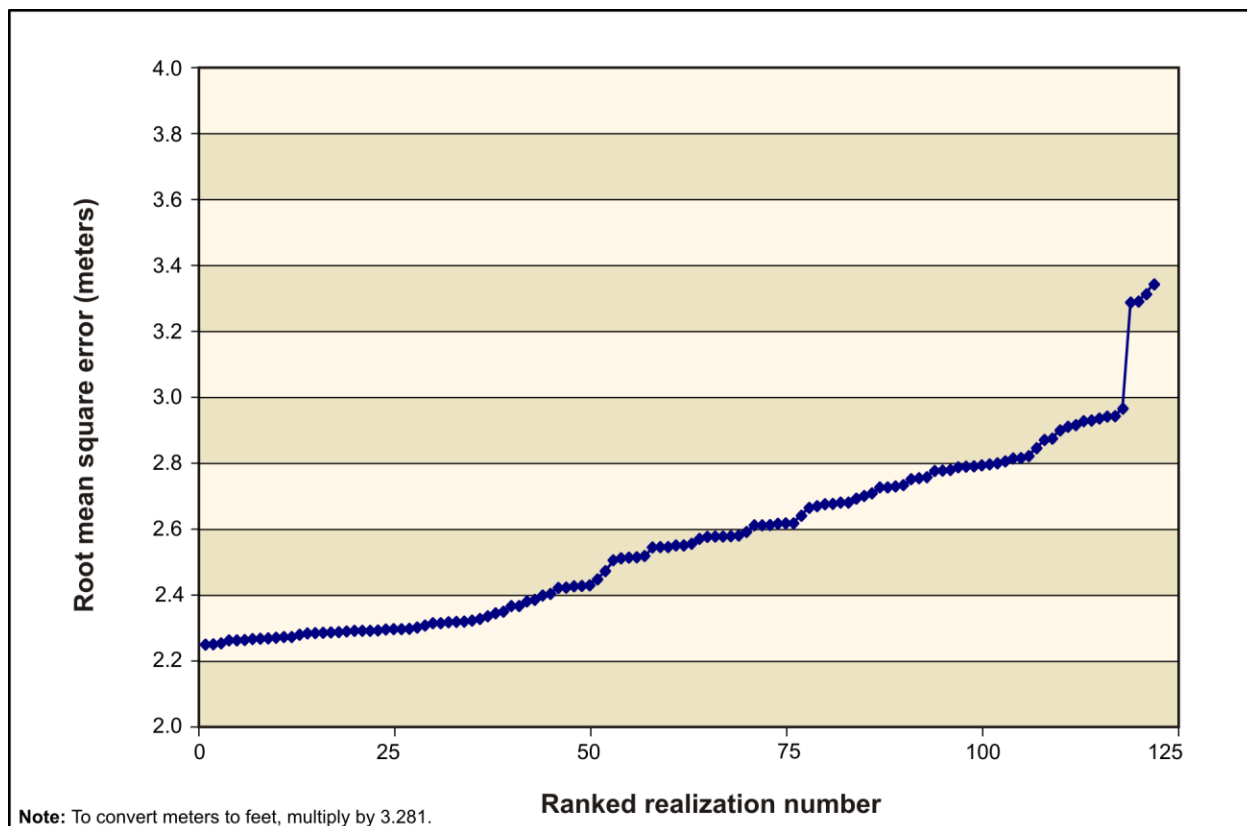


Figure L–27. Range of Root Mean Square Error for Varying Generalized Head Boundary Conductance Values

L.7.4 Background and Anthropogenic Recharge

L.7.4.1 Background Recharge

No changes to background recharge values were made in the *Final TC & WM EIS* flow model. To determine the sensitivity of the model to varying the background recharge values across a reasonable range, recharge values for sitewide and City of Richland recharge zones in the model were varied as shown in Table L–13.

Table L-13. Range of Background Recharge Values Considered

Recharge Zone	Recharge Values (millimeters per year)
Sitewide	0.5
	1.5
	2.5
	3.5
	4.5
	5.5
	6.5
	7.5
	8.5
	9.5
	10.5
City of Richland	5
	15
	25
	35
	45
	55
	65
	75
	85
	95
	105

This structured approach to varying the background recharge values (including those of the Base Case) resulted in 122 model realizations, all of which converged. The results of this analysis show that the model was not sensitive (in terms of RMS error) to changes in background recharge values across the ranges listed. Figure L-28 shows the range of RMS error values resulting from the 122 converged model runs.

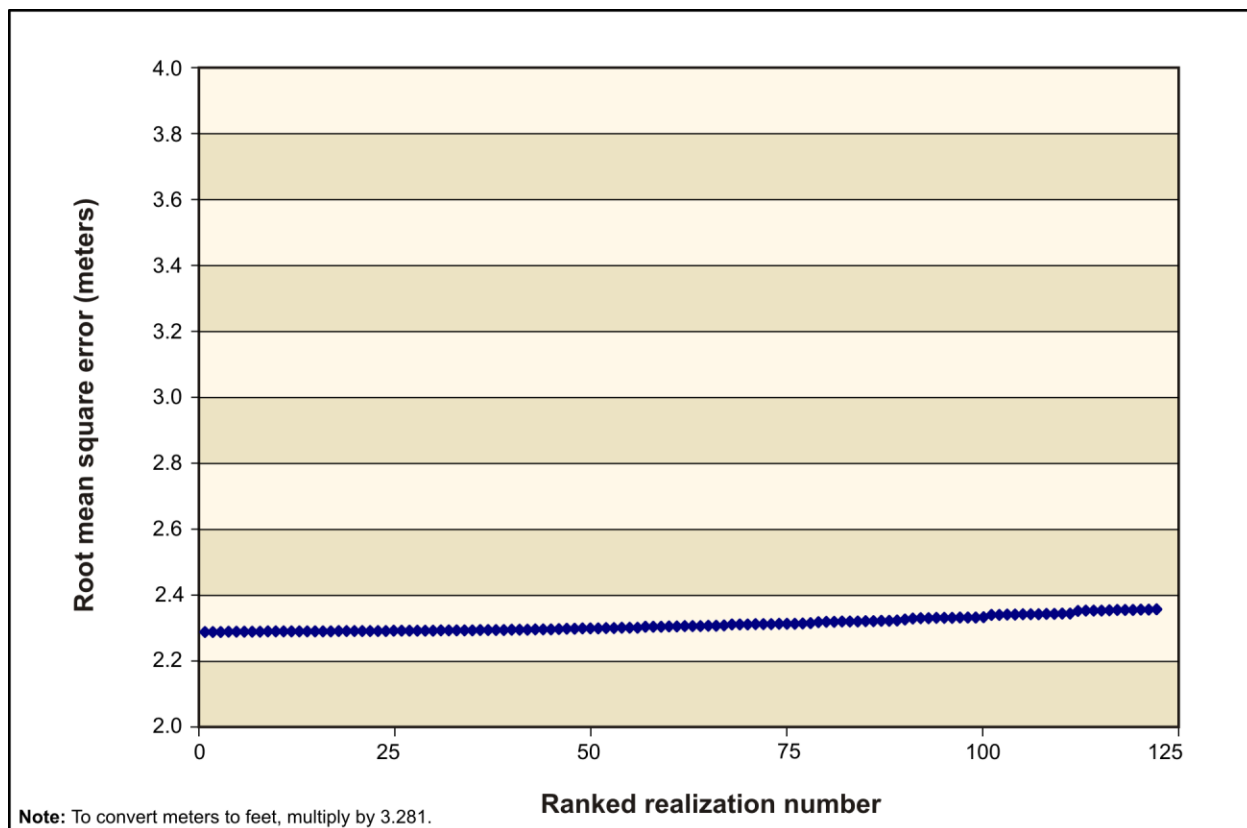


Figure L-28. Range of Root Mean Square Error for Varying Background Recharge Values

L.7.4.2 Anthropogenic Recharge

No changes to anthropogenic recharge values were made in the *Final TC & WM EIS* flow model. To determine the sensitivity of the model to varying the anthropogenic recharge values across a reasonable range, recharge values for approximately 130 recharge zones were varied randomly between 50 percent and 150 percent of the base values. Each recharge zone was varied independently from all other recharge zones in each of 5,000 model realizations, most of which converged. The results of this analysis show that the model was not sensitive (in terms of RMS error) to changes in anthropogenic recharge values across the ranges listed. Figure L-29 shows the range of RMS error values resulting from the 4,970 converged model runs.

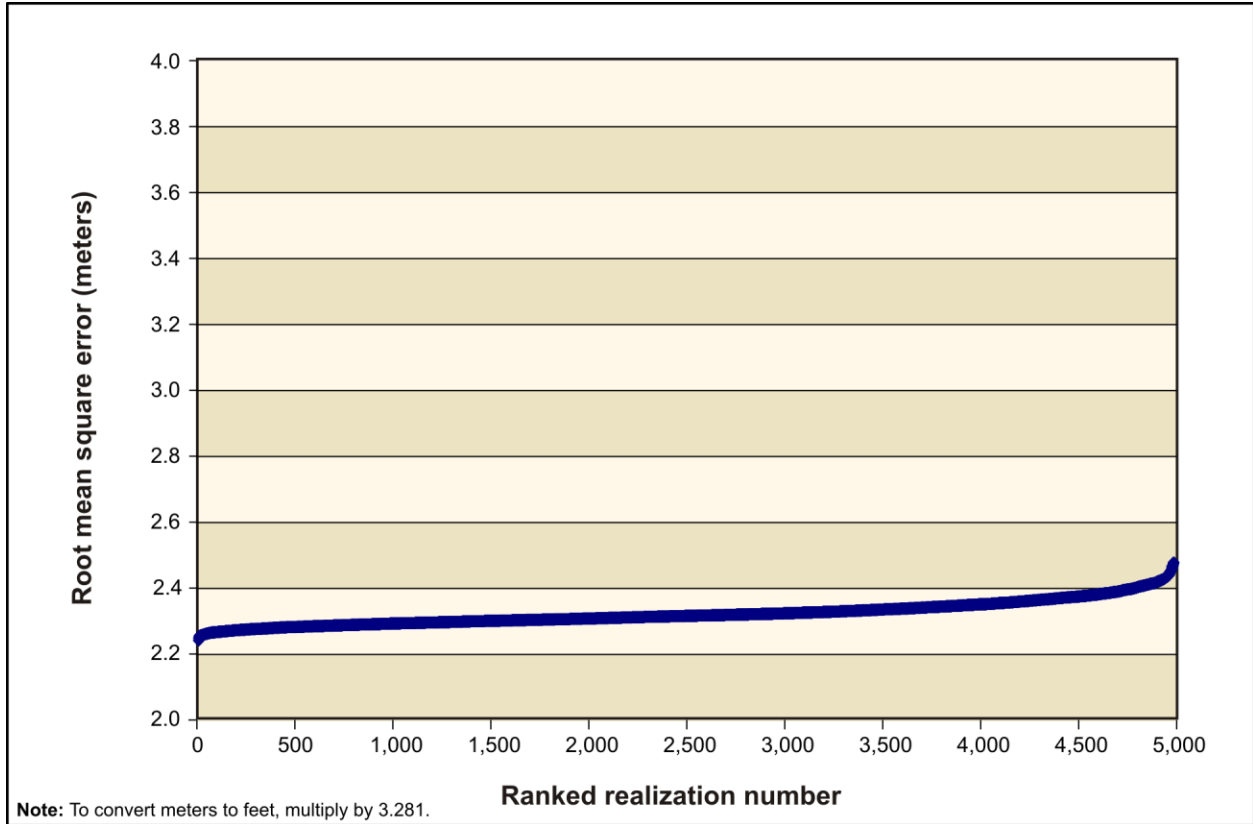


Figure L-29. Range of Root Mean Square Error for Varying Anthropogenic Recharge Values

L.7.5 River Conductance

No changes to river conductance values were made in the *Final TC & WM EIS* flow model. To determine the sensitivity of the model to varying the river conductance values across a reasonable range, river conductance values were varied using seven multipliers (0.1, 0.2, 0.5, 1.0, 2.0, 5.0, and 10.0) applied independently to the Columbia River and Yakima River reach base conductance values. Varying the conductance values in this structured way resulted in 49 model realizations, most of which converged. The results of this analysis show that the model was not sensitive (in terms of RMS error) to changes in river conductance values across the ranges listed. Figure L-30 shows the range of RMS error values resulting from the 48 converged model runs.

The above analyses demonstrated that the model was sensitive to changes in hydraulic conductivity values and not highly sensitive to the remaining parameters that were evaluated. The following section provides detailed results from three models that span the best one-third (in terms of RMS error) of models evaluated in the above hydraulic conductivity analysis.

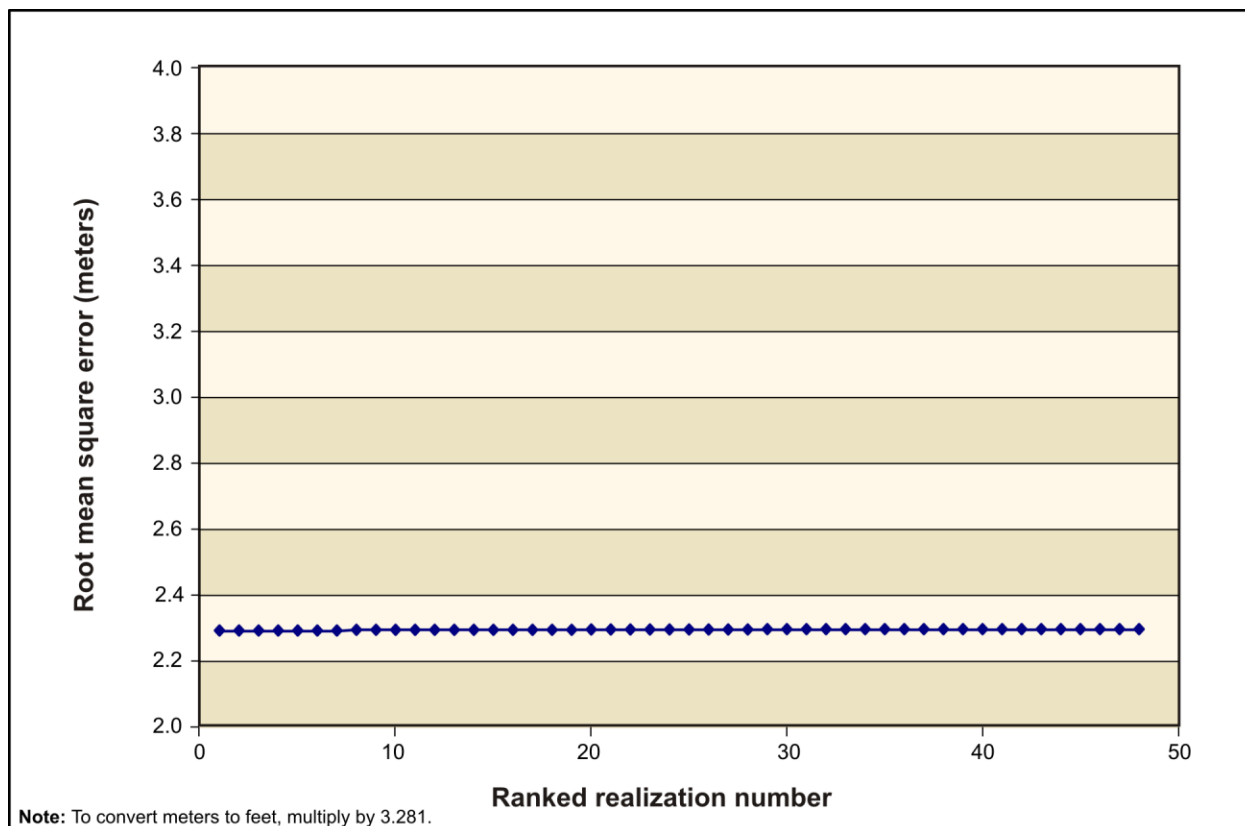


Figure L-30. Range of Root Mean Square Error for Varying River Conductance Values

L.8 FLOW MODEL PERFORMANCE – TOP ONE-THIRD OF MODELS

Results from three models that are among the best one-third (in terms of RMS error) evaluated in the preceding section's sensitivity analysis for hydraulic conductivity are provided below. The ranking identifiers for each of the three models are as follows:

- 95th percentile (better than 95 percent of model realizations in terms of lowest RMS error), this being selected as the *Final TC & WM EIS* Base Case flow model.
- 100th percentile (best model realization in terms of lowest RMS error).
- 66th percentile (better than 66 percent of model realizations in terms of lowest RMS error).

The purpose of reviewing and evaluating the results of these three models is to determine whether there are significant differences in the model behavior across the top one-third of the flow models as ranked in the hydraulic conductivity sensitivity analysis.

L.8.1 Results from the 95th Percentile (Base Case) Flow Model

L.8.1.1 Calibration Acceptance

Table L–14 provides a restatement of the flow model calibration criteria discussed in Section L.6.2, along with an assessment of the 95th percentile (Base Case) flow model’s performance against each criterion. Specific data illustrative of such performance are reflected in Tables L–15 and L–16 and Figures L–31 through L–42.

**Table L–14. Summary of the 95th Percentile (Base Case) Flow Model
Performance Compared with the Calibration Acceptance Criteria**

Flow Model Calibration Acceptance Criteria	95th Percentile (Base Case) Flow Model Performance
Residual distribution should be reasonably normal.	Residual distribution is reasonably normal (see Figure L–31).
The mean residual should be approximately 0.	Residual mean = 0.122 meters (0.400 feet) (see Figure L–32).
The number of positive residuals should approximate the number of negative residuals.	Positive residuals approximately equal negative residuals (see Figure L–31).
The correlation coefficient (calculated versus observed) should be greater than 0.9.	Correlation coefficient = 0.973 (see Figure L–32).
The root mean square (RMS) error (calculated versus observed) should be less than 5 meters (16.4 feet), approximately 10 percent of the gradient in the water table elevation.	RMS error = 2.281 meters (7.484 feet) (see Figure L–32).
Residuals in the 200-East Area should be distributed similarly to those in the 200-West Area.	Residuals in the 200-East and 200-West Areas are distributed similarly (see Figures L–33 and L–34).
The residuals should be evenly distributed over time.	Residuals are approximately evenly distributed over time (see Figures L–35, L–36, L–37, and L–38).
The residuals should be evenly distributed across the site.	Residuals are approximately evenly distributed across the site (see Figures L–39, L–40, and L–41).
The calibrated parameters should compare reasonably well with field-measured values.	Calibrated hydraulic conductivity values are listed in Table L–15 and compare reasonably with field-measured values for material types to which the model is sensitive (i.e., Hanford formation and Ringold Formation material types). Figure L–42 provides field-measured values from aquifer pumping tests (Cole et al. 2001).
Parameters should be reasonably uncorrelated.	Hydraulic conductivity parameters are reasonably uncorrelated (see Table L–15 for the key to model material type zones and Table L–16 for the correlation coefficient matrix).

**Table L–15. 95th Percentile (Base Case) Flow Model
Calibrated Hydraulic Conductivity Values**

Material Type (Model Zone)	Hydraulic Conductivity (K _x) ^a	Hydraulic Conductivity (K _y) ^b	Hydraulic Conductivity (K _z) ^c
Hanford mud (1)	0.171	0.171	0.0171
Hanford silt (2)	6.8	6.8	0.68
Hanford sand (3)	123.6	123.6	12.36
Hanford gravel (4)	156.0	156.0	15.6
Ringold sand (5)	3.57	3.57	0.357
Ringold gravel (6)	19.2	19.2	1.92
Ringold mud (7)	1.514	1.514	0.1514
Ringold silt (8)	1.51	1.51	0.151
Plio-Pleistocene sand (9)	96.8	96.8	9.68
Plio-Pleistocene silt (10)	5.81	5.81	0.581
Cold Creek sand (11)	99.13	99.13	9.913
Cold Creek gravel (12)	62.7	62.7	6.27
Highly conductive Hanford formation (13)	3982.0	3982.0	398.2
Activated basalt (14)	0.001	0.001	0.0001

^a Hydraulic conductivity with respect to the *x* axis, meters per day.

^b Hydraulic conductivity with respect to the *y* axis, meters per day.

^c Hydraulic conductivity with respect to the *z* axis, meters per day.

Note: To convert meters to feet, multiply by 3.281.

Table L–16. Flow Model Hydraulic Conductivity Parameter Correlation Coefficient Matrix

Model Zone	1	2	3	4	5	6	7	8	9	10	11	12	13
1	1.00	-0.01	0.00	0.02	-0.02	0.00	0.00	0.02	0.00	0.04	0.00	0.01	0.01
2	-0.01	1.00	0.02	0.03	-0.03	0.01	-0.01	0.00	-0.03	0.02	-0.02	-0.01	-0.02
3	0.00	0.02	1.00	-0.03	0.02	0.00	0.02	-0.02	-0.02	0.01	0.01	-0.02	-0.02
4	0.02	0.03	-0.03	1.00	0.00	-0.03	-0.01	0.00	0.02	0.02	-0.01	-0.02	0.02
5	-0.02	-0.03	0.02	0.00	1.00	-0.02	0.01	-0.01	0.00	0.02	-0.02	0.00	-0.01
6	0.00	0.01	0.00	-0.03	-0.02	1.00	-0.03	-0.01	-0.01	0.01	0.03	-0.02	0.00
7	0.00	-0.01	0.02	-0.01	0.01	-0.03	1.00	0.00	0.00	0.00	0.01	0.00	-0.03
8	0.02	0.00	-0.02	0.00	-0.01	-0.01	0.00	1.00	-0.01	0.01	0.01	0.01	-0.01
9	0.00	-0.03	-0.02	0.02	0.00	-0.01	0.00	-0.01	1.00	0.02	0.01	0.00	-0.03
10	0.04	0.02	0.01	0.02	0.02	0.01	0.00	0.01	0.02	1.00	0.02	0.00	-0.03
11	0.00	-0.02	0.01	-0.01	-0.02	0.03	0.01	0.01	0.01	0.02	1.00	0.02	-0.02
12	0.01	-0.01	-0.02	-0.02	0.00	-0.02	0.00	0.01	0.00	0.00	0.02	1.00	0.01
13	0.01	-0.02	-0.02	0.02	-0.01	0.00	-0.03	-0.01	-0.03	-0.03	-0.02	0.01	1.00

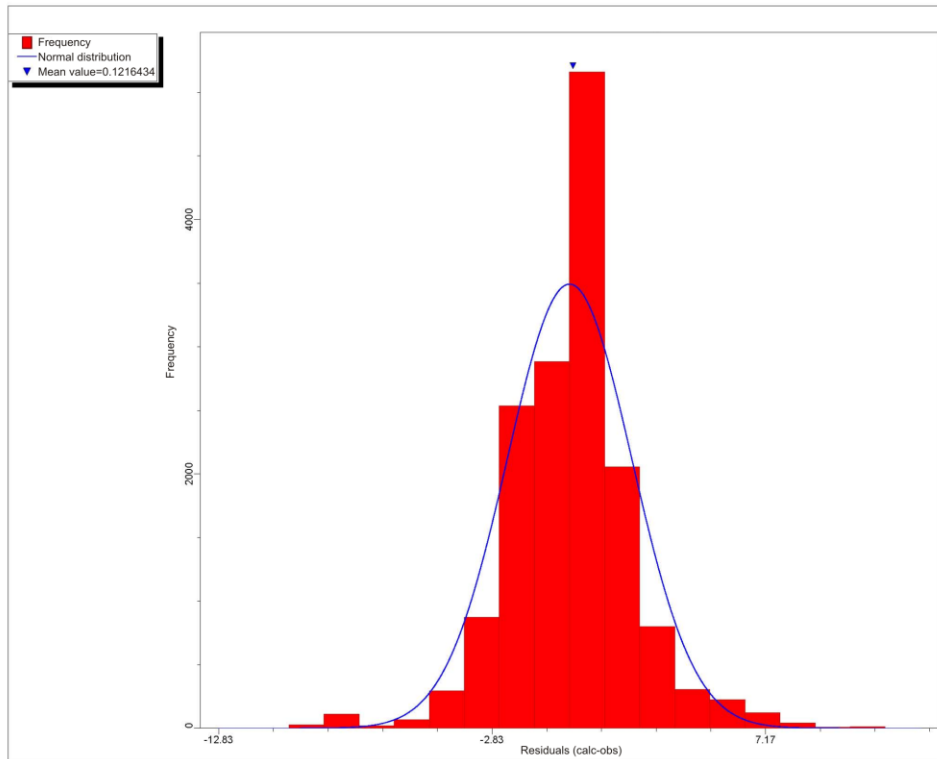


Figure L-31. 95th Percentile (Base Case) Flow Model Residual Distribution

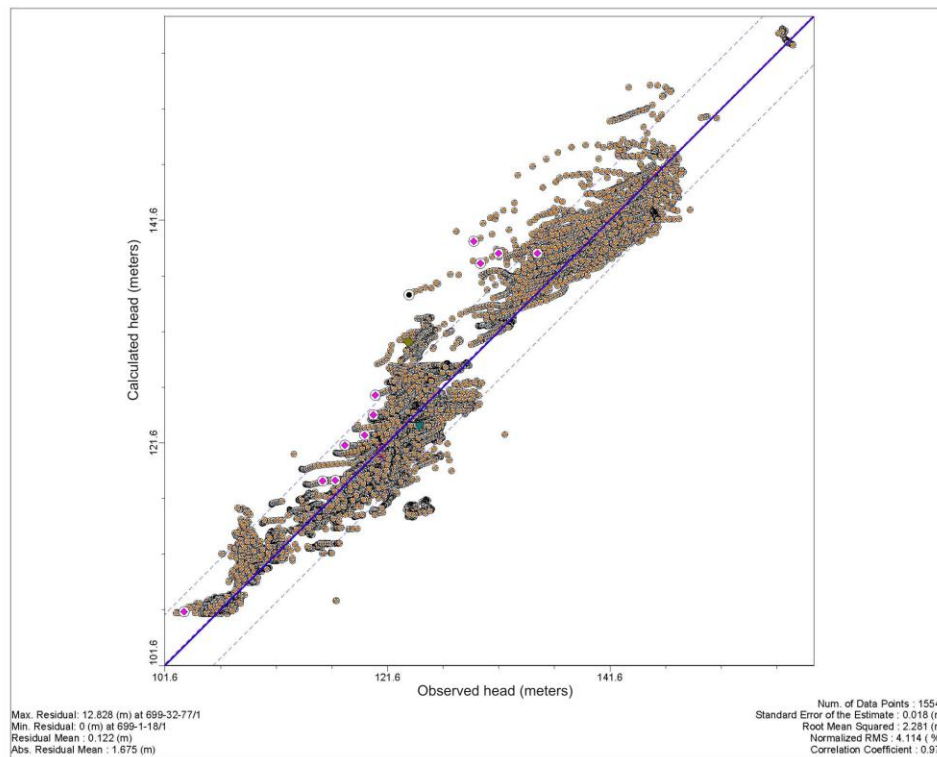


Figure L-32. 95th Percentile (Base Case) Flow Model Calibration Graph and Statistics

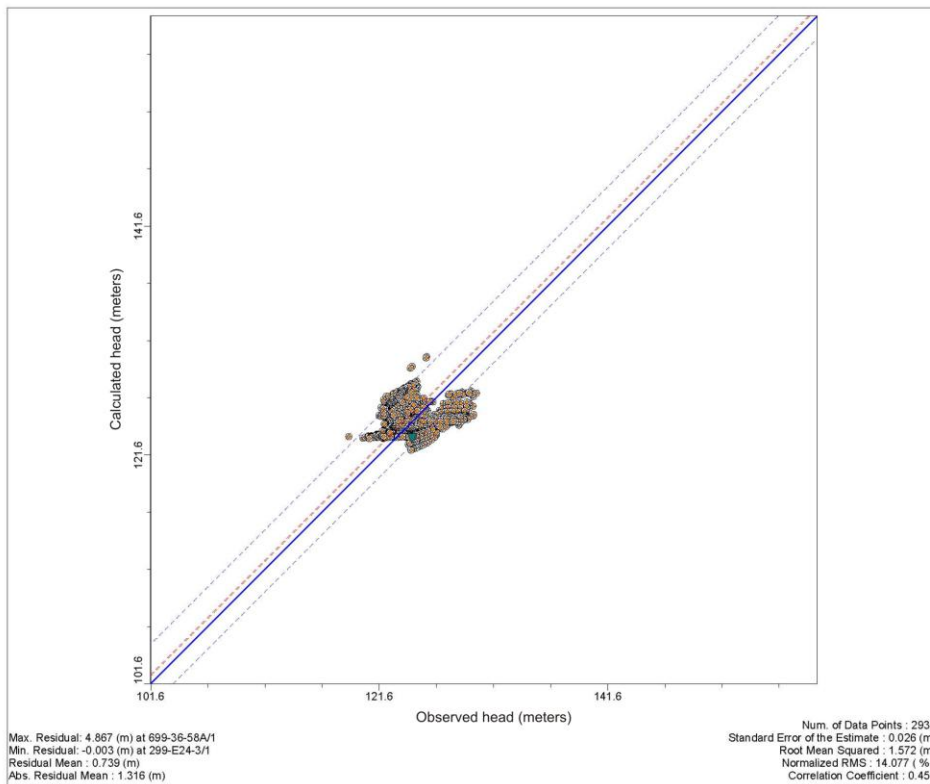


Figure L-33. 95th Percentile (Base Case) Flow Model Residuals – 200-East Area

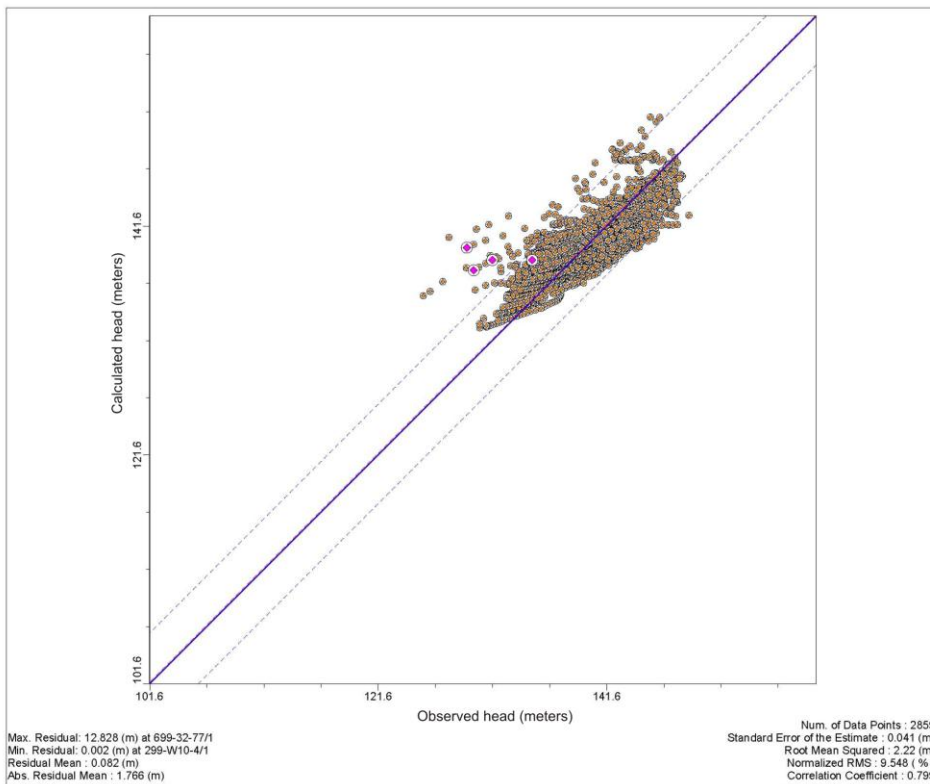


Figure L-34. 95th Percentile (Base Case) Flow Model Residuals – 200-West Area

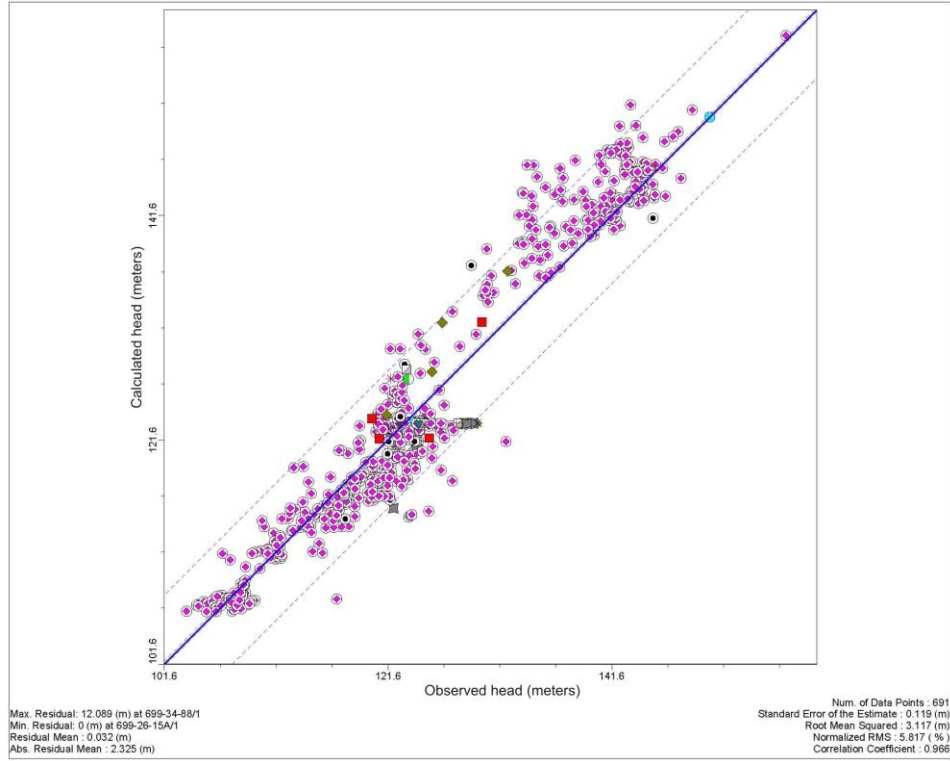


Figure L-35. 95th Percentile (Base Case) Flow Model Residuals, Calendar Year 1955

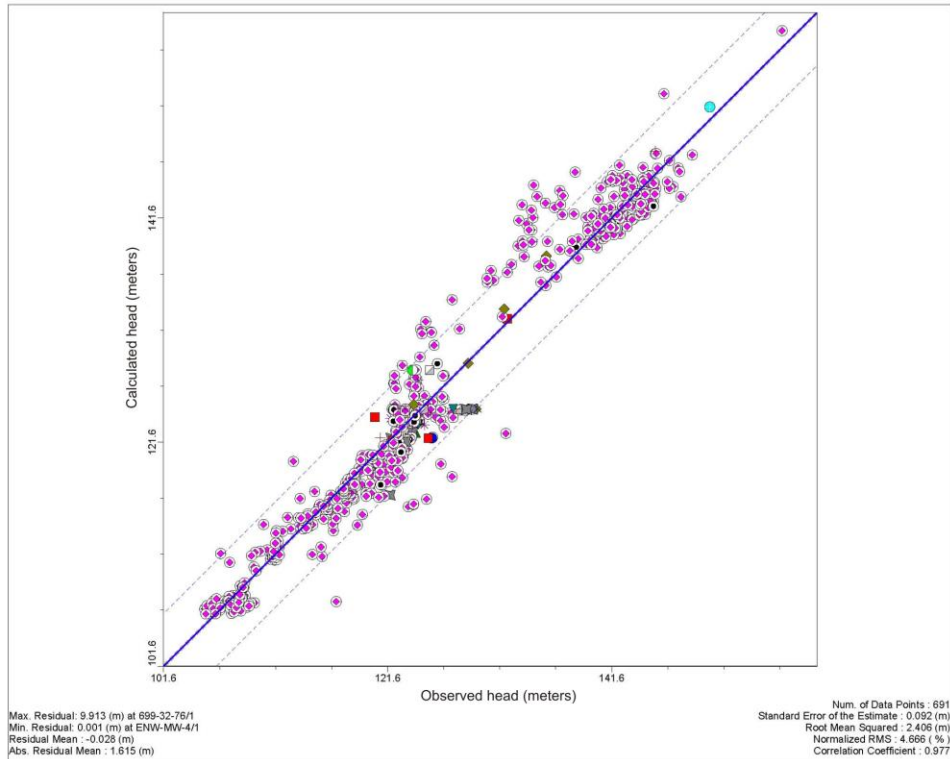


Figure L-36. 95th Percentile (Base Case) Flow Model Residuals, Calendar Year 1975

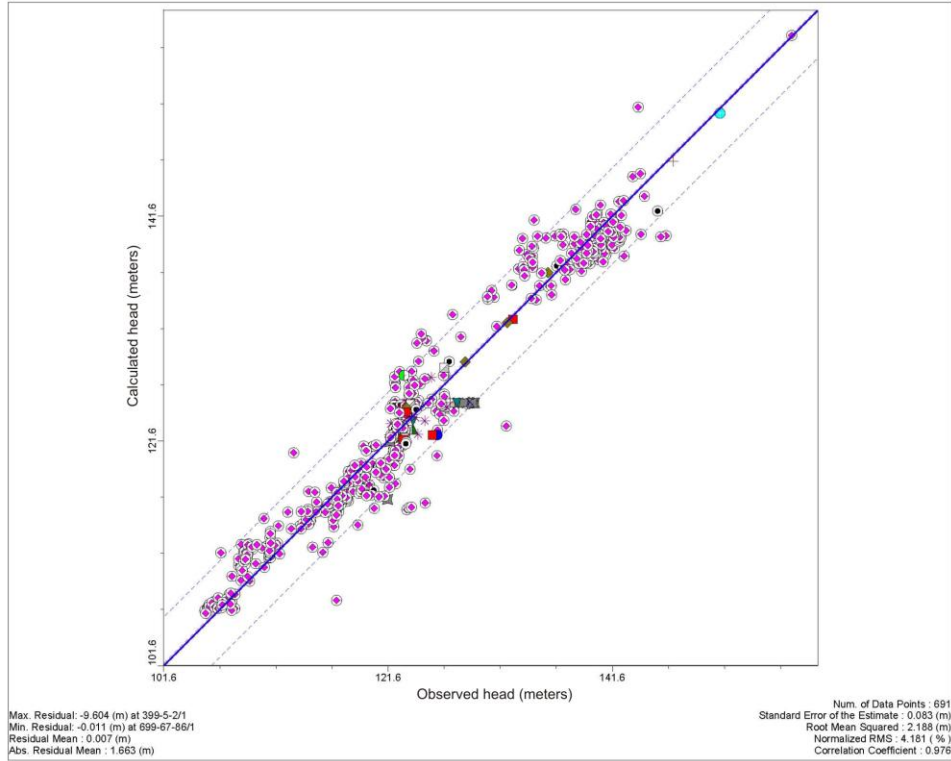


Figure L-37. 95th Percentile (Base Case) Flow Model Residuals, Calendar Year 1995

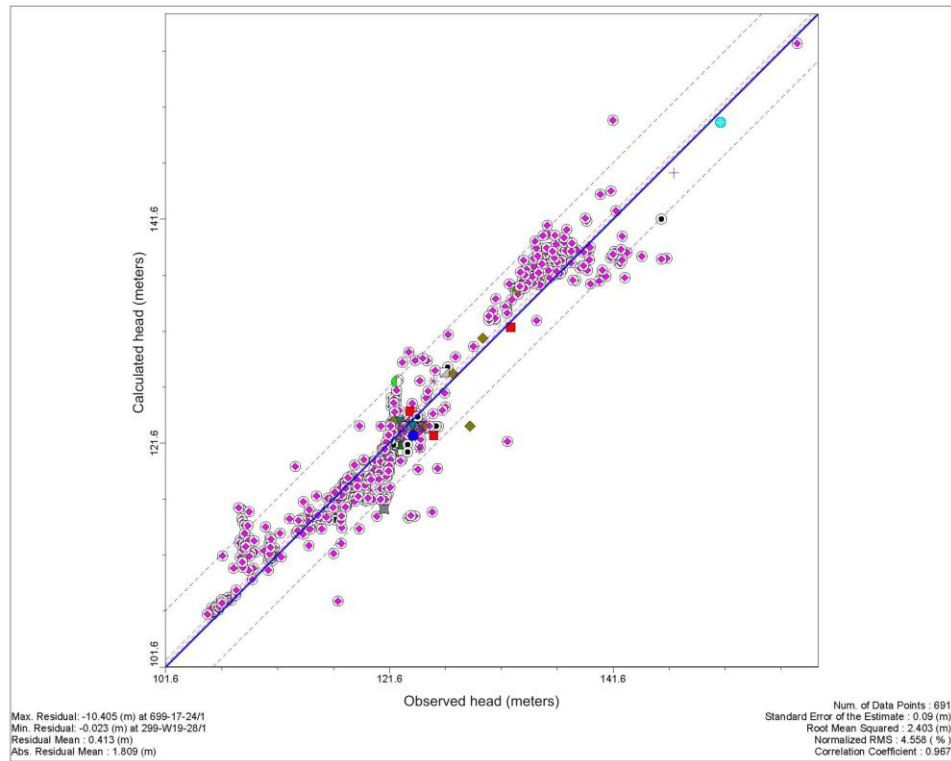


Figure L-38. 95th Percentile (Base Case) Flow Model Residuals, Calendar Year 2010

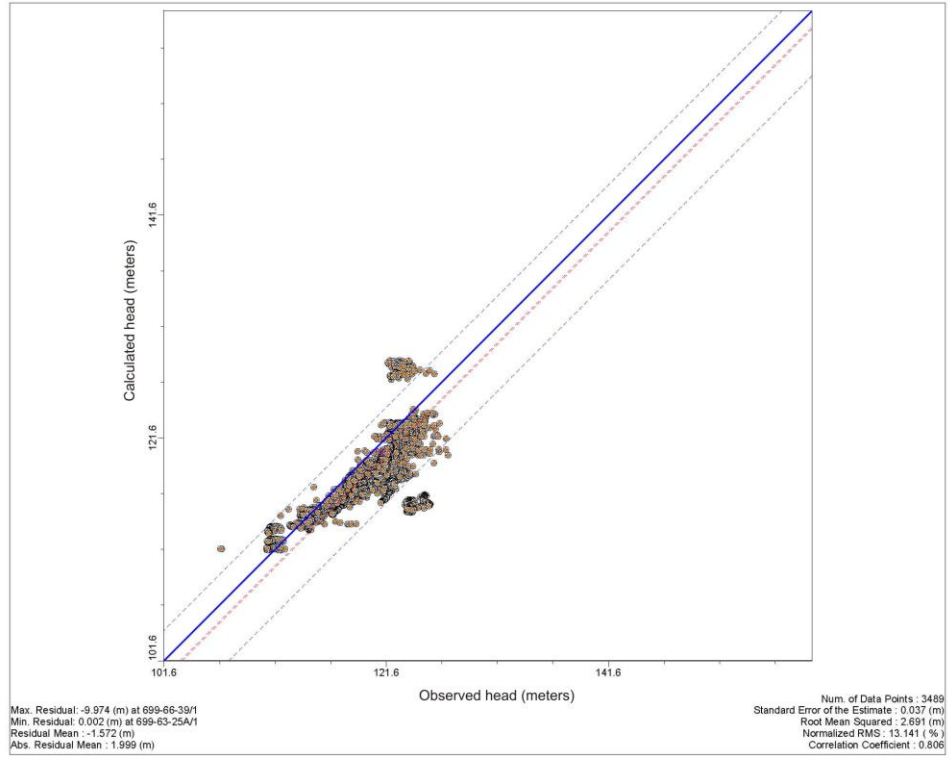


Figure L-39. 95th Percentile (Base Case) Flow Model Residuals in Northern Region of Model

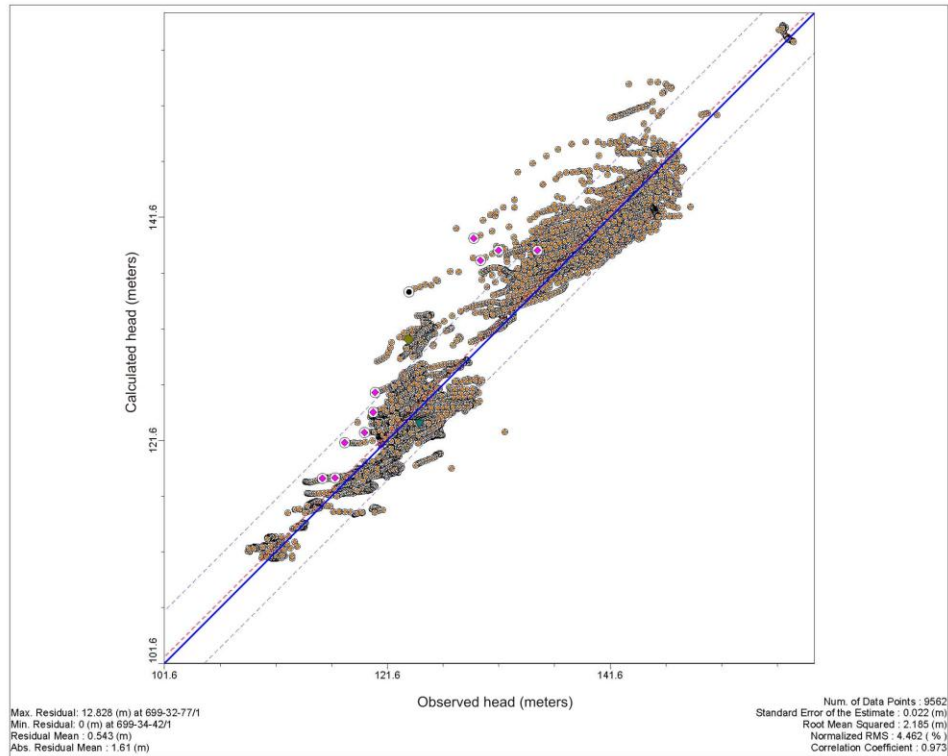


Figure L-40. 95th Percentile (Base Case) Flow Model Residuals in Central Region of Model

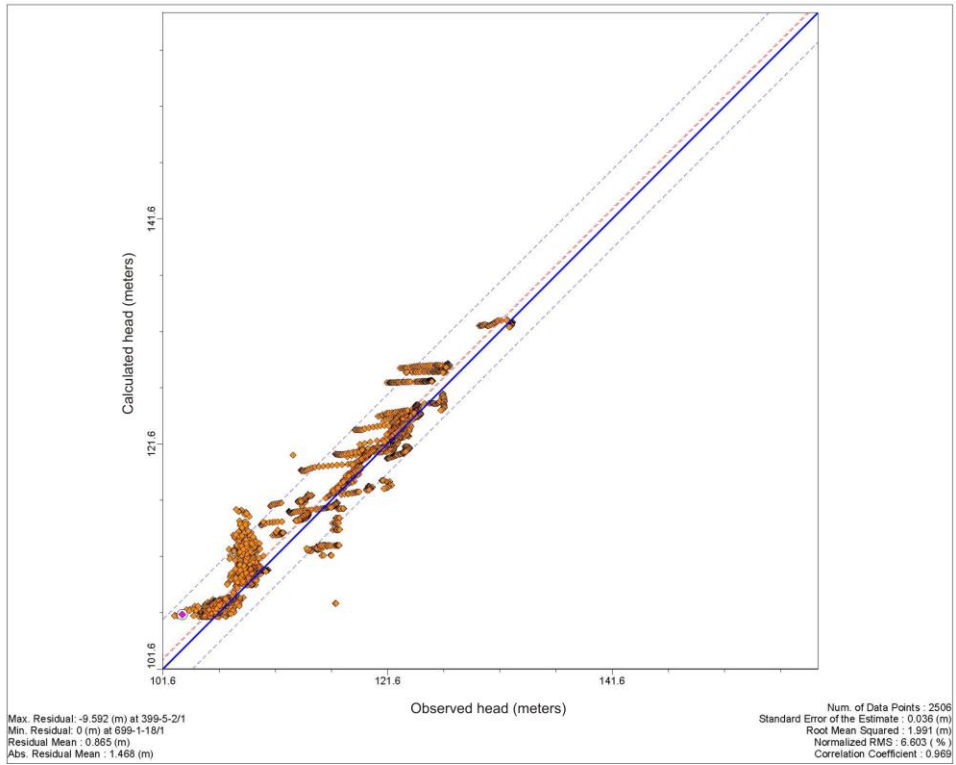


Figure L-41. 95th Percentile (Base Case) Flow Model Residuals in Southern Region of Model

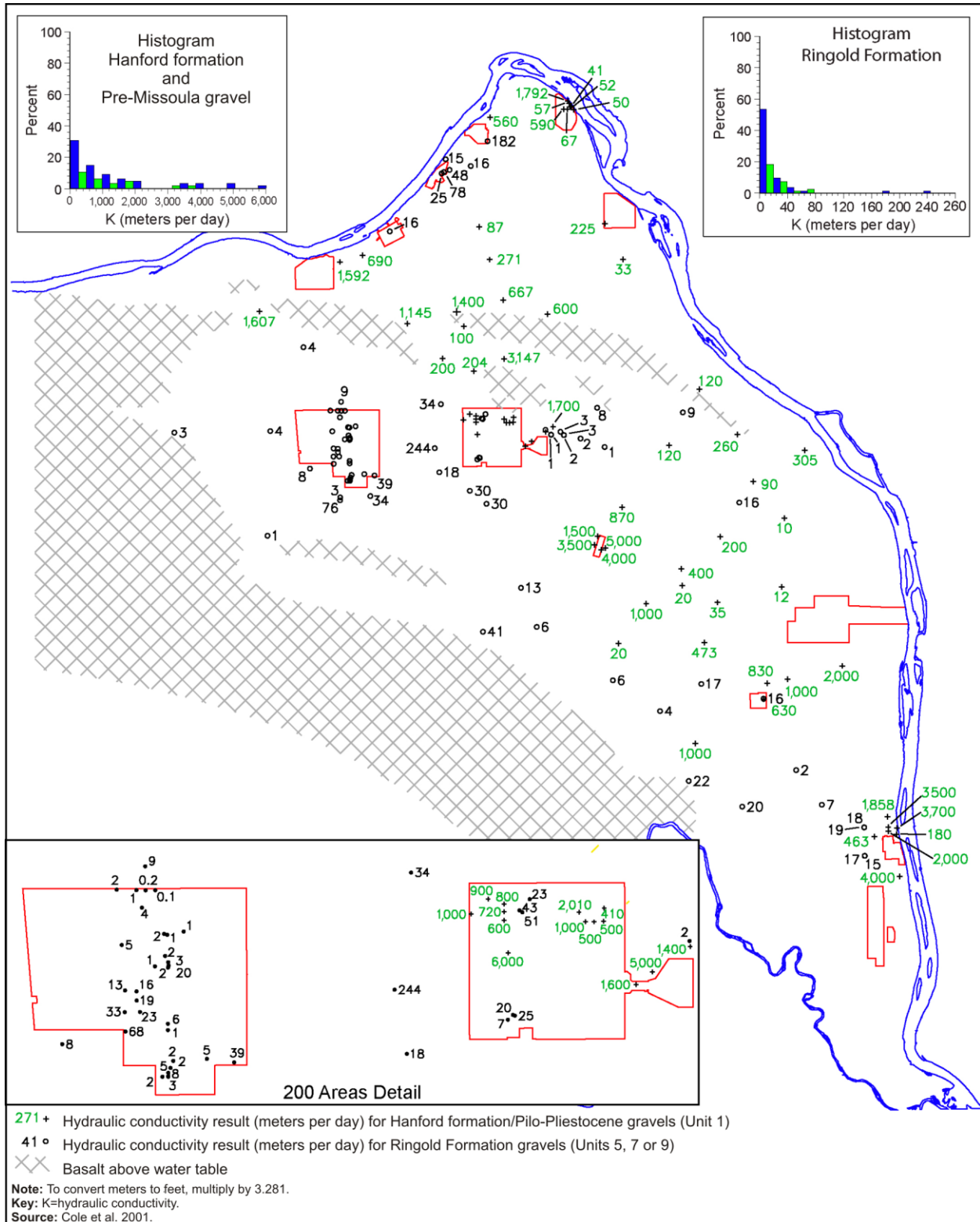


Figure L-42. Distribution of Wells with Hydraulic Conductivity Determined from Aquifer Pumping Tests

In addition to the calibration acceptance criteria, water (or mass) balance and a long-term, steady state condition must be achieved in the calibrated flow model. Cumulative mass water balance data are shown in Figure L-43, indicating a cumulative mass balance error of approximately -1.6 percent. Total water balance and storage data as a function of time are shown in Figure L-44. The Figure L-44 data show storage values relative to the total water balance and indicate that storage-in is approximately equal to storage-out in model year 261 (CY 2200). This indicates that a long-term, steady state condition is achieved. Note that, in Figure L-44, there is a spike in “storage” at model year 82. This spike is the result of a time-stepping change at the beginning of the final long-term stress period. As a result, the model is moving from a relatively long time step at the end of the previous stress period (model year 82) to a relatively short time step at the beginning of the final stress period.

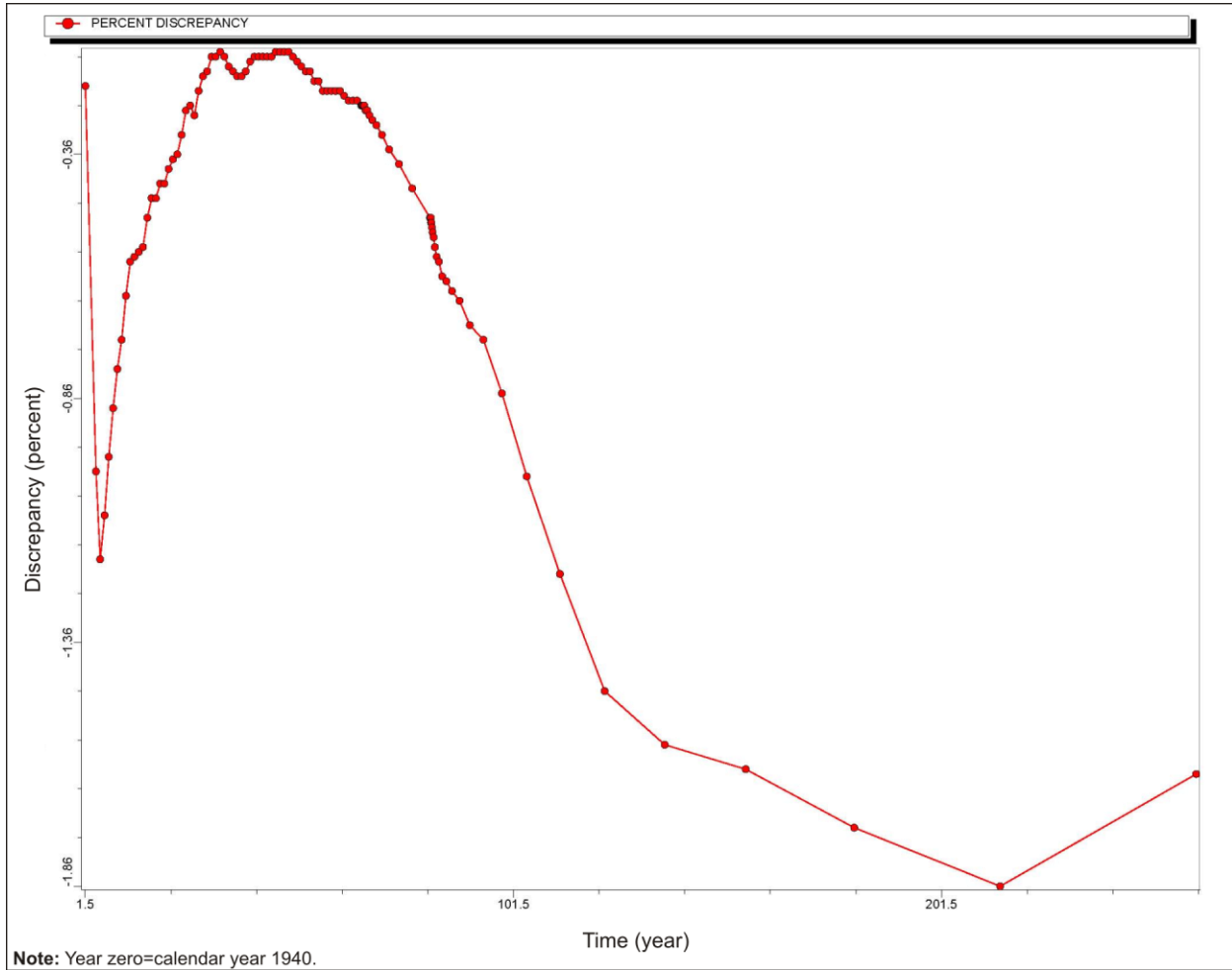


Figure L-43. 95th Percentile (Base Case) Flow Model Cumulative Water Balance Discrepancy

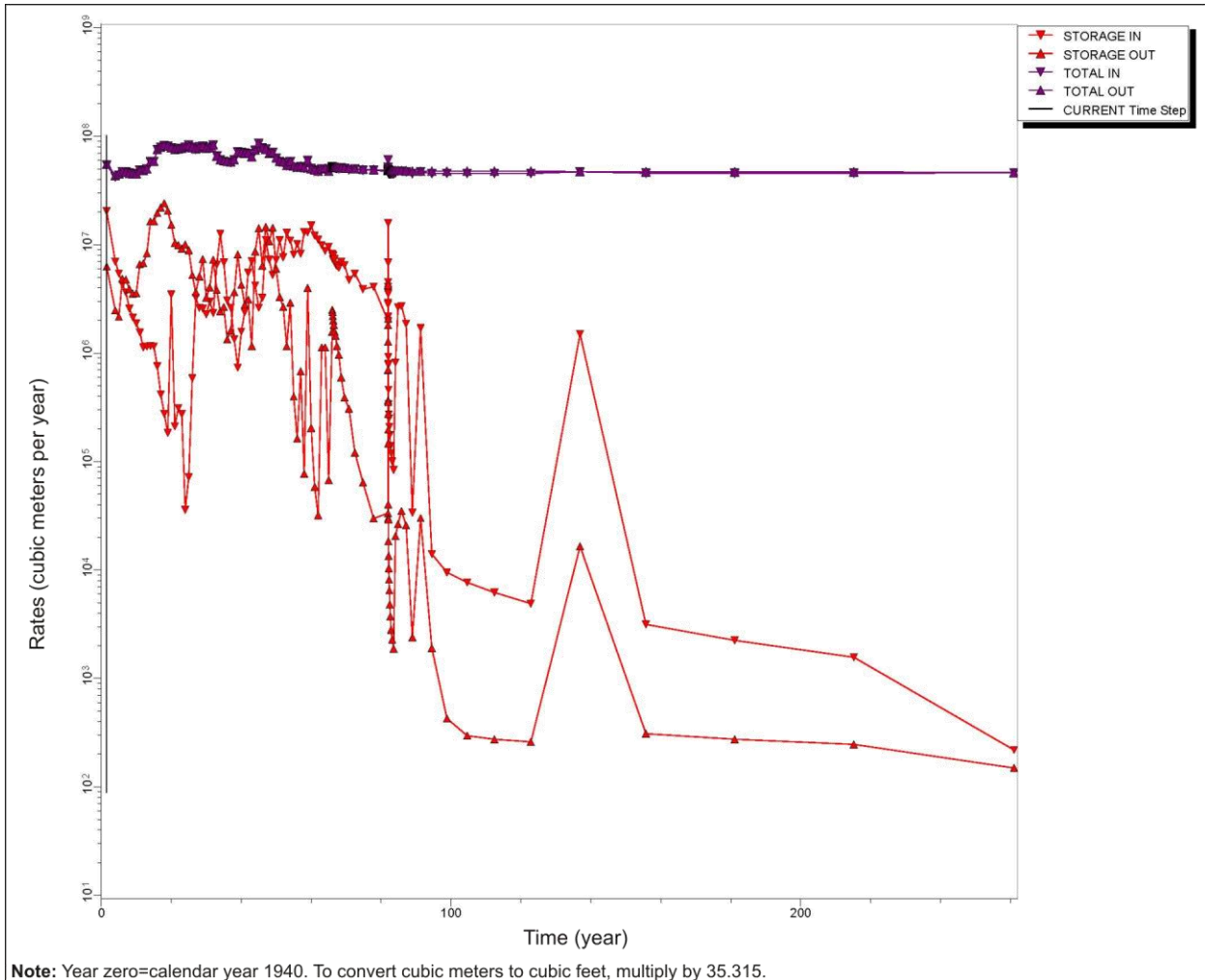
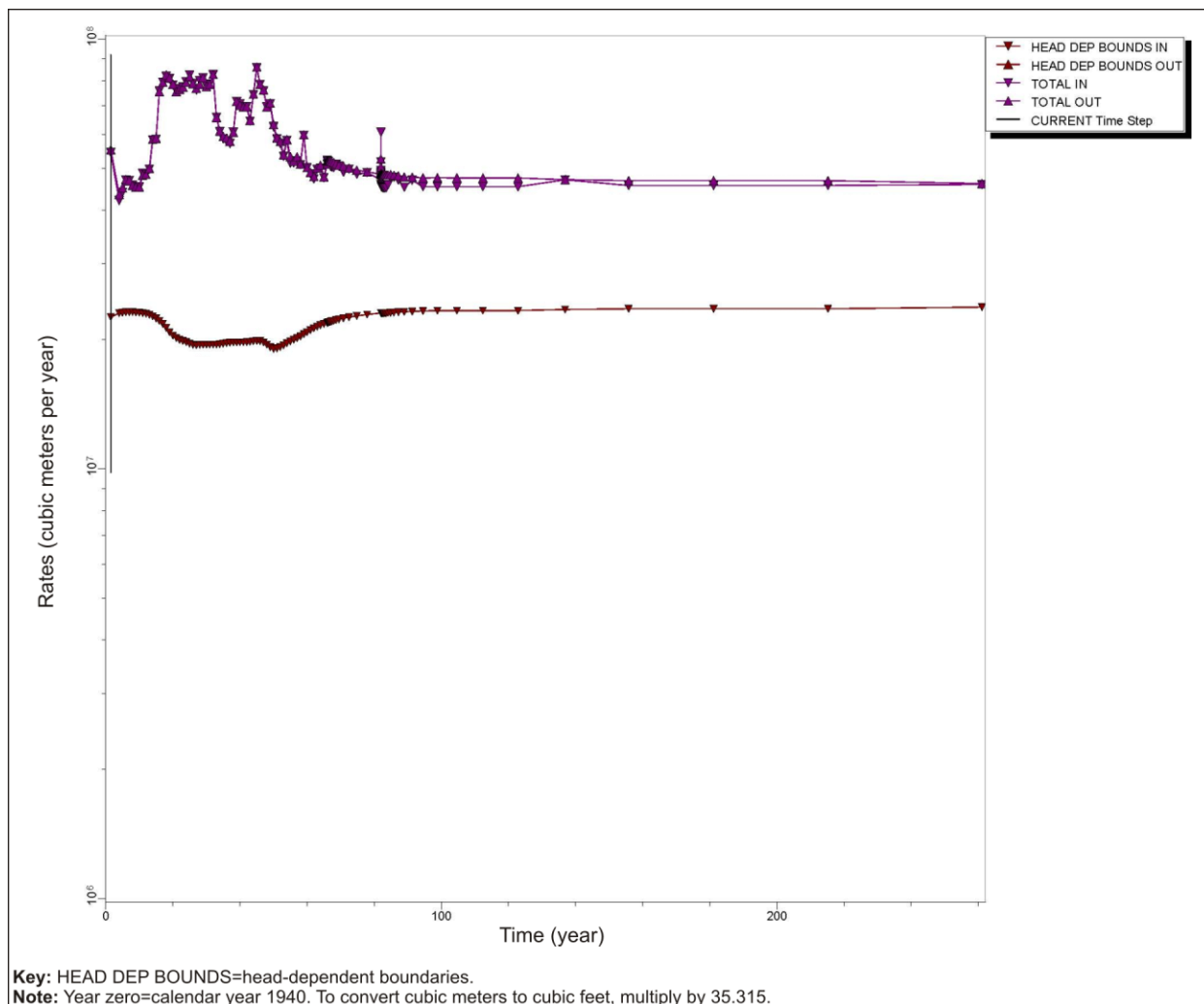


Figure L-44. 95th Percentile (Base Case) Flow Model Total Water and Storage Rates over Time

Additional water balance results for the 95th percentile (Base Case) flow model are shown in Figures L-45, L-46, and L-47 for GHBs, river boundaries, and recharge boundaries, respectively. In Figure L-47, the 'Recharge Out' value goes to zero at model year 82. This reduction occurs because the cells below the water extraction zone in the model become dry at this time during the model simulation and do not rewet for the remainder of the simulation.



**Figure L-45. 95th Percentile (Base Case) Flow Model
 Total Water and Generalized Head Boundary Rates over Time**

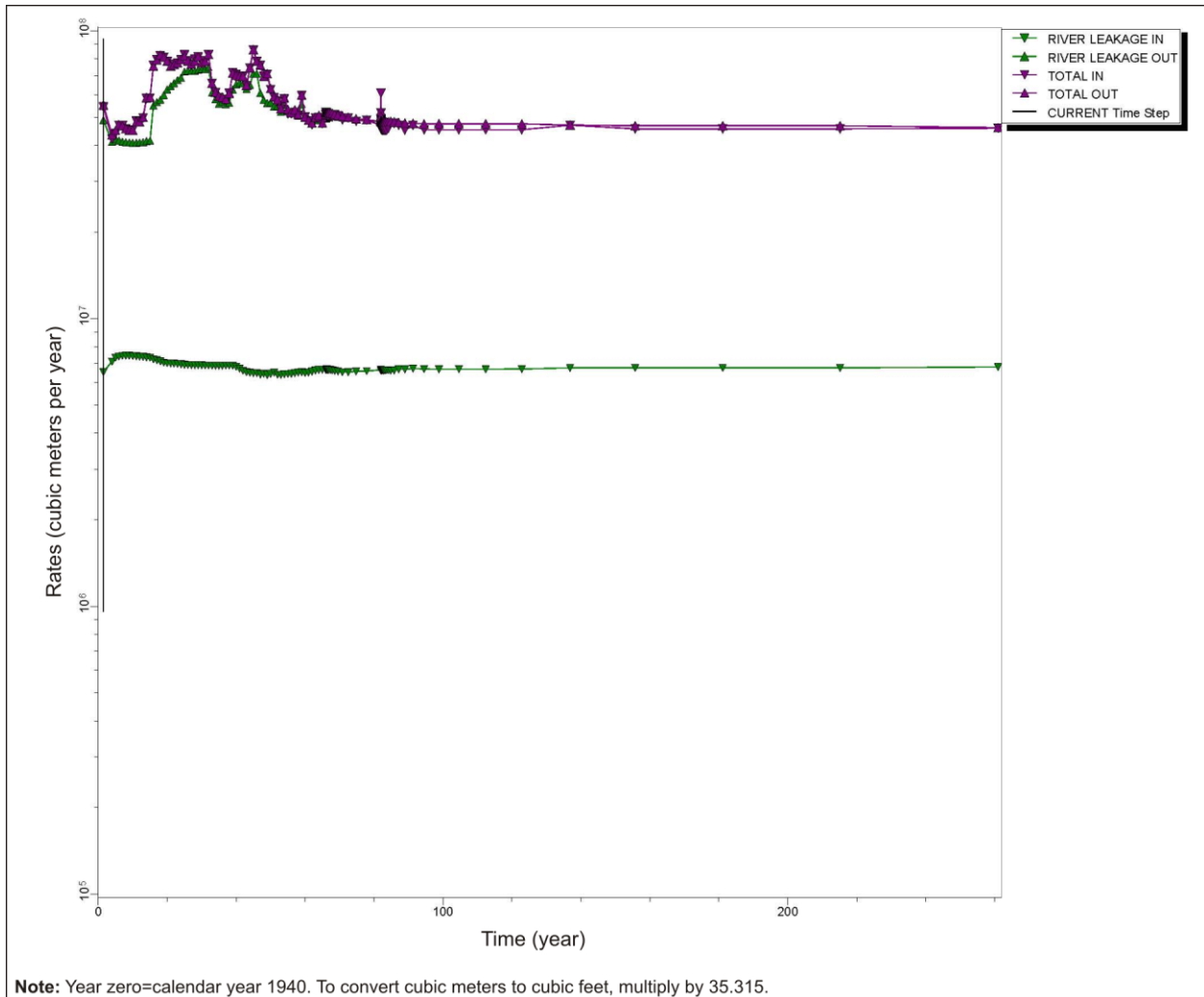


Figure L-46. 95th Percentile (Base Case) Flow Model Total Water and River Rates over Time

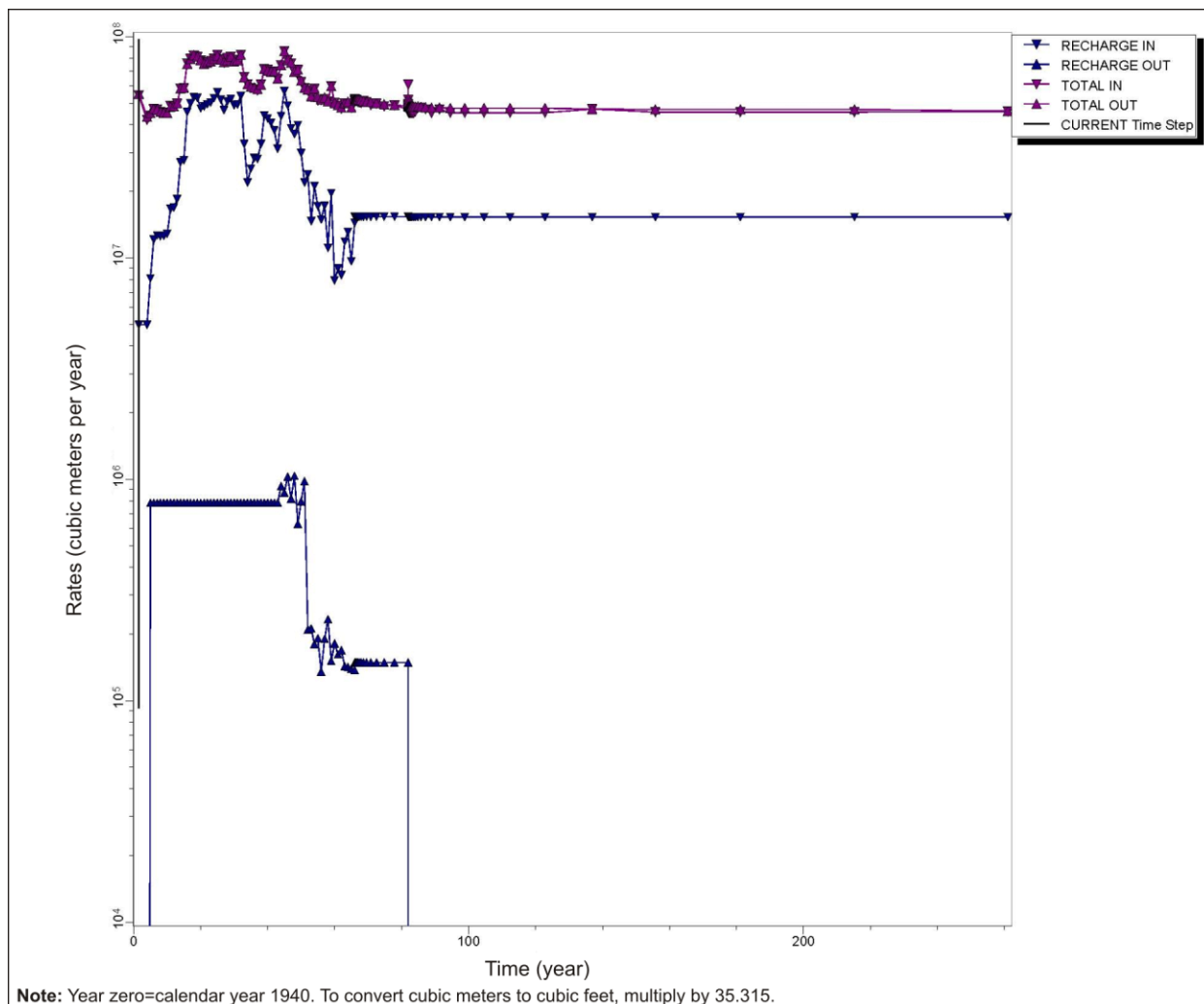


Figure L-47. 95th Percentile (Base Case) Flow Model Total Water and Recharge Rates over Time

L.8.1.2 95th Percentile (Base Case) Potentiometric Head Distribution

A goal for the Base Case flow model is to produce a potentiometric distribution of heads that shows a steep water table in the 200-West Area and a relatively flat water table in the 200-East Area. The pre-Hanford potentiometric surface is assumed to be approximately the same as the post-Hanford long-term steady state condition, with water table mounding occurring below areas where, and at times when, Hanford operational discharges were released at the ground surface. Figures L-48, L-49, and L-50 are Base Case flow model simulations of the potentiometric surface in CY 1944 (pre-Hanford), CY 1975 (Hanford operations), and CY 2200 (post-Hanford), respectively.

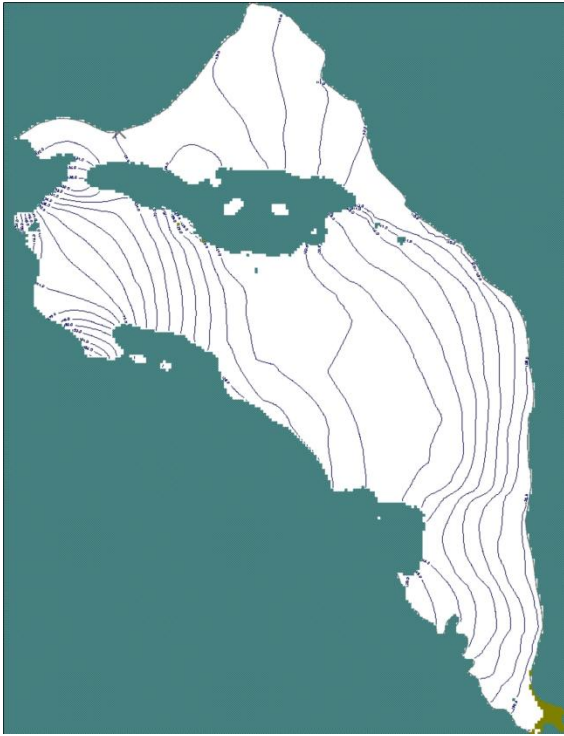


Figure L-48. 95th Percentile (Base Case) Flow Model Potentiometric Head Distribution, Calendar Year 1944

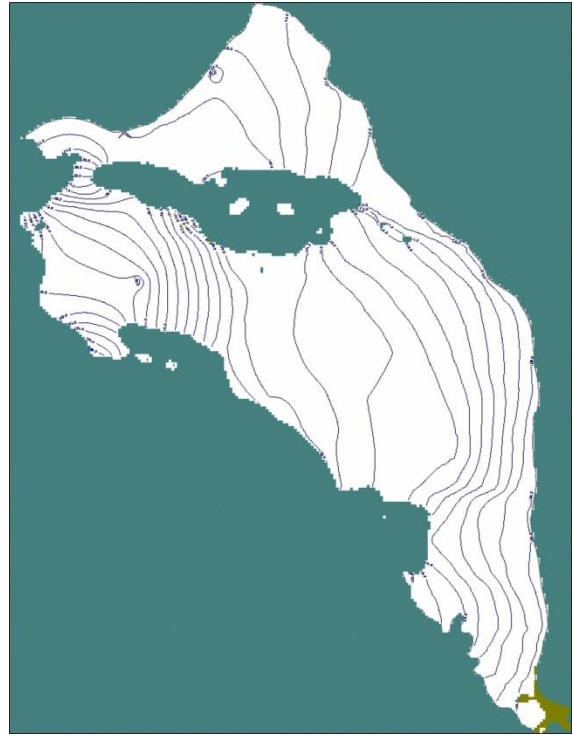


Figure L-49. 95th Percentile (Base Case) Flow Model Potentiometric Head Distribution, Calendar Year 1975

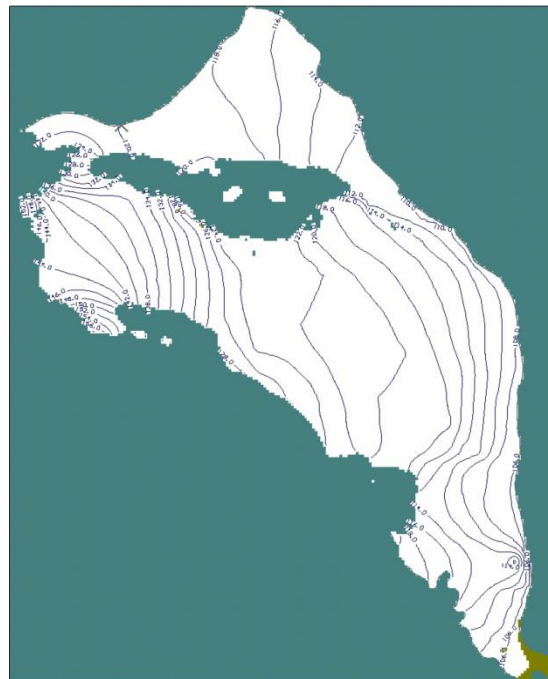


Figure L-50. 95th Percentile (Base Case) Flow Model Potentiometric Head Distribution, Calendar Year 2200

L.8.1.3 95th Percentile (Base Case) Flow Model Velocity Field

The 95th percentile (Base Case) flow model velocity field is variable in both magnitude and direction over time and across the model domain. This variability at selected locations within the model is shown in Figures L-51 through L-56. As expected, the velocities simulated in the 200-West Area are generally lower than those simulated in the 200-East Area, particularly at the 200-East Area BY Cribs. An additional observation is that the velocity directions are highly variable during the Hanford operational period, particularly at the 200-East Area BY Cribs; there the velocity directions change by approximately 180 degrees due to water table mounding, coupled with this source's proximity to Gable Gap, where water table velocity and direction are sensitive to water table elevation.

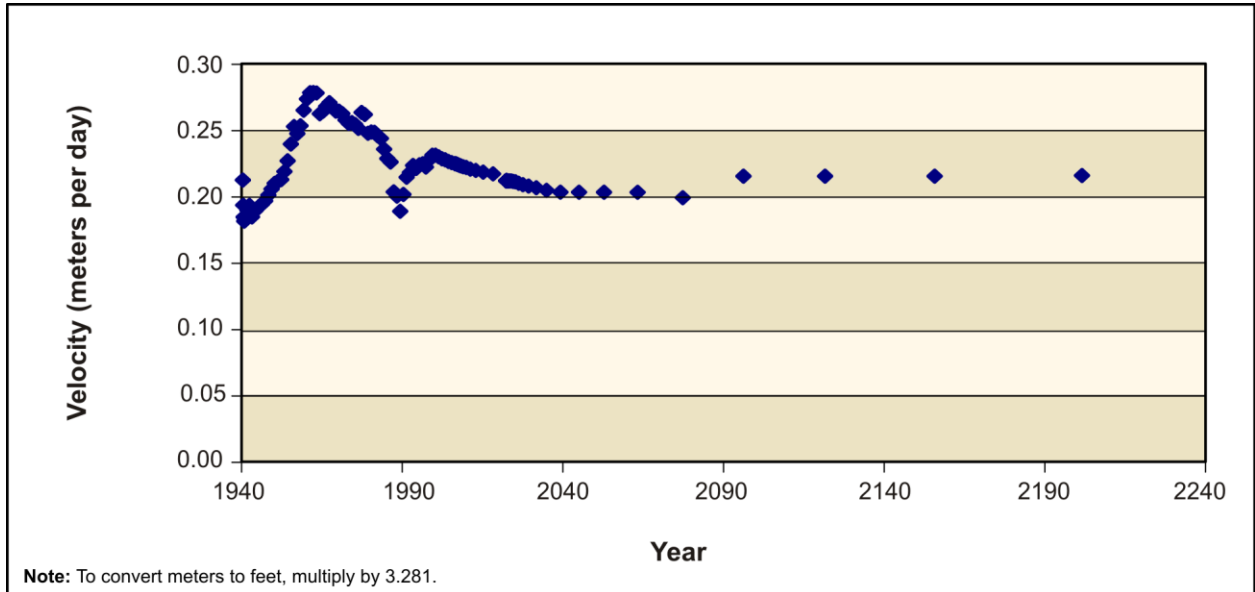


Figure L-51. 95th Percentile (Base Case) Flow Model Velocity Magnitude at 216-B-26 (BC Cribs in 200-East Area)

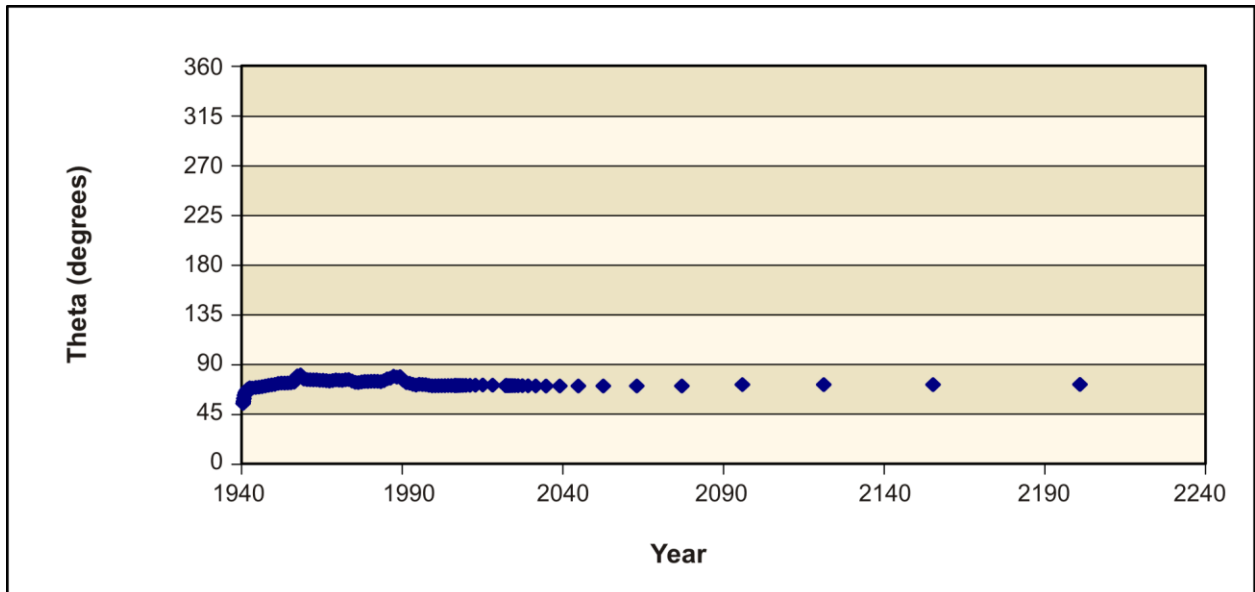


Figure L-52. 95th Percentile (Base Case) Flow Model Velocity Direction at 216-B-26 (BC Cribs in 200-East Area)

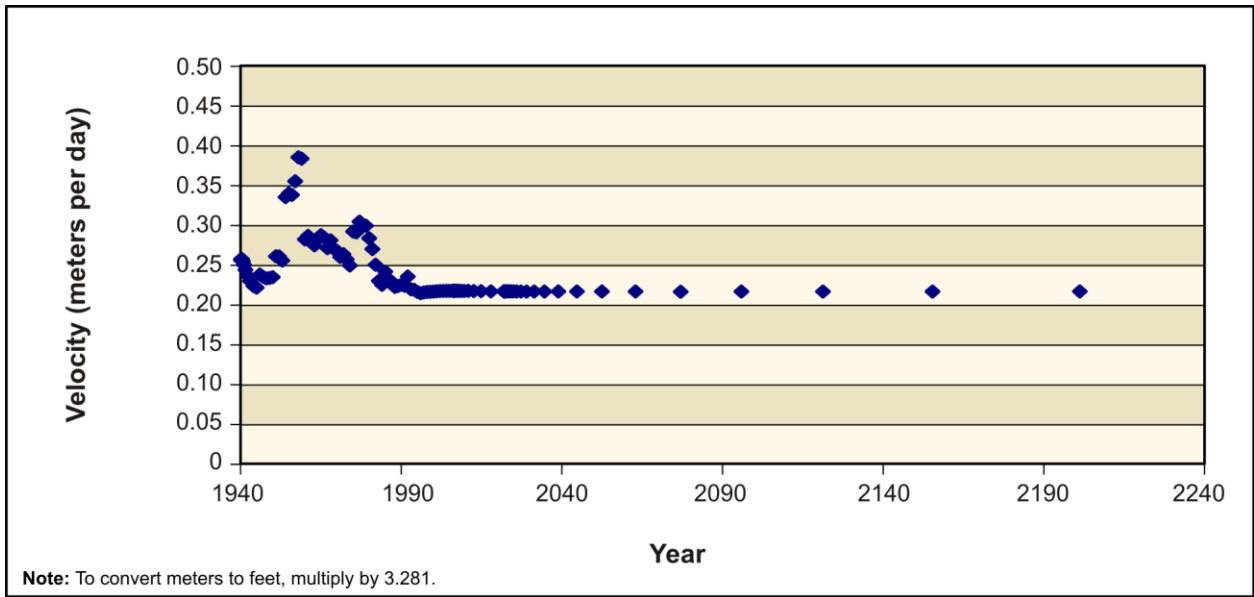


Figure L-53. 95th Percentile (Base Case) Flow Model Velocity Magnitude at 216-T-28 (200-West Area)

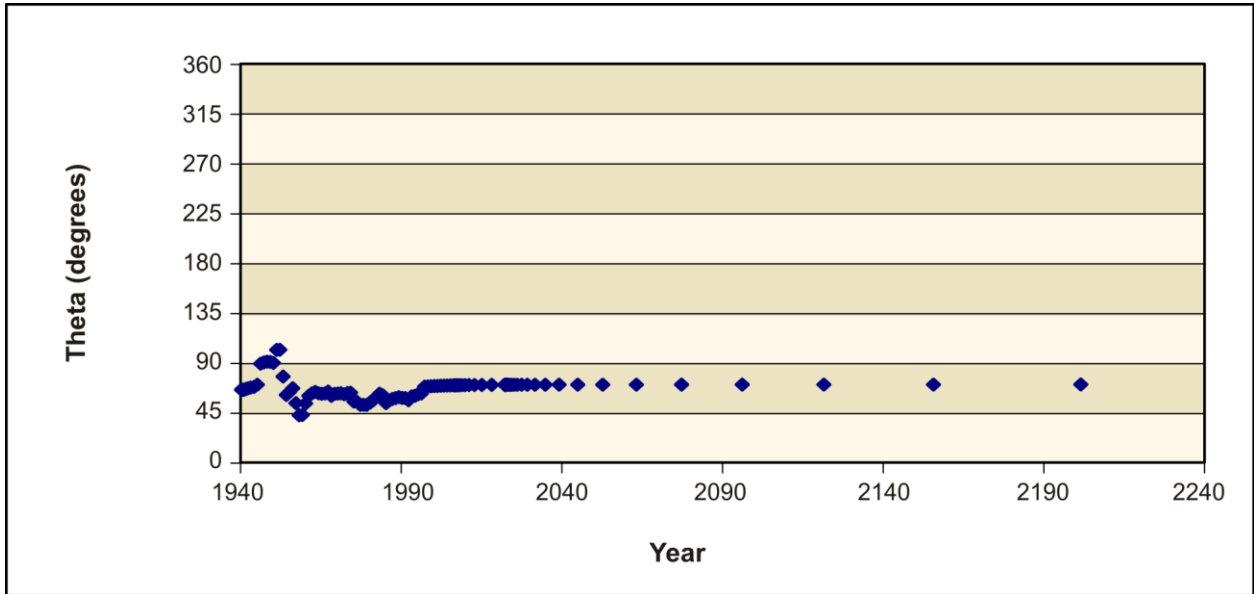


Figure L-54. 95th Percentile (Base Case) Flow Model Velocity Direction at 216-T-28 (200-West Area)

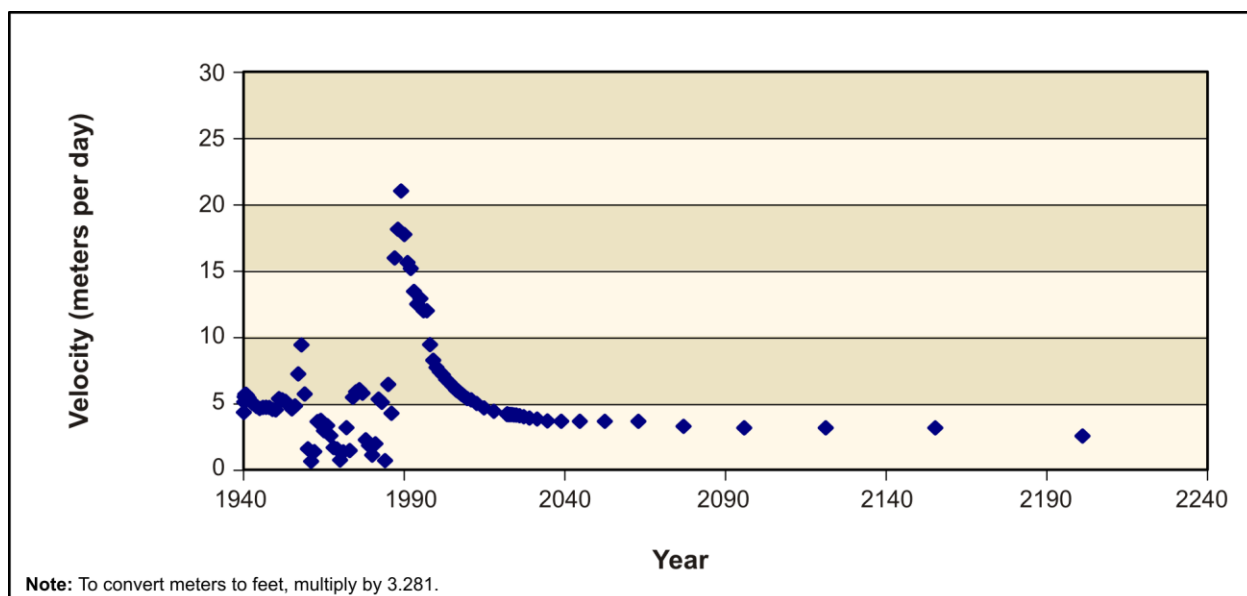


Figure L-55. 95th Percentile (Base Case) Flow Model Velocity Magnitude at BY Cribs (200-East Area)

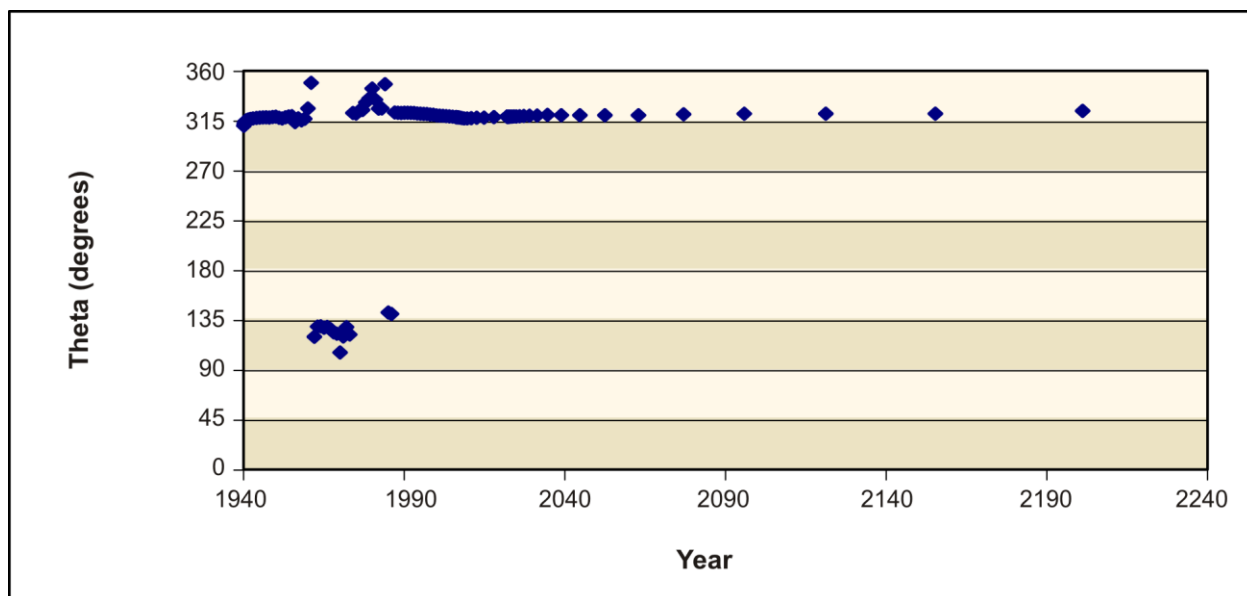


Figure L-56. 95th Percentile (Base Case) Flow Model Velocity Direction at BY Cribs (200-East Area)

L.8.1.4 95th Percentile (Base Case) Flow Model Central Plateau Pathline Analysis

Pathline analysis determined the number of particles (measured in area) released in the Central Plateau area that would move to the north through Gable Gap and the number that would move to the east toward the Columbia River. As discussed in Section L.1.5, in the *Draft TC & WM EIS*, the pathline analysis to demonstrate the area of northerly versus easterly flow from the Central Plateau depended primarily on hydraulic conductivity distribution rather than on uncertainties in the TOB surface. Comparison of this analysis with the 66th and 100th percentile cases (see Sections L.8.2.4 and L.8.3.4) confirms this observation. This pathline analysis included a MODFLOW and MODPATH [MODFLOW particle-tracking postprocessing package] model run, releasing a uniformly distributed set of particles across the

Central Plateau area. The Central Plateau is depicted as a rectangular boundary that includes all of the 200-East and 200-West Areas, as well as other areas between and outside the 200 Areas. Figure L-57 shows that, in terms of area, the flow of the Base Case flow model is predominantly eastward from the Central Plateau.

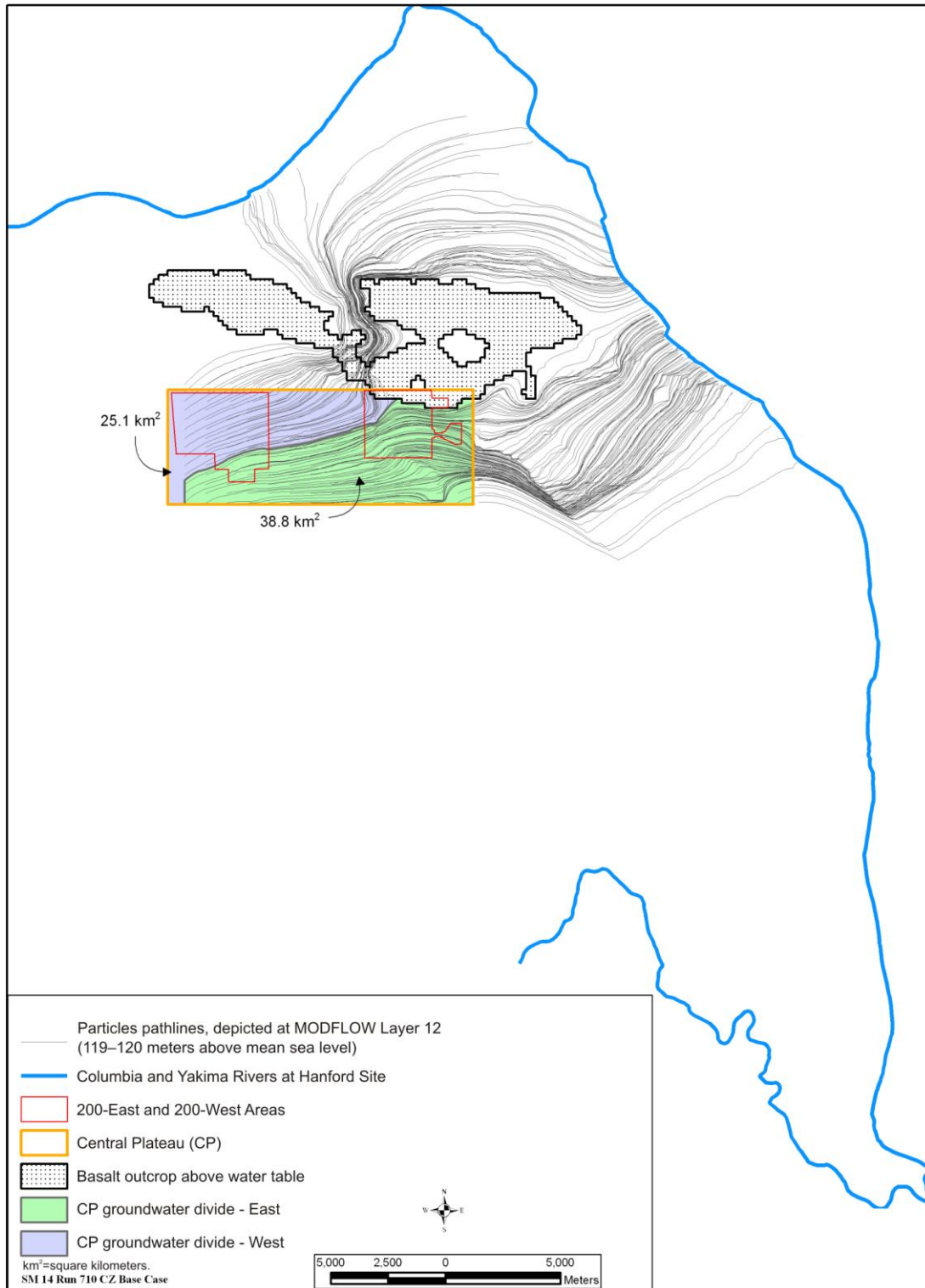


Figure L-57. 95th Percentile (Base Case) Flow Model Central Plateau Pathline Analysis

The computer program MODPATH was developed by the USGS to calculate three-dimensional particle-tracking pathlines from steady state and transient flow simulation output obtained using MODFLOW (SWS 2009).

L.8.1.5 95th Percentile (Base Case) Flow Model Zone Budget Analysis

A zone budget analysis was completed to determine simulated water flow volumes from south of Gable Mountain and Gable Butte through Umtanum Gap, through Gable Gap, and easterly toward the Columbia River. Table L-17 provides total water flow volumes through these areas for CY 2200. These results show that about 17 percent of the total volume of water entering the Columbia River passes through Umtanum Gap, about 15 percent through Gable Gap, and about 68 percent directly east to the Columbia River. Comparison of these results with those of the 66th and 100th percentile cases shows that in terms of volumetric flow, rather than in terms of geometric position of the flow divide across the Central Plateau (see Section L.8.1.4), the model is less sensitive to variations in hydraulic conductivity.

Table L-17. 95th Percentile (Base Case) Flow Model – Simulated Water Flow Volumes Through Selected Areas, Calendar Year 2200

Water Flow Through	Water Volume (cubic meters per year)
Umtanum Gap	4,332,200
Gable Gap	3,714,000
East to Columbia River	16,954,000

Note: To convert cubic meters to cubic feet, multiply by 35.315.

L.8.1.6 95th Percentile (Base Case) Flow Model – Transport Model Concentration-Versus-Time Results

Groundwater transport modeling was completed using the 95th percentile flow model. Figures L-58 and L-59 show the concentration-versus-time results measured at the Core Zone Boundary and at the Columbia River for technetium-99 under Tank Closure Alternative 2B and Waste Management Alternative 2, Disposal Group 1, Subgroup 1-A, respectively. Figures L-58 and L-59 are comparable to Figures L-86 and L-87, respectively, for the 100th percentile model, and comparable to Figures L-114 and L-115, respectively, for the 66th percentile model. These comparisons show that the three flow models result in similar technetium-99 concentrations over time for the two alternatives presented. See Chapter 2 of this *TC & WM EIS* for a description of these alternatives.

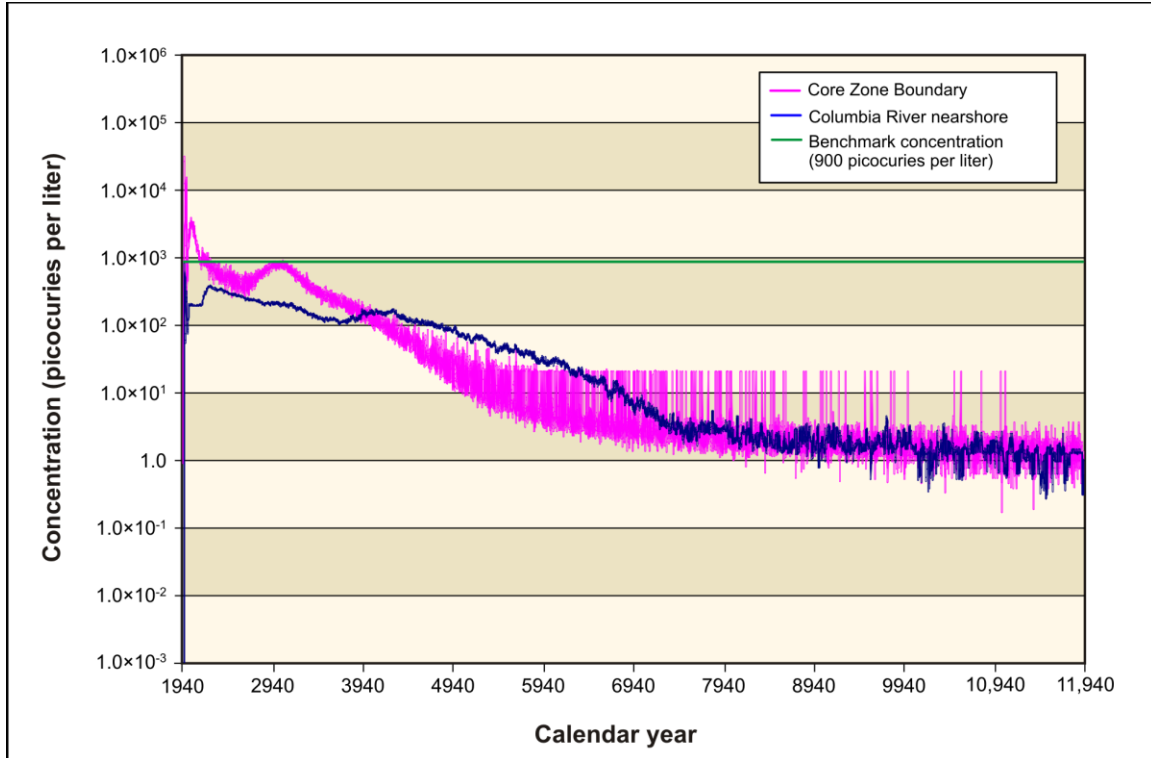


Figure L-58. Tank Closure Alternative 2B 95th Percentile (Base Case) Flow Model Concentration-Versus-Time Results for Technetium-99

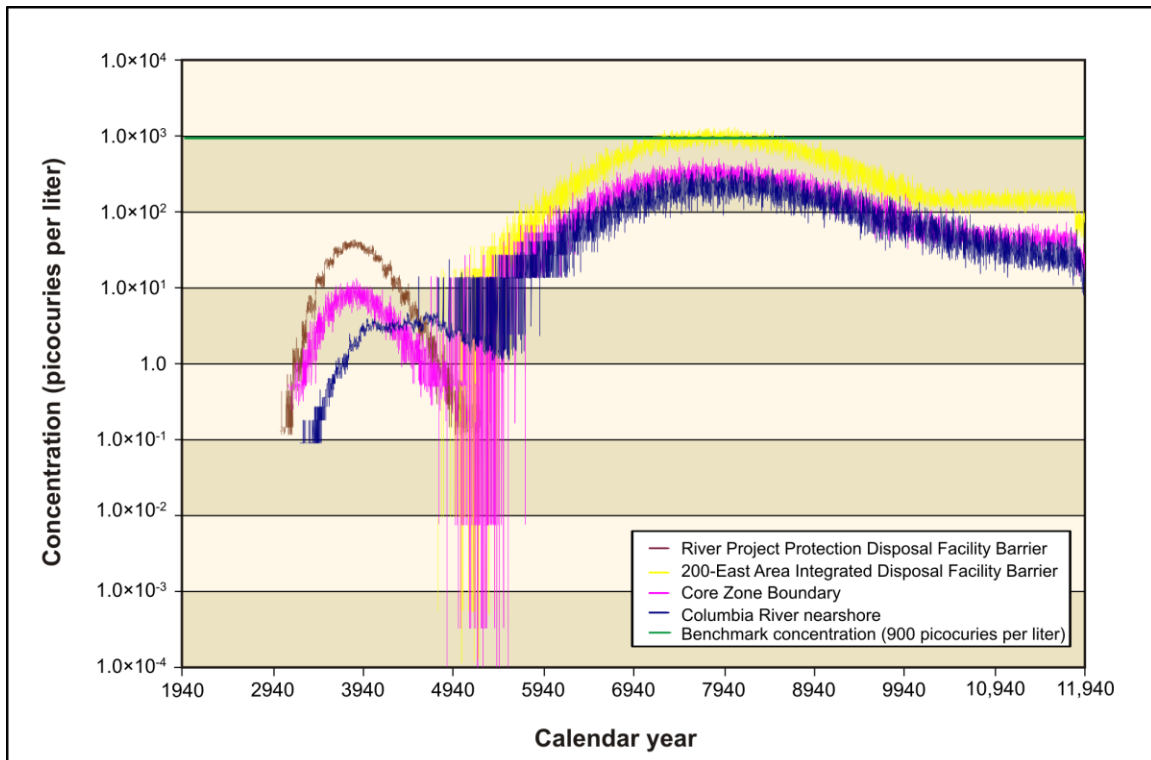


Figure L-59. Waste Management Alternative 2, Disposal Group 1, Subgroup 1-A, 95th Percentile Flow Model Concentration-Versus-Time Results for Technetium-99

L.8.2 Results from the 100th Percentile Flow Model

L.8.2.1 Calibration Acceptance

Table L–18 provides a restatement of the flow model calibration criteria discussed in Section L.6.2, along with an assessment of the 100th percentile flow model’s performance for each criterion. Specific data illustrative of such performance are reflected in Table L–19 and Figures L–60 through L–70.

Table L–18. Summary of the 100th Percentile Flow Model Performance Compared with the Calibration Acceptance Criteria

Flow Model Calibration Acceptance Criteria	100th Percentile Flow Model Performance
Residual distribution should be reasonably normal.	Residual distribution is reasonably normal (see Figure L–60).
The mean residual should be approximately 0.	Residual mean = –0.108 meters (–0.354 feet) (see Figure L–61).
The number of positive residuals should approximate the number of negative residuals.	Positive residuals approximately equal negative residuals (see Figure L–60).
The correlation coefficient (calculated versus observed) should be greater than 0.9.	Correlation coefficient = 0.974 (see Figure L–61).
The root mean square (RMS) error (calculated versus observed) should be less than 5 meters (16.4 feet), approximately 10 percent of the gradient in the water table elevation.	RMS error = 2.25 meters (7.382 feet) (see Figure L–61).
Residuals in the 200-East Area should be distributed similarly to those in the 200-West Area.	Residuals in the 200-East and 200-West Areas are distributed similarly (see Figures L–62 and L–63).
The residuals should be evenly distributed over time.	Residuals are approximately evenly distributed over time (see Figures L–64, L–65, L–66, and L–67).
The residuals should be evenly distributed across the site.	Residuals are approximately evenly distributed across the site (see Figures L–68, L–69, and L–70).
The calibrated parameters should compare reasonably well with field-measured values.	Calibrated hydraulic conductivity values are listed in Table L–19 and compare reasonably with field-measured values for material types to which the model is sensitive (i.e., Hanford formation and Ringold Formation material types). Figure L–42 provides field-measured values from aquifer pumping tests (Cole et al. 2001).
Parameters should be reasonably uncorrelated.	Hydraulic conductivity parameters are reasonably uncorrelated (see Table L–19 for the key to model material type zones and Table L–15 for the correlation coefficient matrix).

Table L–19. 100th Percentile Flow Model Calibrated Hydraulic Conductivity Values

Material Type (Model Zone)	Hydraulic Conductivity (K _x) ^a	Hydraulic Conductivity (K _y) ^b	Hydraulic Conductivity (K _z) ^c
Hanford mud (1)	0.28	0.28	0.028
Hanford silt (2)	3.79	3.79	0.379
Hanford sand (3)	49.6	49.6	4.96
Hanford gravel (4)	223.64	223.64	22.364
Ringold sand (5)	1.89	1.89	0.189
Ringold gravel (6)	19.51	19.51	1.951
Ringold mud (7)	1.95	1.95	0.195
Ringold silt (8)	2.12	2.12	0.212
Plio-Pleistocene sand (9)	40.71	40.71	4.071
Plio-Pleistocene silt (10)	4.7	4.7	0.47
Cold Creek sand (11)	83.95	83.95	8.395
Cold Creek gravel (12)	79.7	79.7	7.97
Highly conductive Hanford formation (13)	4,793.76	4,793.76	479.376
Activated basalt (14)	0.001	0.001	0.0001

a Hydraulic conductivity with respect to the x axis, meters per day.

b Hydraulic conductivity with respect to the y axis, meters per day.

c Hydraulic conductivity with respect to the z axis, meters per day.

Note: To convert meters to feet, multiply by 3.281.

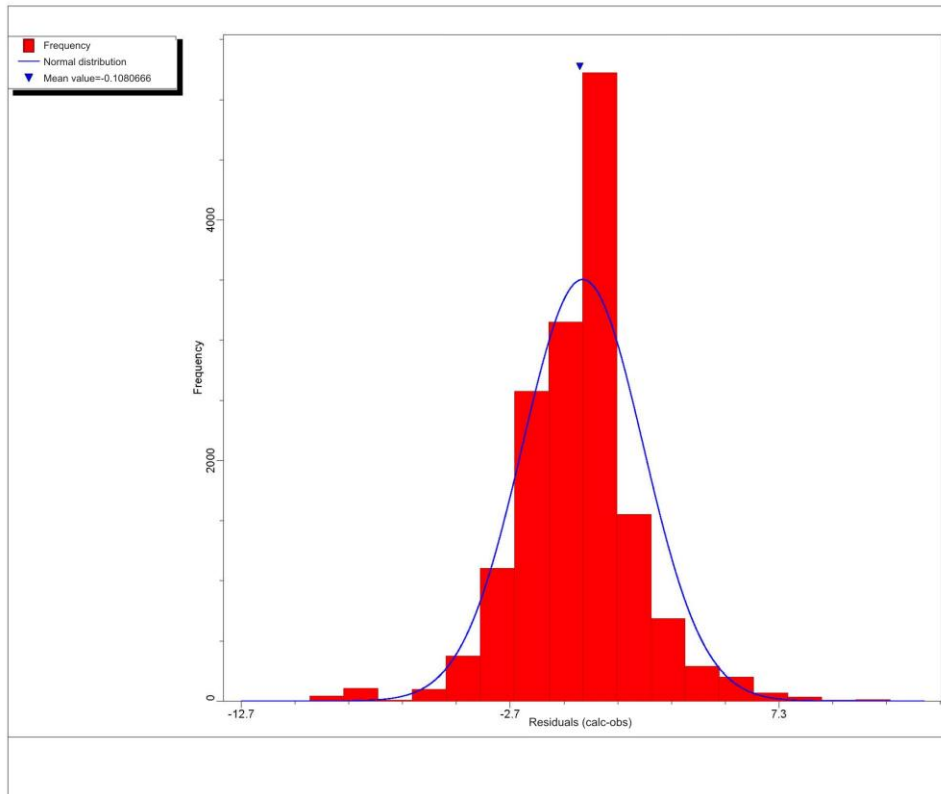


Figure L–60. 100th Percentile Flow Model Residual Distribution

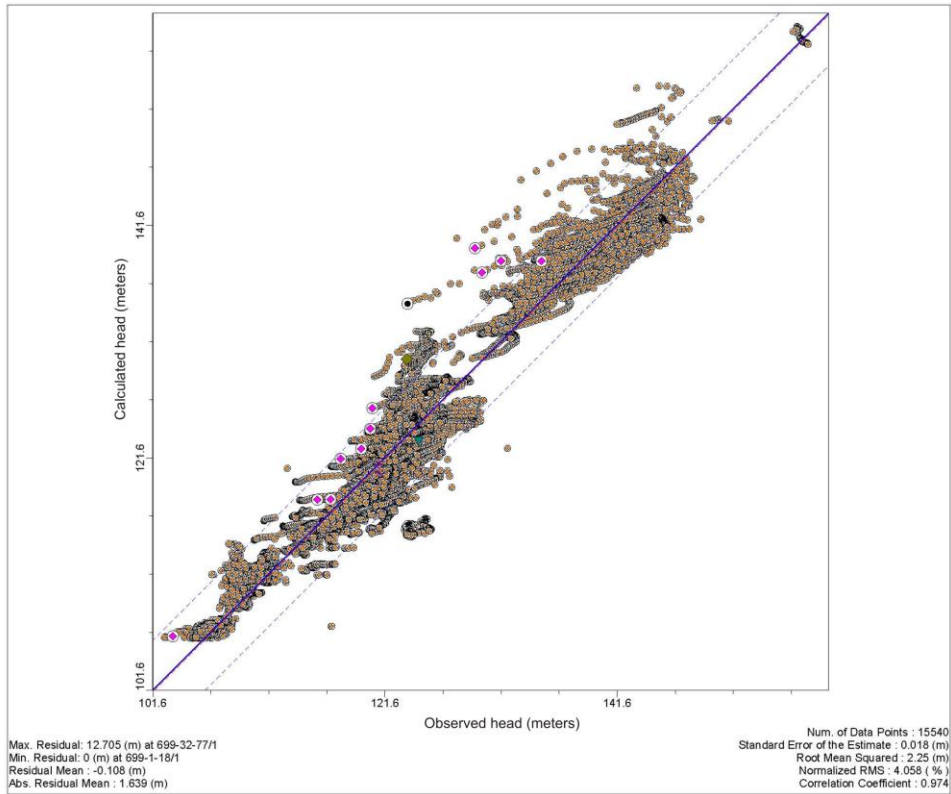


Figure L-61. 100th Percentile Flow Model Calibration Graph and Statistics

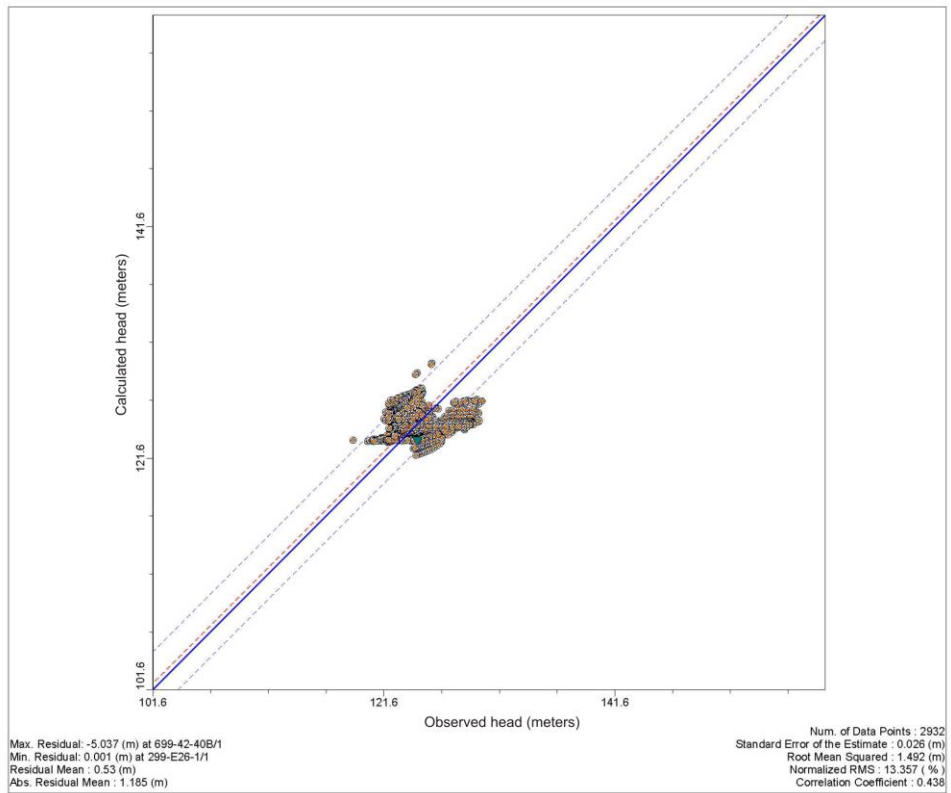


Figure L-62. 100th Percentile Flow Model Residuals – 200-East Area

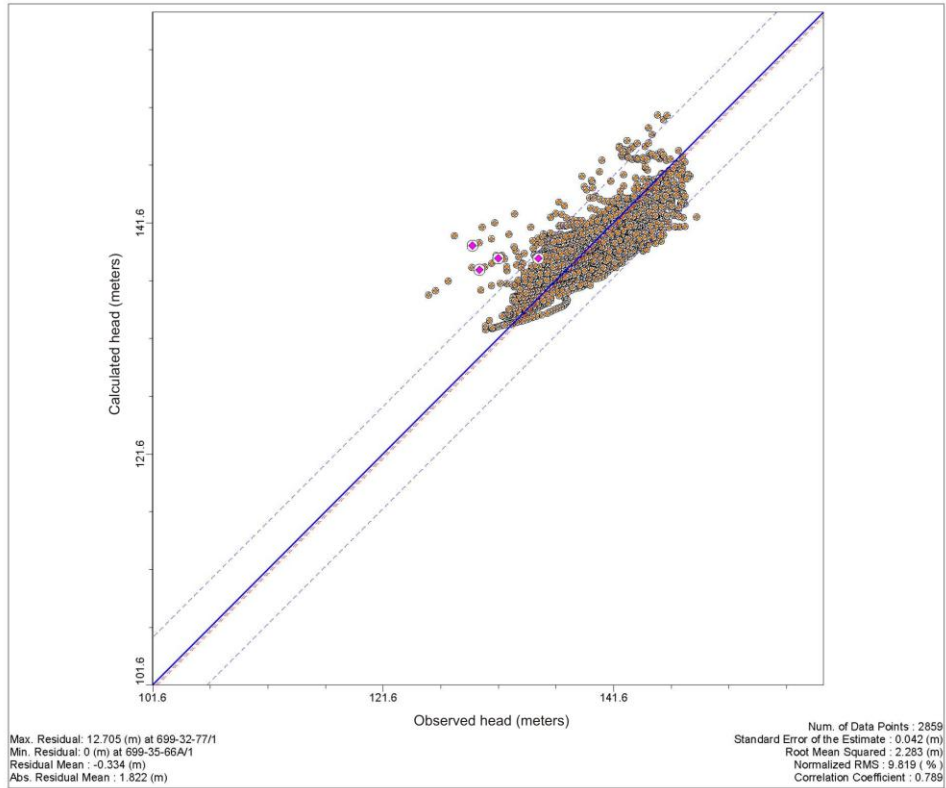


Figure L-63. 100th Percentile Flow Model Residuals – 200-West Area

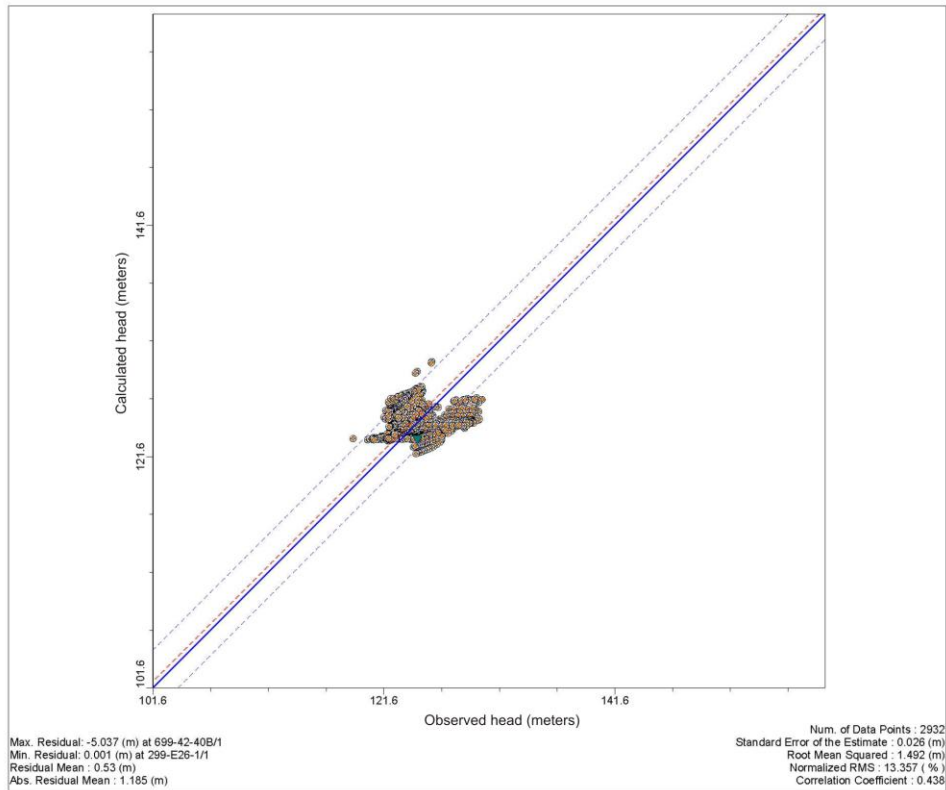


Figure L-64. 100th Percentile Flow Model Residuals, Calendar Year 1955

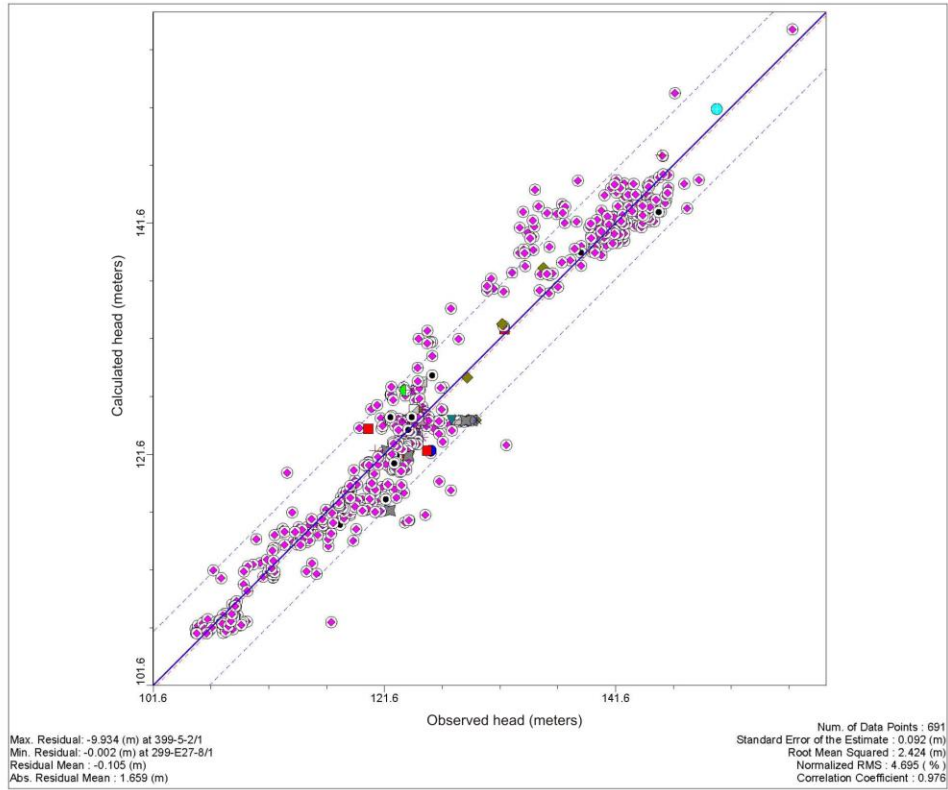


Figure L-65. 100th Percentile Flow Model Residuals, Calendar Year 1975

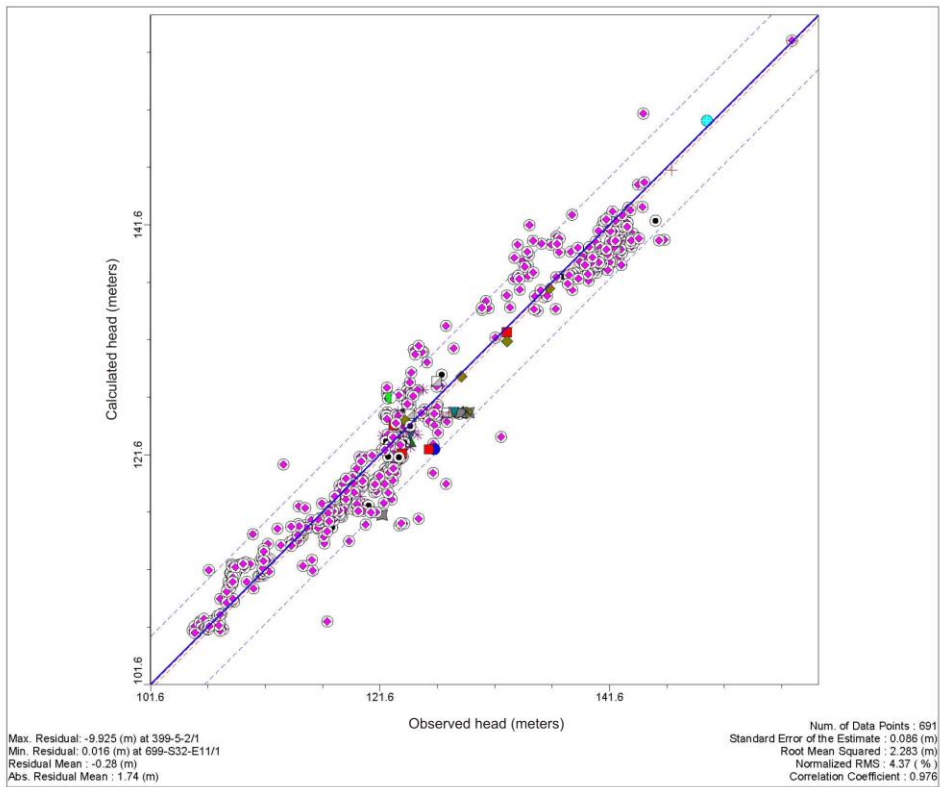


Figure L-66. 100th Percentile Flow Model Residuals, Calendar Year 1995

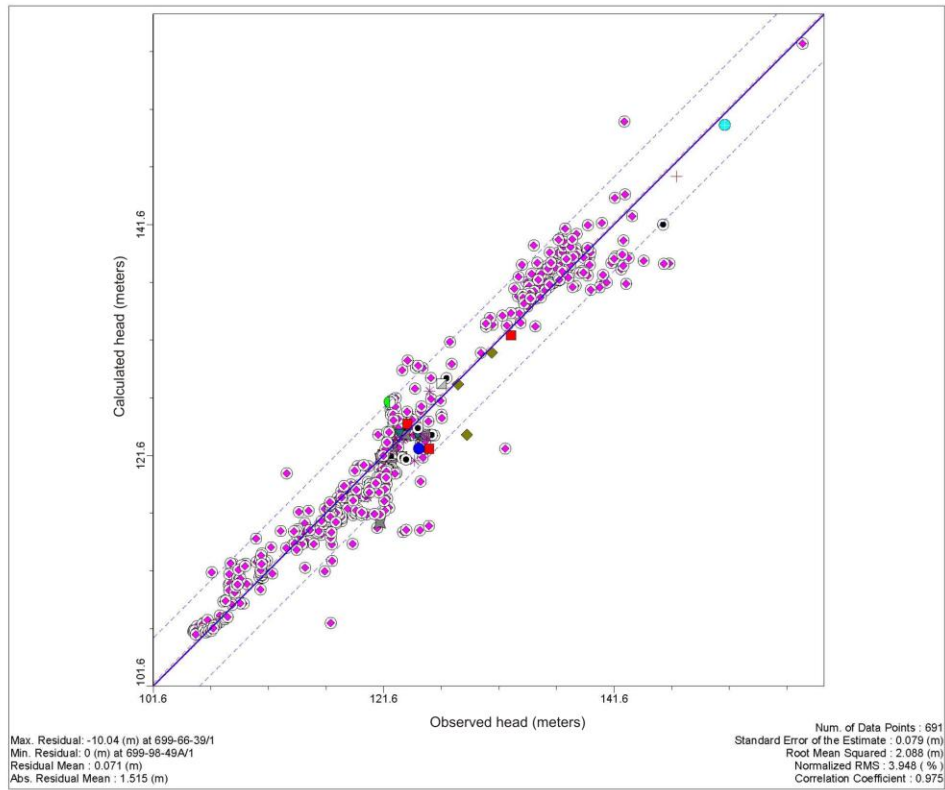


Figure L-67. 100th Percentile Flow Model Residuals, Calendar Year 2010

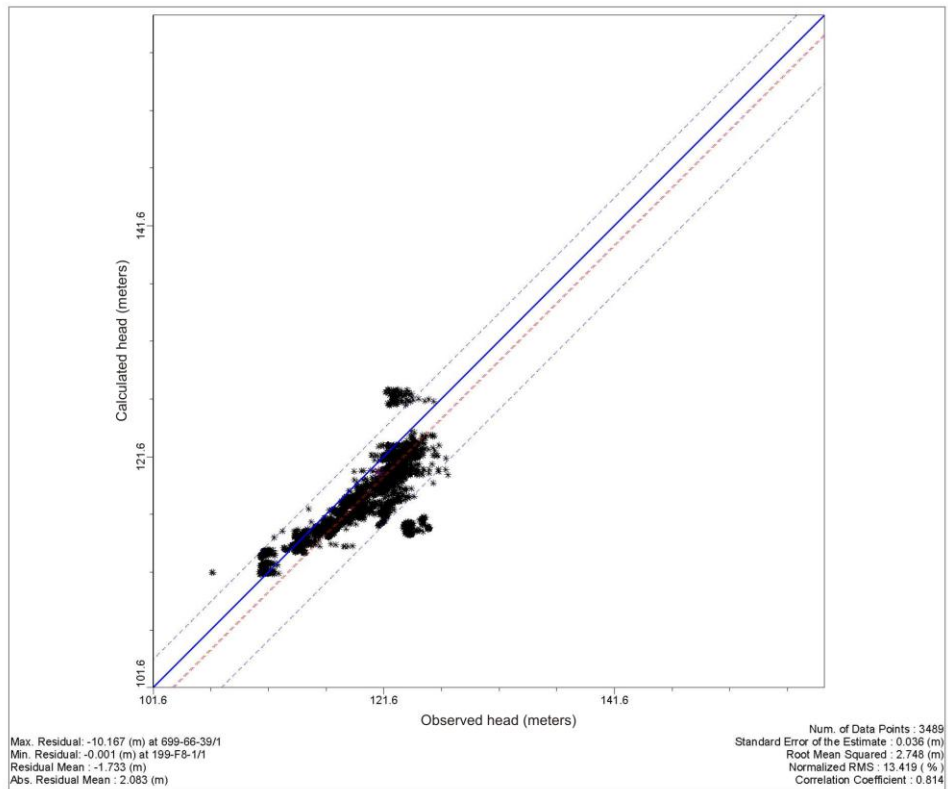


Figure L-68. 100th Percentile Flow Model Residuals in Northern Region of Model

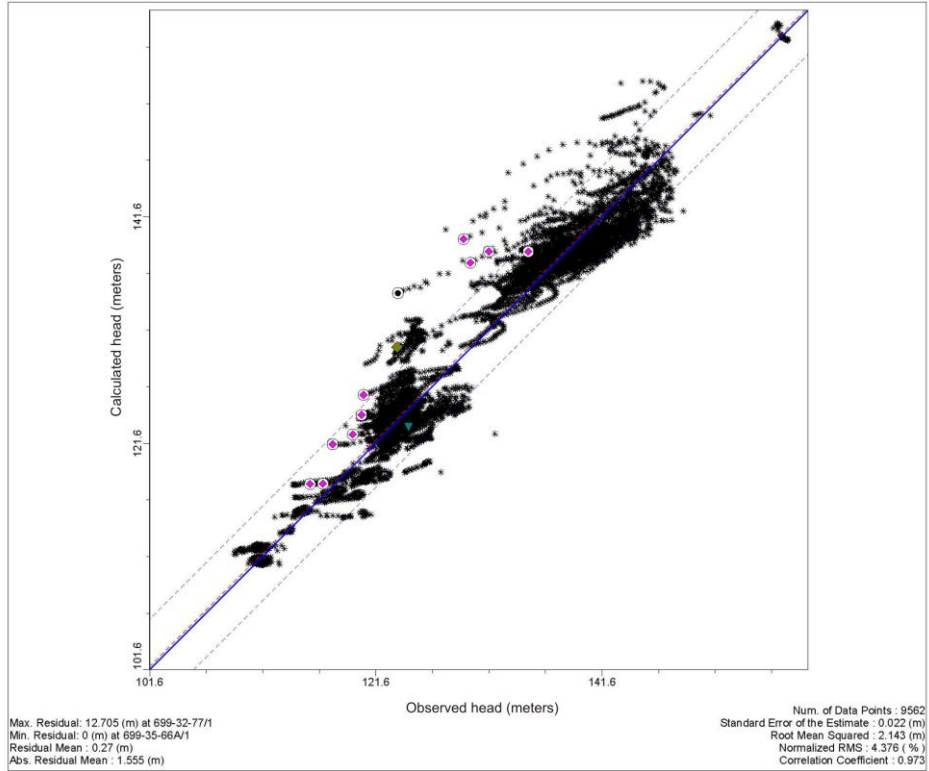


Figure L-69. 100th Percentile Flow Model Residuals in Central Region of Model

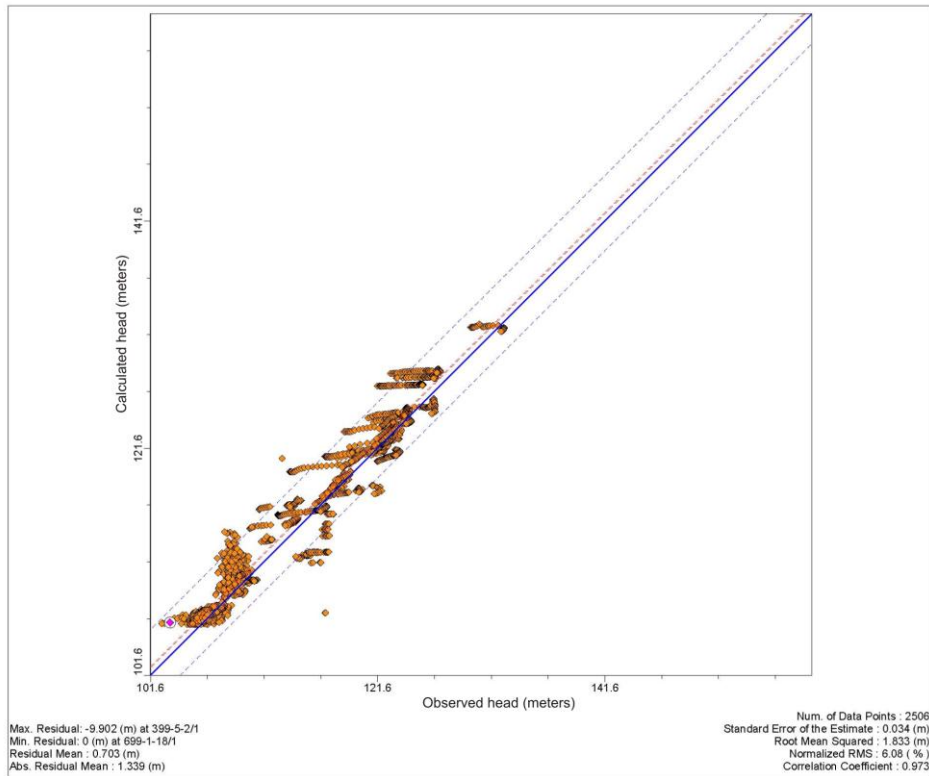


Figure L-70. 100th Percentile Flow Model Residuals in Southern Region of Model

In addition to the calibration acceptance criteria, water (or mass) balance and a long-term, steady state condition must be achieved in the calibrated flow model. Cumulative mass water balance data are shown in Figure L-71, indicating a cumulative mass balance error of approximately -1.4 percent. Total water balance and storage data as a function of time are shown in Figure L-72. The Figure L-72 data show storage values relative to the total water balance and indicate that storage-in is approximately equal to storage-out in model year 261 (CY 2200). This indicates that a long-term steady state condition is achieved. Note that, in Figure L-72, there is a spike in “storage” at model year 82. This spike is the result of a time-stepping change at the beginning of the final long-term stress period. As a result, the model is moving from a relatively long time step at the end of the previous stress period (model year 82) to a relatively short time step at the beginning of the final stress period.

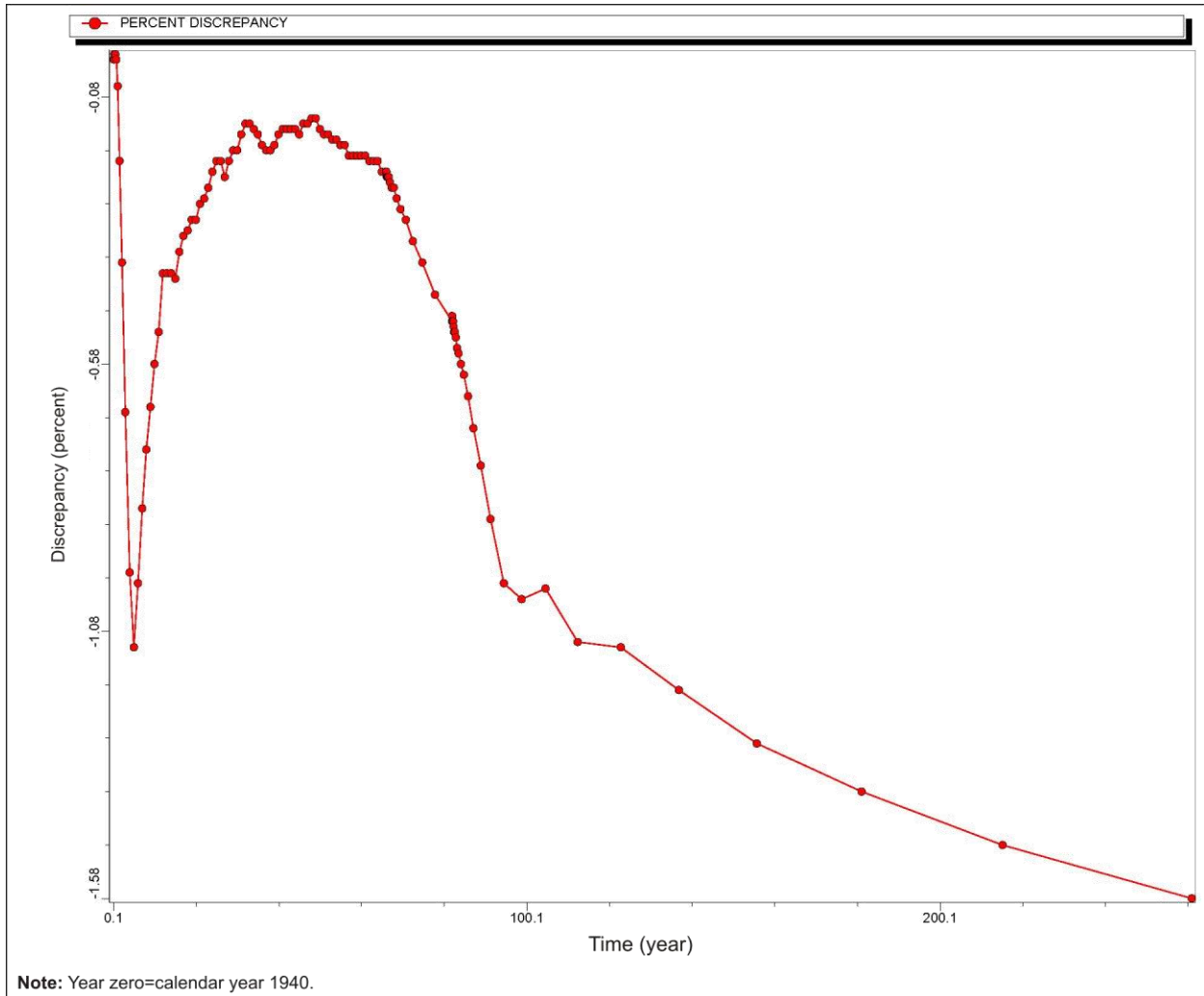


Figure L-71. 100th Percentile Flow Model Cumulative Water Balance Discrepancy

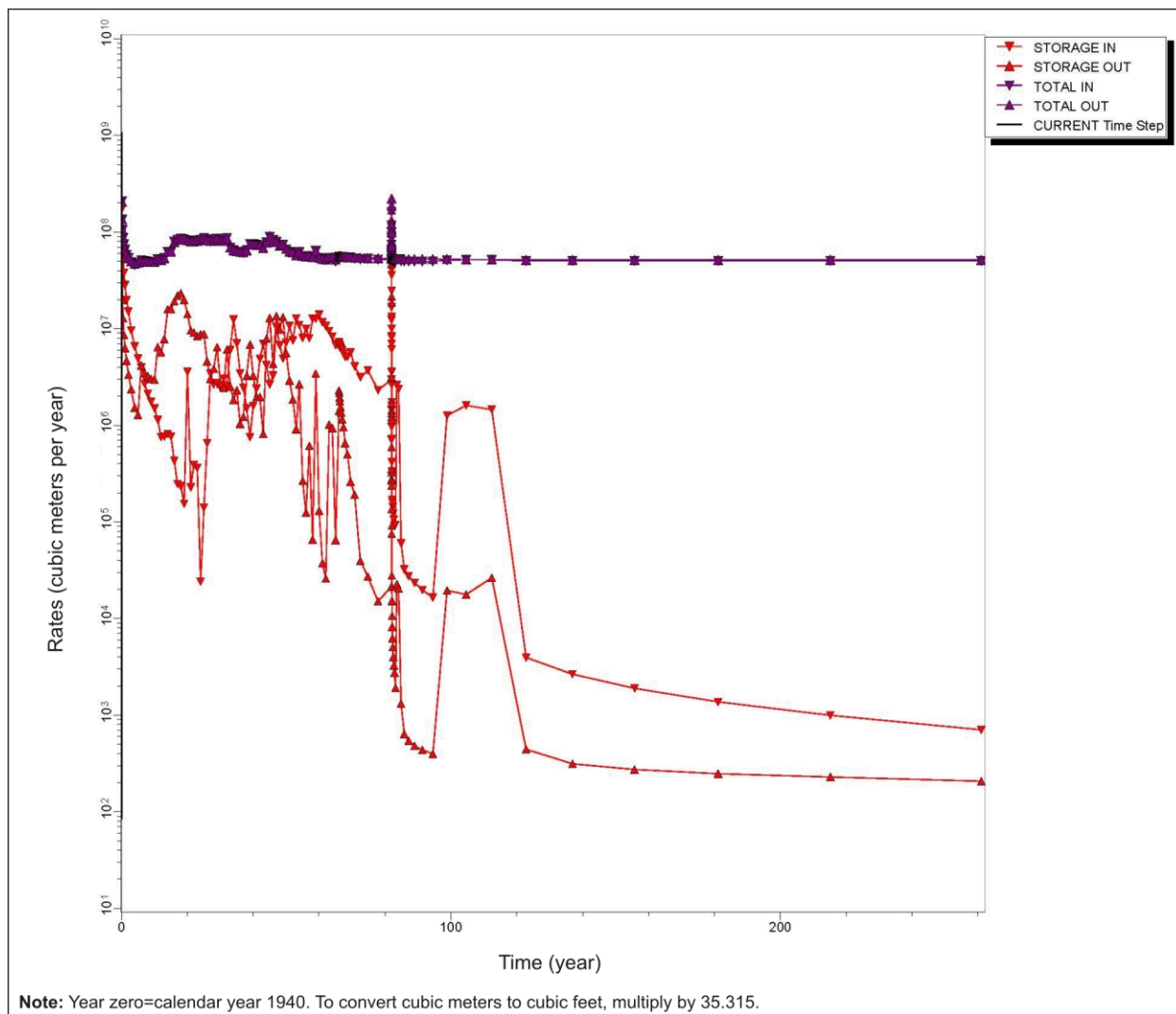
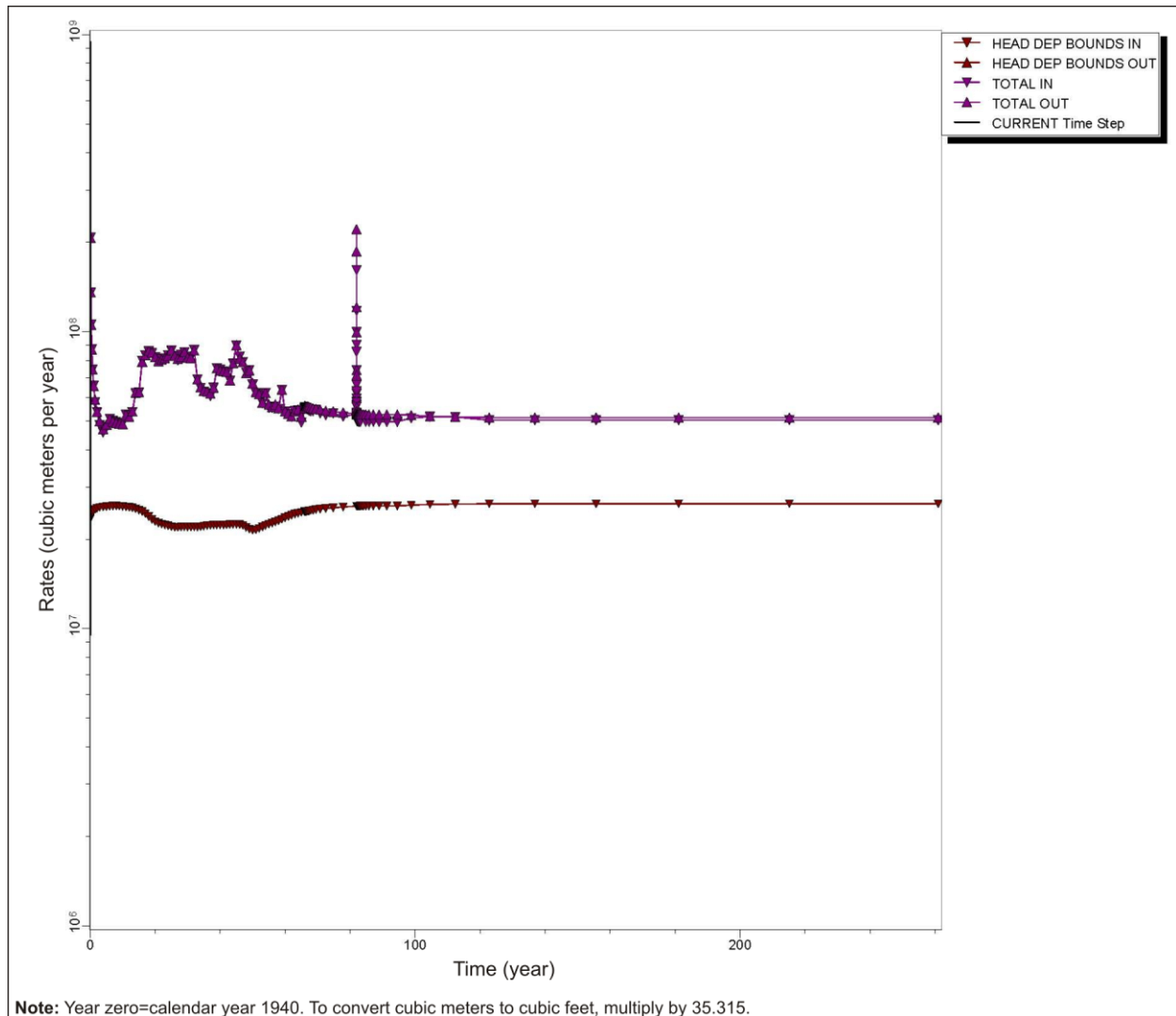


Figure L-72. 100th Percentile Flow Model Total Water and Storage Rates over Time

Additional water balance results for the 100th percentile flow model are shown in Figures L-73, L-74, and L-75 for GHBs, river boundaries, and recharge boundaries, respectively.



**Figure L-73. 100th Percentile Flow Model
Total Water and Generalized Head Boundary Rates over Time**

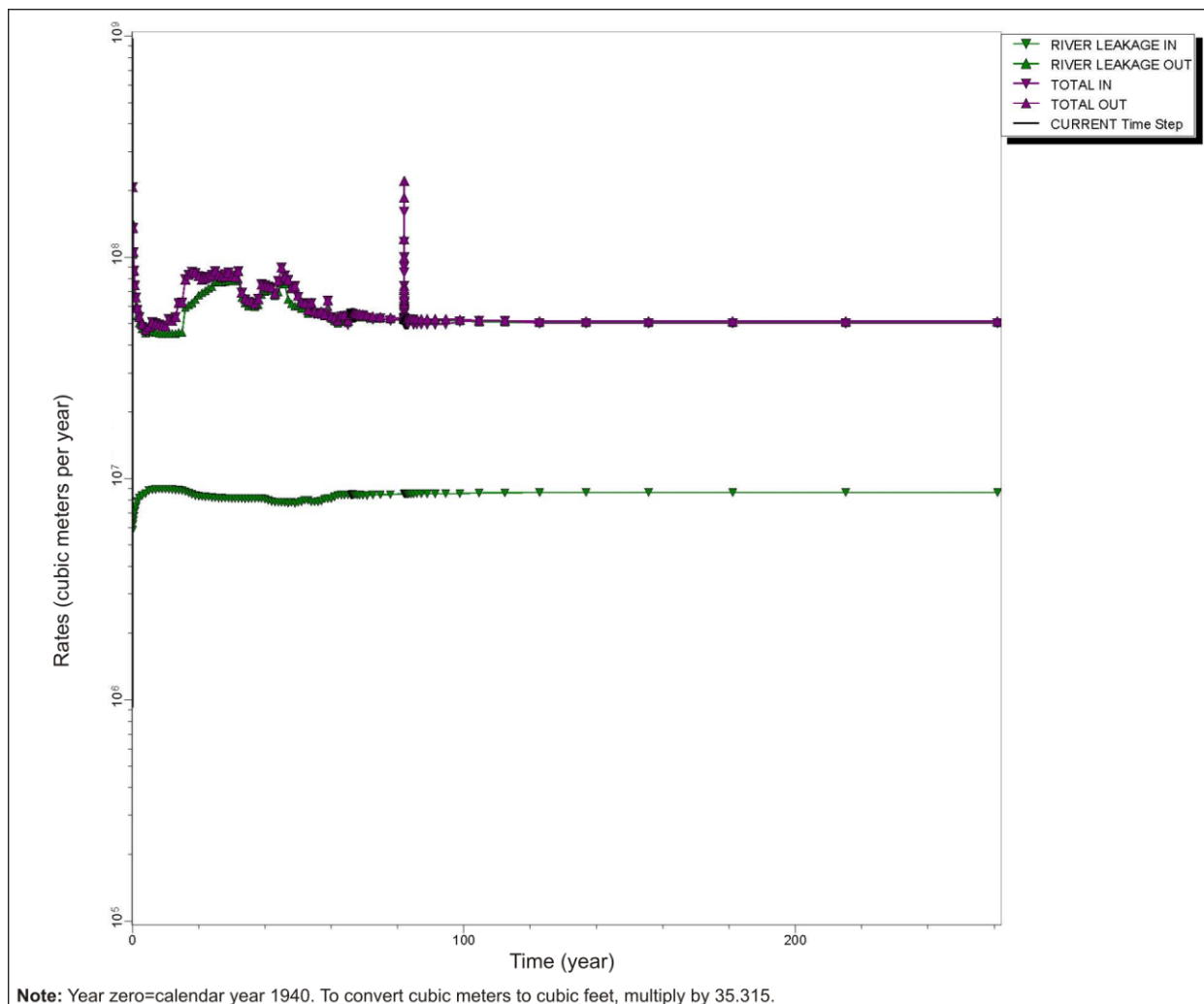
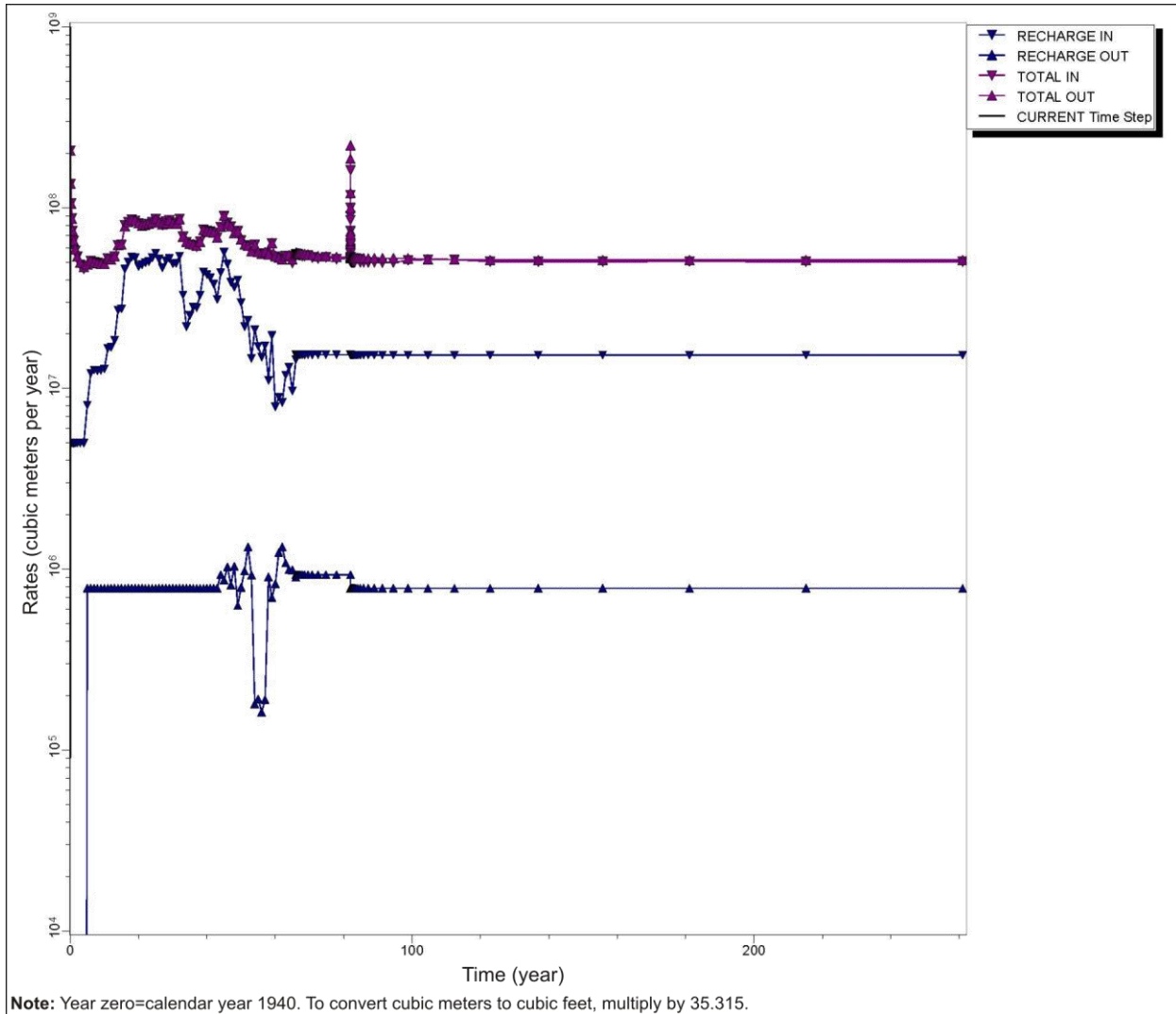


Figure L-74. 100th Percentile Flow Model Total Water and River Rates over Time



Note: Year zero=calendar year 1940. To convert cubic meters to cubic feet, multiply by 35.315.

Figure L-75. 100th Percentile Flow Model Total Water and Recharge Rates over Time

L.8.2.2 100th Percentile Potentiometric Head Distribution

A goal for the flow model is to produce a potentiometric distribution of heads that shows a steep water table in the 200-West Area due to the low-conductivity material types in that area and a relatively flat water table in the 200-East Area where high-conductivity material types are present. The pre-Hanford potentiometric surface is assumed to be approximately the same as the post-Hanford long-term, steady state condition, with water table mounding occurring below areas where, and at times when, Hanford operational discharges were released at the ground surface. Figures L-76, L-77, and L-78 are 100th percentile flow model simulations of the potentiometric surface in CY 1944 (pre-Hanford), CY 1975 (Hanford operations), and CY 2200 (post-Hanford), respectively.

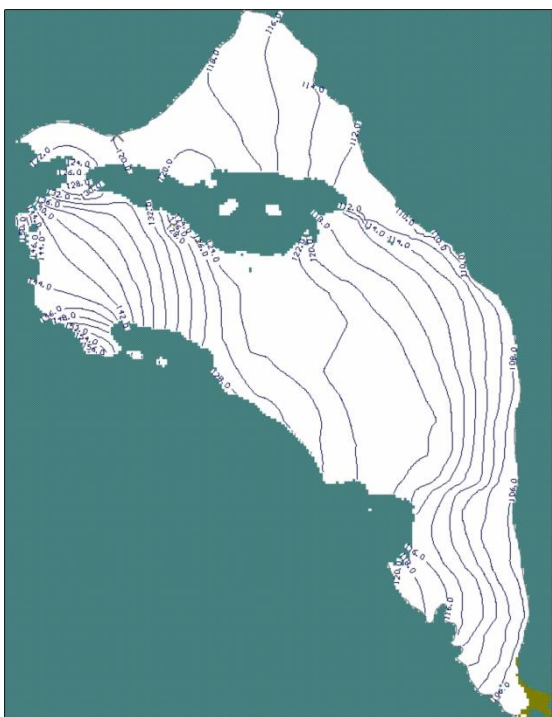


Figure L-76. 100th Percentile Flow Model Potentiometric Head Distribution, Calendar Year 1944

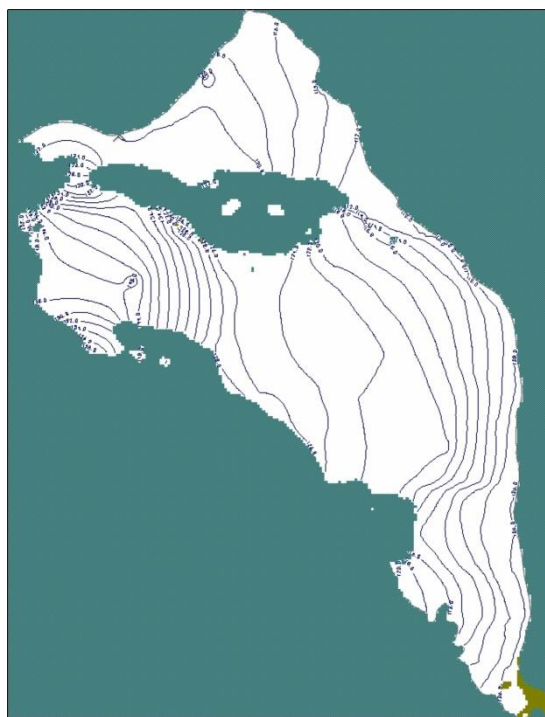


Figure L-77. 100th Percentile Flow Model Potentiometric Head Distribution, Calendar Year 1975

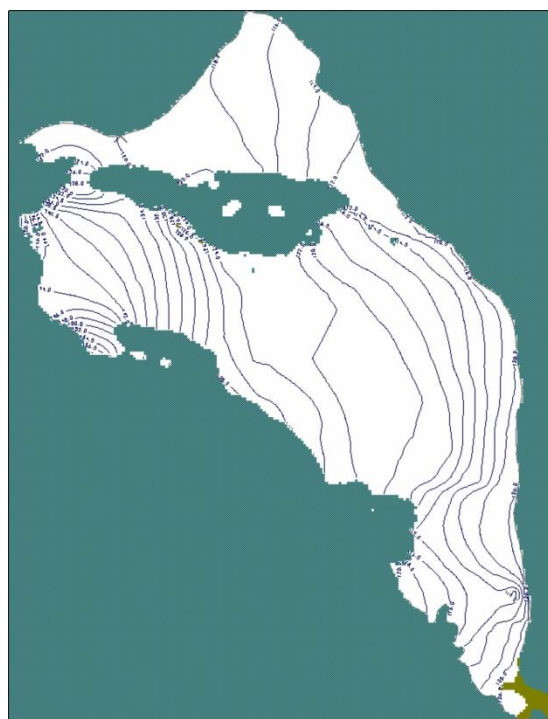


Figure L-78. 100th Percentile Flow Model Potentiometric Head Distribution, Calendar Year 2200

L.8.2.3 100th Percentile Flow Model Velocity Field

The 100th percentile flow model velocity field is variable in both magnitude and direction over time and across the model domain. This variability at selected locations within the model is shown in Figures L-79 through L-84. As expected, the velocities simulated in the 200-West Area are generally lower than those in the 200-East Area, particularly at the 200-East Area BY Cribs. An additional observation is that the velocity directions are highly variable during the Hanford operational period, particularly at the 200-East Area BY Cribs; there the velocity directions change by approximately 180 degrees due to water table mounding, coupled with this source's proximity to Gable Gap, where water table velocity and direction are sensitive to water table elevation.

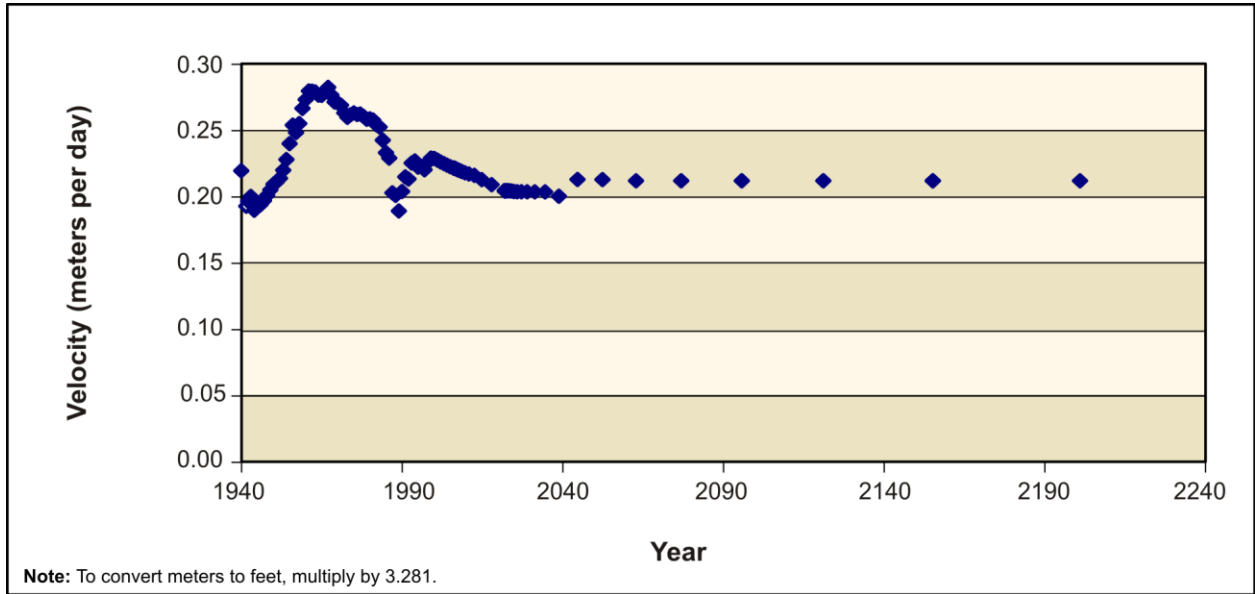


Figure L-79. 100th Percentile Flow Model Velocity Magnitude at 216-B-26 (BC Cribs in 200-East Area)

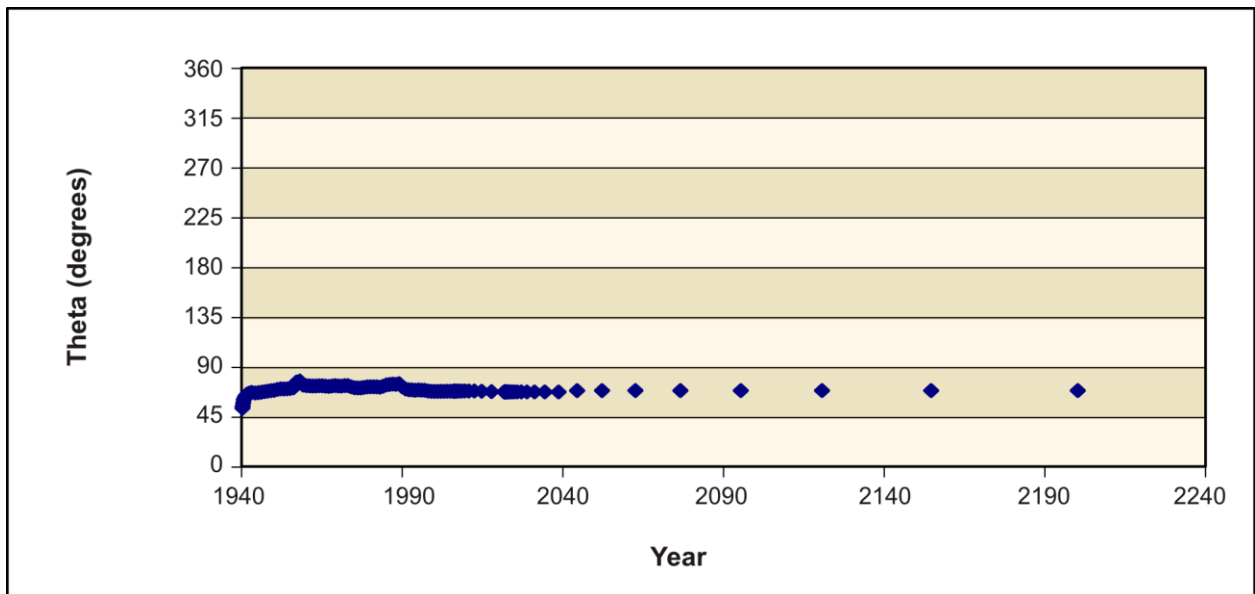


Figure L-80. 100th Percentile Flow Model Velocity Direction at 216-B-26 (BC Cribs in 200-East Area)

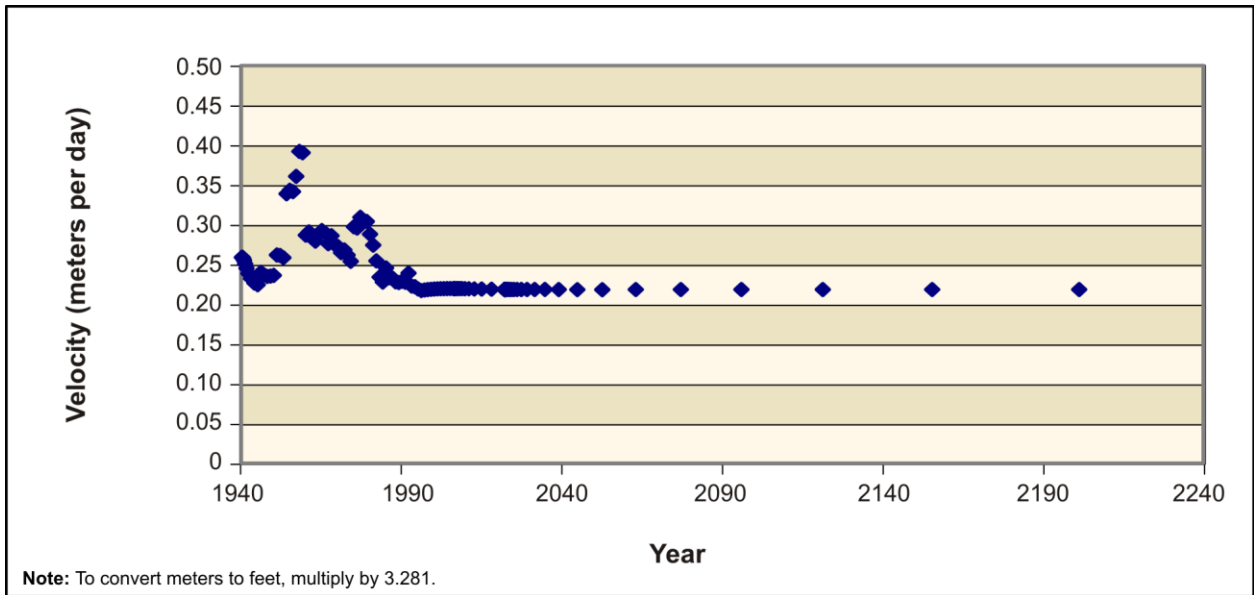


Figure L-81. 100th Percentile Flow Model Velocity Magnitude at 216-T-28 (200-West Area)

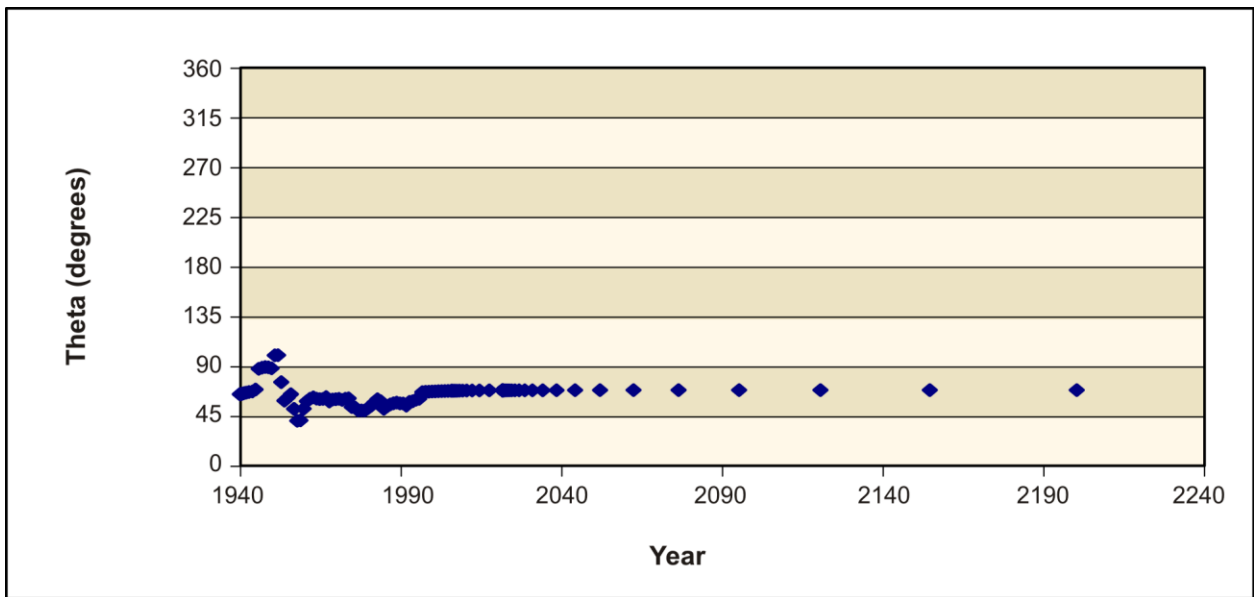


Figure L-82. 100th Percentile Flow Model Velocity Direction at 216-T-28 (200-West Area)

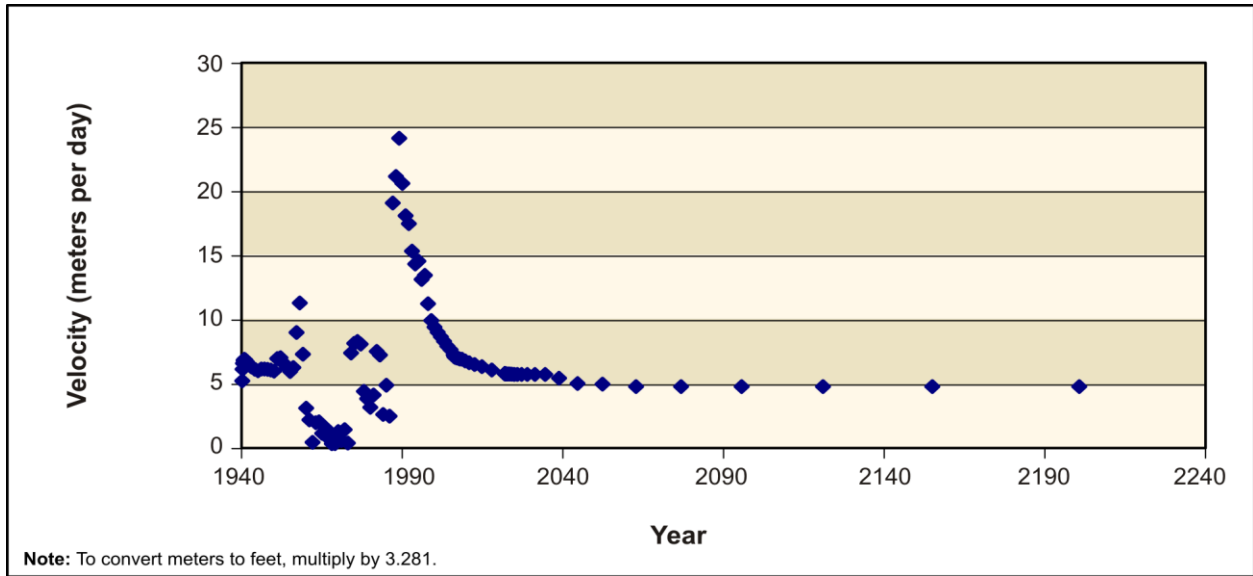


Figure L-83. 100th Percentile Flow Model Velocity Magnitude at BY Cribs (200-East Area)

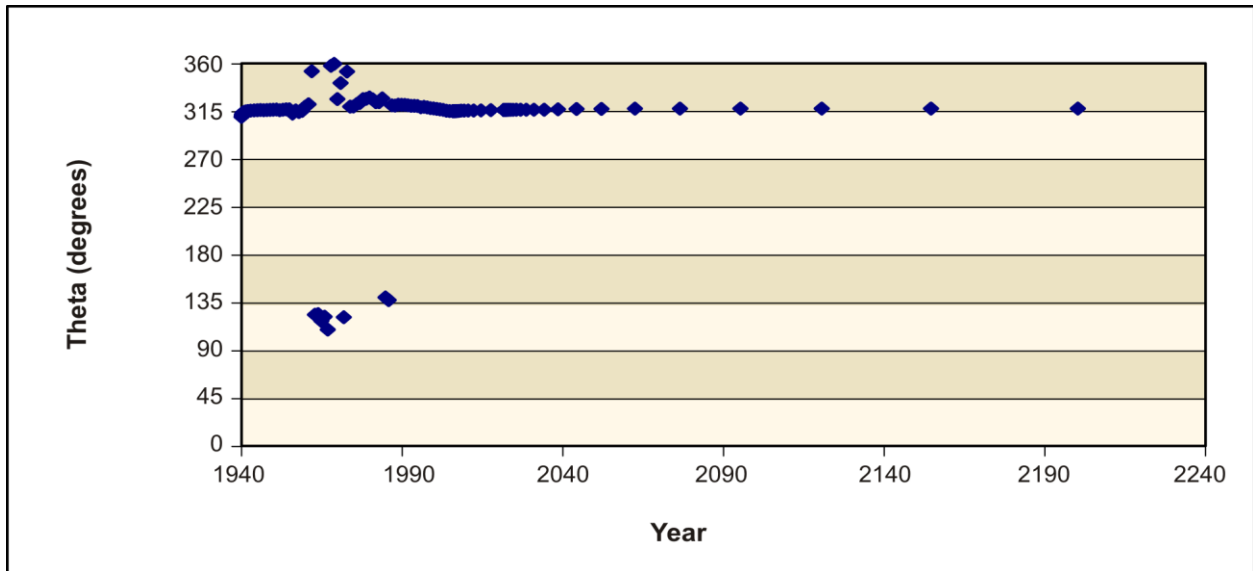


Figure L-84. 100th Percentile Flow Model Velocity Direction at BY Cribs (200-East Area)

L.8.2.4 100th Percentile Flow Model Central Plateau Pathline Analysis

Pathline analysis determined the number of particles (measured in area) released in the Central Plateau area that would move to the north through Gable Gap and the number that would move to the east toward the Columbia River. As discussed in Section L.1.5, in the *Draft TC & WM EIS*, the pathline analysis to demonstrate the area of northerly versus easterly flow from the Central Plateau depended primarily on hydraulic conductivity distribution rather than on uncertainties in the TOB surface. Comparison of this analysis with the 66th and 95th percentile cases (see Sections L.8.1.4 and L.8.3.4) confirms this observation. This pathline analysis included a MODFLOW and MODPATH model run, releasing a uniformly distributed set of particles across the Central Plateau area. The Central Plateau is depicted as a rectangular boundary that includes all of the 200-East and 200-West Areas, as well as other areas between and outside the 200 Areas. Figure L-85 shows that, in terms of area, the flow of this model is predominantly eastward from the Central Plateau.

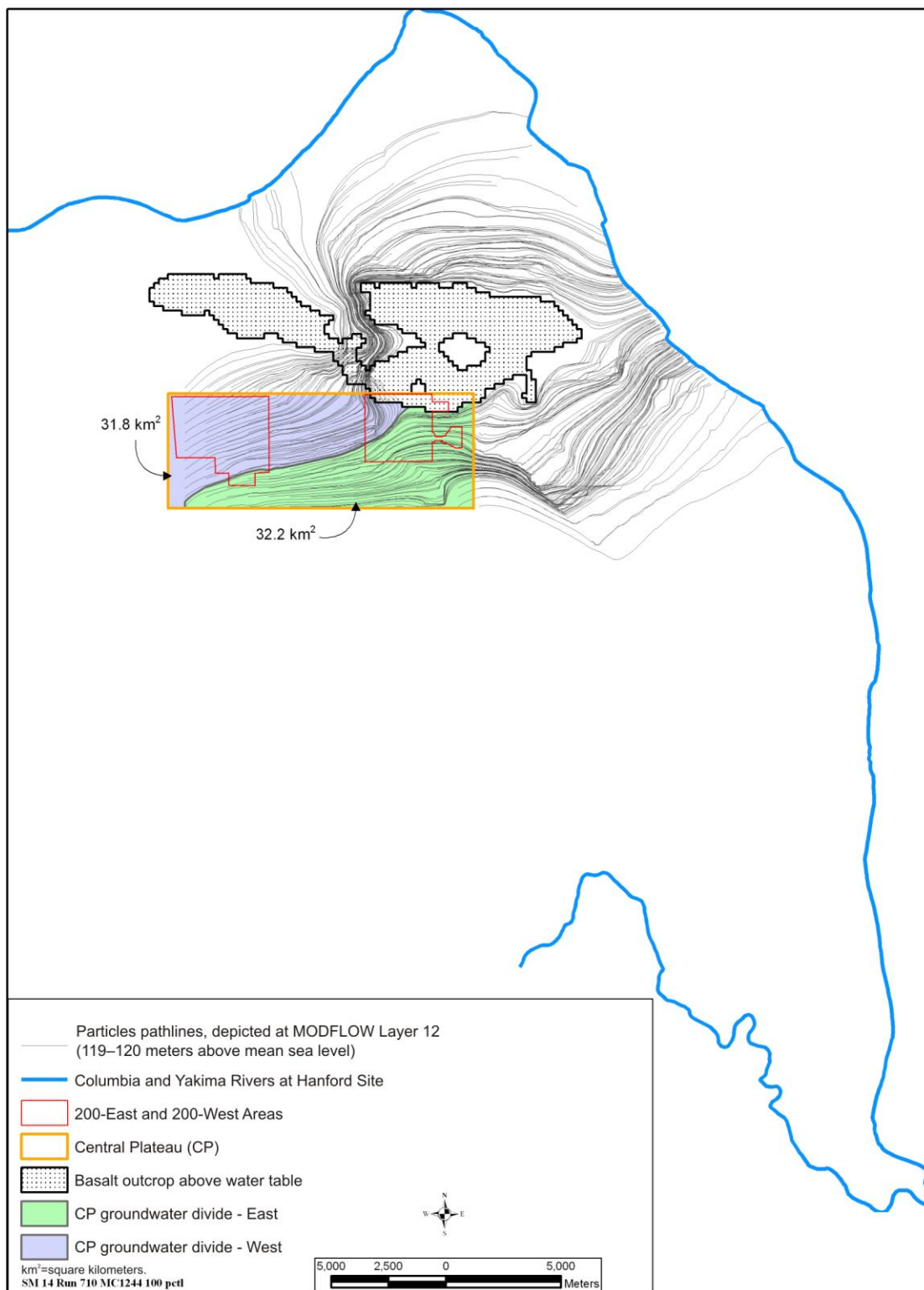


Figure L-85. 100th Percentile Flow Model Central Plateau Pathline Analysis

L.8.2.5 100th Percentile Flow Model Zone Budget Analysis

In addition to the particle pathline analysis described in the previous section, a zone budget analysis was completed to determine simulated water flow volumes from south of Gable Mountain and Gable Butte through Umtanum Gap, through Gable Gap, and easterly toward the Columbia River. Table L-20 provides total water flow volumes through these areas for CY 2200. These results show that about 17 percent of the total volume of water entering the Columbia River passes through Umtanum Gap, about 15 percent through Gable Gap, and about 68 percent directly east to the Columbia River. Comparison of these results with those of the 66th and 95th percentile cases shows that in terms of volumetric flow, rather than in terms of geometric position of the flow divide across the Central Plateau (see Section L.8.2.4), the model is less sensitive to variations in hydraulic conductivity.

**Table L-20. 100th Percentile Flow Model –
Simulated Water Flow Volumes Through Selected Areas, Calendar Year 2200**

Water Flow Through	Water Volume (cubic meters per year)
Umtanum Gap	4,615,600
Gable Gap	4,294,500
East to Columbia River	18,977,000

Note: To convert cubic meters to cubic feet, multiply by 35.315.

L.8.2.6 100th Percentile Flow Model – Transport Model Concentration-Versus-Time Results

Groundwater transport modeling was completed using the 100th percentile flow model. Figures L-86 and L-87 show the concentration-versus-time results measured at the Core Zone Boundary and at the Columbia River nearshore for technetium-99 under Tank Closure Alternative 2B and Waste Management Alternative 2, Disposal Group 1, Subgroup 1-A, respectively. Figures L-86 and L-87 are comparable to Figures L-58 and L-59, respectively, for the 95th percentile flow model, and comparable to Figures L-114 and L-115, respectively, for the 66th percentile flow model. These comparisons show that the three flow models result in similar technetium-99 concentrations over time for the two alternatives presented. See Chapter 2 for a description of these alternatives.

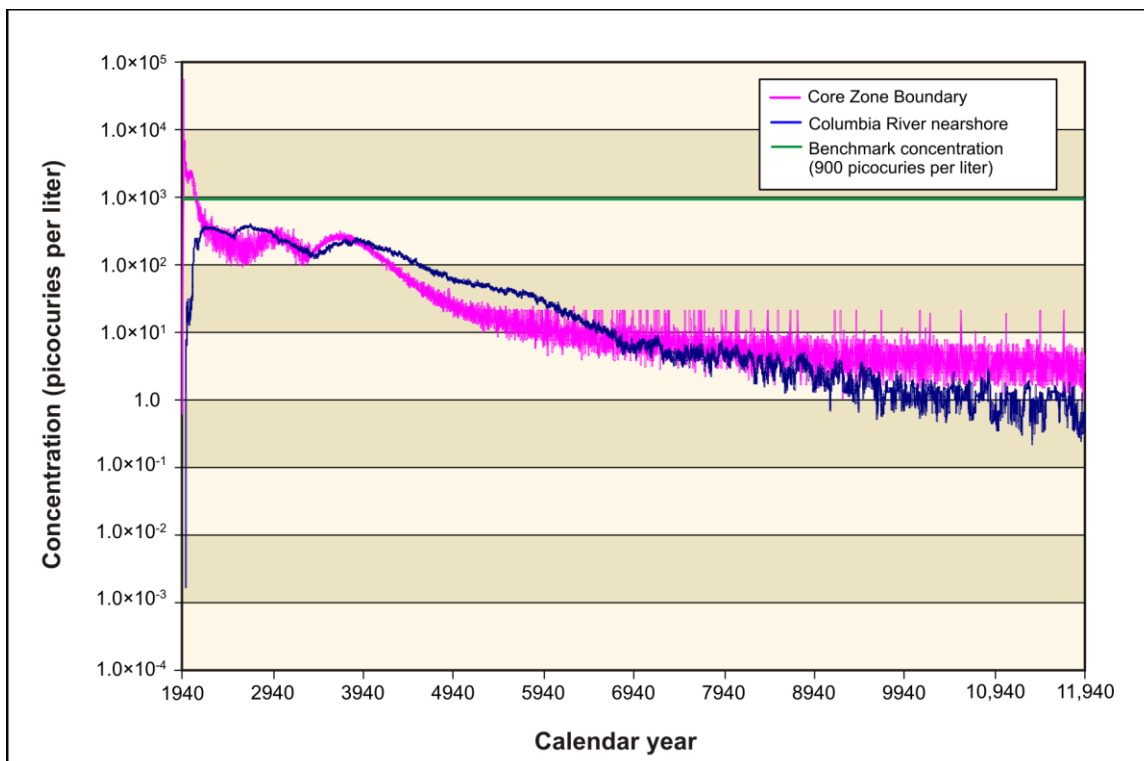


**Figure L-86. Tank Closure Alternative 2B 100th Percentile Flow Model
Concentration-Versus-Time Results for Technetium-99**

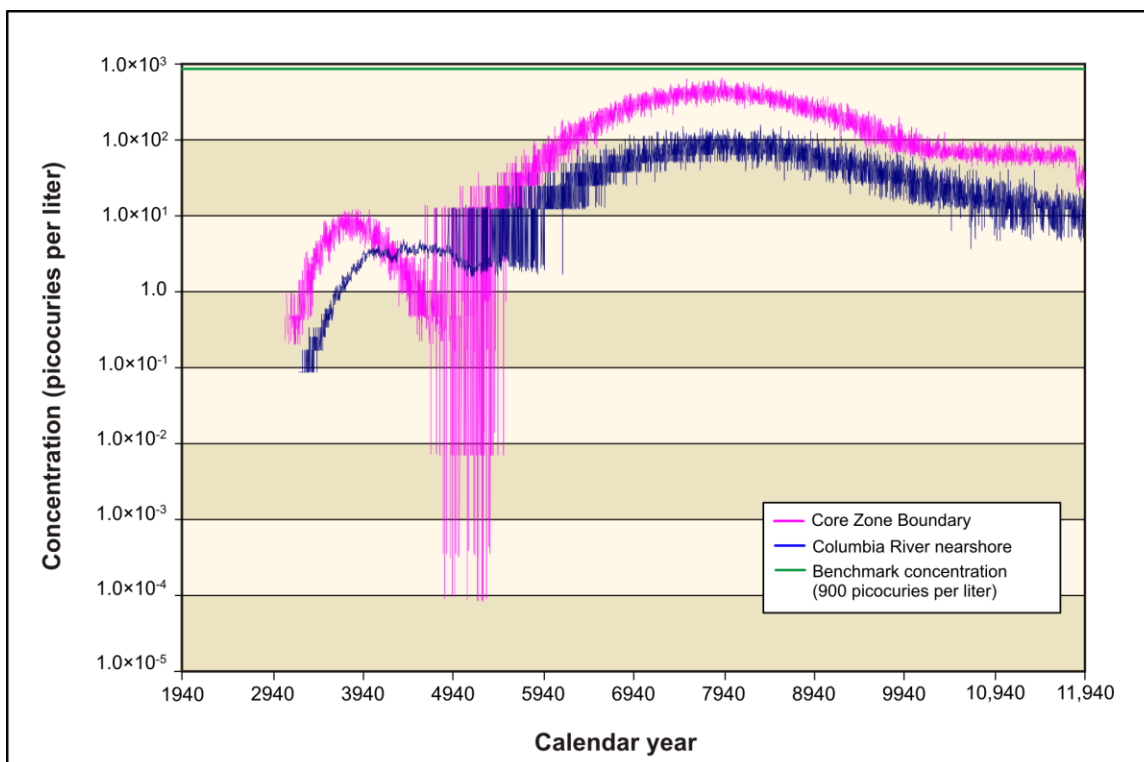


**Figure L-87. Waste Management Alternative 2, Disposal Group 1, Subgroup 1-A,
100th Percentile Flow Model
Concentration-Versus-Time Results for Technetium-99**

L.8.3 Results from the 66th Percentile Flow Model

L.8.3.1 Calibration Acceptance

Table L-21 provides a restatement of the flow model calibration acceptance criteria discussed in Section L.6.2, along with an assessment of the 66th percentile flow model's performance for each criterion. Specific data illustrative of such performance are reflected in Table L-22 and Figures L-88 through L-98.

**Table L-21. Summary of the 66th Percentile Flow Model
Performance Compared with the Calibration Acceptance Criteria**

Flow Model Calibration Acceptance Criteria	66th Percentile Flow Model Performance
Residual distribution should be reasonably normal.	Residual distribution is reasonably normal (see Figure L-88).
The mean residual should be approximately 0.	Residual mean = 0.462 meters (1.516 feet) (see Figure L-89).
The number of positive residuals should approximate the number of negative residuals.	Positive residuals approximately equal negative residuals (see Figure L-88).
The correlation coefficient (calculated versus observed) should be greater than 0.9.	Correlation coefficient = 0.972 (see Figure L-89).
The root mean square (RMS) error (calculated versus observed) should be less than 5 meters (16.4 feet), approximately 10 percent of the gradient in the water table elevation.	RMS error = 2.412 meters (7.913 feet) (see Figure L-89).
Residuals in the 200-East Area should be distributed similarly to those in the 200-West Area.	Residuals in the 200-East and 200-West Areas are distributed similarly (see Figures L-90 and L-91).
The residuals should be evenly distributed over time.	Residuals are approximately evenly distributed over time (see Figures L-92, L-93, L-94, and L-95).
The residuals should be evenly distributed across the site.	Residuals are approximately evenly distributed across the site (see Figures L-96, L-97, and L-98).
The calibrated parameters should compare reasonably well with field-measured values.	Calibrated hydraulic conductivity values are listed in Table L-22 and compare reasonably with field-measured values for material types to which the model is sensitive (i.e., Hanford formation and Ringold Formation material types). Figure L-42 provides field-measured values from aquifer pumping tests (Cole et al. 2001).
Parameters should be reasonably uncorrelated.	Hydraulic conductivity parameters are reasonably uncorrelated (see Table L-22 for the key to model material type zones and Table L-15 for the correlation coefficient matrix).

Table L–22. 66th Percentile Flow Model Calibrated Hydraulic Conductivity Values

Material Type (Model Zone)	Hydraulic Conductivity (K_x) ^a	Hydraulic Conductivity (K_y) ^b	Hydraulic Conductivity (K_z) ^c
Hanford mud (1)	0.88	0.88	0.088
Hanford silt (2)	9.86	9.86	0.986
Hanford sand (3)	103.13	103.13	10.313
Hanford gravel (4)	278.63	278.63	27.863
Ringold sand (5)	3.69	3.69	0.369
Ringold gravel (6)	17.0	17.0	1.7
Ringold mud (7)	0.97	0.97	0.097
Ringold silt (8)	0.59	0.59	0.059
Plio-Pleistocene sand (9)	93.9	93.9	9.39
Plio-Pleistocene silt (10)	23.73	23.73	2.373
Cold Creek sand (11)	107.08	107.08	10.708
Cold Creek gravel (12)	43.73	43.73	4.373
Highly conductive Hanford formation (13)	2411.55	2411.55	241.155
Activated basalt (14)	0.001	0.001	0.0001

^a Hydraulic conductivity with respect to the x axis, meters per day.

^b Hydraulic conductivity with respect to the y axis, meters per day.

^c Hydraulic conductivity with respect to the z axis, meters per day.

Note: To convert meters to feet, multiply by 3.281.

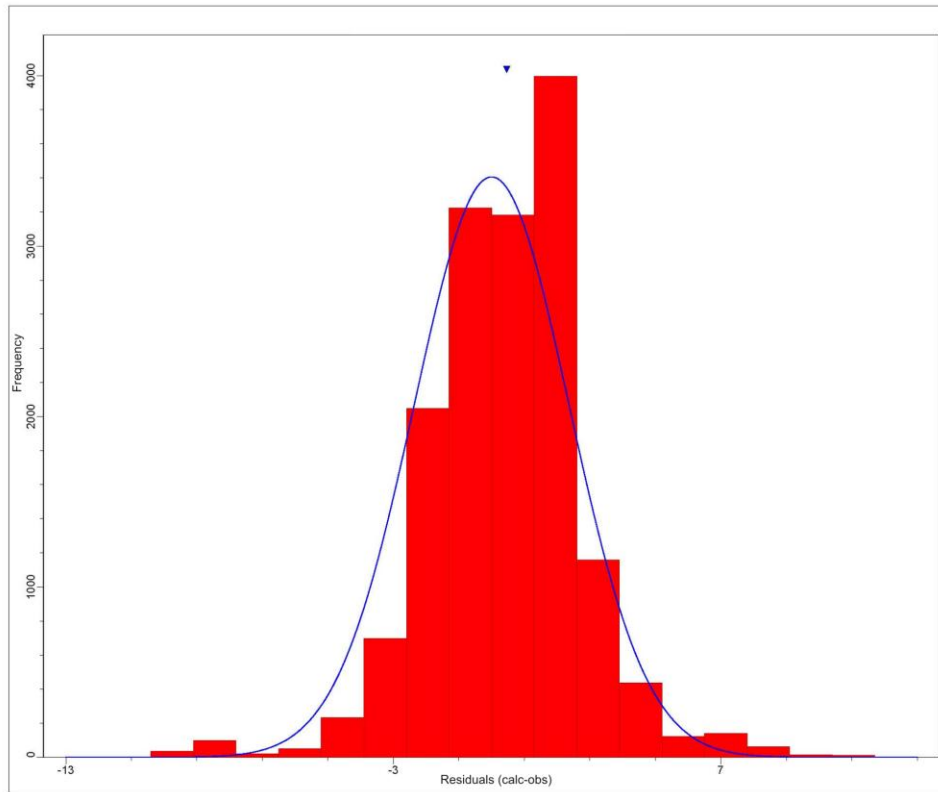


Figure L–88. 66th Percentile Flow Model Residual Distribution

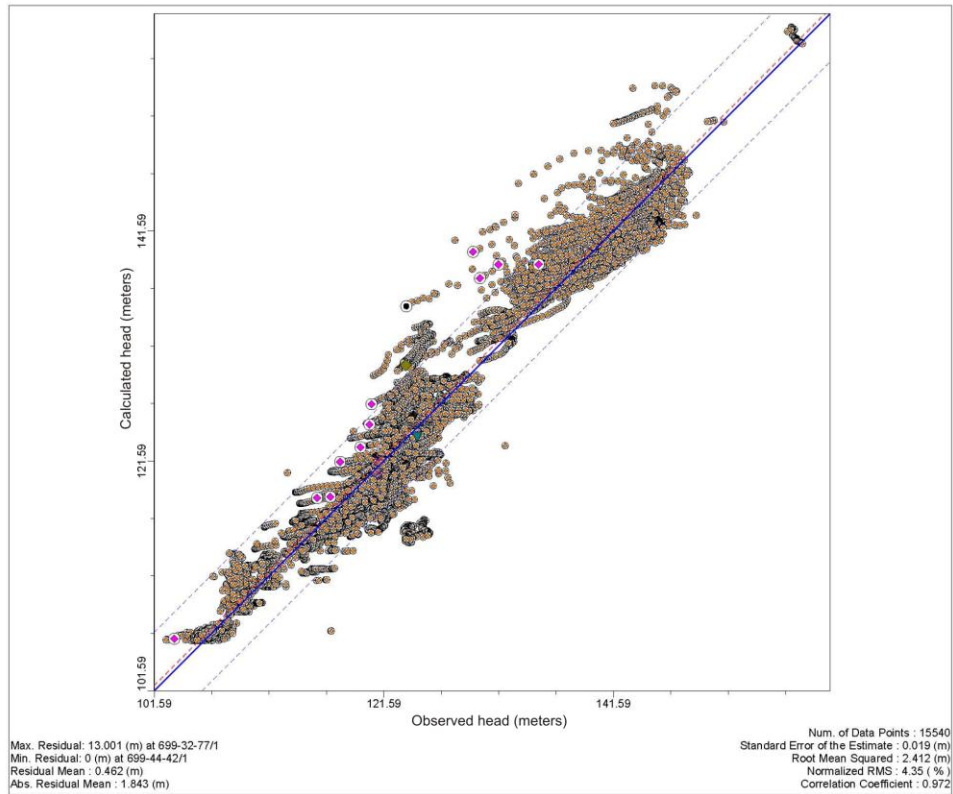


Figure L-89. 66th Percentile Flow Model Calibration Graph and Statistics

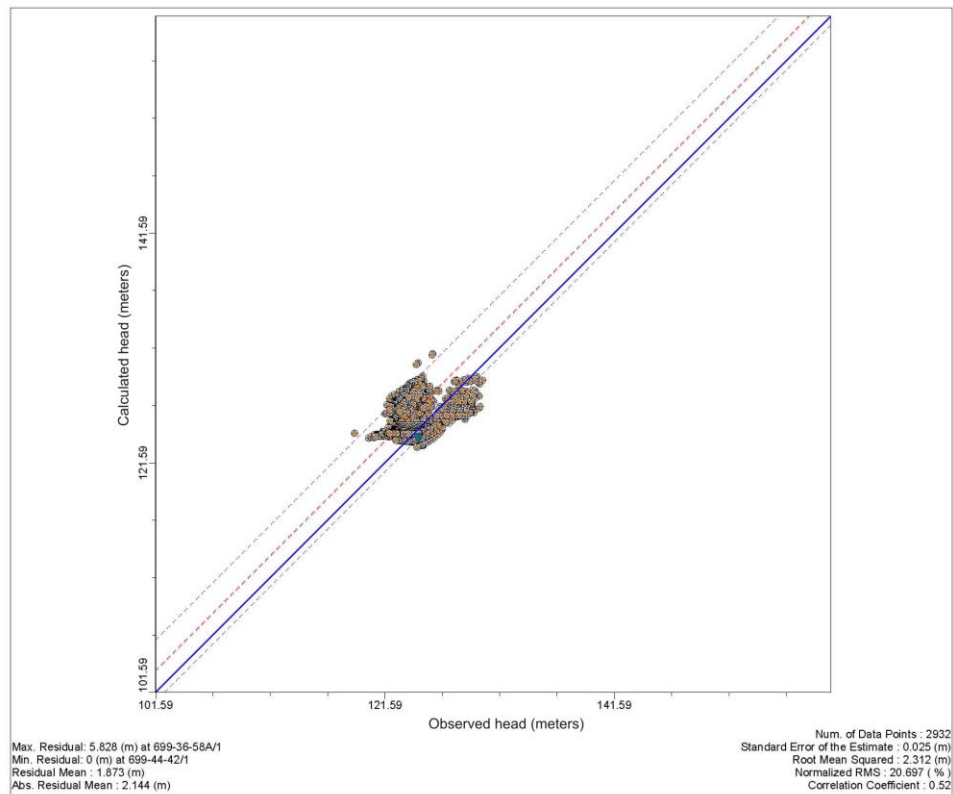


Figure L-90. 66th Percentile Flow Model Residuals - 200-East Area

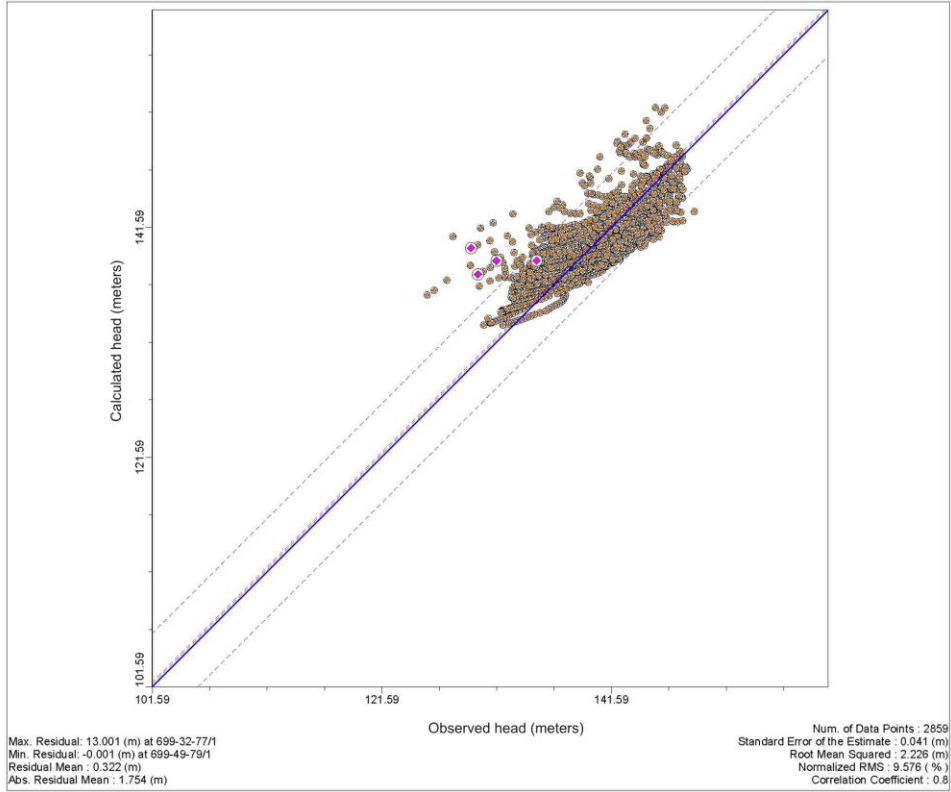


Figure L-91. 66th Percentile Flow Model Residuals – 200-West Area

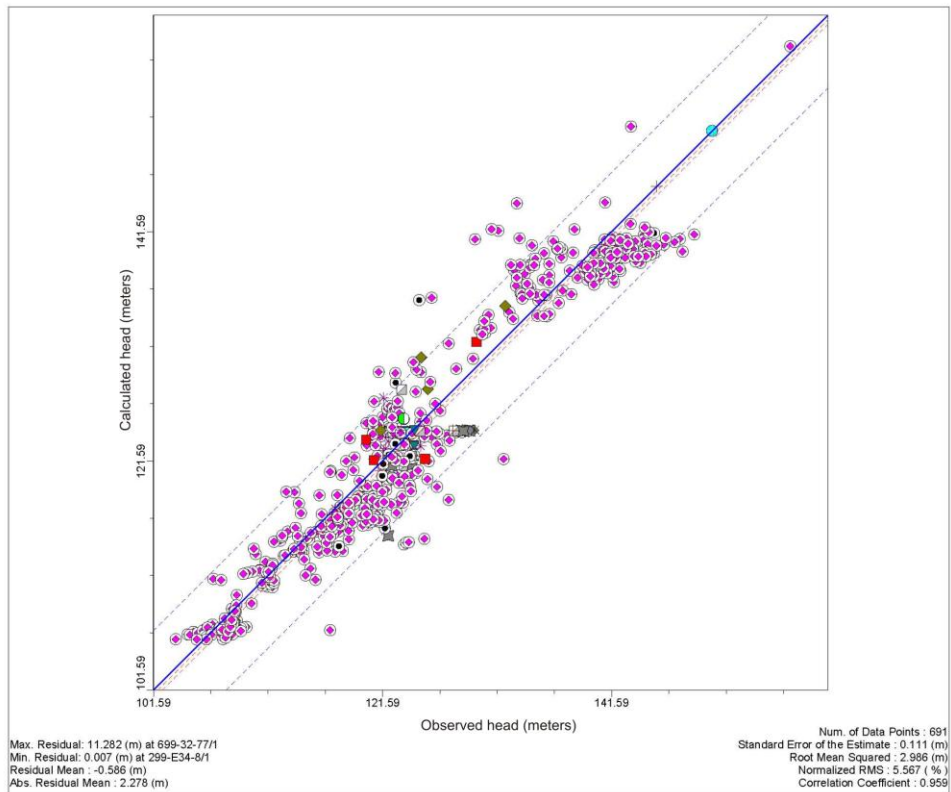


Figure L-92. 66th Percentile Flow Model Residuals, Calendar Year 1955

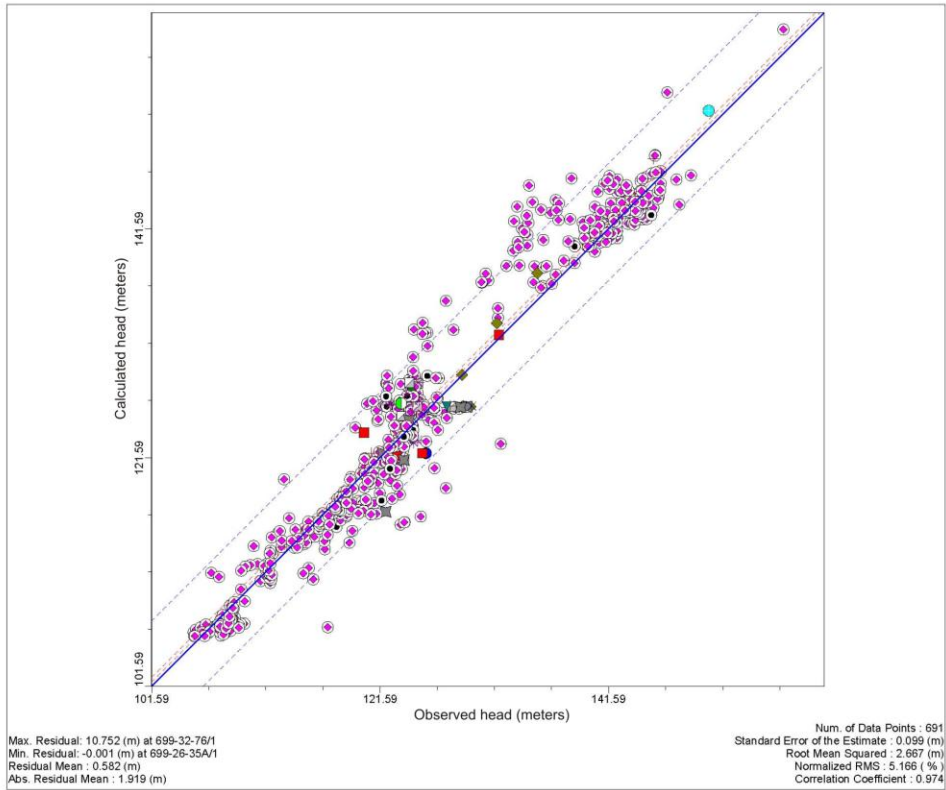


Figure L-93. 66th Percentile Flow Model Residuals, Calendar Year 1975

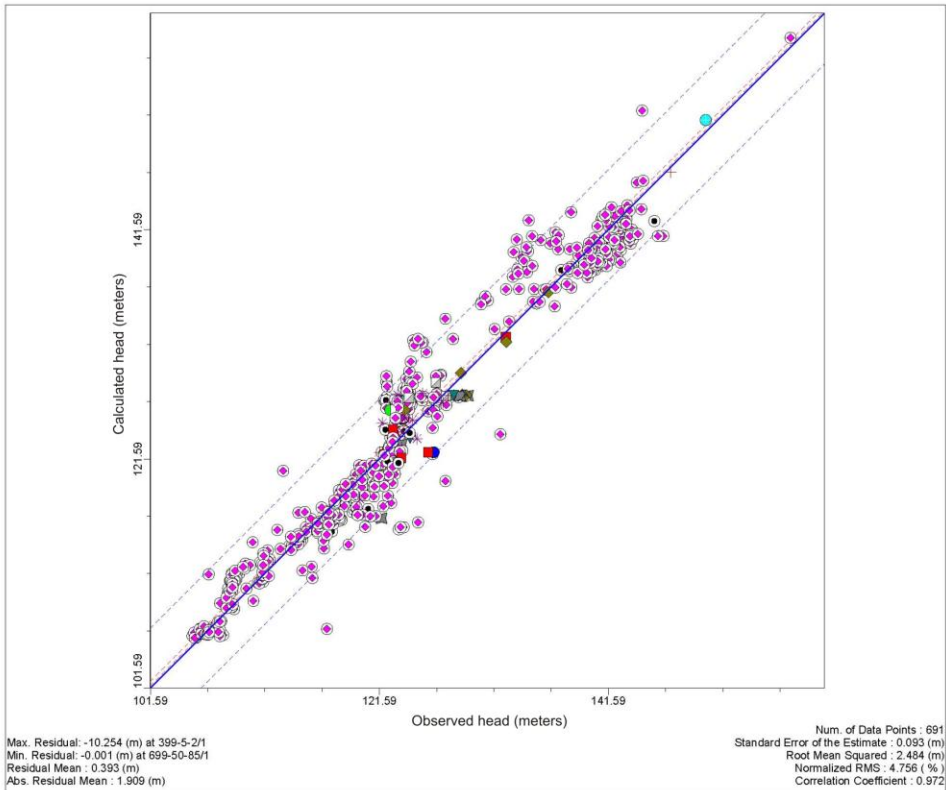


Figure L-94. 66th Percentile Flow Model Residuals, Calendar Year 1995

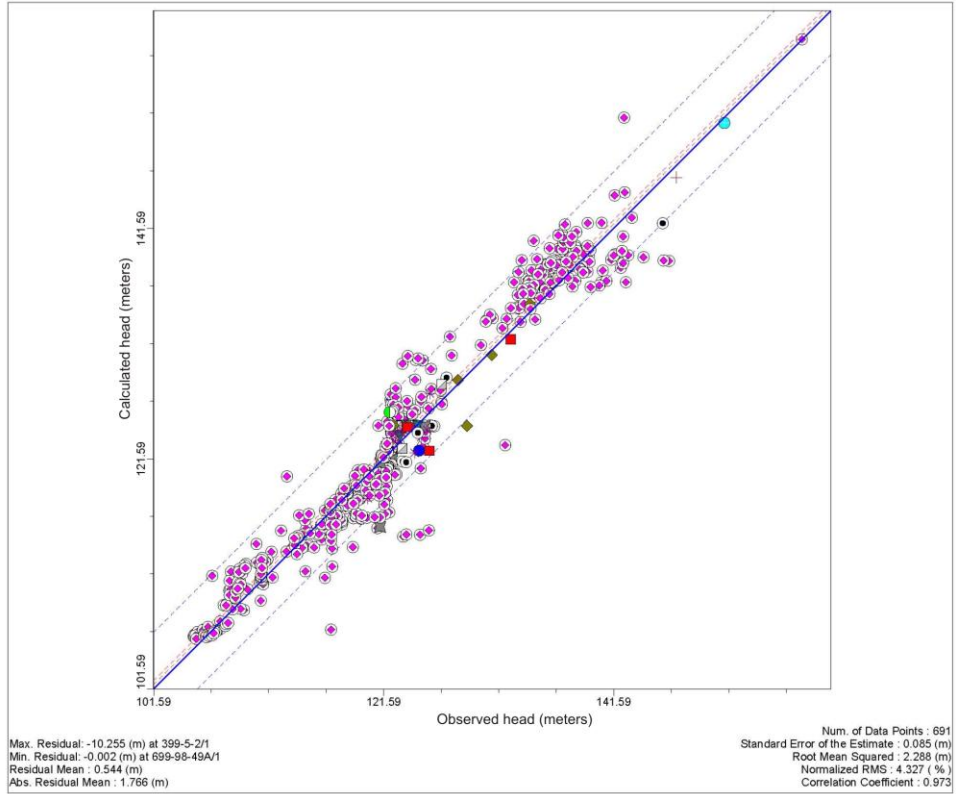


Figure L-95. 66th Percentile Flow Model Residuals, Calendar Year 2010

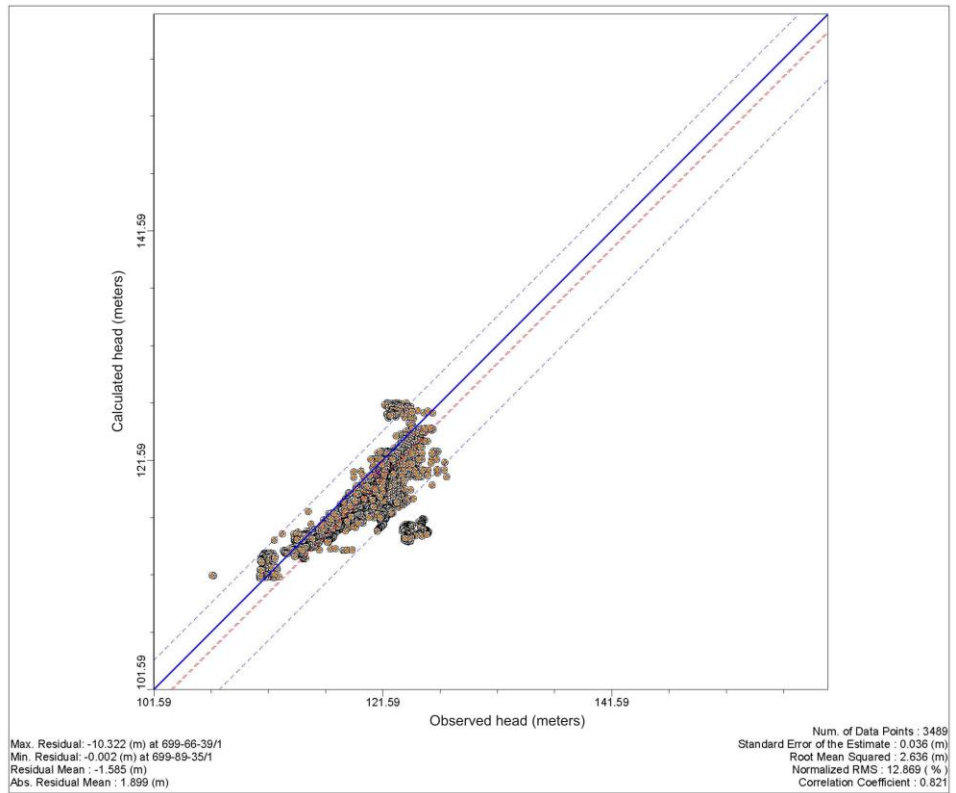


Figure L-96. 66th Percentile Flow Model Residuals in Northern Region of Model

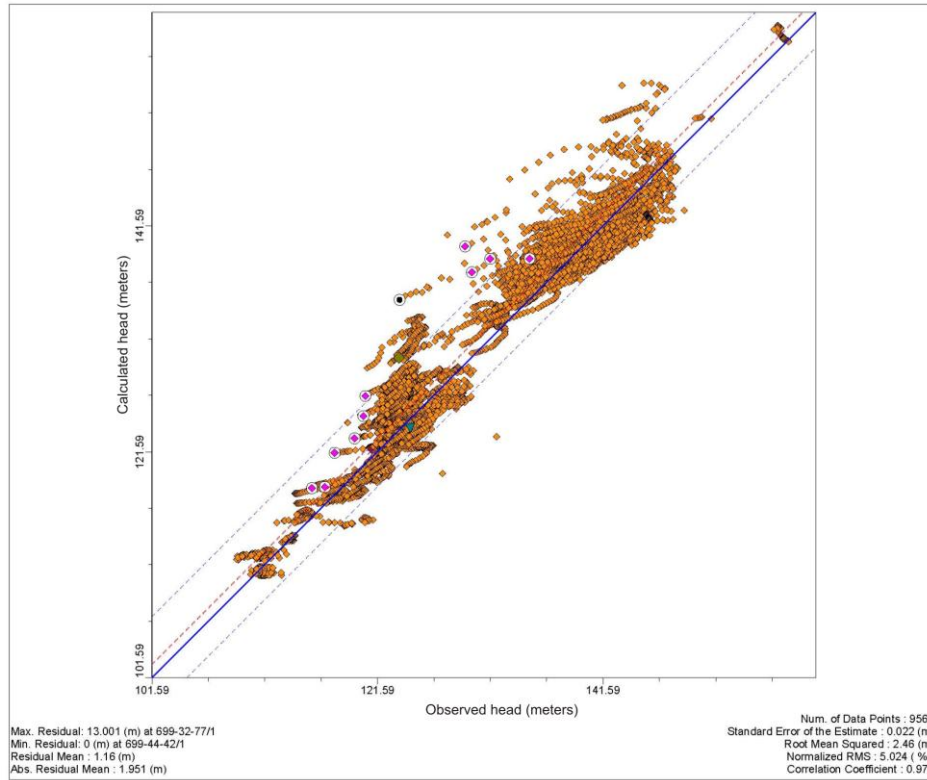


Figure L-97. 66th Percentile Flow Model Residuals in Central Region of Model

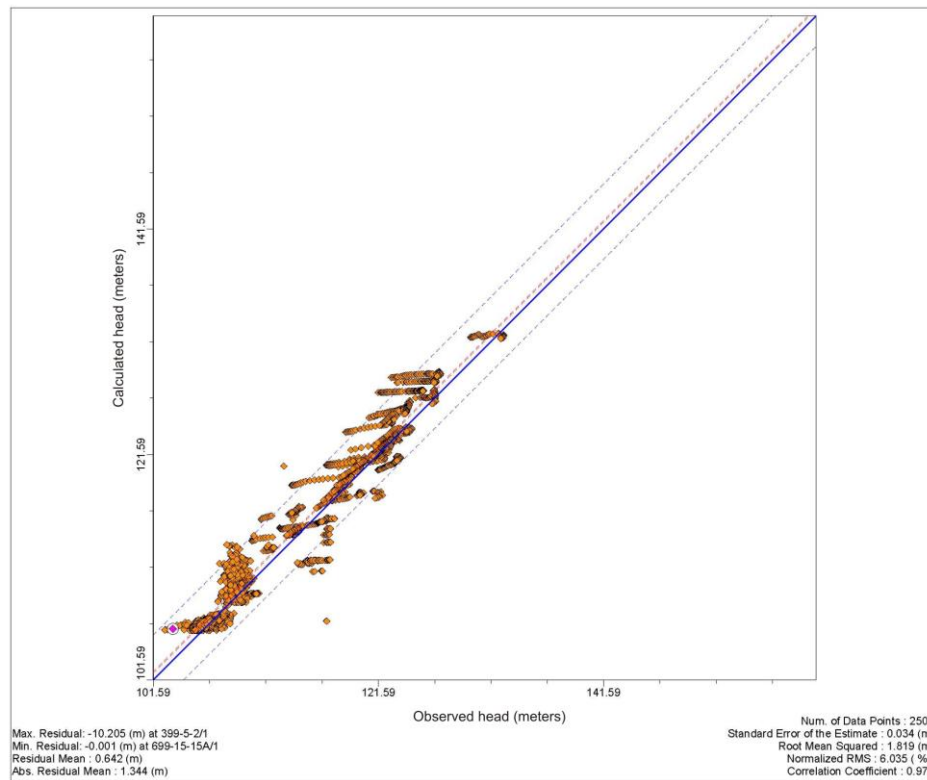


Figure L-98. 66th Percentile Flow Model Residuals in Southern Region of Model

In addition to the calibration acceptance criteria, water (or mass) balance and a long-term, steady state condition must be achieved in the calibrated flow model. Cumulative mass water balance data are shown in Figure L-99, indicating a cumulative mass balance error of approximately -1.4 percent. Total water balance and storage data as a function of time are shown in Figure L-100. The Figure L-100 data show storage values relative to the total water balance and indicate that storage-in is approximately equal to storage-out in model year 261 (CY 2200). This indicates that a long-term, steady state condition is achieved. Note that, in Figure L-100, there is a spike in “storage” at model year 82. This spike is the result of a time-stepping change at the beginning of the final long-term stress period. As a result, the model is moving from a relatively long time step at the end of the previous stress period (model year 82) to a relatively short time step at the beginning of the final stress period.

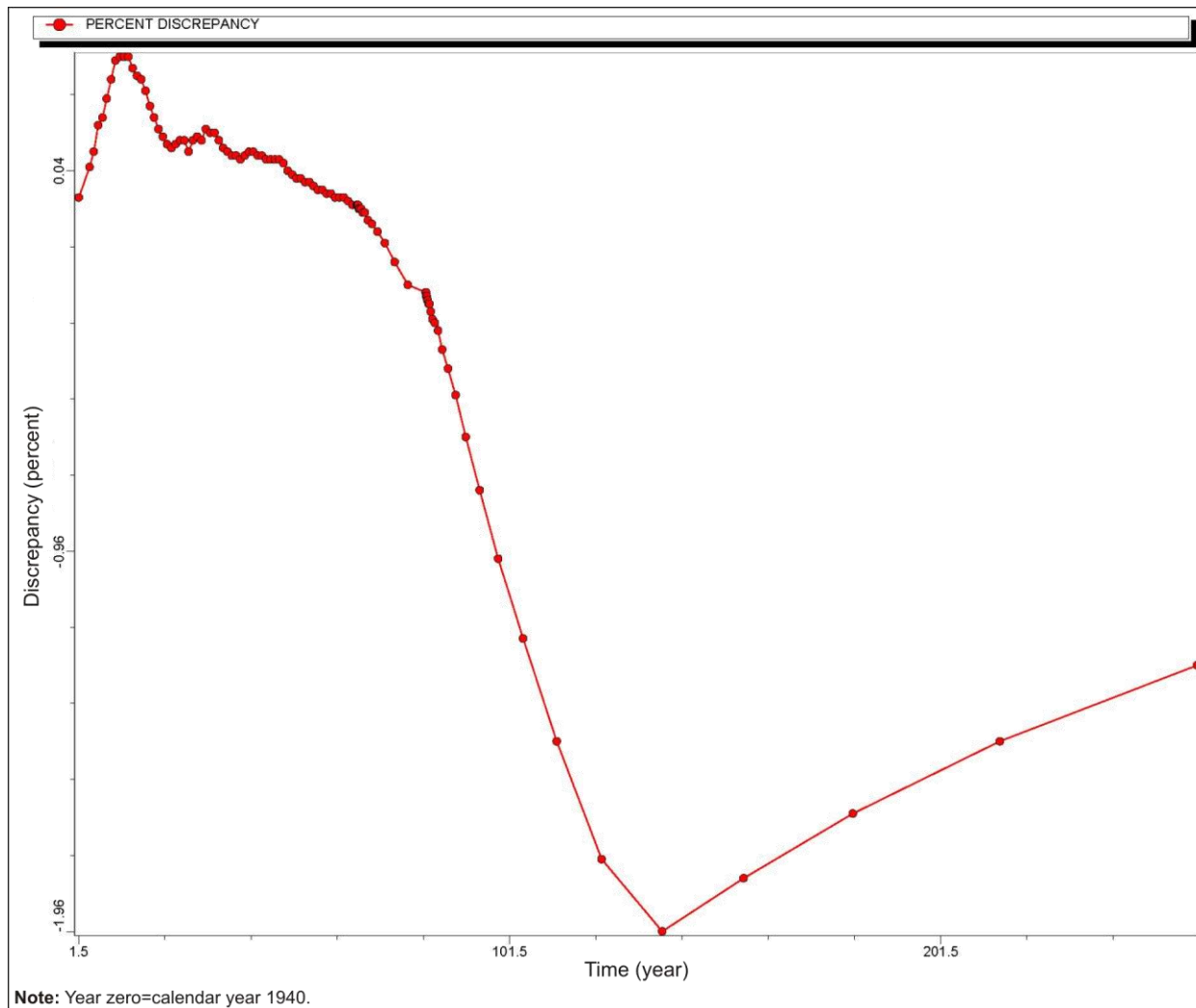


Figure L-99. 66th Percentile Flow Model Cumulative Water Balance Discrepancy

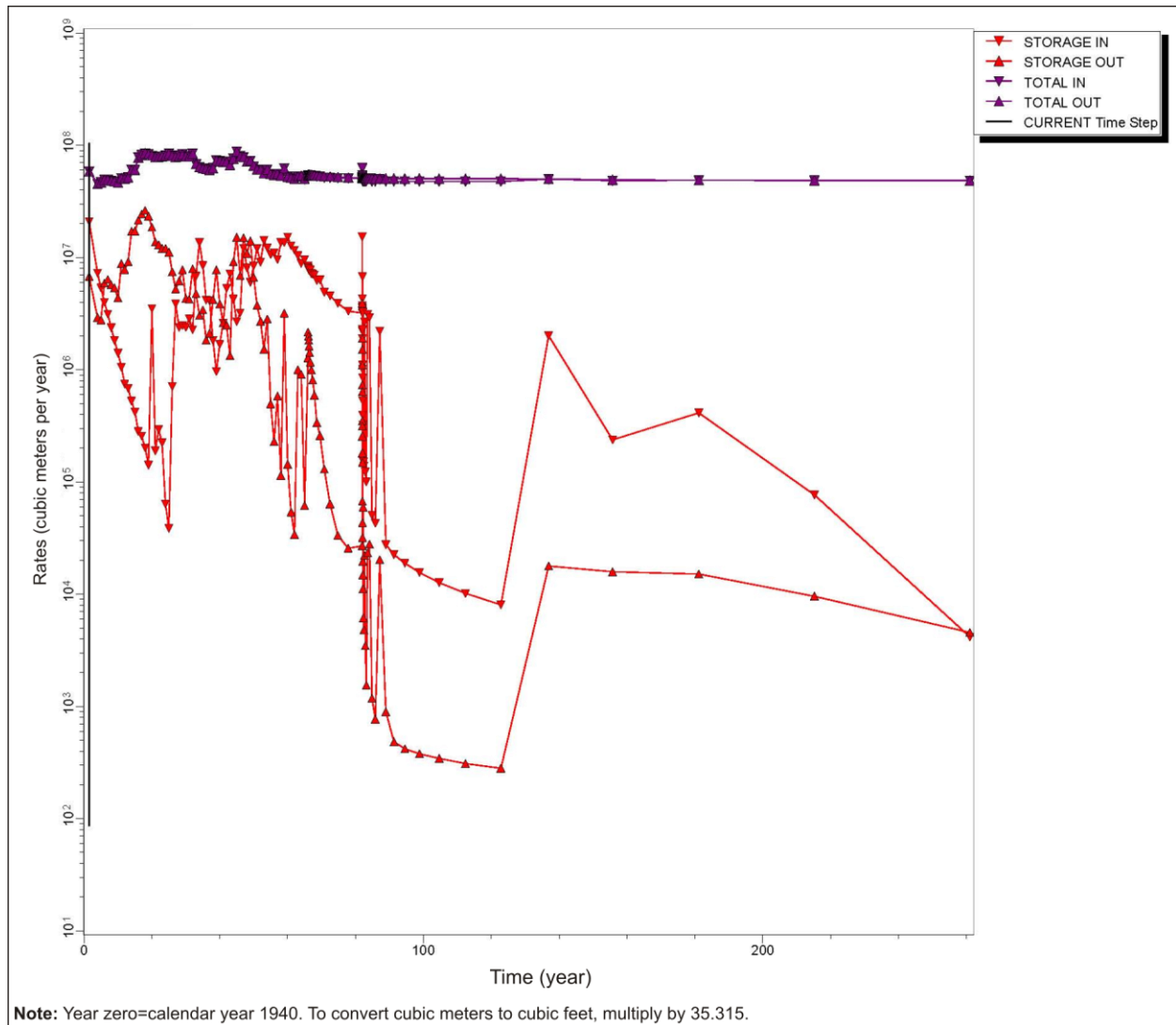
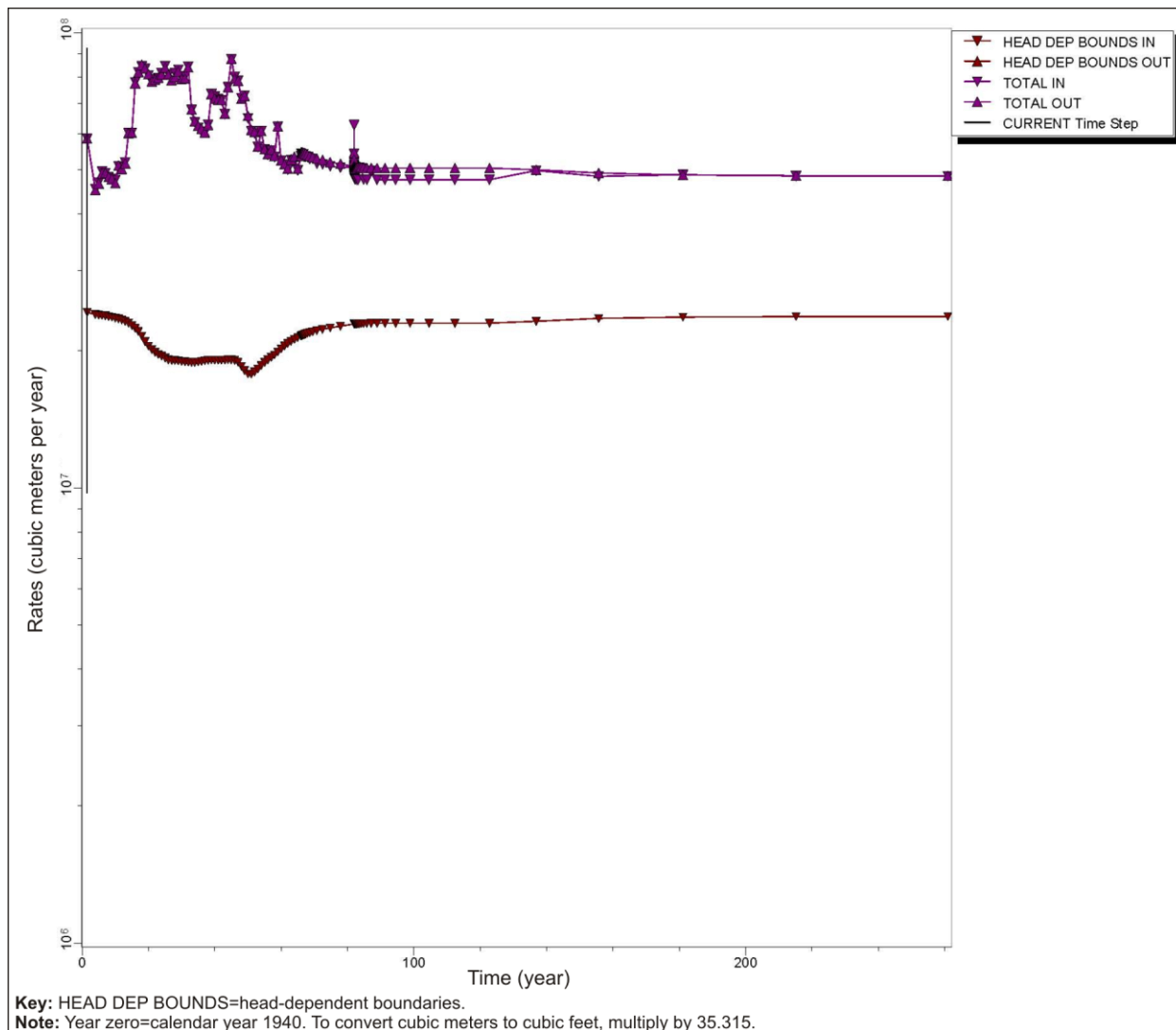
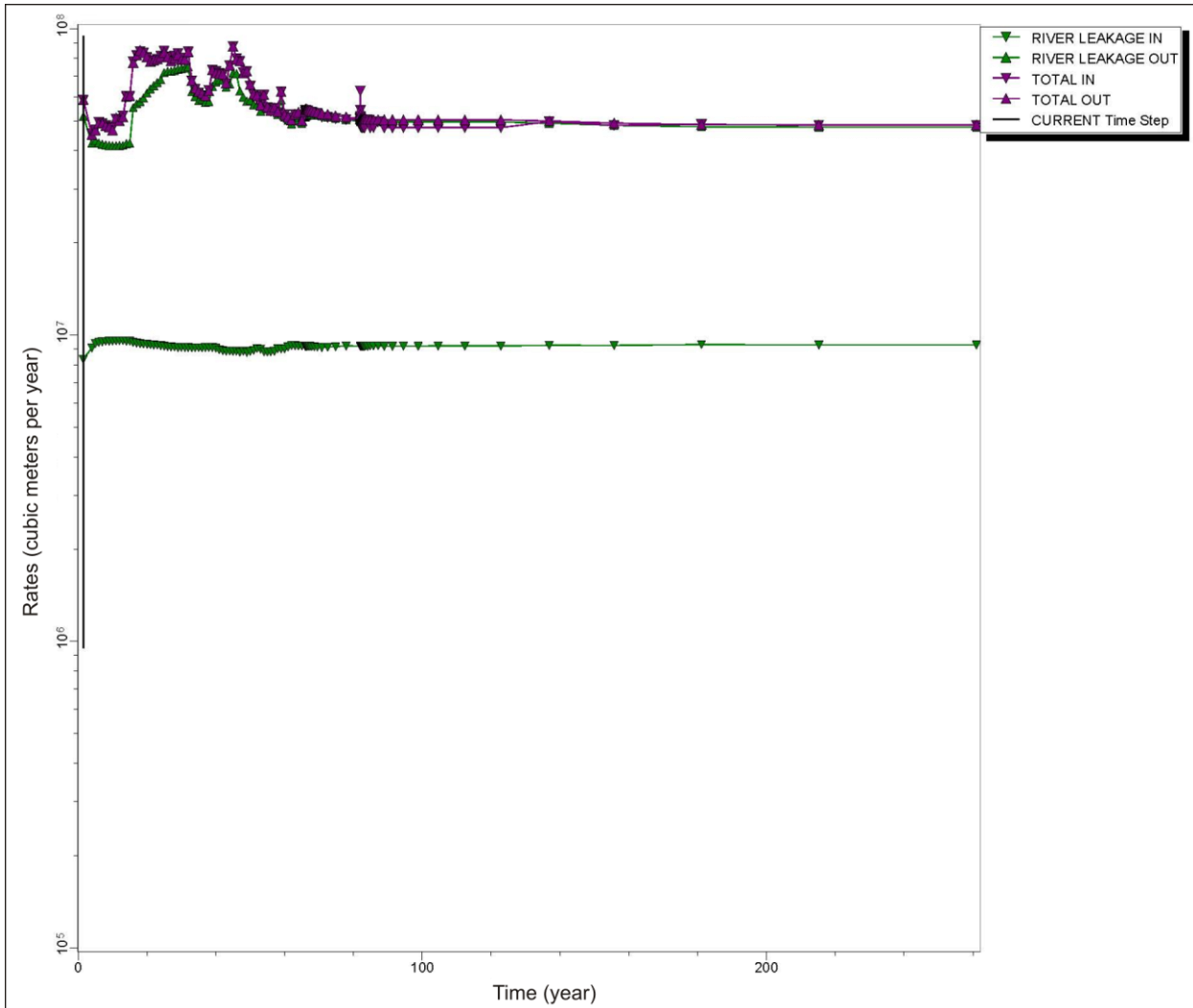


Figure L-100. 66th Percentile Flow Model Total Water and Storage Rates over Time

Additional water balance results for the 66th percentile flow model are shown in Figures L-101, L-102, and L-103 for GHBs, river boundaries, and recharge boundaries, respectively.



**Figure L-101. 66th Percentile Flow Model
 Total Water and Generalized Head Boundary Rates over Time**



Note: Year zero=calendar year 1940. To convert cubic meters to cubic feet, multiply by 35.315.

Figure L-102. 66th Percentile Flow Model Total Water and River Rates over Time

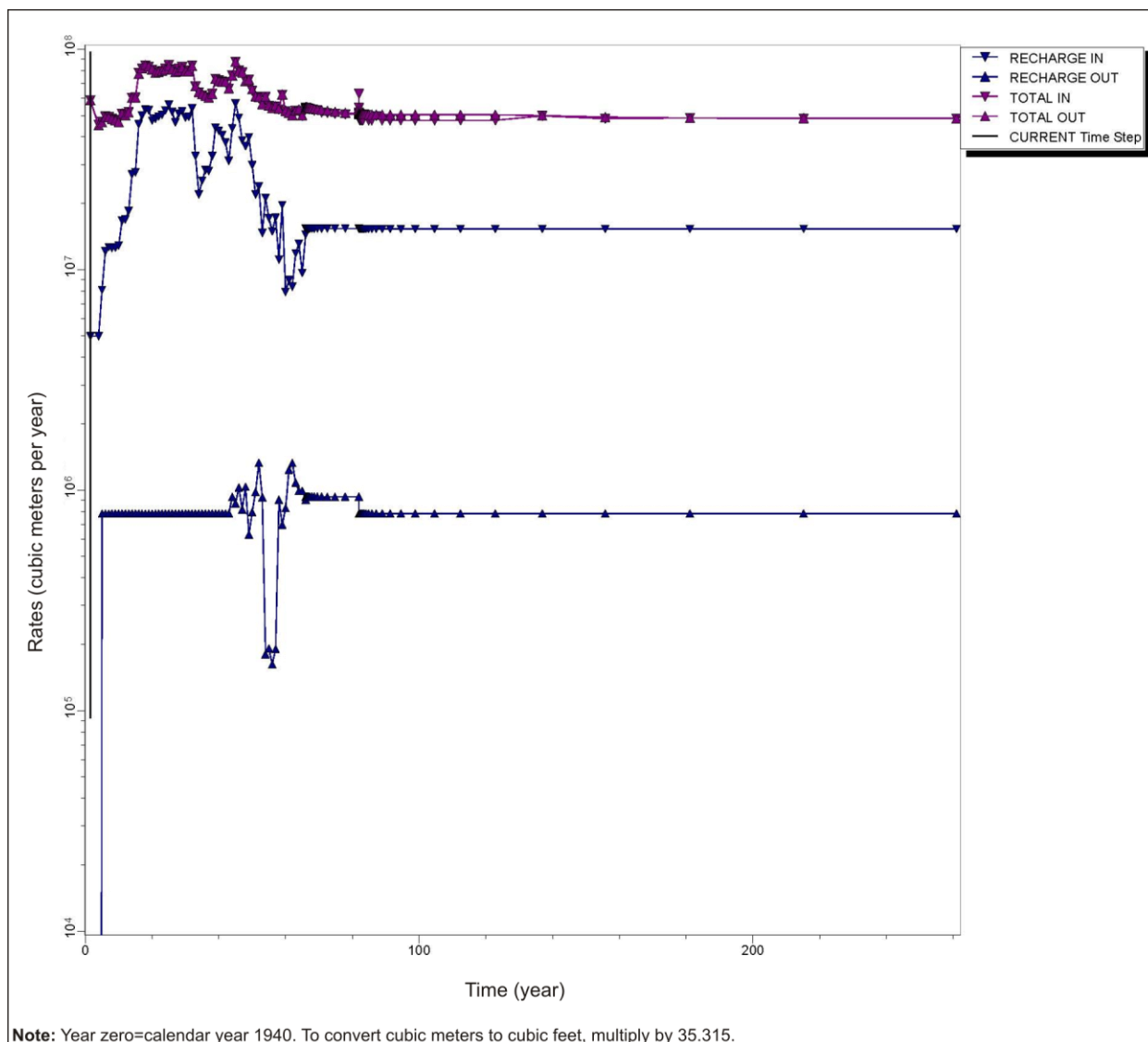


Figure L-103. 66th Percentile Flow Model Total Water and Recharge Rates over Time

L.8.3.2 66th Percentile Potentiometric Head Distribution

A goal for the flow model is to produce a potentiometric distribution of heads that shows a steep water table in the 200-West Area due to the low-conductivity material types in that area and a relatively flat water table in the 200-East Area where high-conductivity material types are present. The pre-Hanford potentiometric surface is assumed to be approximately the same as the post-Hanford long-term, steady state condition, with water table mounding occurring below areas where, and at times when, Hanford operational discharges were released at the ground surface. Figures L-104, L-105, and L-106 are 66th percentile flow model simulations of the potentiometric surface in CY 1944 (pre-Hanford), CY 1975 (Hanford operations), and CY 2200 (post-Hanford), respectively.

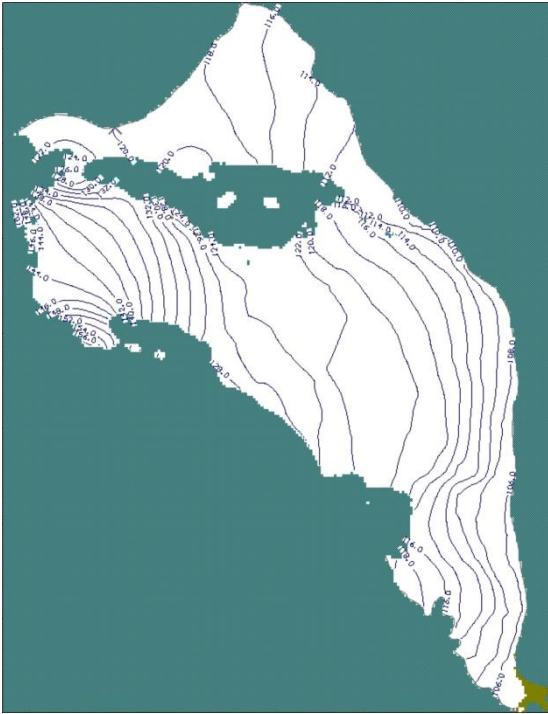


Figure L-104. 66th Percentile Flow Model Potentiometric Head Distribution, Calendar Year 1944

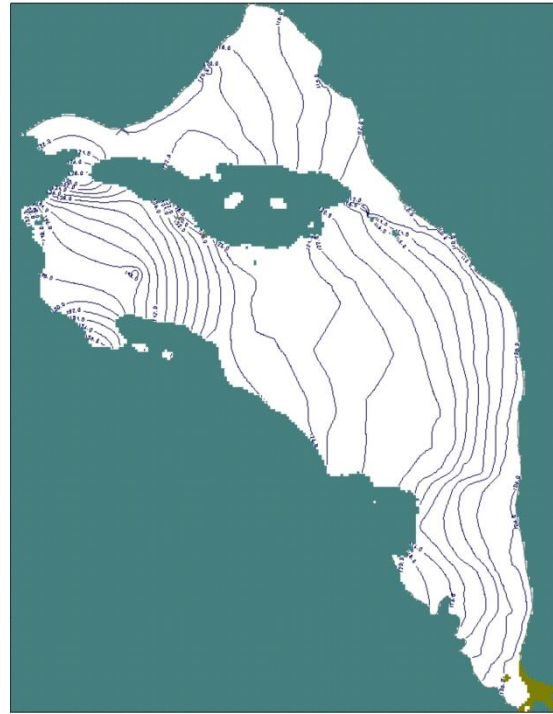


Figure L-105. 66th Percentile Flow Model Potentiometric Head Distribution, Calendar Year 1975



Figure L-106. 66th Percentile Flow Model Potentiometric Head Distribution, Calendar Year 2200

L.8.3.3 66th Percentile Flow Model Velocity Field

The 66th percentile flow model velocity field is variable in both magnitude and direction over time and across the model domain. This variability at selected locations (BC Cribs, 216-T-26 Crib, and BY Cribs) within the model is shown in Figures L-107 through L-112. As expected, the velocities simulated in 200-West Area are generally lower than those simulated in the 200-East Area, particularly at the 200-East Area BY Cribs. An additional observation is that the velocity directions are highly variable during the Hanford operational period, particularly at the 200-East Area BY Cribs; there the velocity directions change by approximately 180 degrees due to water table mounding, coupled with this source's proximity to Gable Gap, where water table velocity and direction are sensitive to water table elevation.

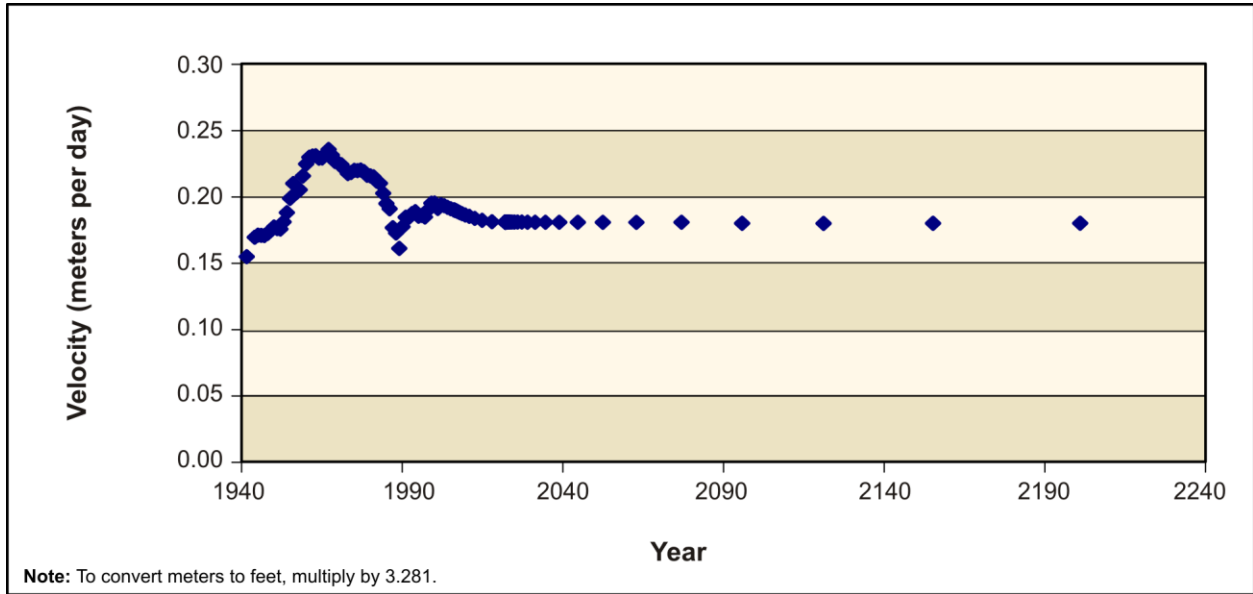


Figure L-107. 66th Percentile Flow Model Velocity Magnitude at 216-B-26 (BC Cribs in 200-East Area)

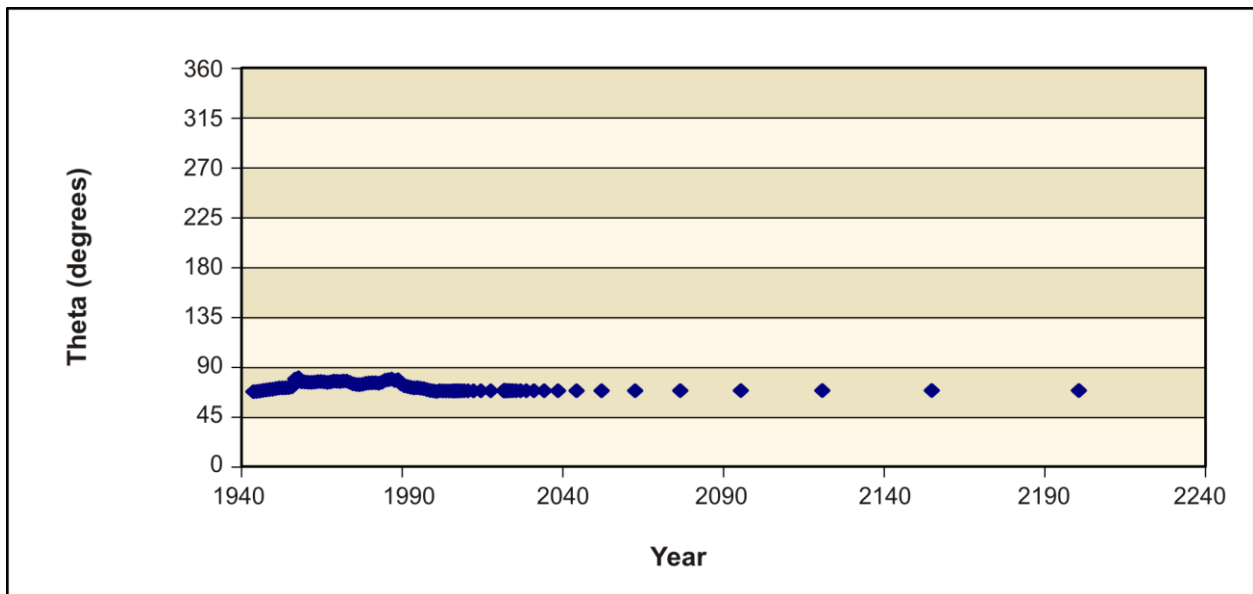
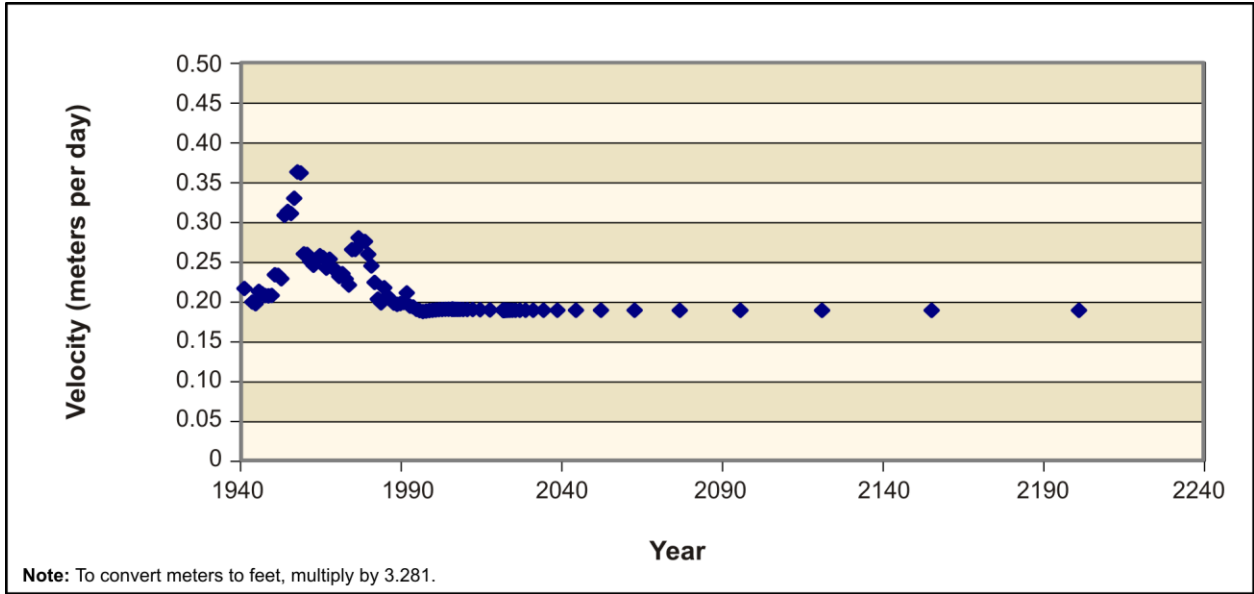
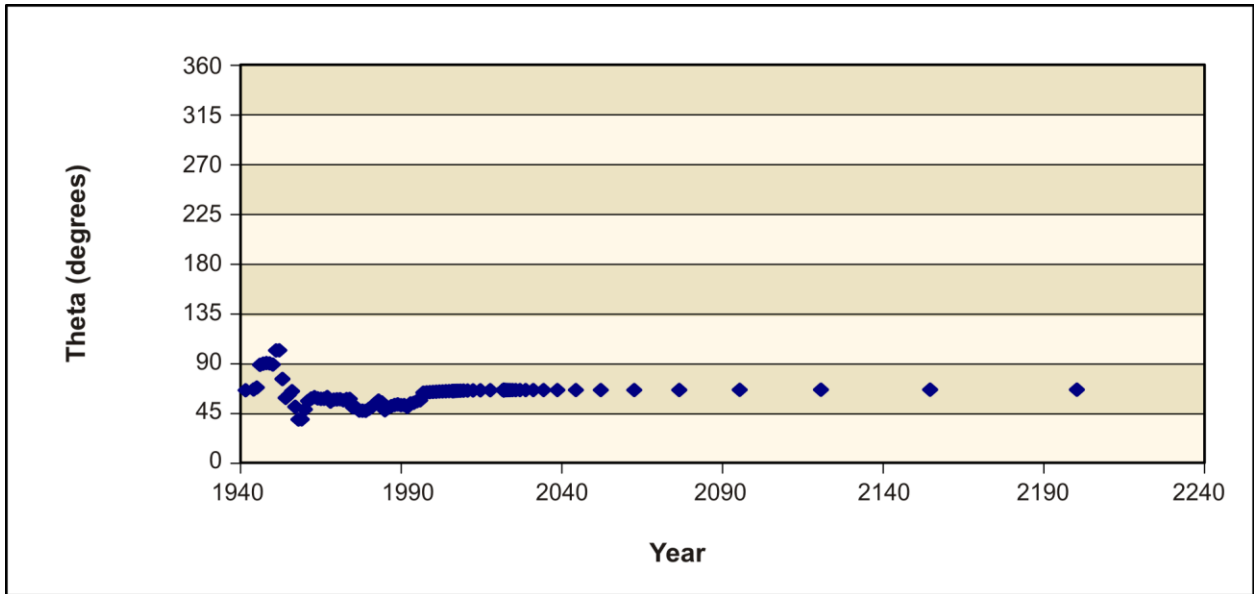


Figure L-108. 66th Percentile Flow Model Velocity Direction at 216-B-26 (BC Cribs in 200-East Area)



**Figure L-109. 66th Percentile Flow Model
Velocity Magnitude at 216-T-28 Crib (200-West Area)**



**Figure L-110. 66th Percentile Flow Model
Velocity Direction at 216-T-28 Crib (200-West Area)**

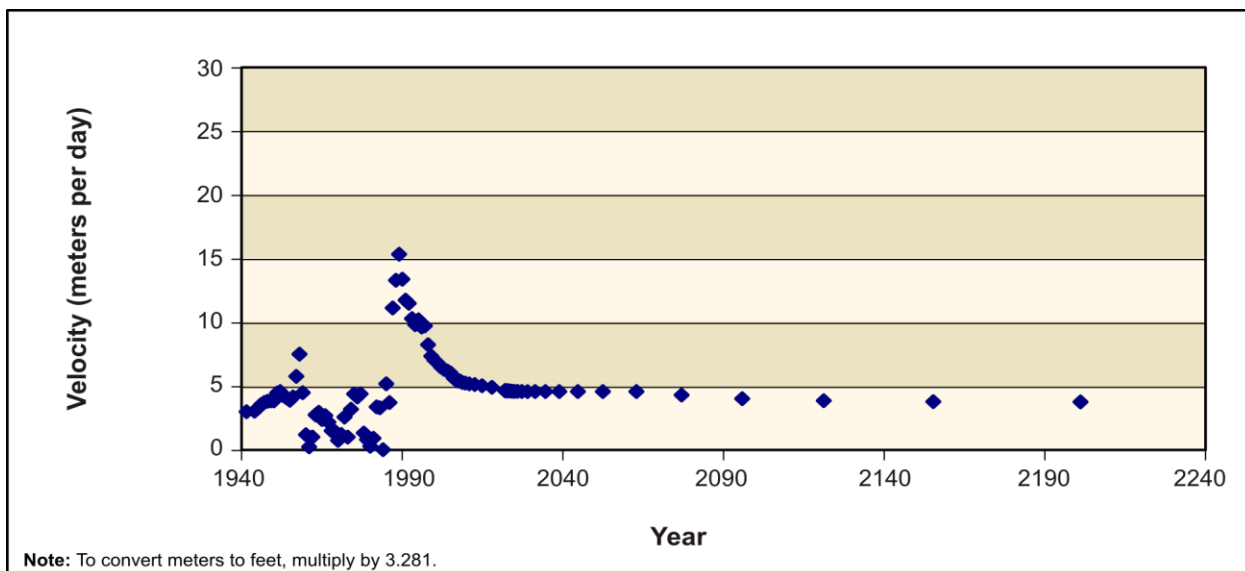


Figure L-111. 66th Percentile Flow Model Velocity Magnitude at BY Cribs (200-East Area)

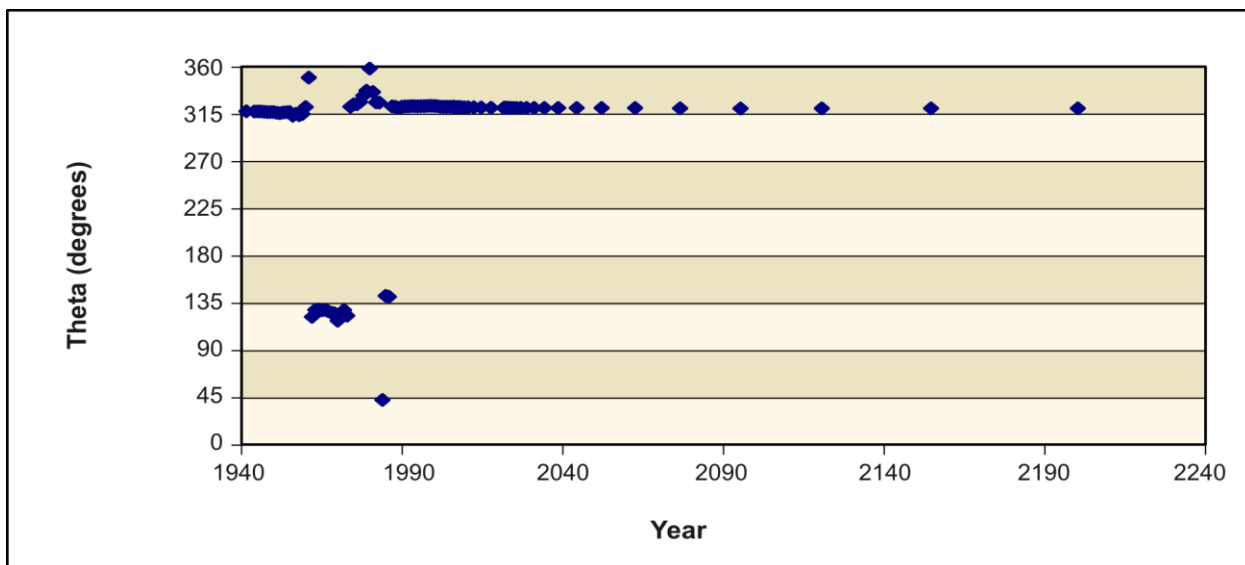


Figure L-112. 66th Percentile Flow Model Velocity Direction at BY Cribs (200-East Area)

L.8.3.4 66th Percentile Flow Model Central Plateau Pathline Analysis

Pathline analysis determined the number of particles (measured in area) released in the Central Plateau area that would move to the north through Gable Gap and the number of particles that would move to the east toward the Columbia River. As discussed in Appendix L, Section L.1.5, in the *Draft TC & WM EIS*, the pathline analysis to demonstrate the area of northerly versus easterly flow from the Central Plateau depended primarily on hydraulic conductivity distribution rather than on uncertainties in the TOB surface. Comparison of this analysis with the 95th and 100th percentile cases (see Sections L.8.1.4 and L.8.2.4) confirms this observation. This pathline analysis included a MODFLOW and MODPATH model run, releasing a uniformly distributed set of particles across the Central Plateau area. The Central Plateau is depicted as a rectangular boundary that includes all of the 200-East and 200-West Areas, as well as other areas between and outside the 200 Areas. Figure L-113 shows that, in terms of area, the flow of this model is predominantly northward from the Central Plateau.

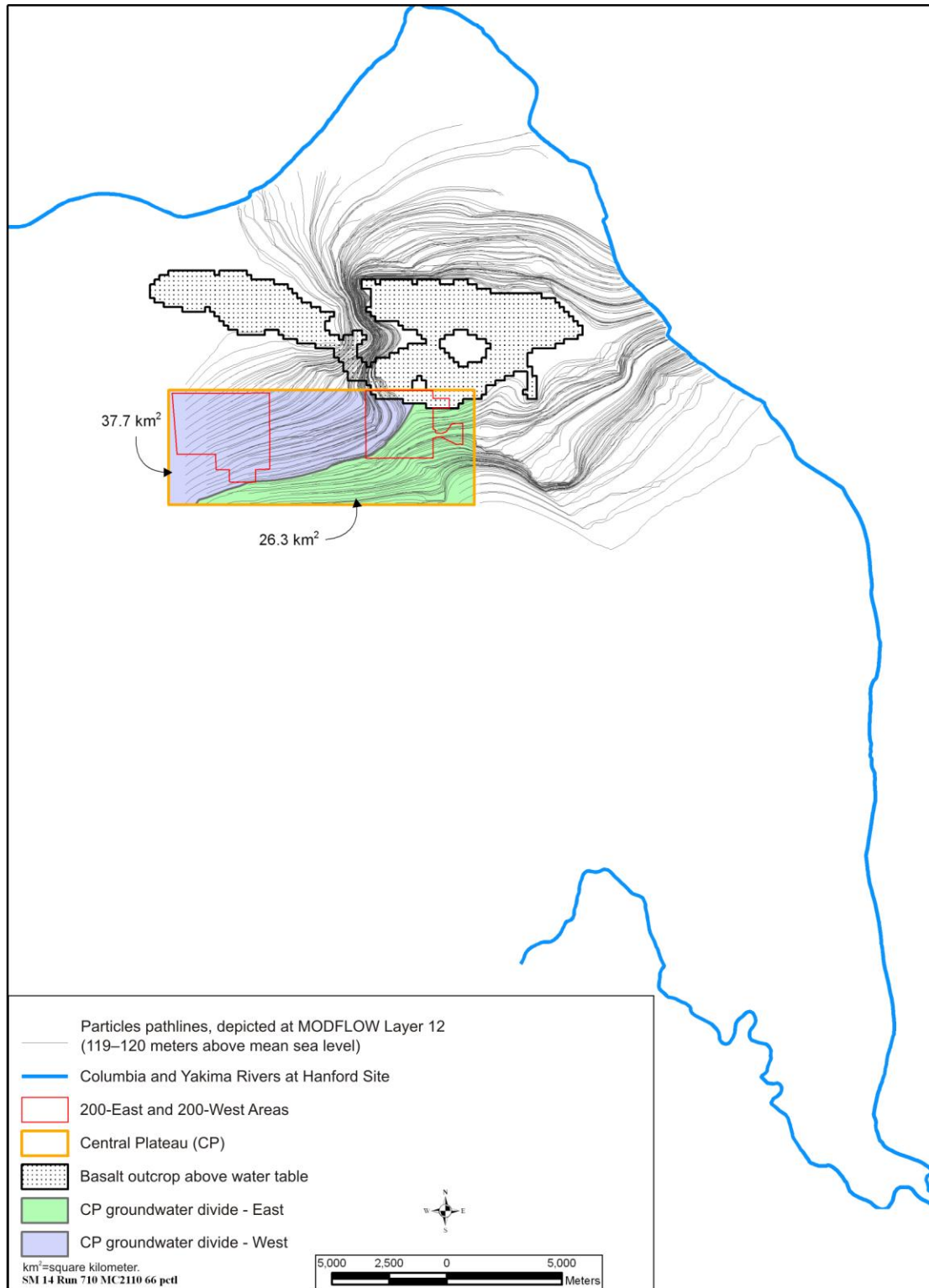


Figure L-113. 66th Percentile Flow Model Central Plateau Pathline Analysis

L.8.3.5 66th Percentile Flow Model Zone Budget Analysis

In addition to the particle pathline analysis described in the previous section, a zone budget analysis was completed to determine simulated water flow volumes from south of Gable Mountain and Gable Butte through Umtanum Gap, through Gable Gap, and easterly toward the Columbia River. Table L–23 provides total water flow volumes through these areas for CY 2200. These results show that about 18 percent of the total volume of water entering the Columbia River passes through Umtanum Gap, about 16 percent through Gable Gap, and about 66 percent directly east to the Columbia River. Comparison of these results with those of the 95th and 100th percentile cases shows that in terms of volumetric flow, rather than in terms of geometric position of the flow divide across the Central Plateau (see Section L.8.3.4), the model is less sensitive to variations in hydraulic conductivity.

**Table L–23. 66th Percentile Flow Model –
Simulated Water Flow Volumes Through Selected Areas, Calendar Year 2200**

Water Flow Through	Water Volume (cubic meters per year)
Umtanum Gap	4,458,400
Gable Gap	3,945,100
East to Columbia River	16,532,000

Note: To convert cubic meters to cubic feet, multiply by 35.315.

L.8.3.6 66th Percentile Flow Model – Transport Model Concentration-Versus-Time Results

Groundwater transport modeling was completed using the 66th percentile flow model. Figures L–114 and L–115 show the concentration-versus-time results measured at the Core Zone Boundary and at the Columbia River for technetium-99 under Tank Closure Alternative 2B and Waste Management Alternative 2, Disposal Group 1, Subgroup 1-A, respectively. Figures L–114 and L–115 are comparable to Figures L–58 and L–59 (respectively) for the 95th percentile flow model, and comparable to Figures L–86 and L–87 (respectively) for the 100th percentile flow model. These comparisons show that the three flow models result in similar technetium-99 concentrations over time for the two alternatives presented. See Chapter 2 of this *TC & WM EIS* for a description of these alternatives.

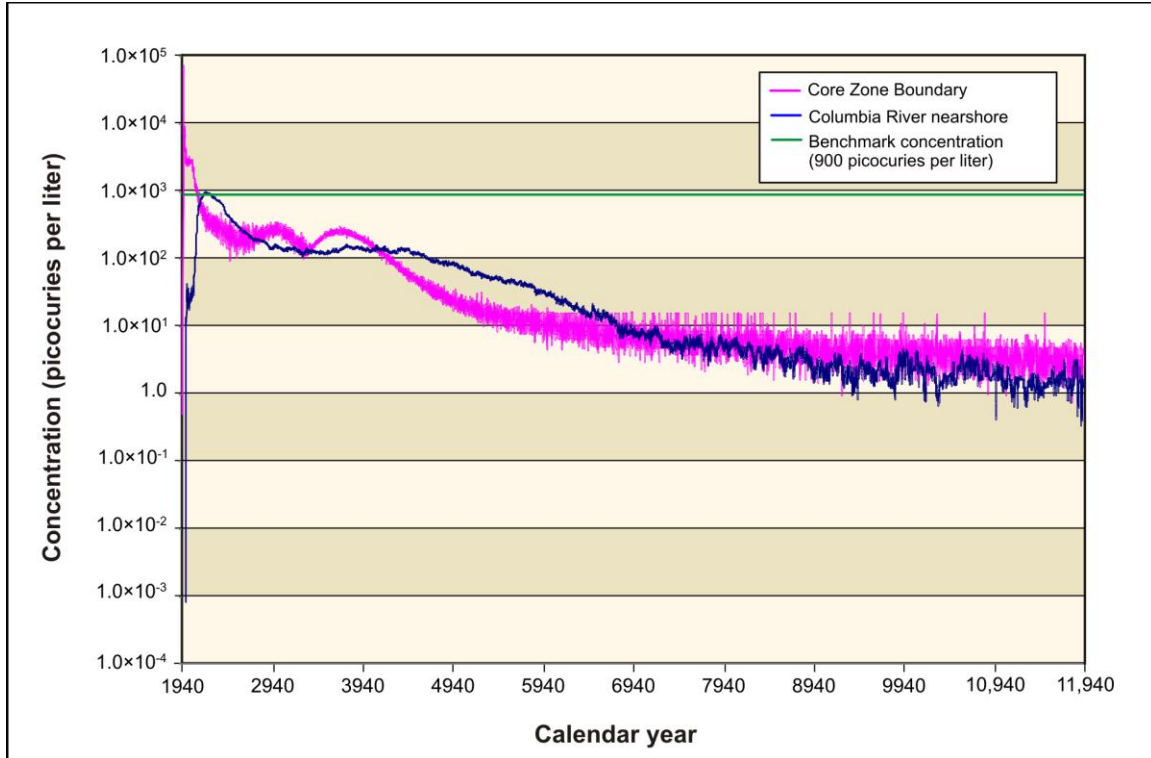


Figure L-114. Tank Closure Alternative 2B 66th Percentile Flow Model Technetium-99 Concentration-Versus-Time Results

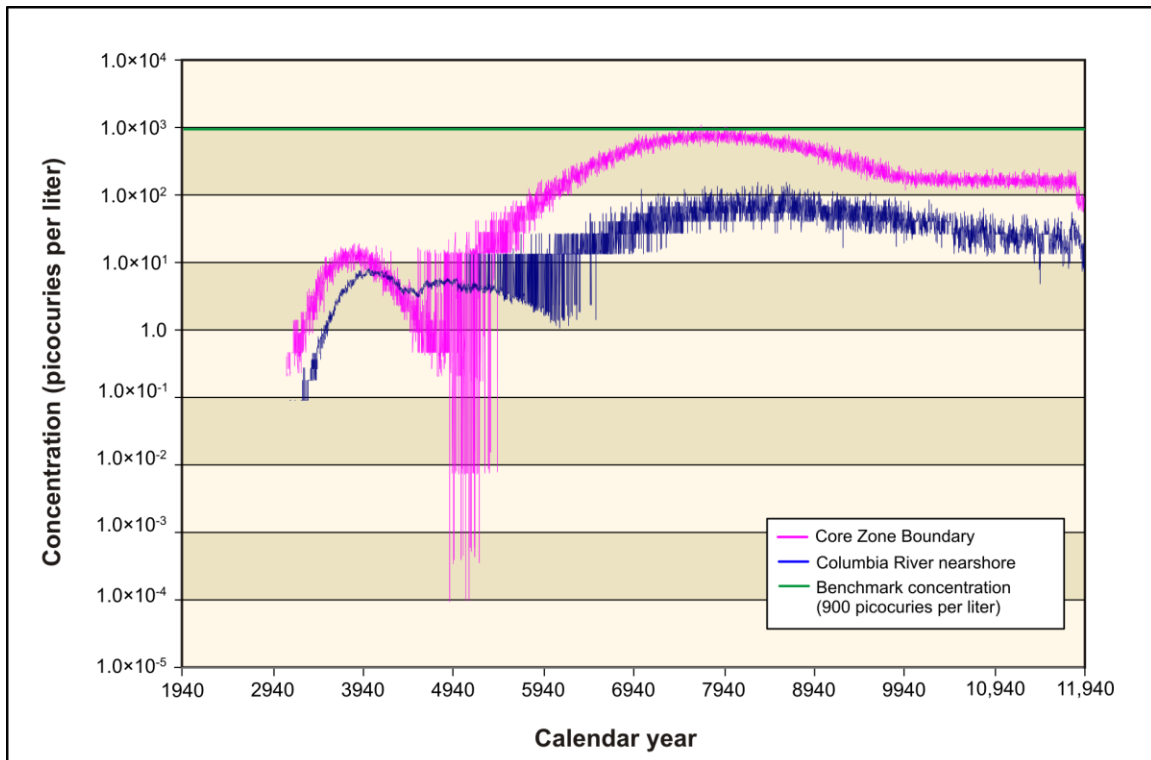


Figure L-115. Waste Management Alternative 2, Disposal Group 1, Subgroup 1-A, 66th Percentile Flow Model Technetium-99 Concentration-Versus-Time Results

L.8.4 Conclusions

Section L.10 provides a summary of the results produced by three models from the 5,000 hydraulic conductivity model runs described in Section L.7. These results show that any of the top one-third of models, as measured by RMS error when varying hydraulic conductivity values, achieves the EIS groundwater model calibration criteria. Therefore, it would be acceptable to use any of these models as the Base Case for analysis in this *Final TC & WM EIS*. The 95th percentile model was selected for analysis in this *Final TC & WM EIS* because its hydraulic conductivity values are identical to those assigned in the groundwater flow model used in the *Draft TC & WM EIS* analysis.

L.9 FLOW FIELD EXTRACTION

To support analysis of transport in the saturated zone, the MODFLOW groundwater flow model developed for this *Final TC & WM EIS* was used as the basis for particle-tracking simulations. The selected particle-tracking code does not directly read MODFLOW output files to calculate the heads and velocities required as input; instead, the MODFLOW files must be independently processed to generate these heads and velocities.

The Base Case flow model data files were processed by extracting hydraulic heads and velocities at each active cell within the model domain at selected times for use in groundwater transport modeling (see Appendix O of this *TC & WM EIS*). Table L-24 gives the times selected for extracting the head and velocity data.

Table L-24. Selected Times for Extracting the Base Case Head and Velocity Data Files

Stress Period	Time Step	Model Year	Calendar Year
1	100	4	1943
2	10	5	1944
3	10	6	1945
4	10	7	1946
5	10	8	1947
6	10	9	1948
7	10	10	1949
8	10	11	1950
9	10	12	1951
10	10	13	1952
11	10	14	1953
12	10	15	1954
13	10	16	1955
14	10	17	1956
15	10	18	1957
16	10	19	1958
17	10	20	1959
18	10	21	1960
19	10	22	1961
20	10	23	1962
21	10	24	1963
22	10	25	1964
23	10	26	1965
24	10	27	1966
25	10	28	1967
26	10	29	1968
27	10	30	1969

Table L–24. Selected Times for Extracting the Base Case Head and Velocity Data Files (continued)

Stress Period	Time Step	Model Year	Calendar Year
28	10	31	1970
29	10	32	1971
30	10	33	1972
31	10	34	1973
32	10	35	1974
33	10	36	1975
34	10	37	1976
35	10	38	1977
36	10	39	1978
37	10	40	1979
38	10	41	1980
39	10	42	1981
40	10	43	1982
41	10	44	1983
42	10	45	1984
43	10	46	1985
44	10	47	1986
45	10	48	1987
46	10	49	1988
47	10	50	1989
48	10	51	1990
49	10	52	1991
50	10	53	1992
51	10	54	1993
52	10	55	1994
53	10	56	1995
54	10	57	1996
55	10	58	1997
56	10	59	1998
57	10	60	1999
58	10	61	2000
59	10	62	2001
60	10	63	2002
61	10	64	2003
62	10	65	2004
63	10	66	2005
64	70	67	2006
64	90	67.9	2006.9
64	100	68.6	2007.6
64	110	69.5	2008.5
64	120	70.8	2009.8
64	130	72.5	2011.5
64	140	74.8	2013.8
64	150	77.9	2016.9
64	160	82	2021

Table L–24. Selected Times for Extracting the Base Case Head and Velocity Data Files (continued)

Stress Period	Time Step	Model Year	Calendar Year
65	230	83.2	2022.2
65	250	84.1	2023.1
65	270	85.8	2024.8
65	280	87.2	2026.2
65	290	88.9	2027.9
65	300	91.3	2030.3
65	310	94.5	2033.5
65	320	98.8	2037.8
65	330	104.6	2043.6
65	340	112.4	2051.4
65	350	122.8	2061.8
65	360	136.9	2075.9
65	370	155.7	2094.7
65	380	181.1	2120.1
65	390	215.2	2154.2
65	400	261	2200

L.10 SUMMARY

A three-dimensional transient flow model was developed in accordance with the *Technical Guidance Document* (DOE 2005) to support the *TC & WM EIS* analyses of alternatives and cumulative impacts. The flow model was developed using the MODFLOW 2000 engine within the Visual MODFLOW framework. The site conceptual model consists of an unconfined, heterogeneous aquifer bounded at the bottom by an impermeable basalt surface. Water enters the model from several sources: mountain-front recharge along Rattlesnake Mountain; the Yakima River; areal recharge; and operational discharges, primarily at the Central Plateau of Hanford. Water leaves the model via the Columbia River and several pumping wells. The operational discharges and pumping well withdrawals vary with time, providing the transient drivers to the model.

Standard data gathering and encoding techniques were used to develop the model extents, gridding, TOB topography, location and elevation of the Columbia and Yakima Rivers, lithology, and artificial discharges and withdrawals. These elements of the model were encoded directly from site-specific data. The background areal recharge was encoded as specified by the *Technical Guidance Document* (DOE 2005). Initial estimates for GHB heads and conductances, riverbed conductances, and material properties were encoded and refined through a flow calibration process as documented in the *Draft TC & WM EIS*, Appendix L. These parameter sets are unchanged in the *Final TC & WM EIS* model.

Internal reviews and public comment on the *Draft TC & WM EIS* motivated additional sensitivity analyses in this *Final TC & WM EIS* for a better understanding of the uncertainties in the parameter sets used for modeling. To that end, this *Final TC & WM EIS* includes a more extensive sensitivity analysis of a variety of boundary condition and material property parameter values, including the following:

- Hydraulic conductivity
- Storage properties (Sy)
- GHB head and conductance
- Background and anthropogenic recharge
- River conductance

These analyses show that the model is sensitive to changes in hydraulic conductivity values, but not highly sensitive to changes in the other parameters.

The results of the sensitivity analysis led to further evaluation of the performance of the top one-third of models, as ranked by RMS error in the hydraulic conductivity sensitivity analysis. This evaluation was completed by selecting the 66th, 95th, and 100th percentile models from this set and extracting detailed flow model results from each. These results are presented in this appendix. Evaluation of the results from these three models revealed that all achieve the calibration criteria, and thus any one of them could have been selected as the Base Case model for use in the *Final TC & WM EIS* analysis. The 95th percentile flow model was selected because it has the same parameter set values as the Base Case model used in the *Draft TC & WM EIS*.

The flow field from the 95th percentile model (Base Case) was extracted for use with contaminant transport modeling in the long-term groundwater impact analyses (see Appendix O). This flow field reflects the magnitude and direction of the pore water velocity throughout the active model domain. This Base Case model was used for additional analyses to determine the model's sensitivity to changes in recharge, GHB heads, and Columbia River heads. This analysis is presented in Appendix V.

L.11 REFERENCES

Bjornstad, B.N., and D.C. Lanigan, 2007, *Geologic Descriptions for the Solid-Waste Low-Level Burial Grounds*, PNNL-16887, Pacific Northwest National Laboratory, Richland, Washington, September.

Bjornstad, B.N., P.D. Thorne, B.A. Williams, G.V. Last, G.S. Thomas, M.D. Thompson, J.L. Ludwig, and D.C. Lanigan, 2010, *Hydrogeologic Model for the Gable Gap Area, Hanford Site*, PNNL-19702, Pacific Northwest National Laboratory, Richland, Washington, September.

CHPRC (CH2M HILL Plateau Remediation Company), 2009a, *Water Level Data*, Data Form 312, Richland, Washington, June 30.

CHPRC (CH2M HILL Plateau Remediation Company), 2009b, *Hanford Well Information System (HWIS)*, accessed through <http://prc.rl.gov/rapidweb/EDM/index.cfm?Pagenum=8>, July 8.

CHPRC (CH2M HILL Plateau Remediation Company), 2010, *Soil and Groundwater Remediation Project*, accessed through <http://prc.rl.gov/rapidweb/SGPR>, September 29.

Cole, C.R., M.P. Bergeron, C.J. Murray, P.D. Thorne, S.K. Wurstner, and P.M. Rogers, 2001, *Uncertainty Analysis Framework – Hanford Site-Wide Groundwater Flow and Transport Model*, PNNL-13641, Pacific Northwest National Laboratory, Richland, Washington, November.

DOE (U.S. Department of Energy), 1988, *Consultation Draft, Site Characterization Plan, Reference Repository Location, Hanford Site, Washington*, DOE/RW-0164, Office of Civilian Radioactive Waste Management, Washington, D.C., January.

DOE (U.S. Department of Energy), 2005, *Technical Guidance Document for Tank Closure Environmental Impact Statement Vadose Zone and Groundwater Revised Analyses*, Final Rev. 0, Office of River Protection, Richland, Washington, March 25.

DOE (U.S. Department of Energy), 2010, *Hanford Site Cleanup Completion Framework*, DOE/RL-2009-10, Rev. 0, Richland Operations Office and Office of River Protection, Richland, Washington, July.

Ecology (Washington State Department of Ecology), 2003, *Well Logs*, accessed through <http://apps.ecy.wa.gov/welog/testsearch.asp>, February 12.

Ecology, EPA, and DOE (Washington State Department of Ecology, Olympia, Washington; U.S. Environmental Protection Agency, Washington, D.C.; and U.S. Department of Energy, Richland, Washington), 1989, Hanford Federal Facility Agreement and Consent Order, 89-10, as amended, accessed through <http://www.hanford.gov/tpa/tpahome.htm>, May 15.

Hartman, M.J., and W.D. Webber, eds., 2008, *Hanford Site Groundwater Monitoring for Fiscal Year 2007*, DOE/RL-2008-01, Rev. 0, U.S. Department of Energy, Richland Operations Office, Richland, Washington, March.

Hill, M.C., 1990, *Preconditioned Conjugate-Gradient 2 (PCG2)*, A Computer Program for Solving Ground-Water Flow Equations, Water-Resources Investigations Report 90-4048, U.S. Geological Survey, Denver, Colorado.

Johnston, K., J.M. Ver Hoef, K. Krivoruchko, and N. Lucas, eds., 2001, *Using ArcGIS Geostatistical Analyst*, Environmental Systems Research Institute, Inc., Redlands, California.

Lindsey, K.A., 1995, *Miocene- To Pliocene-Aged Suprabasalt Sediments of the Hanford Site, South-Central Washington*, BHI-00184, Rev. 00, Bechtel Hanford, Inc., Richland, Washington, July.

National Research Council, 1996, *The Hanford Tanks: Environmental Impacts and Policy Choices*, Committee on Remediation of Buried and Tank Wastes, Board on Radioactive Waste Management, Commission on Geosciences, Environment, and Resources, National Academy Press, Washington, D.C.

Reidel, S.P., D.G. Horton, Y.-J. Chen, and D.B. Barnett, 2006, *Geology, Hydrogeology, Geochemistry, and Mineralogy Data Package for the Single-Shell Tank Waste Management Areas at the Hanford Site*, RPP-23748, Rev. 0, CH2M Hanford Group, Inc., Richland, Washington, May.

Reidel, S.P., and M.A. Chamness, 2007, *Geology Data Package for the Single-Shell Tank Waste Management Areas at the Hanford Site*, PNNL-15955, Pacific Northwest National Laboratory, Richland, Washington, January.

Richland (City of Richland), 1981–2005, *Water Treatment Plant, Richland Water System Monthly Report*.

SAIC (Science Applications International Corporation), 2006, *Cumulative Impacts Analysis, Inventory Development*, Rev. 4, Germantown, Maryland, October 2.

Serne, R. J., B.N. Bjornstad, J.M. Keller, P.D. Thorne, D.C. Lanigan, J.N. Christensen, and G.S. Thomas, 2010, *Conceptual Models for Migration of Key Groundwater Contaminants Through the Vadose Zone and Into the Unconfined Aquifer Below the B-Complex*, PNNL-19277, Pacific Northwest National Laboratory, Richland, Washington, July.

SWS (Schlumberger Water Services), 2009, *Visual MODFLOW, Version 2009.1 Pro*, Waterloo, Ontario, Canada.

Thorne, P.D., M.P. Bergeron, M.D. Williams, and V.L. Freeman, 2006, *Groundwater Data Package for Hanford Assessments*, PNNL-14753, Rev. 1, Pacific Northwest National Laboratory, Richland, Washington, January.

USGS (U.S. Geological Survey), 2004, *MODFLOW 2000 Engine, Version 1.15.00*, August 6.

WHI (Waterloo Hydrogeologic, Inc.), 2005, *HydroGeo Analyst v. 3.0 User's Manual – Database Utilities, Borehole Logging/Reporting, 2D Mapping and Cross Sections, and 3D Visualization*, Waterloo, Ontario, Canada.

Wurstner, S.K., P.D. Thorne, M.A. Chamness, M.D. Freshley, and M.D. Williams, 1995, *Development of a Three-Dimensional Ground-Water Model of the Hanford Site Unconfined Aquifer System: FY 1995 Status Report*, PNL-10886, Pacific Northwest National Laboratory, Richland, Washington, December.

Code of Federal Regulations

10 CFR 1021, U.S. Department of Energy, “National Environmental Policy Act Implementing Procedures.”

40 CFR 1500–1508, Council on Environmental Quality, “Regulations for Implementing the Procedural Provisions of the National Environmental Policy Act.”

40 CFR 1502.1, Council on Environmental Quality, “Environmental Impact Statement: Purpose.”

40 CFR 1502.2(b), Council on Environmental Quality, “Environmental Impact Statement: Implementation.”

Federal Register

62 FR 8693, U.S. Department of Energy, 1997, “Record of Decision for the Tank Waste Remediation System, Hanford Site, Richland, WA,” February 26.

United States Code

42 U.S.C. 4321 et seq., National Environmental Policy Act of 1969.